UNIVERSITY OF BIRMINGHAM

SURFACE PASTEURISATION OF FOOD PACKAGES BY THE INVERSION METHOD

by

FLORA P. CHALLOU

A thesis submitted to
The University of Birmingham
for the degree of
DOCTOR OF PHILOSOPHY

School of Chemical Engineering
College of Engineering and Physical
Sciences
The University of Birmingham
January 2016

Abstract

Thermal processing is the most widely used and well established preservation method used in the food industry for ensuring food safety and extending the shelf life of food products. Besides from the food product, the package needs also to be decontaminated to achieve the required safety goals. This research is concerned with surface pasteurisation treatments in food packages by the method of inversion, primarily for hot-filled food products. Starch solutions and tomato soup, used as model fluids in the current work, were hot-filled in glass jars, were sealed and then inverted for thirty seconds at a filling temperature of $80^{o}C$ for achieving a target process equivalent of 5 min at $70^{o}C$; the inversion step was used as a thermal treatment of the headspace and the lid. The inverted jars showed significantly higher process values for the headspace and the lid with the filling temperature being the most important parameter.

The effectiveness of the inversion step during hot-fill treatments was quantified by the use of two monitoring techniques, the traditional temperature sensors and the alternative, enzymic based *(Bacillus amyloliquefaciens* α-amylase) Time Temperature Integrators (TTIs). TTIs are small devices with kinetics similar to the microorganisms, whose level of degradation is measured at the end of the thermal process. The enzyme activity obtained is integrated and the temperature history can be quantified. TTIs were tested for their reliability and accuracy under isothermal and non-isothermal conditions, and were then used for validating the hot-fill process.

The behaviour of the model fluids was investigated by performing rheological analysis and by the development of a mathematical model. The rheological experiments showed that the food fluids are shear-thinning ($n < 1$), temperature, frequency, stress and strain dependent and have dominant elastic properties, rather than viscous. The fluids' behaviour was also described by the development of a mathematical model. Transient flow patterns and temperature profiles during the cooling phase of the heat treatment were predicted and modelled by a finite element method. Good agreement between the experimental and predicted data, which was confirmed by the calculation of the Root Mean Sum Error (RMSE), validated the developed model, making it a promising tool in predicting thermal processes.

Acknowledgements

Table of Contents

Chapter 4 - Modelling of temperature distributions in hot-filled food packages

List of Figures

Chapter 2 - Literature Review

Chapter 3 - Pasteurisation of model food packages by the inversion method

Chapter 4 - Modelling of temperature distributions in hot-filled food packages

Chapter 5 - TTI validation for hot-fill processes

List of Tables

Chapter 2 - Literature Review

Chapter 3 - Pasteurisation of model food packages by the inversion method

Chapter 4 - Modelling of temperature distributions in hot-filled food packages

Chapter 5 - TTI validation for hot-fill processes

Nomenclature

A_o / A_f	Initial and final enzyme activity
a_w	Water activity
C_{BAA}	Concentration of BAA or BLA (mol l^{-1})
C_p	Heat capacity (J kg^{-1} K^{-1})
C_1 / C_2	concentration of microorganisms at times t_1 and t_2
c and d	Consistency and index constants
R	Diameter of the container (m)
D_T	Decimal Reduction Time (min)
D_o	Decimal Reduction Time at a reference temperature T_o (min)
F	Sterilisation value (min) and volume force (N m^{-3})
F_o	Target lethality at the coldest spot (min)
F_s	Integrated lethality (min)
G´ / G´´ / G*	Storage / loss / complex modulus (Pa)
Gr	Grashof number (dimensionless)
g	Acceleration of gravity (m s^{-2})
h_c	Heat transfer coefficient (W m^{-2} K^{-1})
H	Height of the container (m)
i	Complex number ($\sqrt{-1}$)
k	Thermal conductivity (W m K^{-1})
$k^{'}$	Constant reaction rate
L	Lethality (min) and length of container (m)
M	Percentage of components on wet basis
N_o / N_f	Initial and final number of microorganisms
N_1 / N_2	Number of spores at time t_1 and t_2
N_t	Number of spores at time t
P	Pasteurisation value (min)
p	Initial pressure (Pa)
Pr	Prandtl number (dimensionless)
q	Inward heat flux (W m^{-2})

r_A	Reaction rate (mol s^{-1})
Ra	Rayleigh number (dimensionless)
Re	Reynolds number (dimensionless)
t	Duration of the heat treatment (min)
$T(t)$	Product temperature (°C)
T_{ref}	Reference temperature (°C)
u	Instantaneous velocity (m s^{-1})
U	Typical velocity (m s^{-1})
x_wall / x_bot / x_lid	Wall / bottom / lid thickness (m)
$X_{a,c,f,p,w}$	Mass fraction of ash, carbohydrates, fat, protein, water
z	z -value (number of degrees Celsius to bring about a ten-fold change in Decimal reduction time) (°C)

Greek symbols

α	Thermal diffusivity (m s^{-2})
β	Thermal expansion coefficient (K^{-1})
$\dot{\gamma}$	Shear rate (s^{-1})
$\gamma_{max} / \gamma_{min}$	Minimum and maximum shear rate (s^{-1})
δ	Phase angle (degrees)
δ_M / δ_T	Momentum and thermal boundary layer thickness (m)
η_0 and η_∞	Viscosities at shear rate $\dot{\gamma} = 0$ and $\dot{\gamma} = \infty$ respectively
μ	Dynamic viscosity (Pa s)
ν	Kinematic viscosity (m^2 s^{-1}) and velocity (m s^{-1})
ρ	Density (kg m^{-3})
τ_{min} / τ_{max}	Minimum and maximum shear stress (Pa)
σ	Surface tension (N m^{-1})

Abbreviations

2D	Two dimensional
3D	Three dimensional
12-D	12-log decimal reduction of microorganisms
ANOVA	Analysis of Variance
BAA	*Bacillus amyloliquefaciens*
BLA	*Bacillus licheniformis*
CCRFA	Campden and Chorleywood Food Research Association
CFD	Computational Fluid Dynamics
CFL	Courant Friedrichs Lewy condition
CMC	Carboxymethyl Cellulose
df	Degrees of freedom
DRT	Decimal Reduction Time
EO	Ethylene Oxide
FD	Finite Difference
FE	Finite Element
HACCP	Hazard Analysis Critical Control Point
HCl	Hydrochloric acid
HTST	High Temperature Short Time
IR	Infrared Radiation
LLP	Least Lethality Point
LVR	Linear Viscoelastic Region
MRI	Magnetic resonance imaging
MS	Mean Squared Error
NAS	National Academy of Sciences
PEPT	Positron Emission Particle Tracking
PPC	Post Pasteurisation Contamination
RMSE	Root Mean Square Error
SS	Sum of Squares
TDT	Thermal Death Time
TTI	Time Temperature Integrators

Tris	Tris hydroxymethyl aminomethane
UHT	Ultra High Temperature
UV	Ultra Violet

Chapter 1 - Introduction

Thermal processing has always been key in ensuring the microbiological safety of long-life food and beverage products, whether that be a full sterilisation, aimed at a 12-Log reduction of *Clostridium botulinum*, or a lesser pasteurisation heat treatment targeting less heat-resistant organisms (e.g. *Listeria monocytogenes, Escherichia coli O157, Salmonella*) with other inhibiting steps (pH control, water activity, etc.) (Holdsworth, 1997).

Manufacture of a thermally processed food consisted of two basic steps (Fellows, 2000):

- Heat application to the food product to reduce microbial population to a level that is acceptable; i.e. to achieve a statistically small probability of growth of pathogenic and spoilage organisms under the intended storage conditions.
- Sealing of the food product within a hermetic package to prevent re-infection.

In traditional preservation methods, such as canning, the food is sealed in its package before heat is applied to it, whereas in aseptic treatments such as, hot-fill, cook-chill and cook-freeze the food is heated before being dispensed into the pack (Rickman, 2007). The most heat-resistant pathogen that survives thermal processing of low-acid foods is the spore-forming organism *Clostridium botulinum*; a sterilisation process is established based on the 12-log reduction of the *Clostridium botulinum* spores (i.e. 1 spore surviving in 10^{12} packs). However, there is a growing trend to apply additional hurdles to microbial growth that allow the processor to use milder heat treatments such as pasteurisation; the treatment is extensively used in the production of many different types of food, such as fruit products, pickled vegetables, jams and ready meals (CCFRA, 1992a). Food may be delivered in-pack

(analogous to canned foods), or in continuous processes (analogous to aseptic filling operations). The target aimed during pasteurisation processes is usually a 5 or 6-log reduction of the target organism. However, pasteurised foods are not free from microorganisms and rely on other preservative mechanisms to ensure their extended stability for the desired length of time (Montville,2005).

Of primary interest in the current work are foods that are given a mild heat treatment, more specifically the hot-filled ones. Food products with a shelf-life of up to 10-days are recommended to receive a pasteurisation treatment at least equivalent to 2 min at 70°C at the product's thermal centre, i.e. the coldest point (CCFRA, 2006). This assumes that no other preservation hurdle (e.g. salt, sugar or preservatives) is used, apart from chilled storage. Examples of food products receiving this type of treatment are soups, sauces, cooked poultry, ready meals and a wide range of pies and pastries.

With the number of products and their variety increasing, food companies are faced with the challenge of proving that their products are safely pasteurised. Their ability to validate this can be challenging if conventional temperature probe systems cannot be used. This might be due to complexities introduced by products cooked in continuous ovens or fryers (e.g. poultry joints, bread) or by particulate products cooked in agitated vessels or heat exchangers (e.g. ready meals, soups, dressings) (Tucker et al., 2000). Thus, alternative validation approaches are required.

The use of correct guidance and statistical models to validate and optimise processes can result in several benefits, including significant cost reduction through use of less energy and shorter process cycle times, which increases productivity and plant efficiency. It may also lead to the improved retention of various nutrients in food products (Âvila and Silva, 1999).

1.1   Objectives

The objectives of the current study are:

- To investigate the effectiveness of the inversion step in hot-fill processes as a thermal treatment of the headspace and lid, for reducing post-pasteurisation treatments.

- To test the reliability and accuracy of TTIs, when subjected to a variety of time-temperature profiles, relevant to industrial thermal processes ;

- To test the effectiveness of TTIs as a monitoring technique, for validating pasteurisation processes.

- To develop a valid mathematical model that would be able to accurately predict temperature profiles and flow patterns of complex processes; simulating the inversion step of the hot-fill treatment is one such a challenge.

1.2   Thesis chapters

This thesis has the following structure:

Chapter 2 reviews:

−   The food preservation methods used in the food industry, with thermal processing being more extensively analysed;

−   The development of the TTI systems and their application up to date;

−   The development of a kinetic and heat transfer model used for designing, controlling and optimising thermal processes

Chapter 3 refers to the experimental work carried out for investigating the effectiveness of the inversion step as a treatment of the headspace and the lid, in hot-fill treatments. The method aims at a target process of 5 min at 70°C for food products with a chilled shelf-life up to 10 days.

Chapter 4 illustrates the effectiveness of the finite element mathematical method in predicting the flow behaviour of a starch solution and tomato soup during the cooling phase of the hot-filling process. The model is validated by experimental data.

Chapter 5 investigates:

− The sensitivity and accuracy of TTIs under isothermal and non-isothermal condition;

− Their effectiveness as an alternative monitoring technique in monitoring pasteurisation treatments, by being compared to temperature probes.

Chapter 6 summarises the conclusions of the current work and refers to future work recommendations.

Publications: Papers and Posters are given in the CD included with this work at the back of the thesis

Journal (Peer-Reviewed)

Peter J. Fryer, Mark J.H. Simmons, Phil W. Cox, K. Mehauden, Suwijak Hansriwijit, Flora Challou, Serafim Bakalis, (2011). Temperature Integrators as tools to validate thermal processes in food manufacturing. *Procedia Food Science*. 1, 2011, 1272 - 1277, doi:10.1016/j.profoo.2011.09.188.

Conferences

- Flora Challou, M. J. Simmons, P. J. Fryer (2014). Surface Pasteurisation of Food Packages by the Inversion Method and evaluation of Time Temperature Integrators. *Institute of Food Technologists* (IFT14), New Orleans, LA, USA, June 2014 (Poster presentation)

- Flora Challou, M. J. Simmons, P. J. Fryer (2015). Surface Pasteurisation of Food Packages by the Inversion Method. *International Congress of Engineering and Food* (ICEF12), Quebec City, Canada, June 2015, (Oral presentation).

Chapter 2 - Literature Review

2.1   Introduction

Consumers' demand for safe and high quality food products is ensured by the application of different preservation techniques. Whilst the heat treatment of food products has been extensively studied, no guidelines exist currently for the surface treatment of food packages (CCFRA, 2012). Hot-fill treatment is based on the assumption that the heat transferred from the pasteurised food is sufficient to decontaminate the package. That is true for the surfaces that come in contact with the product, but it is not the case for the headspace and the lid of the package. It is thus usual that foods are either over-processed before filling, or the product is given a further heat treatment after filling. Usually, the after filling step is followed by a top-up pasteurisation which includes either:

o Passing the food packages (jars or bottles) through a pasteurisation tunnel where water is sprayed at high temperatures (around 95°C), or

o Inverting the package for pasteurising the headspace and the lid; the latter has been extensively used in the food industry for filling into glass jars, plastic pots and pouches, cartons and plastic trays.

Quantifying the heat treatment given to food packages during hot-fill operations would potentially increase line efficiency and reduce waste and energy input (CCFRA, 2011).

In the current chapter, the state of work on heat treatment quantification by a variety of validation techniques and optimisation methods is detailed.

2.2   Food processing technology

Food processing is more than merely a necessity to preserve foods; multiple objectives are served until the food product reaches the consumer. For instance, freezing technology both preserves foods and offers convenience, while heating or fermentation of foods like soy makes them edible and prevents them from mild toxicity caused by hemagglutinens (Floros, 2008). Food processing operations dealing with raw materials or ingredients that carry pathogens are tightly controlled by regulations associated with detection and inactivation of food-borne microorganisms in order to ensure that the final product delivered to the consumers is safely delivered and of high quality. New, innovative technologies have been developed to ensure not only the safety and quality of food products, but also to produce foods with unique attributes (e.g. functional foods) (Cardello, 2002).

Most food preservation techniques are designed to create unfavourable conditions for microbial growth. Some of the most important growth requirements of microorganisms, associated with food preservation are presented in Table 2.1.

Table 2.1: Growth requirements of microorganisms in foods (adjusted from ICMSF, 1996).

Environmental factor	Microorganism type	Growth requirements
Temperature	Psychrotrophic	Grow at refrigerated temperatures
	Mesophilic	$20\text{-}36^{o}C$
	Thermophilic	$24\text{-}55^{o}C$
Oxygen	Aerobic	O_2 required
	Anaerobic	Don't grow with O_2 present
Water*	Bacteria	$a_w \geq 0.99$
	Yeasts	$a_w \geq 0.88$ (some grow at $a_w=0.70$)
	Moulds	$a_w \geq 0.80$ (some grow at $a_w=0.60$)
Acidity	All	Range of tolerance: pH 4.0 to 8.0; some yeast and moulds very acid tolerant.
Nutrients	All	Wide range of specific requirements for different organisms

*water expressed in terms of water activity (a_w)

Food processing technology aims at a number of objectives that benefit the consumers and society:

Preservation: It is the most common and important purpose of food processing, as it prevents food spoilage and extends the shelf life of foods. Food spoilage can be caused by microorganisms, undesirable enzymes and /or chemical reactions (e.g. Maillard browning and lipid oxidation), and change in food physical structure (e.g., sugar crystallisation, starch gelatinisation) (Gould, 1989).

Microbial food spoilage is the most important type of spoilage as it can cause quality and safety deterioration that can range from merely a poor, non–nutritive product to food poisoning (Miller, 1989).

Safety: The major concern and challenge of food processing operations is to inactivate pathogenic microorganisms which are related to health hazards. The pathogens of concern vary significantly in terms of heat resistance; *Campylobacter*, *Salmonella*, and *Listeria* are heat-labile and can be inactivated by mild heat treatments such as pasteurisation, whilst *Bacillus cereus* survives pasteurisation and low temperatures (Hammer, 1999).

Clostridium botulinum is the most heat-resistant bacteria which make it a good indicator for the validation of thermal processes such as sterilisation and canning (Holdsworth, 1997). Besides from the foodborne pathogens, other microorganisms such as yeasts, moulds, and gas-producing bacteria can also cause food spoilage and thus must be inactivated (Sivertsvik et al., 2004). The behaviour of microorganisms changes according to the environment they are submitted to. Environmental factors such as the pH, water activity, chemical composition and the properties of the foods themselves affect the microorganisms' heat resistance and behaviour. Thus, the type of microbial flora associated with raw materials or ingredients is important to be known, before any thermal process is applied. Another important factor to be taken into consideration is the re-infection of the product, which can cause problems in the thermal treatment (Lioliou et al., 2004). Safety is also associated with other factors such as pesticides, natural toxins, antibiotics and environmental contaminants (NAS, 1973). Managing microbiological risks is not the only task that ensures the safety of a final product: good agricultural and manufacturing practices that address chemical and physical hazards are also of great importance (Hall, 1977).

Quality: It refers to attributes such as colour, taste, texture, nutrient content (e.g. vitamins) and aroma. The quality of most attributes starts declining at the moment the foods or ingredients are harvested or collected (Kader, 2005). Thus, processing operations need to ensure that the rate of decline of the quality attributes is slowed down and the losses are minimised. A good example is the blanching of vegetables after they have been harvested; the nutrients are almost kept at their initial level (Barrett, 2007). The challenge that food manufacturers have to face is to ensure safety, without compromising quality. Therefore, it is important to understand the reaction kinetics in relation to microbial inactivation, chemical damage, enzyme inactivation and physical changes.

Availability and sustainability: The increased demand for access to a variety of food products all year along requires food processes to be fast and efficient. Controlled atmosphere for stored fruits and vegetables is an example of retaining freshness and extending shelf-life (Rickman, 2007b). The goal of sustainability is to maximise the utilisation of the raw materials required for manufacturing purposes, and the integration of the activities from the production to the consumption stages (Bongiovanni, 2004). To maximise the conversion of raw materials into final products, postharvest losses need to be reduced and the utilisation of by-products need to be increased. Then, efforts need to be made for ensuring that resources such as energy and water are efficiently used, with minimal environmental impact. Refrigeration of fresh food products is an example of minimising loss and increasing the edible life of the product (Mattsson, 2003).

Convenience, Health and Wellness: Food processing is also used for preparing ready-to-eat foods and meals that need a limited amount of effort to be cooked before consumption. For instance, many frozen or refrigerated products only need to be microwave-heated for only a few minutes. Snacks are another example of convenience products achieved by food processing. Besides meeting nutritional requirements, food can also be processed in ways that provide them with optimised properties, promoting health and wellness. Refining of anti-nutritional compounds in vegetables, extraction of carotenoids from tomatoes, for improving bioavailability and nutritional quality, are some of the techniques used to optimise quality of foods (ILSI, 2004a). Some products are designed and produced to respond to specific nutritional needs of the consumers, such as gluten free products, sugar free, reduced salt, etc. Other products are enriched with vitamins, minerals or other nutrients (e.g. addition of calcium in orange juice, stanols in margarine) for bone and heart health respectively. These products are called functional foods and are required to also meet the consumers' expectations of flavour and texture (Rosetta Newsome, 2007).

With preservation being the most important objective of food processing, the following technologies are used to control the different spoilage types in food products:

Thermal processing: Thermal processes can range from mild, such as blanching and pasteurisation, to severe, such as sterilisation and canning (Leistner, 1995). Depending on the resistance of the attribute targeted, a variety of time-temperature combinations is applied. In the case of mild processes, vegetative pathogens, yeasts, moulds and/or enzymes are targeted and need to be inactivated. When the spore-forming and toxic pathogens are targeted, more severe conditions need to be applied and destroy the microorganisms implicated. The high temperature exposure of foods ensures safety, but at the same time causes quality alterations.

When the quality attributes (e.g. nutritional value, texture, flavour, etc.), are changed in an undesirable way, the thermal process is referred to as "thermal damage", but when desirable, the process is known as "cooking". The preservation by heat will be further discussed in § 2.2.1.

Low-temperature processing: When compared to heating processes, the activity of the microorganisms and enzymes, under low temperatures, is not destroyed or inactivated but depressed, for as long as the applied temperature conditions (chilling or freezing) are kept constant. Unlike heat preservation, low temperature preservation is reversible, and once temperature is increased, microorganisms and enzymes will be reactivated. Hence, it is critical to maintain the required low temperatures throughout the product's shelf life. Low temperature preservation can be divided into two processes; chilling, where the food is kept at a low temperature above its freezing point, and freezing, where the food is kept at a temperature below its freezing point (Fellows, 2000). Besides from temperature differences, the processes differ also in terms of phase change that happens during freezing, due to reduced molecular mobility. The water transition to ice in freezing results in water activity reduction in the rest of the food that is not ice and consequently microbial and enzymic depression. The phase transitions during freezing can also lead to undesirable and irreversible changes, such as texture alteration (Heldman and Hartel, 1997; Boonsupthip, 2007).

Dehydration: The process is one of the oldest and most energy intensive food preservation techniques used (Von Loesecke, 1943; Saravacos, 1965; King, 1968; Thijssen, 1979). It aims at slowing the growth of microorganisms and rate of chemical reactions. The method offers many advantages to food processors, since volume and weight of the product are reduced by

water removal, the shelf life is extended, and liquids are converted into powders, such as instant coffee. Water is usually evaporated, vaporised, or sublimated in the case of freeze-drying by means of a simultaneous heat, mass, and momentum transfer mechanism (Whitaker, 1977) within the food and between the food and the drying medium. In addition to water removal, other reactions that modify the original structure of the food material also occur (Viollaz and Alzamora, 2005); chemical reactions such as Maillard browning of amino acids/reducing sugars, sugar caramelisation, protein denaturation, and pyrolysis of organic constituents, as well as loss of volatile compounds and gelatinisation of starches, are some of them.

Water activity (a_w) preservation: Many processes and products have been successfully designed based upon the a_w concept (Alzamora et al., 2003). Unlike water content, a_w can give information about the shelf stability of the food. The free water available in fruit and vegetables supports microbial growth, chemical reactions and acts as a transporting medium for compounds, whilst the bound water does not participate in these reactions since it is bound by water soluble compounds such as salt, sugar, gums, etc. and by the surface effect of the substrate matrix binding (Barbosa-Canovas et al., 2007). The moisture conditions in which spoilage microorganisms cannot grow is very important for food preservation; each microorganism has a critical a_w below which it cannot grow. At $a_w=0.3$, food products are very stable in terms of enzyme activity, non-enzymatic browning, lipid oxidation and microbial parameters. As a_w increases, the probability of the food product deteriorating increases (Barbosa-Canovas et al., 2007).
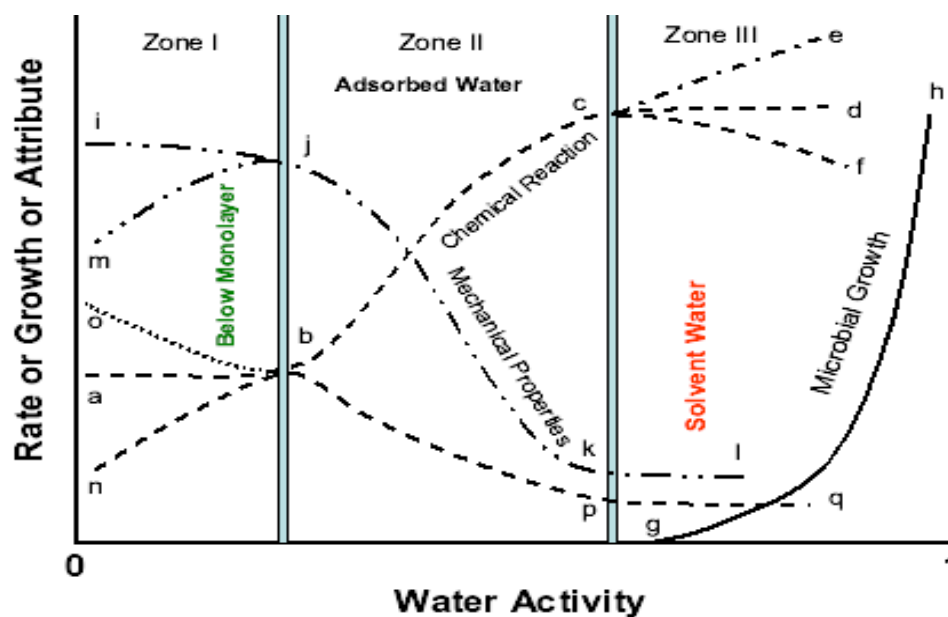
Figure 2.1: Stability diagram based on the water activity concepts (Powitz, 2007)

Packaging: Food is primarily packaged to contain the product, protect it from contamination, enable convenience, and provide information (Paine, 1991; Robertson, 1993; Yam et al.*, 2005; IFT, 2008). In addition, it extends the shelf life of the product by acting as a physical barrier to the atmospheric factors such as oxygen, moisture and any others that would cause product deterioration. Packaging also provides legally required information, through labels, that inform the consumer about the product identity, ingredients, nutrient content, expiration date, quantity, and commercial source.

Packaging has advanced from glass bottles and cans towards flexible, rigid, active and intelligent packaging (Floros et al.*, 1998; Ozdemir and Floros, 2004; Yam et al.*, 2005; Han and Floros, 2007). That was due to consumers' desire for more convenient, sustainable packaging and demands for global and fast transport of food (Suppakul et al.*, 2003). Aseptic packaging offers increased safety, quality, convenience and availability, while reducing the energy usage needed to preserve and store certain foods. It differs from traditional packaging methods because the product and the package are sterilised separately, resulting in a shelf-

stable final product with high quality and extended shelf life; that is mainly due to the milder heat treatment that the product undergoes compared to the traditional thermal process (Floros, 1993).

Chemical preservation: This type of preservation is based on the addition of chemicals in foods, known as food preservatives; salting is one of the oldest and most common chemical preservation techniques. Smoking can also be used as a chemical preservation method due to the deposition of naturally produced chemicals resulting from thermal breakdown of wood and salting; the incorporation of smoke flavour and the development of colour are highly desirable in the developed societies (McGee, Harold, 2004).

Most of the food pathogens cannot grow or survive at low pH conditions; compounds that lower the pH of the food product or its surrounding environment need to be used. Such compounds can be acids (e.g. citric acid, vinegar, acetic acid, lactic acid produced by fermentation), herbs and spices, or non-natural chemicals (e.g. sorbic acid, sulphur dioxide) (Jay, 1995).

Novel, alternative processes: The new processing technologies include microwave, ionizing radiation, pulsed electric fields, ultra-high pressure, high-intensity pulsed light and ohmic heating (Raso, 2003). These are claimed to deliver safe and shelf-stable food products much faster than canning or other conventional thermal processes, but have not yet been widely used in the industry. The novel processes, primarily developed to replace the conventional thermal processes and have the potential to be used in a variety of food products that will meet consumers' growing demands for fresh-like and nutritious foods. Each of the emerging

technologies has unique characteristics and potential applications in a variety of food products.

o   *Microwave Heating:* A well-known and widely accepted technology by the consumers for heating prepared foods and cooking raw ones.

o   *Ohmic Heating:* The process passes electricity through the food via contact with charged electrodes, resulting in rapid and more uniform heating of the product. Heat is generated instantly inside the food, and its amount is directly related to the voltage gradient, and the electrical conductivity (Sastry and Li, 1996). The lack of high wall temperatures, the short processing time and the maintained quality factors such as colour and nutritional value are some of the an advantages of ohmic treatments over conventional methods (Wang and Sastry, 2002; Castro et al., 2004a; Icier and Ilicali, 2005a; Leizerson and Shimoni, 2005a, b; Vikram et al., 2005). Ohmic treatment is used in a wide range of applications such as blanching, pasteurisation and sterilisation (Lima and Sastry, 1999), and mostly for heat-sensitive foods (Ramaswamy et al., 2005), such as fruit and liquid eggs.

o   *High-Pressure Processing:* a cold pasteurisation method according to which food products are sealed, placed into a containing liquid chamber, and pumps are used to create high hydrostatic pressures (HHP) of up to 600 MPa for a few seconds to a few minutes. The technique is a promising preservation method that respects the quality attributes of food, since the reduction in microbial populations can be accomplished without significant increase in product temperature. HPP is especially efficient on food products, such as yogurts and fruits (Brown, 2007) as pressure-tolerant spores do not survive at low pH levels (Adams & Moss,

2007). A number of ready-to-eat meats and other refrigerated items have been treated by high pressure, resulting in high-quality products with increased shelf life (Jay et al., 2005).

o *Pulsed Electric Fields (PEF):* The method uses high voltage (>20 kV) and short (µs) electric pulses to liquid or semi-solid food products placed between two electrodes. It aims for microbial inactivation, whilst causing minimal effect on food quality attributes (Quass, 1997), making the technology highly advantageous as compared to traditional thermal processing. Most of the PEF studies are concerned with the microbial inactivation in liquid foods (Qin et al., 1995). However, recent research has shown that PEF is very effective for inactivation of microorganisms, increasing the pressing efficiency and enhancing the juice extraction from food plants, and for intensification of the food dehydration and drying (Barsotti and Cheftel, 1998, 1999; Estiaghi and Knorr, 1999; Vorobiev et aI., 2000, 2004; Bajgai and Hashinaga, 2001; Bazhal et aI., 2001; Taiwo et aI., 2002).

Hurdle technology: It is based on the principle that the combined effect of different preservation techniques is more efficient than using each technique separately (Leistner, 2002). For instance, the process of dried sausages includes steps that need to ensure low pH, low water activity, low temperatures, salting, smoking, and the addition of herbs or spices. The required, preserved final product is achieved by the combination of all the steps, as each one individually would not be sufficient.

Table 2.2: Principal hurdles used for food preservation (Leistner, 1995; Lee, 2004).

Parameter	Symbol	Application
High temperature	**F**	Heating
Low temperature	**T**	Chilling, freezing
Reduced water activity	$\mathbf{a_w}$	Drying, curing, conserving
Increased acidity	**pH**	Acid addition or formation
Reduced redox potential	$\mathbf{E_h}$	Removal of oxygen or addition of ascorbate
Bio-preservatives		Competitive flora such as microbial fermentation
Other preservatives		Sorbates, sulfites, nitrites

2.2.1 *Thermal processing of food products*

The application of high temperatures on food products, their surrounding environment and package, is the basis of heat preservation, which is the most common type of preservation method. It is the principle preservation method used in the canning industry. Thermal processes can be mild, as in the case of blanching and pasteurisation or more severe as in canning operations, all relying on the application of heat. Depending on the intensity of the thermal process food safety and quality are affected accordingly. The reasons why foods are heated are numerous, with preservation being the primary one, as it is associated with the microbiological safety of a product, which can be at risk if certain heat-resistant food pathogens are not destroyed or inactivated (CODEX, 1997).

The effectiveness of a thermal process is dependent on the formulation and composition of the food product, the heat resistance of the microorganisms present in each of the products, the heating rate of the specific product and the container's characteristics. The product's physical thermal properties, especially its rheology (if a liquid), have a significant effect on the heat

transfer mode and the heat penetration speed (Lewis, 2002). In a pure solid and liquid food, heat will be transferred by conduction and convection, respectively, but for most viscous fluids or solid-liquid mixtures the heat transfer mechanisms will lie between the above two extremes. According to HACCP procedures, it is important to find the coldest spot, i.e. the point in the pack or vessel that heats slowest.

Thermal transfer to this point is the slowest and thus controls the process. That can be an easy task when it comes to solid products, where the cold spot is located in the centre of the container, but not as easy when complex food products such as viscous fluids or particulate mixtures are involved; for locating their slowest heating point, the determination of heat penetration data is of great importance. Another reason for heat to be applied in foods is associated with quality issues. Chemical reactions like protein denaturation and starch gelatinisation are promoted, and the quality attributes of the final product are affected either advantageously or not. For instance, the gelation of evaporated milk is prevented by heat application, and the texture of yoghurt is improved, while in other products foods where a natural and fresh appearance is required such as in drinkable milk or fruit juices the sensory and nutritional quality is damaged by heat. Enzyme activity may also result in quality changes; some enzymes need to be inactivated for avoiding changes like fruit browning by polyphenol oxidases and minimising quality changes such as flavour, caused by lipases, whilst other enzyme action can improve the taste and structure of products like bread, biscuits, wine and beer (Campbell et al., 1999).

Safety and quality issues can conflict in cases where severe heat treatments are applied; microbial inactivation is achieved, but at the same time the quality of the product deteriorates. Most biochemical reactions involved in quality degradation are catalysed by heat-sensitive enzymes (Meade et al., 2005). Hence, the quality deterioration can be prevented and the food

quality can be retained. Similarly, a food product is microbiologically stable, when the heat applied is sufficiently high and it is hermetically sealed. Therefore, to extend the shelf-life of a food product, the denaturation of enzymes, destruction of bacterial spores, and the inactivation of vegetative pathogens, need to be achieved. To achieve all three objectives would result in a stable product with a much extended shelf-life. Generally, the thermal processes aiming at each of the above objectives, besides cooking, are blanching, pasteurisation and sterilisation, with the latter two being tightly controlled and regulated by government and state agencies, due to their impact on health and wellness (Singh et al., 2004).

Blanching

Blanching is a mild, pre-heating step that is applied to food products at temperatures <100°C for a couple of minutes and it is usually followed by other heat treatments, such as freezing and drying (Van Buggenhout 2005). Due to being mild, the process has limited effect on nutrients. Blanching may simply be a cooking process wherein foods, normally vegetables and some fruits are immersed in boiling water or are steamed for a very short time (seconds to a couple of minutes) and are then immediately cooled down into cold/ice, for the cooking treatment to be halted, which can lead to quality deterioration of the products. The cooking of asparagus and protein-based salads are characteristic examples of blanching. They are boiled for 30 seconds and then chilled rapidly. Blanching is also used to inactivate anti-nutritional properties (e.g. trypsin inhibitor found in soybeans), and reduce oxidation by removing air in the food tissues (Selman., 1987).

Pasteurisation

Pasteurisation is also a relatively mild heating regime, in which food is heated to < 100ºC, and it aims to inactivate heat labile microorganisms, such as vegetative bacteria, yeasts, moulds, and/or enzymes that may cause food spoilage. It is applied to a wide, diverse range of foods such as dairy products, fruit, vegetables, drinks, meat, fish, sauces, etc. in order to extend their shelf-life from a few days up to several months, depending on their acidity. The heat treatment is in most cases combined with rapid cooling and refrigeration, in order to avoid post-pasteurisation contamination (PPC) from occurring. Some examples of food products and the reasons they are pasteurised, are presented in Table 2.3.

Table 2.3: Pasteurisation processes for different foods (Adapted from Anon, 2007a; Campden BRI technical manuals, 2006b).

Food product	Purpose	Factors	Target organism	Processing conditions
Acidified vegetables	Ambient shelf stable	pH must be < 4.0	Butyric anaerobes	15 min at 100°C (retort) Equivalent process: 5 min at 85°C
Beer	Ambient shelf stable	CO_2 acts as inhibitor	Yeasts	20 min at 60°C
Brown sauce	Ambient shelf stable	pH=3.6±0.3 acetic acid, salt, sugar, spices	Yeasts, moulds, lactic acid bacteria	30 s at 90°C (plate heat exchanger)
Canned plums	Ambient shelf stable	pH=3.5 sugar 30°Brix	Enzyme inactivation, yeasts	125 min at 101°C (retort) Equivalent process: 5 min at 85°C
Canned tomato sauce	Ambient shelf stable	pH=4.2 citric acid, salt, sugar	Butyric anaerobes	70 min at 105°C (continuous steriliser)

Food product	Purpose	Factors	Target organism	Processing conditions
Carrots and onions in wine sauce	Ambient shelf stable	pH must be < 4.0	Enzyme inactivation	10 min at 110°C (retort) Equivalent process: 5 min at 85°C
Milk	Pathogen destruction and extended chilled shelf-life at T≤3°C	Chill storage	*Pathogens (Mycobacterium tuberculosis)*	15 s at 72°C (heat exchanger)
Fish pate	Short shelf life-chilled stability at T≤3°C	a_w=0.97	Listeria	4 h at 82°C (oven) Equivalent process: 12 min at 70°C
Meat	Chilled stability at T≤3°C (6 weeks shelf life)	Salt 2.5%	*Psychrotrophic C.botulinum*	7.75 h at 78°C (oven) Equivalent process: 10 min at 90°C
Soft drinks	Ambient shelf stable	pH=3.2-3.5	Yeasts	4-10 s at 90-95°C (heat exchanger)
Tomato ketchup	Unopened ambient shelf life	pH=3.8-3.9 acidity 1.5% sugar 26% salt 2.9%	*Z.bailii*	2.3 min at 82°C (min. in bottle) Equivalent process: 3 min at 82°C

Pasteurisation can be delivered 'in-pack' or to products that are thermally processed before being filled. In-pack pasteurisation is a very conventional concept, as the food product is sealed in a container and then thermal process is applied to both the food product and the container. The thermal process may be batch, with the retort being used for the heating, holding and cooling phases of the treatment, or continuous, where the food products roll on conveyors into a tunnel with the three sections of heating, holding, and cooling (Fellows, 1997). In a hot-fill process, the food is pasteurised before being filled into the package,

assuming that the temperature given to the food will sufficiently pasteurise the package. However, no guidance exists on this subject (CCFRA, 2007) and the uncertainty has led the hot-filled products to often be processed to higher temperatures than necessary before filling, or the product to be given a further heat treatment after filling and sealing the package (Figure 2.2). It is often the case that the food product temperature drops dramatically as it comes into contact with the food pack and, consequently, provides little thermal decontamination on the inside pack surface. Experimental results obtained from industrial trials showed that there was a significant temperature decrease in certain containers after the hot-fill treatment (CCFRA, 2014); a temperature reduction of up to 20˚C was observed on glass jar packages, 5-10˚C for plastic surfaces and up to 3˚C for pouch surfaces, as compared to the temperature recorded at the bulk of the food product. This suggests that hot-filling alone is not realistic for achieving even a minimum of 70°C for 2 minutes process, if the packages is not pre-heated or/and post-pasteurised.
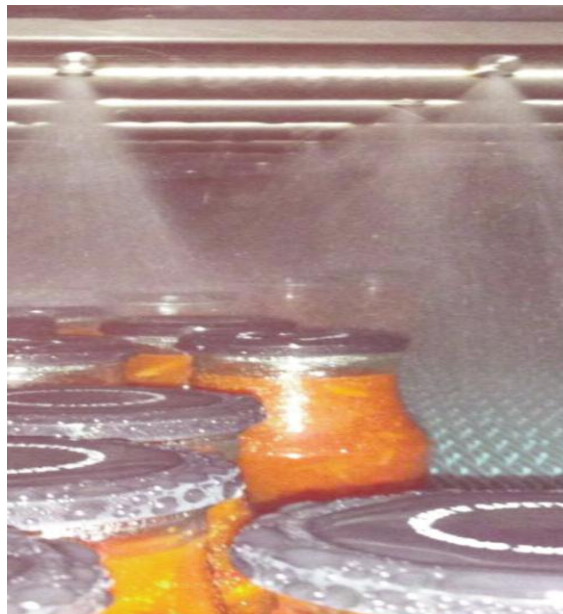
Figure 2.2: Typical post-filling pasteurisation tunnel

In hot-filling processes, products are thoroughly cooked before being filled into the package. Thus, any spoilage occurring in the final products, would probably be due to either insufficient heating of the internal surfaces of the package, or because of post-process contamination caused by failure of the package (Bown, 2003).

Both in-pack and hot-fill methods are time-consuming and expensive, and often require significant additional processing capability. The quantification of hot-fill operations would potentially be advantageous in saving water and energy, reduce waste and have great environmental impact.

Research concerning the application of hot-fill treatment in products like fruits, fruit purees, tomato sauces and pastes, has been covered in literature. A standard procedure for the hot-fill treatment of fruits with a pH < 4.0, was recommended by the National Canners Association (Brown, 1984) and includes the following conditions: filling temperature >85°C, can sealing, water processing for 2 minutes at 88°C, steam can also be used, and cooling. The above conditions appeared to be ineffective, however, when applied in Indian canneries, due to the long holding time (10-30 min) between sealing and processing (Silva, 1997). Nanjundaswamy et al., (1973) evaluated the impact of the hot-fill process in canned mango products, and concluded that yeast and peroxidase inactivation, as well as the reduction of the overall process time, are significantly affected by the filling temperature. Cans of a 570 mL capacity, were hot-filled at temperatures from 76 to 80°C, sealed, inverted for 2-3 minutes and cooled down. The conditions used proved sufficient for the product to be pasteurised. The validation of the process was based on the analysis of the final enzymic and microbiological activity. Nath & Ranganna, (1983a) studied the impact of the hot-fill treatment on guava pulp, and managed to determine heat transfer characteristics and process requirements.

Sterilisation

Sterilisation is the heat treatment primarily used to inactivate microorganisms that cause food-borne disease such as botulism, and other microorganisms related to food spoilage, such as yeasts and moulds. Sterilisation can be delivered in two ways (Nelson, 2010):

o   The food is sealed in a container and then it is thermally processed, together with the package, referred to as canning or in-container processing.

o   The food is sterilised, it is filled into pre-sterilised containers, within a sterile environment and it is finally sealed. The method is referred to as aseptic processing. Whatever the process, the safety and quality of the food need to be ensured. With *Clostridium botulinum* being the critical target microorganism in sterilisation processes, low-acid food products with a pH>4.5 would be the ones of interest. For a 12D reduction of *C. botulinum*, that would ensure the required safety, the low-acid foods need to be processed for 3 min at 121°C, also referred as a $3F_{o}$ process. The process value of the sterilised products is determined by measuring the time-temperature history of the product at the slowest heating point, using a z-value of 10°C, for *C. botulinum.* The ideal sterilisation process would involve the heat to be instantaneously transferred to the food, so that the same temperature is reached by all food parts, at the same time. In that case sterilisation reactions would predominate over the quality ones (Fryer, 1997).

Ultra High Temperature (UHT) and High Temperature Short Time (HTST) processes are considered to follow the above ideal concepts. In both processes food is rapidly heated at about 130-140°C, is held for a few seconds at high temperatures, and then cooled down in the same rate, in order to avoid product degradation. Both processes result in products with substantially improved quality attributes compared to conventional heat treatments (Simpson et al*.,* 2000). More specifically, in the HTST process the food product is sterilised before it is

filled into the package, which is also pre-sterilised using either steam or hydrogen peroxide. The heat rates of HTST process are significantly higher than in canning, making the process ideal for continuous operations.

The rate at which microorganisms are destroyed is increased with temperature. The same thing happens with the rate at which a quality factor changes. However, the microbial destruction rate is from four to seven times more temperature sensitive than the quality degradation rate (Martinez et al., 1999; Holdsworth, 2004). Therefore, for every 10°C increase in processing temperature, the cooking effect will be doubled, whereas the microbial death rate will increase by a factor of ten (Table 2.4).

Table 2.4: z-values for heat-sensitive food components (Holdsworth, 1992).

Component	z-value (^{o}C)
Bacterial spores	7-12
Microbial cells	4-8
Enzymes	3-50
Vitamins	25-30
Proteins	15-37
Sensory factors	
Overall	25-47
Texture-softening	25-47
Colour	24-50

Thus, processing at high temperatures, and shortened processing time, the product delivered would potentially be safe with a reduced quality loss. The question is how fast can the product be heated and cooled. The UHT process has been used mostly for dairy products, especially milk, when the conventional sterilisation processes cause sensory problems. UHT heat processing results in ambient stable and better quality food products, as compared to conventional sterilisation process. A comparison between conventional and aseptic processes used in food industries, is illustrated in Figure 2.3.
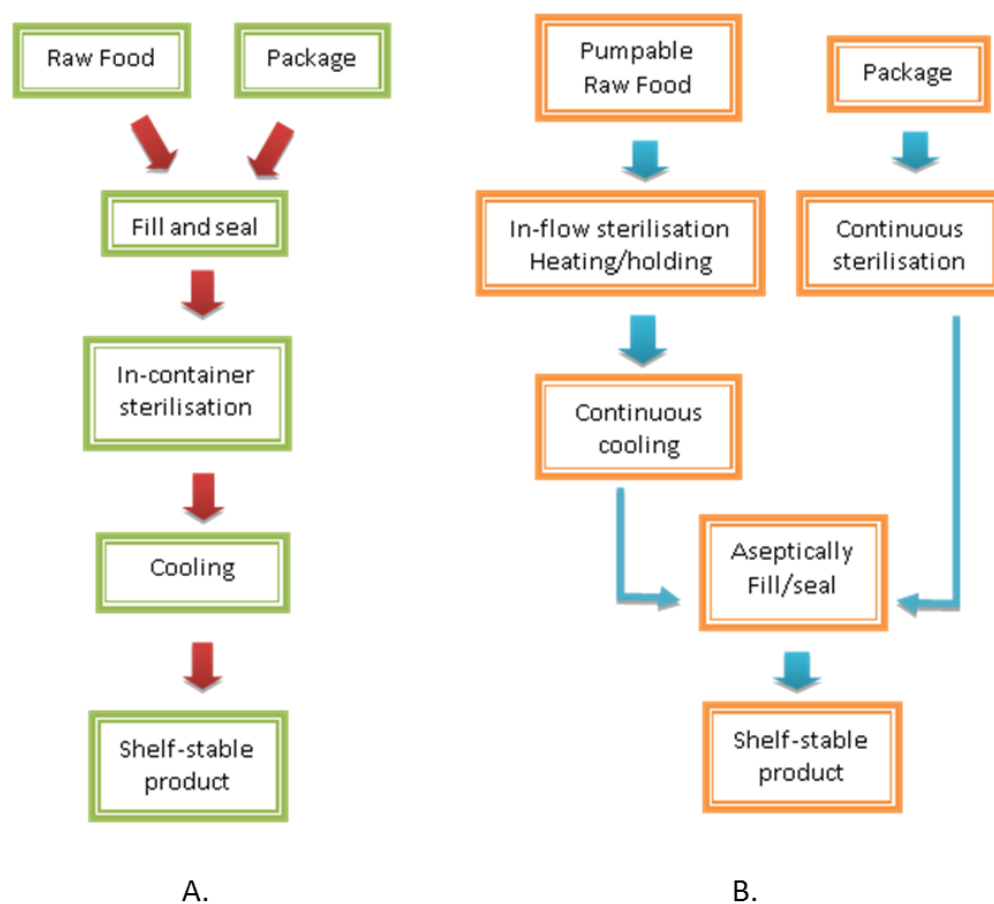
Figure 2.3: Comparison of A. conventional and B. aseptic processing for the production of shelf stable foods (Nelson, 2010).

2.2.2   *Surface decontamination of food packages*

Most of the food contamination studies carried out in factories and labs refer to the microorganisms present in the food. Hence, little information on package contamination, and guidelines on the controls that need to be implemented for ensuring the required food safety and quality, is available. The first step in understanding the degree of decontamination needed to be achieved on the food package, is knowledge of the type and load of the microorganisms, or enzymes present. Then, the extent of the heat treatment applied to the surface of the package needs to be determined (CCFRA, 2012).

Aseptic packages utilise plastics, foil containers or paperboard for packing the sterilized product. In hot-fill treatments, glass jars, laminated cardboard and plastic tubs are of particular interest. Experiments conducted on concentrated tomato paste, hot-filled in glass jars, showed that spoilage microorganisms such as *Bacillus coagulans* were not inactivated after the application of the hot-fill treatment (Sandoval et al.*,* 1994). Hersom and Hulland, (1964) supported the above findings by spotting remaining *Clostridium* spores after hot-filling. Vegetative pathogens, yeasts and moulds were observed by Tucker et al.*,* (2004), on the packaging used for dairy products, before they were hot-filled. The highest contamination level appeared to be found on polystyrene surfaces, as compared to materials such as glass. That is assumed to be because of the higher electrostatic charge observed on polystyrene, and in plastic packages in general, making them a significant source of contamination.

The most common packaging heat treatments used include thermal processing (including saturated and superheated steam), radiation, chemical methods and a combination of the above (Ansari and Datta, 2003). Some of the methods used for sterilising aseptic packages are summarised in the following paragraphs:

Thermal process methods

As mentioned above, heat processing is still the most commonly used method for food preservation and package decontamination. When heat is used, the nature of the material of package needs to be taken into account. The low thermal conductivity of plastics and cartons makes it more difficult to sterilise them as compared to metal packages.

Thermal processes do not cause environmental hazards, since they don't deposit any undesirable residues on the surface being treated.

−   *Saturated steam and hot air (moist heat):* It is mainly used for the sterilisation of thermostable plastic cups and metal surfaces, such as homogenisers and fillers in the hold tube. The moulded cups and foil lids are subjected to saturated steam at 165°C and 6 bar after deep drawing. At the same time, the external cup surface is cooled by applying air to limit the effect of the short time heat application on the material, by reducing the pressure, as the materials cannot otherwise withstand the high temperatures for long (Larousse and Brown, 1997).

−   *Superheated steam and hot air (dry heat):* The heat delivered is not as effective as the one obtained from moist heat at the same temperature for sterilisation, therefore higher temperatures are required (Larousse and Brown, 1997).

The hot-air method is preferred over the saturated heat, when paper-based packaging is involved, due to condensation and for food products with a pH of <4.6. The method can ensure safety without any effect on packaging material quality (Toledo, 1986). Hot air sterilisation has been commercially used for juice and beverages.

o   *Heating by extrusion:* It is a form, fill, seal packaging system that relies on the temperatures reached by thermoplastic resin, during the co-extrusion process. The high extrusion temperatures result in a sterile product contact surface. During the process, a multi-layer package material is fed into the machine and is delaminated under sterile conditions. A layer of material is then removed, and the product contact surface is exposed; the container material is then thermoformed into cups (Bauser, 2006). The method has only been used for acidic products with pH less than 4.6, due to concerns about its efficacy (Reuter, 1988).

Chemical methods

A variety of chemicals, either in a liquid or gas form are used as an alternative method for surface decontamination of packages. The most commonly used ones are the following:

o   *Hydrogen Peroxide:* It is the most widely used chemical disinfectant for packaging materials, and it is efficient either at ambient temperatures and high concentrations, or at increased ambient temperatures and lower concentrations. That is due to the slow reaction rate of the chemical on the surface of the package, at ambient temperature. Swartling and Lindgren (1968) note that spores of *Bacillus subtilis* were reduced by a 4-log, when the food package was immersed for 15 seconds in a bath consisted of 20% of hydrogen peroxide, at $80^{o}C$. Rutherford et al., (2000) reported that the mechanisms of inactivation are different between spores and vegetative cells. Hydrogen peroxide can be commercially applied to packages by dipping (a bath consisted of 30-33% of hydrogen peroxide, where the package is immersed), spraying (dispersed droplets of hydrogen peroxide are sprayed on the package surface), and rinsing (substitutes the other two, when not feasible). Recent studies have been

referring to hydrogen peroxide vapour (HPV), which is beneficial in disinfecting hard to reach and complex surfaces (Johnston et al., 2005).

o   *Ethylene Oxide (EO):* It is used mainly used as a chemical intermediate in the manufacture of detergents, solvents, and textiles, but it has also been used in sterilising packages for aseptically processed foods, dried fruits and spices (ATSDR, 1990). EO has been successfully used for spice sterilisation with alkylation as a mechanism of action. Usage of EO as a food sanitation method accelerated dramatically in the 1960s, when EO fumigation was reported to significantly reduce spoilage organisms in spices and spice blends (Radomyski, 1994). It is temperature, humidity and concentration dependent and is generally carried out at temperatures of 30 °C to 60 °C with relative humidity above 30%, for sterilising objects sensitive to temperatures greater than 60°C. The EO has been shown to be effective when diffused freely throughout the product being treated, which means that the package used needs to be breathable (Council of Agricultural Science and Technology, 1995).

Radiation methods

When thermal and chemical methods are not feasible, radiation methods are used as an alternative approach which is becoming increasingly popular; Figure 2.4 illustrates the mechanism of radiation, when applied to a surface. The packaging materials commonly used in radiation are: PVC, polyethylene (PET), polypropylene, polyester, nylon, etc. (Ansari and Datta, 2003). Radiation methods are classified as follows:

o   *Ultraviolet (UV) Ray:* Both vegetative pathogens and heat-resistant spore-forming bacteria are UV sensitive and are effectively destroyed at the range of 200-315 nm

(Bachmann, 1975). UV light has been used in the food industry for disinfecting surfaces of equipment in bakeries, cheese and meat plants, food packages such as bottles, boxes, foils, caps, cartons and films and for decontamination of conveyor surfaces (C.A.C., 1994). UV light has been effectively used to disinfect smooth surfaces, but its application in food processing industry is still limited. Reasons for that can be the restricted range of commercially available equipment for disinfecting solids and the fact that the kinetic data for microbial inactivation are mostly obtained from in suspension in aqueous media or air (F.D.A., 1997). A few studies have been reported on the use of UV irradiation for the inactivation of *Salmonella typhimurium* on poultry carcasses (Wallner-Pendelton et al.*,* 1994), *Escherichia coli* and *Salmonella* on pork skin and muscle (Wong et al.1998); and *Listeria monocytogenes* on chicken meat (Kim et al.*,* 2002). The above studies showed that UV light has the potential to decontaminate food surfaces from bacterial contamination and therefore could possibly be used as post lethality treatment to control *L. monocytogenes* and other pathogens of concern. A commercially available food surface decontamination system, called the UV tumbling process was developed by C&S Equipment Company The system has been recommended for the treatment of fresh fruits and vegetables, meats, frozen foods (fruits, vegetables, meats, seafood, bakery products), and cooked, refrigerated products (pasta, cheese) (Chapman, 2003).

o   *Infrared Radiation (IR):* It is commonly used for decontaminating the interior of lids, coated with aluminium and its working principle is based on the conversion of the radiation into sensible heat, when it is in contact with an absorbent surface (Ansari and Datta, 2003).
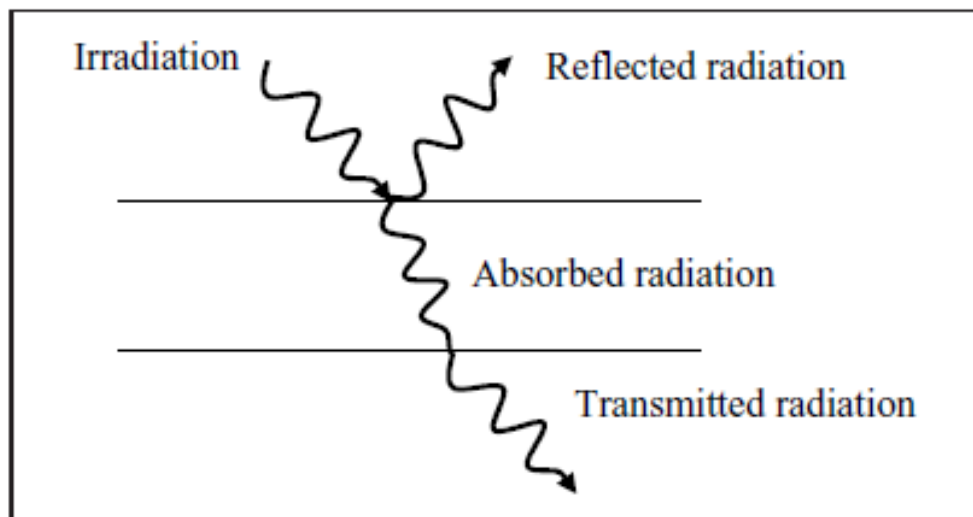
Figure 2.4: Extinction of radiation (Pan et al., 2010)

Application of IR in food processing has gained popularity due to its advantages over conventional heating. It has been applied in a variety of processes such as drying, baking, roasting, blanching, pasteurisation, and sterilisation of food products, showing a potential to produce high-quality foods at low-cost (Sakai and Hanzawa, 1994). When used for dehydrating foods, IR radiation is very advantageous since the drying time is reduced, the energy efficiency is increased and there is uniform temperature throughout the product while drying. Thus, the necessity air flow across the product is reduced and better-quality finished products are obtained (Dostie et al., 1989; Navari et al., 1992; Mongpreneet et al., 2002). Because of the its advantageous effect in the drying process, IR has been successfully applied for drying fruit and vegetable products such as potatoes (Afzal and Abe, 1998), sweet potatoes (Sawai et al., 2004), onions (Sharma et al.,2005), kiwifruit (Fenton and Kennedy, 1998), and apples (Nowak and Levicki, 2004; Togrul, 2005). Infrared drying has also been used in food analysis to measure water content in food products (Hagen and Drawert, 1986; Anonymous, 1995).

o   *Ionising Radiation:* It has been mainly used for the sterilisation of medical equipment; its use in sterilisation of food products is still contentious. In the 1980s, the World Health Organisation (WHO) and Food Agriculture Organisation (FAO), approved the use of radiation as a treatment for foodstuffs at a defined dosage of <10 kGy (WHO, 1994; FAO, 1984). FAO reports that approximately 25% of the food production is lost due to bacteria, insects, and rodents after harvesting. Radiation can inhibit the sprouting, delay ripening, and help with the disinfestations of insects and parasites when applied at a dose of <1 kGy. When a medium dose of 1 to 10 kGy is used, the number of spoilage organisms and pathogens is reduced, whilst at a high dose of >10kGy, sterility can be achieved (Farkas, 1998). It has been affective towards *Campylobacter, Yersinia* and *Vibrio spp.*, as well as *E. coli* (Formanek et al., 1996).

Concerns still remain though over the effect of irradiation on the organoleptic characteristics of the foods (Venugopal, 1999). Another important fact is that irradiation does not inactivate the bacterial toxins, which means that by destroying the bacteria does not guarantee food safety (Weissmann et al., 2002).

o   *Light Pulse treatments:* It is a food preservation method that combines intense and short duration pulses of broad-spectrum "white light"; the spectrum includes wavelengths in the ultraviolet (UV) to the near infrared region of light for pulsed light treatment. The technology is mainly used for decontaminating the surface of food packages and sterilizing pharmaceutical products. The surface to be sterilised is exposed to a pulse of light with a duration range from 1 μs to 0.1 s (Dunn, 1996). In aseptic processing, the packaging material is usually sterilized chemically, most frequently with hydrogen peroxide, which may leave

undesirable residues in the food or package (Barbosa-Cánovas et al., 1997). Light pulses can be used to reduce the need for chemical disinfectants and extend the shelf life of the product.

Combination methods

As with the hurdle technology used in thermal processing, radiation methods can be combined with chemical or even thermal methods, in the case of *Clostridium* spores destruction, resulting in a greater overall lethality (Marquenie 2003).

Combined treatment, such as in the case of low heat with a low dose of irradiation, can slow down ripening, reduce losses in fruits and delay the development of ripe skin colour (Gagnon et al., 1993; Lacroix et al., 1995). It has been supported that irradiation improves the effectiveness of subsequent processes to further reduce microbial contamination (Farkas, 1999). In the case of dried foods such as spices, where irradiation has been applied the most, the microbial contamination levels decline with storage time, since the microorganisms treated with radiation cannot reproduce anymore. This has been reported to be the case, even when the product was stored at elevated temperatures and high humidity for a few months (Marquis, 2007). Furthermore, microorganisms that survive irradiation are more heat sensitive and thus, if kept at constant temperature after heat treatment, they would have an extended shelf-life. Edible coating has been used in combination with gamma irradiation and has proved to be effective in reducing microbial loads and increasing the shelf life of a variety of food products, such as herbs, poultry and beef (Bruhn, 1995; Resurreccion et al., 1995; Farkas and Andrassy, 1996).

2.2.3   Monitoring of thermal processes

The increased demand for a variety of safe food products has made validation of the thermal processes a challenging task. To establish a safe thermal process, accurate measurements of the temperature the products are exposed to and the interpolation of the microbial destruction level need to be taken. Temperature sensors and data loggers provide an economical and flexible way of taking such temperature measurements.

2.2.3.1 Temperature sensors

A temperature measuring system for validating a thermal process consists of a temperature sensor and a data logging device; the sensor type and data logger varies depending on the application. The proper selection of equipment to be used is important, as it would affect the outcome of any trials performed in terms of accuracy. Department of Health Guidelines, (2000) recommends that temperature measurements should be taken to an accuracy of $\pm0.5^{o}$C. Temperature sensors commonly used in thermal processes, are thermocouples and resistance thermometers; the latter are based on the principle of electrical resistance changes due to temperature and they are mainly used to monitor stable temperatures (Tucker et al., 1996). Thermocouples are devices consisted of two insulated, separate wires of dissimilar metals. The wires are joined together at one end, while the other end is connected to a data logger. The junction of the two metals produces an electric potential that is proportional to the temperature difference between the reference, cold junction and the thermocouple junction. The resulting voltage, measured by a voltmeter, is converted into a temperature reading and the electronic signal is converted into temperature data from the data logger. The metals used for the wires, can be figured by the type of thermocouple used (e.g. T, K type).

Thermocouples and data loggers are used to record temperature distributions and to determine the location of the slowest heating point in a retort/tank or product (Shaw, 2000). They are user friendly, easy to use (setting-up and downloading data is straightforward), provide with immediate results (data can be exported instantly) accurate with an offset of $\leq 0.2°C$ and they can record temperature on multiplechannels displaying the data graphically, when the appropriate software is used. One such example, which was used in the current work, is Pico Data Logger.

Thermocouples can also be wireless, which are usually easier to install when compared with cable probes. They are mainly used for continuous processes, sachet filling, internal packaging surfaces and rotary type retorts, where the cable thermocouples cannot be used. They are precise and practical, but the data is downloaded after processing and not Real-Time. Data ValSuite™ Pro Software and Madge Tech Packages are examples of wireless data loggers used in industry.

Figure 2.5: Ellab wireless thermocouples and data loggers.

However, the application of temperature probes is not always convenient and the process validation can be difficult, when complexities are introduced. Complex processes include products that are continuously cooked in an oven, such as burgers and chicken nuggets, or

particulate foods processed in either continuous heat exchangers or agitated batch vessels such as sauces, soups, ready meals and preserves (Tucker et al., 2005). When the use of temperature sensors is not feasible, the thermal process is validated by other monitoring techniques, some of which are listed below:

2.2.3.2 Microbiological methods

They are used when the inactivation kinetics of the microorganisms is similar to that of the target organism; the microbial spores are embedded into calcium alginate beads, which mimic the physical-thermal behaviour of the food particles and pass the process with them (Brown et al., 1984). The remaining organisms are enumerated and the process values can be calculated. A similar procedure has been used when ohmic heating was applied for monitoring the kinetics of *Lactobacillus acidophilus* during a fermentation process, by measuring the current passing through the fermenter (Cho, 1996). The use of Ohmic heating as a monitoring technique has been conducted with liquid crystal and MRI (Sastry and Li, 1998; Ruan et al., 2004). Liquid crystal is a chemical compound which changes its colour as a function of temperature. It can visualise surface temperature changes either by observing the pattern of colour change, or by calibrating it with a thermocouple at a known temperature range.

MRI is another non-invasive technique that maps temperature distribution, by recording real time dynamic changes throughout the process.

The inoculated pack method is another commonly used approach where a solution of spores is distributed throughout the product; the spores are in direct contact with the food product in each pack. The inoculated packs are incubated after the heat treatment and the survivors are recovered. The presence or absence of growth is observed by the gas production and changes in turbidity (NACMCF, 2010).

Impedance microbiology, a rapid technique that enables qualitative and quantitative tracing of food-pathogens by measuring electrical conductivity changes, is another microbiological monitoring method that has been mainly used in food products such as milk and its sub-products (Silley, 1996; Wawerla, 1999).

Other monitoring approaches used for confirming the presence or not of microorganisms in food products are dry plate culturing, biochemical profiling, immunological methods, and bioluminescence applications (Gracias, 2004). Molecular methods, such as those referring to sequent gene coding have gained become popularity recently in studying bacterial communities in environmental samples (Giovannoni et al., 1990, Ward et al., 1990, Muyzer et al., 1993, Ludwig and Schleifer, 1994, Amann et al., 1995 and Head et al., 1998).

Fourier Transform Infrared Spectroscopy (FT-IR) has been used successfully for identifying several foodborne pathogens, such as *Yersinia, Staphylococus, Salmonella, Listeria, Enterobacter* (Gupta et al., 2005; Mossoba et al., 2005). The method is based on the molecular composition of the food sample tested and it is consisted of the infrared source, the sample and the detector (Thomson et al., 2003).

2.2.3.3 Retort simulators

Retort simulators are mostly used for continuous canning systems (e.g. reel cooker-cooler) and are based on replications of heat transfer conditions of a thermal process, carried out in a lab or a pilot plant (CCFRA, 1977; Bee and Park, 1978). These simulators are nowadays substituted by temperature loggers that are self-contained and can actually travel with the cans, such as Ellab sensors and data loggers.

2.2.3.4 Thermochromic inks or dyes

Thermochromic inks or dyes are compounds that are sensitive to temperature, and change colour when exposed to heat. They are used in applications such as clothing, flat thermometers, baby bottles and kettles (Ramaiah, 1997). When used inside a container, they can indicate the cold spot locations and can estimate lethality. According to trials carried out in glass jars filled with water, thermochromic inks proved to be slow, inaccurate, and incapable of providing information about high temperatures However, the method has been extensively used in food industry, to distinguish cooked from uncooked batch products, to avoid cross contamination, and to check temperature abuse during product distribution and storage (Burfoot, 2014). Thermochromic dyes have also been used as microwave temperature indicators on food packaging (Seeboth, 2014).

Figure 2.6: Thermochromatic ink paper and Leuco Dye (www.slideshare.net).

2.2.3.5 Thermal imaging

Thermal imaging is a technique that is based upon the principle that the amount of radiation emitted by an object, which is increased with temperature, is converted into visible images for feature extraction and analysis (Berry, 2000). It is mainly used as a quality assurance tool for

controlling the quality and safety of cooked meat products, predicting fruit yield, detecting bruises in fruits and vegetables, and foreign bodies in food material (http://www.proviso systems.co.uk/index.php). The thermal imaging camera can monitor the temperature of food products, such as chicken tenders in continuous conveyor ovens; it can identify hot/cold spot in microwave heating, for measuring external surface packages and can record the outside wall temperature in hot-fill processes (Vadivambal, 2011).

Infra-red imaging is another example of thermography. It has been mainly used as a method for direct measurement of the surface temperature and it can provide a visual indication of variations in temperature. The method is a non-invasive, non-contact, and non-destructive nature and can be used in thermal validation where conventional probes cannot be applied, requiring knowledge and experimental emissivity data on the packaging surface in order to provide an accurate reading (CCFRA, 2011).
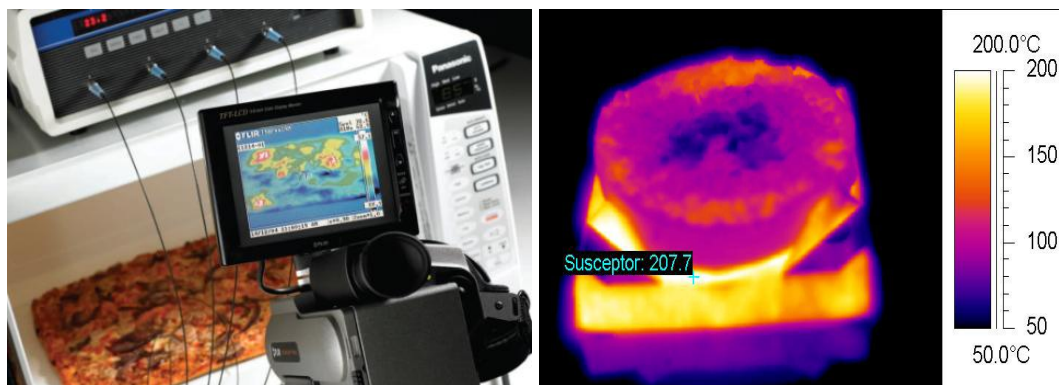
Figure 2.7: Thermal imaging camera and outcome image (plus.maths.org).

2.2.3.6 Process models

They are developed for predicting the time-temperature history of primarily small food particles throughout the thermal process (Heppell, 1985; McKenna & Tucker, 1991). For

larger food particles (>2-3 mm), the microbiological method described above, is mostly used (Fryer et al., 1997).

2.2.3.7 Enzymatic Time-Temperature Integrators (TTIs)

The method was first reported by Hendrickx et al., (1995) and it is based on the denaturation of bacterial amylases that show similar inactivation rates and temperature sensitivity with the microbial breakdown. The method has received considerable attention over the last 20 years (De Cordt et al., 1992; Maesmans et al., 1994; Van Loey et al., 1996). The choice of monitoring technique depends on the nature of the target food, the type of heat process and the costs.

TTIs are used as an alternative means of process validation in complex processes where the conventional thermocouples cannot be used. A TTI is a small, thermally labile measuring device that is time and temperature dependent, is easy to use, and mimics the behaviour of either a safety or quality target attribute, as they undergo the same heat treatment (Taoukis and Labuza, 1989a, b).

An ideal TTI system, applicable to foods products of interest, needs to fulfil certain requirements. Such a system should:

o Undergo irreversible changes and be time-temperature dependent;

o Have same or similar kinetics with the target attribute;

o Be sensitive to various temperature conditions;

o Be reproducible;

o Easy to use, without interfering with the target food and;

o Easily measurable.

Figure 2.8: TTI tubes and particles.

Classification of TTIs: They can be of biological (enzymatic or microbiological), chemical or physical nature. When the kinetics of the TTI system are equal or similar to that of the target attribute, the response is characterised as single, while when the TTI system is consisted of a set of components with dissimilar kinetics, the system is considered to be a multi response. Depending on whether the TTI is added to the food or it is intrinsically present in it, the TTIs are called extrinsic and intrinsic, respectively. The single point (i.e. the cold spot) or volume average impact on a food product can be evaluated by a dispersed, permeable or isolated approach, with regard to the TTI application. The above classification of TTIs is illustrated in Figure 2.9 and further discussed in the following paragraphs.
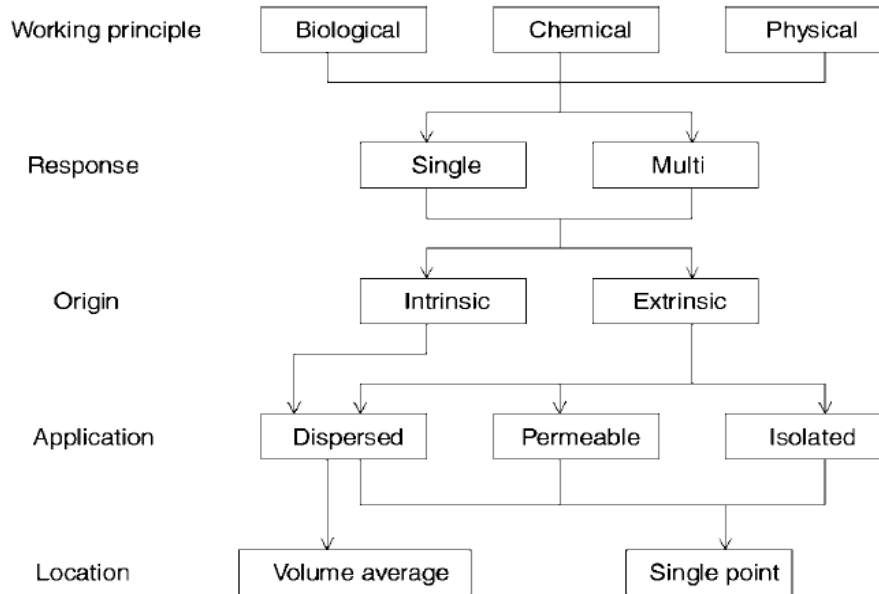
Figure 2.9: Classification of TTIs (Hendrickx et al., 1993).

Working principle of TTIs: The nature of the TTI system affects the time needed for post-processing to obtain the process value at the end of the thermal treatment. Biological TTIs are the most studied systems yet the post-processing is highly-time consuming, as the population of the viable cells needs to be counted. However, the fact that they are heat sensitive over the same temperature range as their target gives them a major advantage. Processes based on enzymic TTIs are more advantageous since their denaturation enthalpy and activity can be more easily and accurately measured and they are small enough to be used in a variety of containers and processes. Microbiological systems need to be calibrated before being used to any thermal treatment evaluation, as the microorganisms can exhibit inherent variability (Pflug and Odlaug, 1987). Enzymatic TTI systems also need to be thoroughly calibrated due to batch differences and storage conditions.

TTI systems of chemical nature are flexible and exhibit analytical precision, but they still have not been applied to thermal processes.

Response types of TTIs: TTIs have a single or multicomponent response, depending on whether or not they have similar kinetics as their target attribute, respectively. In the case of single response, a direct correlation between the TTI system and the target organism can be obtained, whereas in the multicomponent case, knowledge of target's time-temperature profile is needed (Taoukis, 1999). Studies have been carried out for dealing with the multicomponent response by statistically correlating the TTI behaviour with the safety or quality attributes for given time-temperature profiles. The equations used correspond to specific conditions with different kinetics, meaning that if another time-temperature set is needed, extrapolation will be required which can lead to uncertainty and errors. Stoforos and Taoukis, (1998) suggested that components with z-value higher and lower than that of the target organism should be included when multicomponent TTIs are used. Despite its limitations, the complex system of the multiple TTI components can be useful in targeting multiple targets with various z-values, showing potential for further investigation.

Origin: With regard to their origin, the TTIs can be intrinsic or extrinsic. The former, is dispersed in the food product and can be used for either to evaluate a single point in the product, which is usually the cold spot, or the average volume, while the latter is added to the food. Intrinsic TTIs are convenient, as there is no need for a monitoring device, but the fact that they are mixed with the environment they are subjected to, can cause difficulties in determining the kinetics of the TTI and the product, separately. That is the reason why the extrinsic TTIs are encapsulated in a variety of materials that isolates them from the actual food product and the surrounding environment. When TTIs are encapsulated, it is important that the properties (thermal or mechanical) of the carrier material are determined. This is particularly important in the case of aseptically processed liquid or particulate foods. In the

case of non-thermal processing, such as microwave heating, the dielectric properties of the material, such as the penetration depth and the heating rate are important since they have been recognized as potential factors to improve the retention of thermolabile constituents in liquid foods such as milk and fruit juices (Mudgett, 1986). As far as the dispersion of the TTI is concerned, the volume average before and after processing is determined when the target of interest is related to quality attributes (e.g. nutrition retention). When the attribute of interest is related to safety, the TTI should be positioned in the slowest heating point of the product, making sure that the worst-case scenario is taken into account.

Some examples of intrinsic and extrinsic TTIs are presented in Table 2.5.

Table 2.5: Application of intrinsic and extrinsic TTIs
(adjusted from Patterson & Kilpatrick, 1998; Claeys et al., 2002).

Indicator	Principle/reagents	Application
Time-temperature indicator (ext.)	Mechanical, chemical, enzymatic	Food stored under chilled and frozen conditions
Oxygen indicator (int.)	Redox dyes, pH dyes, enzymes	Foods stored in packages with reduced oxygen concentration
Indicator of CO_2 (int.)	Chemical	Foods package in MAP or CAP
Microbial growth indicators (int/ext), **Freshness indicators**	pH dyes, dyes reacting with certain metabolites	Perishable foods such as meat, fish, poultry.
Pathogen indicators (int.)	Various chemical and immunochemical methods reacting with toxins	Perishable foods such as meat, fish, poultry.

Application of TTIs: As already mentioned, TTIs have been used to monitor microorganisms or enzymes with equal z-value (defined in § 2.2.1) or activation energy, when the time-temperature profile of the food being heated is not known. Depending on the process targeted, the range of z-values for the inactivation of vegetative pathogens, yeasts and mould lies in between 5 and $12^{o}C$, which refers to pasteurisation processes, while for quality attributes, such as vitamins and colour, it lies between 25 and $45^{o}C$ (Lund, 1977). The canning process applied in low-acid food products is based on the inactivation of *Clostridium botulinum*, with a z-value of $10^{o}C$.

Most studies regarding TTI development are focused on enzymic and chemical TTIs, which have been evaluated for their reliability and accuracy for a variety of thermal treatments, such as pasteurisation and sterilisation, and semi-industrial processes in pilot plants. TTI systems based on enzymes, originating from bacteria, such as α-amylases, are advantageous over other biological TTI systems. They are convenient, as they are supplied in a powder form, they undergo irreversible changes and they show first order reaction rate when exposed to high temperatures, similar to the microbial destruction rate. Several types of enzymic TTIs have been used to evaluate mild thermal processes; when it comes to more severe processes like sterilisation, there is a limited number of enzymes resistant to temperatures $>100^{o}C$. One such enzyme that can potentially be used in sterilisation processes was isolated from a hyperthermophilic microorganism, *Pyrococcus furiosus*. The amylase extracted is thermostable and can survive throughout processes such as canning, batch vessels and ohmic heating.

Potential TTI systems used in mild processes are reported in the literature. Extrinsic *Bacillus amyloliquefaciens* α-amylase (BAA) based TTIs were used by Van Loey et al., (1996a) to monitor pasteurisation processes with particulate foods and by Tucker et al., (2000) for the

pasteurisation of fruit products in tubular heat exchangers and ohmic heating. Reyes de Corcuera et al., (2005) studied the effectiveness of an exogenous, amperometric glucose oxidase based TTI. The enzyme was entrapped in a thin film and positioned on the interior wall of a capsule. The TTI system was investigated, under isothermal conditions for temperatures 70 to 79.7^{o}C, showing first order kinetics. Vaidya et al., (2003) investigated the potential and effectiveness of a fluorescence emission based TTI system for the inactivation of vegetative pathogens like *Salmonella*. The TTI were tested for temperatures $\geq 62.8^{o}$C and showed good correlation between experimental and theoretical data. Another potential TTI system used for the evaluation of pasteurisation processes was reported by Guiavarc'h et al., (2003); Pectinmethylesterases (PMEs), extracted from cucumber and tomatoes, were subjected at a temperature range of 55–77°C with sugars or polyols being present. Cucumber PMEs showed biphasic behaviour, while the tomato PMEs showed first order kinetics. Fruits and vegetables can be a good source of enzymes, but the steps that need to be taken for preparation and analysis can be time-consuming and excessive.

Enzymic TTIs have also been used for monitoring sterilisation processes. *Bacillus licheniformis* α-amylase (BLA) based TTIs was used by Tucker et al. (2000) to evaluate sterilisation processes and to investigate process value differences between freely moving and fixed particles inside cans. *Bacillus subtilis* α-amylase based TTIs were used for evaluating the end-over-end speed and viscosity influence in sterilised particulate foods (Van Loey et al., 1997b). Spore distribution and leakage of *Bacillus stearothermophilus* spores was evaluated using TTIs in an alginate-starch mushroom puree (Ocio et al., 1997), while Knap and Durance, (1998) used the same spores to evaluate thermally processed particulate foods in an agitating steam-air retort. Pilot plant studies have been carried out for both extrinsic and intrinsic TTI systems, with Rodrigo et al. (1998) investigating the accuracy and performance

of TTIs in a water immersion static retort and Hsu et al., (2000) using triose phosphate isomerase for evaluating roast beef processing, respectively. Another application of the TTIs was based on the formation of 2,3-dihydro-3,5dihydroxy-6-methyl-4(H)-pyran-4-one, for prediction of the cooking effect in an ohmic heater (Eliot-GodeÂreaux et al., 2003).

Other types of TTIs that have been commercially used, include the CheckPoint® TTI (VITSAB International AB, Malmo, Sweden) and the (eO) ® TTI (CRYOLOG SA, France) which are based on pH changes, caused by enzymatic hydrolysis and microbial growth, respectively, expressed in colour changes. Other applications refer to TTIs used as active, smart labels for monitoring time-temperature responses on food packages (e.g. on meals served on flights). 3M Monitor Mark (3M Nederland B.V., Netherlands) is a diffusion-based indicator label that monitors temperature exposure of temperature-sensitive products, such as frozen or refrigerated foods during transportation and storage; the indicator monitors temperature exposure, not product quality and it signals when the product quality should be checked due to temperature exposure. Fresh-Check® (TEMPTIME Corporation, USA) is another time temperature indicator, a self-adhesive device that is specifically formulated to match the shelf life of the food products to which it is affixed. Its active centre circle darkens irreversibly, faster at higher temperatures and slower at lower temperatures, indicating when to USE or NOT USE the food product within the product date codes. As the active centre is exposed to temperature over time it gradually changes colour to show the freshness of the food product.

A.   B.

C.

Figure 2.10: A. Fresh Check, B. 3M Monitor Mark and C. Check Point TTIs.

The above examples indicate the potential of the TTI systems as an alternative monitoring technique to the traditional temperature sensors, for evaluating different heat treatments.

Strengths and weaknesses of TTIs: The ability of the TTIs to quantify, evaluate and finally optimise thermally treated food products, with no prior knowledge of their actual temperature profile, is the TTIs' major strength. Thus, when the physical-mathematical and/or in situ approaches are not convenient, TTIs are used as an alternative method for the design, evaluation and optimisation of a process. This is valid assuming that temperature is the only time dependent factor during the process.

The working principle of all types of TTIs is based on the calculation of the process value at the beginning and the end of the thermal process, as their status changes (e.g. enzymic activity). Thus, the online monitoring of the thermal process by the TTIs is not feasible, that being their major weakness. The TTIs lack predictive power for processing conditions different from the ones under which the experiments are run. Thus, the development of mathematical models would overcome that problem and predict process times and temperatures based on empirical formulae or theoretical heat transfer models. Based on experiments from current work, modelling the heat process would potentially show by how much the TTIs underestimate the process and what would the ideal process conditions for following the thermocouples' trend.

As described above, TTIs are classified according to their working principle, origin, type of response, positioning and application mode, meaning that their strengths and weaknesses will be relative and subject to the type of the TTIs used for different processes. The fact that the TTIs are typically located on the product's surface is another limitation of their use. The temperature difference between the product and surface can be significantly different, depending on product, package and process characteristics. Furthermore, different target microorganisms and quality attributes would require different TTIs, making their application even more challenging.

Recent work on TTIs: studies undertaken in recent years show the extended applicability of TTIs. Claeys et al., (2002) used intrinsic TTIs (heat markers) to assess a high pressure process. The results were not favourable for the use of TTIs at high pressure, but promising for the further research. A TTI system consisted of an enzyme trapped in poly o-phenylenediamine film, coated on the interior wall of a capsule (made of stainless steel) was

studied by Reyes-De-Corcuera et al., (2005). The TTI system was subjected under pasteurisation treatments and was analysed with an amperometer at the end of the treatment. First order kinetics was followed with a *z*- value of 6˚C to 7˚C. The authors concluded that the specific type of TTIs have the potential to validate pasteurisation processes, for targeting *E.Coli* and *Listeria monocytogenes*. A number of studies and work has been done for developing TTI systems that can assess sterilisation treatments; TTIs consisting α-amylase from *Bacillus subtilis* and *Bacillus licheniformis*, have been studied the most (Tucker et al., 2005b). Guiavarc'h et al., (2004a) showed that the *Bacillus licheniformis* based TTI with a *z*-value of 9.4°C was able to monitor a sterilisation process at 121.1°C for up to 30 min, under non isothermal conditions. The authors evaluated *Bacillus subtilis* and *Bacillus licheniformis* TTI systems in an industrial application, where ravioli was processed in a continuous rotary processing plant. TTIs were used together with thermocouples and were compared in terms of process values. *Bacillus licheniformis* and *Bacillus subtilis* α − amylases showed *z*- values of 13.9 and 16.4°C, respectively and were therefore (z-value> 10°C) used together as multi component TTIs. The authors reported that the impact of the thermal process was overestimated, causing food safety issues and that the use of the specific TTIs is complicated in terms of preparation and analysis. TTIs made from *Pyrococcus furiosus* α-amylase, was reported to be a better alternative for sterilisation processes (Tucker et al., 2005; Tucker et al., 2007).

Mehauden et al., (2007) investigated the efficiency of an industrially scaled agitated vessel under pasteurisation conditions, using *Bacillus licheniformis* a-amylase TTIs and thermocouples for viscous model foods. The results showed that the process values obtained by the TTIs were higher than the values of the thermocouples and therefore the TTIs shouldn't be used alone for assessing a thermal process, for safety reasons.

Future trends: When the temperature history of the thermal process can be recorded and controlled on-line, the physical-mathematical approach is preferred instead of the TTIs. Neither of the approaches though, can derive direct measurement and be used as a predictive tool. Thus, the development of predictive methods is essential. Ball, (1923); Ball and Olson, (1957), developed such methods based on empirical/theoretical models constructed for heat transfer predictions. Either temperature sensors are used, in the case of physical mathematical approach, or an enzyme for TTI systems, calibration is a very important task for obtaining accurate results. When predictive models are used accurate properties of the food product processed, its surrounding environment and the packaging need to be determined.

By the use of predictive modeling the batches of food products that undergo process deviation, would be able to be controlled and the process establishment would be more straightforward (Tucker et al., 2003). Stoforos et al., (1997), refer to the TTI systems as an essential complementary step in improving the physical-mathematical approach. Hence, a future, improved plan of processing and design would associate the TTIs with temperature sensors, each being included in a separate risk assessment procedure. The use of TTIs in evaluating safety and/or quality attributes during heat processes or new technologies means that they can also monitor critical control points, necessary in HACCP and be useful companies' demands on microbiological safety.

The reliability and accuracy of TTI systems, already investigated by a number of researchers, will potentially lead to their application to the pharmaceutical and chemical industries, where similar problems and risks to the food industry can be encountered. The development of the various types of TTIs in combination or not with temperature sensors will provide a better understanding of the new, non-thermal technologies that have been developed in the recent years, ensuring safe, high quality foods and will help the food manufacturers to control and

optimise their processes. Fryer and Robbins, (2005), report that the trajectories of the TTIs need to be known in order to be able to use them for assessing heat treatments; that can be achieved by the use of PEPT and PIV flow visualisation techniques.

In the current project, the hot-fill process is validated by a α-amylase based TTI system, which is further discussed in Chapter 5.

2.3   Optimisation of thermal processes

The design and evaluation of thermal processes can be described by two methods; the General and the Formula Method. The former originates from Bigelow et al., (1920) and is considered to be very accurate, as it is based on experimental time-temperature data, but it lacks predictive power. Formula methods have been used extensively since 1923 (Ball, 1923) and combine kinetic and heat transfer models for describing the time dependence of temperature within the product. Thus, for the optimisation of thermal processes, the heat transfer models need to be combined with the kinetic ones (Figure 2.11).

The problems usually identified in optimising thermal processes, include the selection of the design variables to be controlled, the constraints or assumptions made, the mathematical equation used to describe what needs to be optimised and consequently the selection of the proper mathematical model, and finally the choice of the optimisation technique. The accuracy of the parameters chosen to be modelled is of great importance for optimising a thermal process. Heat and mass transport phenomena, as well as the reaction kinetics of the organisms targeted have to be considered.
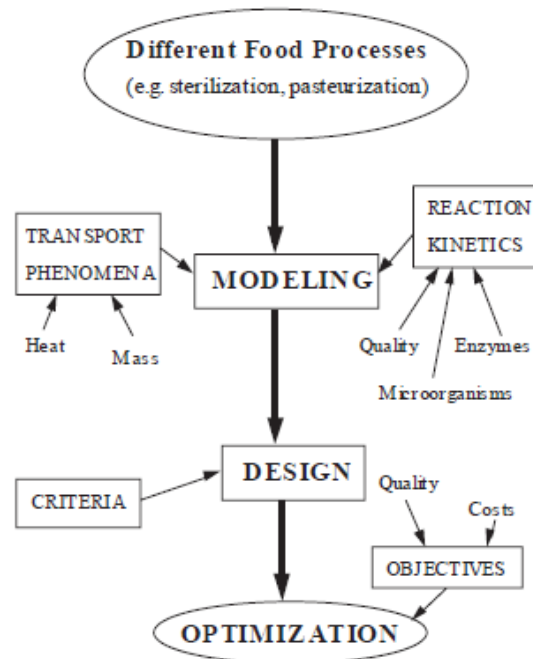
Figure 2.11: Steps for the optimisation of the thermal processing of foods
(Oliveira and Hendrickx, 1996).

The optimisation of thermal processes is possible because the degradation kinetics of quality attributes is significantly less temperature sensitive as compared to the kinetics of microbial or enzymic destruction (Teixeira et al., 1969; Holdsworth, 1985). Although possible, optimisation is still a challenging task, as the right combination of operating variables needs to be determined in order to ensure food safety and minimum quality losses simultaneously (Jung and Fryer, 1999). Most of the studies published in literature focus on finding the optimum conditions for the sterilisation of pre-packaged foods (Holdsworth, 1985; Silva et al., 1992b), in which constant retort temperature is assumed.

The sterilisation of pre-packaged foods can be optimised in terms of process lethality, using two approaches:

o   The target lethality (F_o) at the coldest spot or least-lethality point (LLP), defined as

follows:

$$F_o = \int\limits_0^t 10^{\frac{T-To}{z}} \cdot dt \qquad (2.1)$$

Where: T = temperature at any given time, T_o = reference temperature at 121.1^{o}C and z =

10°C, based on the destruction of *Clostridium botulinum* on low-acid foods.

o   The integrated lethality (F_s) that refers to the average volume of microbial survival

(Stumbo, 1973):

$$F_s = D_o \log\left[\frac{1}{V}\int\limits_0^V 10^{-(1/D_o) \cdot F_o}\, dV\right] \qquad (2.2)$$

Where: V = volume in m^3, D_o = D-value at T_o

The same equations can be used to describe quality attributes which are defined by the 'cook

value' (C-value) instead of the F-value for microbial inactivation, using the appropriate z-

value (Silva et al., 1994a). In the case of the target lethality approach, sensory parameters are

of interest, while the integrated lethality approach is more related to nutritional attributes

(Ohlsson, 1980a).

The target lethality determined at the slowest heating point (or LLP) of a cylindrical

container, is considered to be at its geometrical centre; however, this approach may not be

correct when including the cooling phase in the lethality calculation (Flambert and Deltour,

1972). According to Tucker and Clark, (1990) the cooling phase contributes significantly to

the final sterility of products in rectangular containers. When the cooling phase is included in the lethality calculations, the LLP is observed along the radius or vertical axis, depending on the ratio of half-height to radius and the integrated lethality (F_s) approach needs to be used; if measurements of single point are taken on the surface or the centre of the package, the process will result in under-processing or over-processing, respectively.

Teixeira et al., (1969b) reported that the position of LLP depends on the geometry of the container and the process conditions. Silva and Korczak (1994) also investigated the localisation of the LLP for a product heated through conduction, in a finite cylindrical container. They found that the kinetic parameters of the target organism, the processing temperature, and the target lethality, have no impact on the LLP, while the dimensions of the container and the product's heating rate (surface resistance to heat transfer was taken into account) influence it greatly. Flambert and Deltour, (1972) conducted similar experiments and concluded that the LLP is only affected by the container's dimensions, as surface resistance was assumed negligible.

Silva et al., (1994) and Banga et al., (1993) validated the optimal quality conditions of pre-packaged foods, experimentally; the degradation kinetics and the heat transfer mode into the food were quantified and a quality indicator used. Finally, the best combination of processing variables was chosen and compared to predicted values. The above study is based on the validation of model foods and consequently the parameters taken into consideration are heating by pure conduction, and regular geometries. Information on optimisation of realistic conditions such as irregular geometries, particulate foods or conventional heated foods, is limited. As far as mild heat treatments such as pasteurisation or hot-fill treatments are concerned, there is very limited information on the optimisation of processing conditions. Silva et al., (1997) developed a mathematical model, using a finite difference method, to

describe the hot-fill treatment of fruit purees. Sandoval et al., (1994) predicted the time-temperature profile of hot-filled tomato paste that was air-cooled, using analytical solutions. Glass jars of 0.2, 0.5 and 4 L were hot-filled at 94, 92 and 90°C, respectively, and evaluated for achieving inactivation of *Bacillus coagulans*. The same pasteurisation value of a process can be achieved by several combinations of filling temperature, package size, heating medium properties, etc., but only one pair of conditions can result in optimum quality retention of the fruit preserved. Efforts to generate minimal quality losses of thermally processed foods have been made for a long time, and several studies have been carried out on the development of quality optimisation models (Silva et al., 1994; Fryer et al., 2008). The fact that the degradation kinetics of quality attributes, such as nutrients, texture, colour, or flavour, are less heat-sensitive than the kinetics related to the destruction of microorganisms or inactivation of enzymes (Teixeira et al., 1969; Lund, 1977; Holdsworth, 1985), makes the optimisation possible. Few studies about quality optimisation of foods have been reported in literature. Van Loey et al., (1993) studied the impact of sterilisation on white beans in brine, while Banga et al., (1993) used canned tuna. Kiranoudis and Markatos (2000) used a multi-objective design and a static mathematical model to optimise food dryers. The authors aimed to minimize an economic measure and the colour deviation of the final product, simultaneously. Olmos et al., (2002) considered the constraint approach as a compromise between the process time and the quality of the final product. The approach aims at maximising the final product quality repeatedly subject to a total drying time constraint, which is varies in each optimisation.

2.3.1   Kinetic models

The kinetic models can predict the time-temperature dependence of safety or quality attributes, assuming that accurate reaction kinetics of microbial destruction, enzymic inactivation or quality degradation, depending on the organism targeted, is obtained.

Theory of Microbial Deactivation by Heating

The reactions involved in any thermal process are affected by the contribution of the heating, holding and cooling period to the process. The overall effect (lethality) is determined by evaluating the three different periods individually, as the contribution of each one is significantly different, depending on the process. For instance, when rapid heating and cooling are required, the most important period is the holding period, which will affect the final lethality the most. The temperature during the holding period is constant, which makes it relatively easy to determine the reaction rates of microbial destruction; it is the most convenient period to deal with. The destruction rates have to be observed as a function of temperature. Determining the temperatures at which the various organisms are inactivated, is of great importance in thermal processes. Different microorganisms exhibit different temperature sensitivity, with vegetative pathogens, yeasts and moulds being the most susceptible ones and the endospores being the most resistant ones (e.g. *Bacillus stearothermophilus, B. subtilis*, or *B. cereus*; and *B. stearothermophilus* and *Cl. Thermosaccharolyticum* present in milk and fruits, respectively); viruses lie in between (Johnson et al*.,* 1982; Maggi et al*.,* 1997; Gaze and Brown, 1998). Enzymes, either intracellular or extracellular, also have different temperature resistance and need to be inactivated while the nutritional components are retained (Holdsworth, 1992).

The surrounding medium of the microorganisms, particularly the pH and a_w, and the type and concentration of components the food product is consisted of (e.g. fats, carbohydrates), have substantial impact on the growth of microorganisms. The pH and a_w-value of the medium is mostly associated with the growth of vegetative microorganisms (Brown & Booth, 1991) and has a tremendous impact on microbial death. For example, the vegetative bacteria present in products like butter, are much more resistance than in aqueous environments, such as juices (Herson & Hulland, 1980). The rate of microbial death or quality degradation as a time and temperature function is required in order to evaluate thermal processes. The destruction of microorganisms is assumed to be a first-order reaction, which means that at constant temperature, the rate of the target organism is proportional to its concentration at the particular time. According to the first-order kinetics theory, at a defined time, the number of microorganisms will reduce to the one-tenth of the population at the start of that time interval, regardless of the actual population. In essence, at a constant lethal temperature and after each time interval the number of microorganisms will be reduced by 90% of the original number. Figure 2.12 shows the remaining number of the living cells after each time interval.
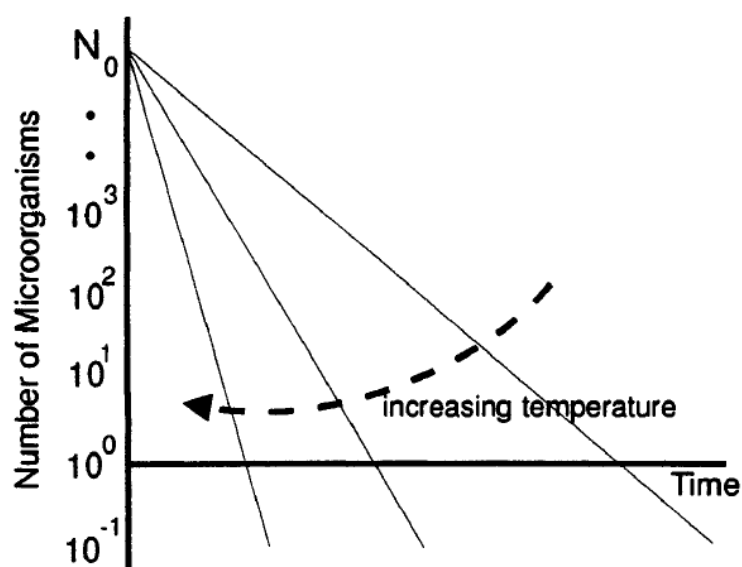
Figure 2.12: Microbial death curve at constant lethal temperature (Lewis, 2000).

The amount of time, in minutes, required for heating a microorganism at a constant lethal temperature, to cause a ten-fold reduction in the number initial living cells, is referred to as The Decimal Reduction Time (DRT). The lethal constant temperature at which the food is subjected to, is the temperature at which microorganisms begin to die. In other words, DRT is the time needed for the spores of a particular food to be reduced by 90%, at a specific temperature. Thus, after a 1D reduction, only 10% of the original spores will survive. It has been accepted that the decrease in the number of microorganisms is nearly logarithmic, as a function of time (Anderson, 1996). The remaining number of organisms can never be zero; there is a finite chance of survival. That chance needs to be reduced to an acceptable level, depending on the food product and the target process, ensuring that the product delivered to the consumer will be free of spoilage microorganisms. The units of the food product that are to be produced and the initial population of microorganisms within it need to be taken into consideration in order to establish the acceptable level of survival.

In low acid foods, pH>4.5, where the target organism is the heat-resistant spore-forming *Clostridium botulinum*, the commercially acceptable level of survival is 1 in 10^{12}, which means that in an initial spore population of 10^{12}, only 1 spore will survive the thermal process. The *Cl. botulinum* survival rate of 10^{12}, which is generally known as the 12D concept, has been alternatively defined in the United Kingdom, as the chance of survival of 1 spore of *Cl. botulinum* in 10^{12} containers rather than 10^{12} initial spores. In any case, the 12D concept is also referred to as a $F_o 3$ process, and was proposed by Stumbo (1965). A $F_o 3$ process means that at a constant reference temperature of $121.1^o C$, 3 minutes are needed for *Cl. botulinum* to be inactivated. The 12-log reduction of the *Cl. Botulinum* spores does not necessarily ensure commercial sterility of the product, as other non-pathogenic bacteria, that are more heat-

resistant, higher D-value, may be still active; in that case, a more severe heat treatment is required, which involves either higher processing temperatures or an additional heating step. Microorganisms that show higher thermal resistance than *Cl. botulinum* are the thermophilic spores, which can grow at ambient temperatures. Their acceptable level of survival lies between 10^5 and 10^7 (5D to 7D reduction), assuming that this still results in a 12D reduction for *Cl botulinum* (Madigan, 2006).

The microbial death by heat can be mathematically expressed by the following equation, in terms of concentration of microorganisms (C):

$$-\frac{dC}{dt} = k \cdot C \tag{2.3}$$

Where: t is the given time, and k is the constant reaction rate

At the different times, t_1 and t_2, at the same temperature the respective concentration of organisms C_1 and C_2 is given by integrating Equation 2.3:

$$\ln \frac{C_1}{C_2} = k(t_2 - t_1) \tag{2.4}$$

By substituting the concentration C of microorganisms with the actual number N present within a container, can be more useful. Thus, Equation 2.4 can be written as follows:

$$\ln \frac{N_1}{N_2} = k(t_2 - t_1) \tag{2.5}$$

Or

$$\log_{10}\left(\frac{N_2}{N_1}\right) = k'(t_2 - t_1) \qquad \text{Where } k' = \frac{k}{2.303} \qquad (2.6)$$

Where: N_1 is the initial number of spores and N_2 is the remaining number of spores after a t_2-t_1 time interval.

The 1/k' term can is replaced by the D-value term and Equation 2.6 is changed to:

$$\frac{N_t}{N_0} = 10^{-t/D} \qquad (2.7)$$

Where: N_0 is the number of spores at t=0, and N_t is the number of spores at time t.

If the $\log_{10} (N_2/N_1)$ were plotted against the heating time, the D-value can be determined, as illustrated in Figure 2.13.
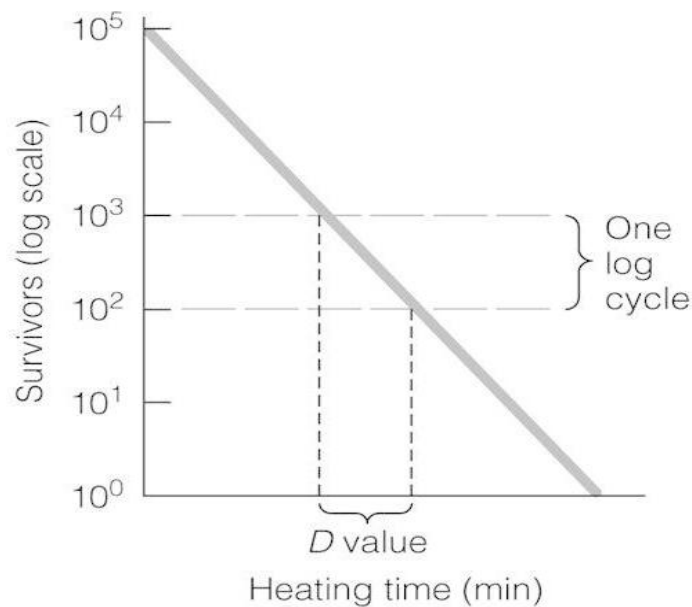
Figure 2.13: Survivor curve and decimal reduction time determination.

When the temperature of the process is increased, the rate at which microorganisms or enzymes are inactivated increases as well and according to Equation 2.5 the decimal reduction time will decrease. The effect of temperature on decimal reduction time has been described by the z-value model and the Arrhenius equation model. The latter has been mostly used to describe the temperature effect on chemical reactions, and data extrapolation is usually required (Jonsson, 1977; Pflug, 1996; Fujikawa, 1998).

In the current project, the temperature effect was described by the z-value model, according to which, when temperature is raised by z degrees C, the decimal reduction time is changed by a factor of 10. Thus, the z-value is the temperature required for achieving a 1-log reduction in the D-value and it is related to the resistance of the microorganism to different temperatures. Bigelow, (1920) showed that there is a linear relationship between the temperature and the logarithm of the D-value; when plotted, the reciprocal of the slope, gives the z-value.

The logarithm of D-values against temperature is illustrated in Figure 2.14 and the curve obtained, is called a thermal death time (TDT) curve; important for calculations required for thermal destruction of microorganisms. The linear slope of the TDT curve shows the temperature sensitivity of the target microorganism. The time–temperature combinations obtained from the points along the TDT line, give equal lethal effect for a given microorganism. Consequently, the z-model, using the D- and z-value constants, can characterise adequately the temperature resistance of safety and quality attributes.
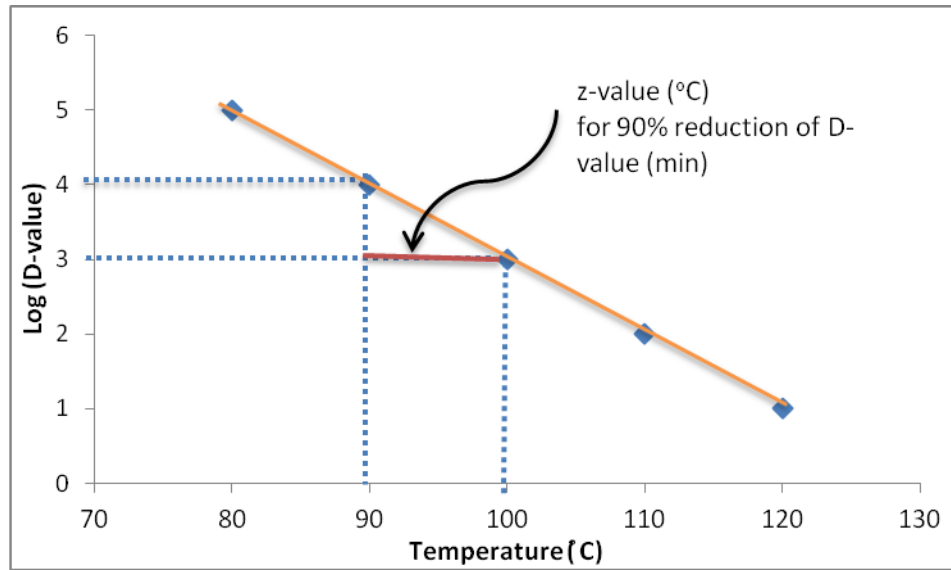
Figure 2.14: Thermal death curve.

The evaluation of thermal processes at a constant lethal temperature is relatively easy; however, the temperature throughout a process can rarely be constant.

The effect of a varying temperature on a thermal process can be described by a term called lethality (L), which is the rate of microbial destruction between a temperature (T) and a reference temperature (T_ref) and is expressed as follows:

$$L = 10^{\frac{T - T_{ref}}{z}} \tag{2.8}$$

The time-temperature combinations used for adequately evaluating a thermal treatment required for a particular food, depends on several criteria.

Thermal death time (TDT), or *F-value* (or process value) is the most commonly used criterion, in the case of commercial sterilisation, introduced by Ball, (1923). Assuming instantaneous heating and cooling, the F-value can be defined as the holding time required

achieving thermal destruction of microorganisms, at a constant reference temperature and is

described by the following equation:

$$F = \int_0^t L \cdot dt = \int_0^t 10^{\frac{T-T_{ref}}{z}} \cdot dt \qquad (2.9)$$

The process value (F and P-value for sterilization and pasteurization, respectively) can be

determined either by being based on the time-temperature history knowledge, or on

measurements of the initial (N_o) and final (N_f) loads of the organism present. The process

value is expressed in the following equation:

$$F \ or \ P = D_T \cdot \log\left(\frac{N_0}{N_f}\right) = \int_0^t 10^{\frac{T_t-T_{ref}}{z}} \cdot dt \qquad (2.10)$$

Where: T (t) is the product temperature at the slowest heating point (°C), T_{ref} is the reference

temperature (°C), t is the process time (min) and z is the value of the temperature required for

a 1D reduction and should be the one of the target organism.

When the target organism refers to enzymes, Equation 2.8 is changed to:

$$F \ or \ P = D_T \cdot \log\left(\frac{A_0}{A_f}\right) = \int_0^t 10^{\frac{T_t-T_{ref}}{z}} \cdot dt \qquad (2.11)$$

Where: A_o and A_f, are the initial and final enzyme activity, respectively.

Besides from the criteria used to characterise the thermal destruction of microorganisms, there are other that are based on biochemical degradation or cooking of a food product. Whatever the target and the criteria used, the reference temperature used should be close to the process temperature, for avoiding data errors (e.g. extrapolation at higher temperatures).

The thermal process criterion should be referred to the organisms most likely to survive the process. For instance, when *Cl. botulinum* is the organism of interest, the F_o (at a T_{ref} of 121.1^{o}C and z-value of 10°C) value is the appropriate one, but in the case of other surviving organisms the process value F should be based on their z-value.

2.3.2   *Mathematical Models*

As mentioned in the previous sections, thermal processing is widely used in the food industry for ensuring safety and delivering quality final products. Foods are complex matrices with varying rheological and thermo-physical properties. They are time and process dependent and therefore it is difficult to make accurate prediction of the process they are involved in (Fryer et al., 2005). Thermal processing of many solid foods is based upon heat and moisture transfer between the solid body and the heating medium. A number of heat transfer mathematical models, based on quantification of heat and mass transfer phenomena have been developed for predicting temperature variation as a function of operating variables, at any location and time (Balsa-Canto et al., 2002a). Most heat transfer models are developed for describing the sterilisation treatment. The requirements imposed to sterilisation processes, which depend on the objectives that need to be satisfied, can be determined analytically or numerically. Both approaches have been used in a number of studies dealing with conduction and convective heated foods, for predicting the time-temperature, velocity, pressure profiles, and fluid flow

behaviour throughout the process. Models referring to conduction heated foods, such as tuna, thick syrups and purees are based on the assumption that the product is heated by pure conduction, it is homogeneous, there is negligible surface resistance to heat transfer, the heating medium temperature is constant and the geometry of the contained is considered to be cylindrical (Perrota, 2011). Complexities during conduction heated foods occur due to the polymorphic nature of food components (Fryer, 2005).

Most commercially processed food products are heated by a combination of conduction and convection; the widely used heat process of canning is one such example. Heat within the can is transferred by a combination of conduction and natural convection. In the case of sterilised liquid foods, both conduction and natural convection have significant effect in heat transfer. Datta et al., (1988); Varma and Kannan, (2006) studied natural convection in canned liquid foods and used numerical solutions to predict transient temperature and velocity profiles. They reached the conclusion that the slowest heating point is observed at approximately the one tenth of the can's bottom. Kumar and Bhattacharya, (1990) studied the sterilisation of viscous, canned liquid foods heated from the side walls, keeping the bottom and top surfaces insulated. Keeping the thermal properties of the liquid food constant and assuming temperature dependent viscosity, the authors found that the slowest heating point moved towards the can's bottom due to natural convection occurrence.

Processing liquid foods is complex due to fluid motion and consequently their simulation is also complicated; equations of continuity, energy and momentum need to be solved simultaneously and more complex boundary conditions need to be considered (Ghani et al., 1999). Owing to the complexity of describing the sterilisation of liquid foods mathematically, equations that include dimensionless parameters, such as Ra, Nu, Re, and Pr number, have been developed (Sablani, 2006).

Regardless of the heat transfer mechanism occurring during thermal processing of foods, either analytical and/or numerical methods can be used.

2.3.2.1 Analytical methods

They are exact solutions of differential equations that are important for the design and optimisation of a process that includes solid food products with simple geometries, such as infinite slab, cylinder, or sphere (Ramaswamy et al., 1984). Laplace transform and separation of variables are included in the solutions, with the latter being used in heat conduction problems with homogeneous boundary and initial conditions (Özisik, 1993). The validation of numerical solutions with uniform boundary conditions and constant thermal properties is a typical application of analytical solutions (Cai et al., 2003).

2.3.2.2 Numerical methods

They are used when analytical solutions are not available; they have the advantage of being flexible, dealing with irregular geometries, complex boundary conditions and temperature dependent thermal properties, but they are not exact solutions. Numerical methods are useful for estimating the thermal behaviour of foods under complex but realistic conditions such as variation in initial temperature, non-linear and non-isotropic thermal properties, irregular-shaped bodies and time dependent boundary conditions (Puri & Anantheswaran, 1993). Numerical modelling technology is a powerful and efficient tool for simulating thermal processes in the food industry (Ahmad & Okos, 2001).

For developing a mathematical model, the problem to be solved needs to be described, to be formulated mathematically and discretised choosing the appropriate numerical solution. The solution is finally visualised and the problem is ideally approximated (Figure 2.15).
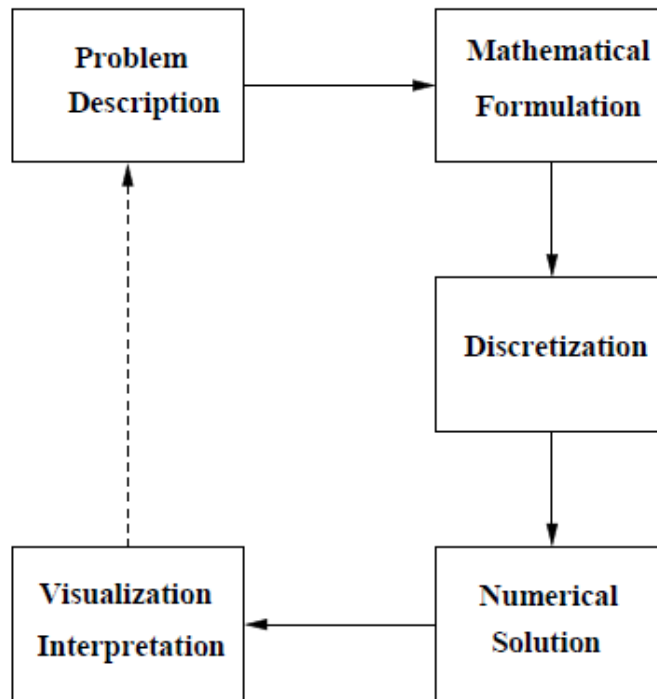
Figure 2.15: Solving a mathematical model (Martin Burger, 2010).

Finite difference, finite element and finite volume methods have widely been used for numerically solving models associated with food processing (Fryer et al., 1995; Erdogdu et al., 1998a; Sun et al., 2000a).

Each method is summarised in the following paragraphs.

Finite Difference method (FD)

The FD method is commonly used for simple geometries such as slab, cylinder and sphere; it can be applied to two or three-dimensional problems and involves simple boundary conditions with constant thermal diffusivity. The method has been widely used to solve heat and mass transfer models of thermal processes such as cooking and frying (Erdogdu et al., 1998a, Pan et al., 2000), drying (Thorvaldsson & Janestad, 1999), and cooling (Chuntranuluck et al.,1998a, b, c). FD method has been used to model the heating process of liquid-solid

systems in processes such as blanching, sous-vide and sterilisation (Farkas et al., 1996b; Wang & Chen, 1999; Davey & Pham, 1997) The heat transferred through a solid food product is described by Fourier's equation of heat conduction, whilst the interaction between the liquid and the solid is considered in the boundary conditions. Fasina & Fleming, (2001) described the heat transfer through a cucumber, during the blanching process using an axi-symmetric, two dimensional FD heat conduction model, assuming a cylinder shape. Ghazala et al., (1995) used FD method to predict the time-temperature history of sous-vide processed fish and meat products of rectangular shape. The convective heat transfer coefficient of the surface is very large and therefore, the authors assumed that its effect on the temperature profiles of the food was negligible. Thus, the heat transfer coefficient was arbitrarily set at a high value during the simulation of a three-dimensional FD heat conduction model. Solid particle foods sterilised in a container with a brine solution is another example of liquid-solid heat process modelled with the FD method. Akterian (1995, 1997) used a one-dimensional model to determine the temperature distribution of canned mushrooms in brine.

The FD method has proved not to be satisfactory for temperature predictions on foods with irregular shapes due to geometric simplification (Coulter et al., 1995; Russell, & James, 1996; Ansari et al., 1999).

<u>Finite Element method (FE)</u>

The FE method has been reported to perform better for irregular geometries and complex boundary conditions than the FD method (Van Der Sluis et al., 1994; Carroll et al., 1996). The FE method concerns the discretisation of a domain into a number of small elements; the developed element equations are then assembled for the whole domain, and solved (Zhao et al., 1998; Wang & Sun, 2003). The discretisation of the differential equations is based on the

interpolation of polynomials in order to describe the variation of a field variable within an element (Rao, 1989). The FE method has been successfully used to solve heat and mass transfer models for cooking (Evans & Warboys, 1997; Wang et al., 1999), drying (Ahmad et al., 2001; Jia et al., 2000a, 2001) and cooling (Van Der Sluis & Rouwen, 1994; Carroll et al., 1996; Wang & Sun, 2002a, b).

FE method has been used to simulate microwave heating of a solid food of cylindrical and rectangular shape (Lin et al., 1995). The authors expressed the microwave power density absorbed at any location within the food product, as a function of the dielectric properties and food geometry; the surface heat losses by convection and evaporation were in the boundary conditions. Zhou et al., (1995), reported that in the case of high amount of moisture loss, a coupled heat and mass transfer model needs to be used, implicating at the same time Fick's law for the moisture transfer through the solid.

FE approach was also used for modelling the process of microwave drying for heat-sensitive foods, such as biscuits (Lian et al., 1997; Ahmad et al., 2001). The prediction of temperature and moisture distribution of regular shaped chicken patties, in an air-convection heating oven was shown to be better predicted by the FE for a coupled heat and mass transfer model, as compared to heat transfer model used alone (Chen et al., 1999). A coupled heat and mass transfer FE model with inner heat generation was also used for the modelling of cooked meat joints in commercial vacuum cooling (Wang & Sun, 2002a, 2003). FE scheme has also been used for modelling convection heated foods. Thermal processes such as sterilisation of canned liquid and spray drying of liquid or powder foods, like in the case of starch dispersion have been predicted using coupled fluid flow and heat transfer models (Yang & Rao, 1998; Straatsma et al., 1999; Verboven et al., 2000a, b). Tewkesbury et al., (2000) used a FE model to predict the cooling of chocolate; the conduction occurring during the cooling phase of

chocolate and the change in specific heat capacity of the product, were modelled as a function of temperature and cooling rate.

A commercial finite element program (FIDAP) has been used by a few authors for simulating processes with complex liquid food systems. The program was used by Kumar and Bhattacharya (1991a) for calculating the lethality of a shear thinning, temperature dependent viscosity fluid along the centreline, whilst Jung and Fryer (1999) used it for estimating the lethality and quality of both a Newtonian and shear thinning fluid in terms of bulk averages. Later, Liao et al., (2000) used the same program to determine the lethality at the slowest heating point of a processed starch suspension.

Despite its advantages, the FE method is complex and computationally expensive, as compared to the FD method.

Finite Volume/Computational Fluid Dynamics (CFD)

CFD is a simulation tool for solving fluid flow and heat transfer problems. The energy conservation, continuity and momentum equation are solved simultaneously to predict velocity, temperature, pressure profiles, and other fluid flow parameters in a system (Sun, 2002). CFD has been mainly applied to automotive and nuclear industries but has been recently used into the food industry. Applications of CFD in the food industry include air flow analyses in ovens and chillers (Foster et al., 2002), fluid flow of particle foods in processing systems (Mirade & Daudin, 2000), convection flow patterns in containers during sterilisation processes (Ghani et al., 1999a, b), and modelling of vacuum cooling processes (Sun & Hu, 2003).

The heat treatment of solid foods in industrial convection ovens, such as hot-air electrical forced convection ovens, can be modelled as a coupled fluid flow and heat transfer problem;

CFD can be used to efficiently analyse the performance of such ovens. The method has also been used to predict transient temperature profiles and flow patterns during the sterilisation of canned liquid foods (Ghani et al., 1999a). Jung & Fryer, (1999) used CFD to describe the laminar flow of food fluids in a circular pipe of uniform wall temperature, for optimising food quality during continuous sterilisation processes such as HTST. CFD has been widely used for simulating gas flow and estimating particle trajectories of droplets during spray drying, as well as for predicting velocity and pressure profiles of heated air in batch type air-dryers for drying fruits and vegetables (Mathioulakis, 1998; Straatsma et al., 1999). Abdhul Ghani et al., (1999) estimated the axial velocity of a viscous canned fluid and modelled the bacterial inactivation. More recently, Bakalis et al., (2003) used positron emission particle tracking (PEPT) examined the three-dimensional flow pattern of liquids in rotating cans allowing the mixing patterns to be quantified.

The application of FD, FE and CFD method in the food industry is summarised in Table 2.6.

Table 2.6: Applications of the various numerical models in the food industry

Finite Difference (FD)		
Process	Food/model properties	Authors
Drying	Potato: 1D, f (T), mass model	Rovedo et al., (1995)
	Aloe Vera: 3D, f (T), mass model	Simal et al., (2000)
	Vegetables: 1D, f (T), mass + heat model	Wang and Chen (1999)
	Shrimp: 2D-axi, f (T), heat model	Erdogdu et al., (1998a, b)
	Bread: 1D, f (T), mass + heat model.	Thorvaldsson and Janestad (1999)
Heating	Hamburger patty: 1D-axi, f (T), mass + heat model	Pan et al., (2000)
	Mushroom: 1D, T=ct, heat model	Akterian (1995, 1997)

Heating	<u>Cucumber:</u> 2D-axi, f (T), heat model	Fasina and Flemiung (2001)
	<u>Carcases:</u> 1D, f (T), heat model	Coulter et al., (1995);
		Davey and Pham (1997)
	<u>Sauce:</u> 1D, T=ct, heat model	Evans et al., (1996)
Cooling	<u>Frozen foods:</u> 3D, f (T), heat model	De Elvira et al., (1996)
	<u>Potato:</u> 1D-axi, T=ct, heat model	Chavez et al., (1996)
Finite Element (FE)		
Drying	<u>Grain:</u> 2D-axi, f (T), mass + heat model	Jia et al., (2000a,b,c,d, 2001))
	<u>Biscuits:</u> 2D-axi, f (T), mass + heat model	Ahmad et al., (2001)
	<u>Chicken:</u> 2D-axi, f (T), heat model	Chen et al., (1999)
	<u>Starch:</u> 2D, f (T), mass + heat model	Wu and Irudayaray (1996);
		Yang and Rao (1998).
Heating	<u>Solid foods:</u> 1D-axi, f (T), mass + heat model	Lin et al., (1995);
		Vilayannur et al., (1998a,b);
	<u>Broccoli:</u> 1D-axi, f (T), heat model	Varga et al., (2000)
	<u>Carcases:</u> 2D, f (T), heat model	Martens et al., (1996)
		Mallikarjunan and Mittal (1994, 1995)
	<u>Apple and Pear:</u> 1D, f (T), heat model	Carroll et al., (1996)
Cooling	<u>Various:</u> 2D, heat model	Comini et al., (1995)
	<u>Cooked meats:</u> 2D-3D, f (T), mass + heat model	Wang and Sun (2002a,b,c,d,e)
	<u>Bakery products:</u> 3D, f (T), mass + heat model	
		Van Der Sluis and Rouwen (1994, 1999).
	<u>Chocolate:</u> 2D-axi, f (T), heat model	Tewkesbury et al., (2000)

Computational Fluid Dynamics (CFD)		
Drying	Particle food: f (T), mass + heat model	Straatsma et al., (1999)
	Fruits & Vegetables: f (T), mass model	Mathioulakis et al., (1998)
	Various	Verboven et al., (2000a,b)
Heating	Canned liquid food: heat model	Ghani et al., (1999a,b, 2001)
	Vegetables: f (T), mass model	Tassou and Xiang (1998)
	Various: f (T), mass+heat model	Jung and Fryer (1999)
Cooling	Various: 3D, f (T), mass+heat model	Cortella et al., (2001)
	Particulated foods: 2D-3D, mass+heat model	Xu and Burfoot (1999a,b)
	Cooked meats: mass model	Hu and Sun (2000, 2001a,b, 2002)

Continuous progress has been made in recent years for improving the accuracy of the developed mathematical models, but more research still needs to be carried out on:

- More accurate estimations of surface heat and mass transfer coefficients (De Elvira et al., 1996; Nicolai et al., 2000);

- Food properties and their interactions;

- Sensitivity analysis for judging assumptions such as temperature and thermal properties of foods (Nicolai et al., 1999; Oliveira, 2000; Verboven et al., 2001).

2.4 Conclusions

In recent years, the increased variety of food products and the consumers' awareness of food safety and quality have led food manufacturers to be faced with the challenge of producing safe and high quality food products. A number of food preservation techniques, such as

thermal and low temperature processing, dehydration, irradiation or a combination of them is applied in order to satisfy the consumers' demands. The common working principle of all processes is the inactivation of microbial growth whilst ideally minimising the physical damage and the possibility for undesirable chemical reactions (Dewanto, 2002).

Thermal processing is the most widely used and well established preservation method in food industry. The application of heat serves a number of objectives, with safety being the primary one; quality is another important reason for heating food products. The degree, at which both safety and quality are affected during heating, is subject to the intensity of the process applied, with sterilisation being the most severe one.

For ensuring safety of the final product, inactivation of the spoilage organisms on the food product alone is not sufficient; package decontamination is equally important (Tucker et al., 2002). The decontamination method applied on the container is dependent on the food target; it can be thermal (application of steam), chemical (e.g. hydrogen peroxide, ethylene oxide), radiation (e.g. UV, IR) or a combination of them.

In order to establish a safe thermal process, accurate validation needs to be performed. Temperature probes and loggers, and microbiological methods are the most widely applied monitoring techniques. The continuously increasing variety of food products has led to the development of novel, more sophisticated validation techniques. Retort simulators, thermal imaging technology and time temperature integrators are such examples.

The ultimate goal of food processing is achieving safety and the highest quality possible at the same time for the final product. For optimising thermal processes the reaction kinetics of the safety and/or quality attributes need to be known in combination with information on the mass and heat transport phenomena occurring during the process applied.

The kinetic models are used to predict the time-temperature dependence of safety or quality attributes and are expressed in terms of lethality; the mathematical models used, intend to predict the dependence of operating variables as a function of temperature distribution by quantifying heat and mass transfer behaviour during the process (Balsa-Canto et al., 2002a).

The progress made during the last decades in optimising thermal processes has been exponential, since the models used have predictive power and can be combined with analytical methods. However, more research needs to be carried out in obtaining deeper understanding of food properties, more accurate estimates of heat and mass transfer coefficients, more sensitive and practical validation techniques and further studying of novel processes.

The current work covers the inversion step as a thermal treatment of the headspace and lid for hot-filled products. The effectiveness of the step in terms of heat transfer enhancement during the cooling phase of the process was simulated and combined with analytical solutions. Kinetic models were used and compared with the simulated models, for validating the process.

References

Adams M. R., Moss M.O., (2007). *Food Microbiology. New Age International.*

Agency for Toxic Substances and Disease Registry (ATSDR), (1990). Toxicological Profile for Ethylene Oxide. U.S. Public Health Service, U.S. Department of Health and Human Services, Atlanta, GA.

Ahmad S.S., Morgan M.T., Okos M.R., (2001). Effects of microwave on the drying, checking and mechanical strength of baked biscuits. *Journal of Food Engineering*, 50, 63–75.

Akterian S.G., (1995). Numerical simulation of unsteady heat transfer in canned mushrooms in brine during sterilisation processes. *Journal of Food Engineering*, 25, 45–53.

Akterian S. G., (1997). Control strategy using functions of sensitivity for thermal processing of sausages. *Journal of Food Engineering*, 31, 449–455.

Alzamora S.M., Tapia M.S., Welti-Chanes J., (2003). The control of water activity. Food Preservation Techniques, Woodhead Publishing, Cambridge, 126-153.

Amann, R.I., Ludwig, W., Schleifer, K.-H., (1995). Phylogenetic identification and in situ detection of individual microbial cells without cultivation. *Microbiol. Rev.*, 59, 143 – 169.

Anderson W.A., McClure P.J., Baird Parker A.C., Cole, M.B., (1996). The application of a log-logistic model to describe the thermal inactivation of *Cl. botulinum 213B* at temperatures below 121.1oC. *Journal of Applied Bacteriology,* 80, 283-290.

Anonymous, (1995). Determination of moisture content in Finnish honey using an infrareddryer. *Food Market Technol*ogy, 9(1), 40–41.

Anonymous, (2007a). Almonds grown in California; outgoing quality control requirements. Federal Register. Agricultural Marketing Service, USDA, 72 (61), 15021–15036.

Ansari F.A, (1999). Finite difference solution of heat and mass transfer problems related to precooling of food. *Energy Conversion & Management*, 40, 795–802.

Ansari M.I.A., Datta A.K., (2003). An overview of sterilisation methods for packaging materials used in aseptic packaging systems. *Trans IChemE*, 81, 57-65.

Ávila I.M.L.B., Silva C.L.M., (1995). Optimum sterilisation conditions for foods inside packs with two divisions. Poster presented at: 9th World Congress of Food Science and Technology, Budapeste (Hungary).

Bachmann R., (1975). Sterilisation by intense ultraviolet radiation. *The Brown Boveri Rev.* 62, 206-209.

Bajgai T. R., Hashinaga E., (2001). High electric field drying of Japanese radish. Drying Technol. 19, 2291-2302.

Ball C.O. (1923). Thermal Process Time for Canned Food, Bulletin of the National Research Council, Washington, DC. Vol. 7, Part 1, Number 37.

Ball C.O. and Olsen, F.C.W. (1957). Sterilization in Food Technology. McGraw-Hill Book Co., New York.

Balsa-Canto E., Banga, J.R, Alonso A.A., (2002). A novel, efficient and reliable method for thermal process design and optimization. Part II: Applications   *Journal of Food Engineering* 52 (3), 235-247.

Bakalis S., Cox P.W., Wang-Nolan W., Parker D.J., Fryer P.J. (2003). Use of Positron Emission Particle Tracking (PEPT) technique for velocity measurements in model food fluids, *Journal of Food Science,* 68, 2684–2692.

Banga J.R., Balsa-Canto E., Moles C.G., Alonso A.A., (2003). Improving food processing using modern optimization methods. *Trends in Food Science & Technology,* 14(4), 131–144.

Barbosa-Canovas G.V., Qin, B.L., Pothakamury, U.R., Swanson B.G., (1996). Non-thermal pasteurization of liquid foods using high-intensity pulsed electric fields *Crit. Rev. Food Science and Nutrition*, 36, 603–627

Barrett D.M, (2006). Maximizing the nutritional value of fruits and vegetables. Review of literature on nutritional value of produce compares fresh, frozen, and canned products and indicates areas for further research.
http://www.fruitandvegetable.ucdavis.edu/files/197179.pdf

Barsotti L., Merle P. P., Cheftel J., (1999). Food processing by pulsed electric fields: Physical aspects. *Food Review Int*ernational, 15(2), 163-180.

Bauser M., Sauer G., Siegert K., (2006). Extrusion, ASM International, p. 270.

Bazhal M.I., (2001). Etude du mecanisme d'electropermeabilisation des tissus vegetux. Application ii l'extraction du jus des pommes, These de Doctorat, Universite de Technologie de Compiegne, France.

Bee G.R., Park D.K., (1978). Heat-penetration measurement for thermal-process design. *Food Technology,* 32(6): 56-58.

Berry B.W., (2000). Use of infrared thermography to assess temperature variability in beef patties cooked from the frozen and thawed states. *Foodservice Research International,* 12(4), 255–262.

Bigelow W.D., Bohart G.S., Richardson A.C., Ball C.O., (1920). Heat penetration in processing canned foods. Bull. Nr 16-L Res. Washington, D.C.: Lab. Natl. Canners Assn.

Bongiovanni R., Lowenberg-Deboer J., (2004). Precision agriculture and sustainability. *Precision Agriculture,* 4(4), 359–387.

Boonsupthip W., Heldman D.R., (2007). Prediction of frozen food properties during freezing using product composition. *Journal of Food Science,* 72 (5), 254-263.

Bown G., (2003). Developments in conventional heat treatment. Food preservation Techniques, Woodhead Publishing, Cambridge, 154-178.

Brown A.C., (2007). Understanding Food: Principles and Preparation *(3 ed.). Cengage Learning*

Brown K.L., Ayres, C.A., Gaze, J.E., Newman, M.E., (1984). Thermal destruction of bacterial spores immobilised in food/alginate particles. *Food Microbiology*, 1, 187-198.

Brown M.H., Booth, I.R., (1991). Acidulants and low pH. In Food Preservatives, pp. 2243. Edited by N. J. Russell & G. W. Gould. Glasgow & London: Blackie.

Bruhn C.M., (1995). Strategies for communicating the facts on food irradiation to consumers. *J. Food Protect*., 58, 213–216.

Burfoot D., Mulvey E., Foy E., Turner R., Bayliss D., McFarland S., Jewell K. (2014). Food surface decontamination to improve food safety and extend shelf life. Campden BRI R&D report no. 358.

Codex Alimentarius Commission (CAC), (1994). Codex General Standard for Irradiated Foods and of untreated and radiation-damaged *Listeria* as affected by Recommended International Codex of Practice for the Opera- environmental factors. *Acta Microbiology and Immunology Hung*. 42, Radiation Facilities used for the Treatment of Food. 19–28. CAC/Vol. XV.-Ed.1. FAO, Rome.

Cai R., Zhang N., (2003). Explicit analytical solutions of 2-D laminar natural convection. *International Journal of Heat Mass Transfer,* 26, 931–934.

Campbell P., Braam J., (1999). In vitro activities of four xyloglucan endotransglycosylases from *Arabidopsis*. *Plant Journal,* 18, 371–382.

Carroll N., Mohtar R., Segerlind L.J., (1996). Predicting the cooling time for irregular shaped food products. *Journal of Food Process Engineering*, 19, 385–401.

Council of Agricultural Science and Technology (CAST), (1995). Food Borne Illnesses: Risks and Consequences. Report No. 122.

Castro I., Macedo B., Teixeira J. A., Vicente A. A. (2004). The effect of electric field on important food-processing enzymes: Comparison of inactivation kinetics under conventional and ohmic heating. *Journal of Food Science, 69*, 696–701.

Campden & Chorleywood Food Research Association (CCFRA), (1977). Guidelines to the establishment of scheduled heat processes for low-acid foods, CCFRA Technical Manual No.3.

Campden & Chorleywood Food Research Association (CCFRA), (2006b). Pasteurisation: A food industry practical guide (second edition). Guideline No.51.

Campden & Chorleywood Food Research Association (CCFRA), (2007). Guidelines for the processing of aseptic packaging Guideline 53.

Campden & Chorleywood Food Research Association (CCFRA), (2011). Energy efficiency by thermal imaging. Brewing analysis leaflet Gary Freeman.

Campden & Chorleywood Food Research Association (CCFRA), (2012). Surface decontamination: A review. Confidential internal publication

Campden & Chorleywood Food Research Association (CCFRA), (2014). Microbiological safety and quality of chilled pasteurised food products: A review. G Betts.

Cho H.Y., Yousef A.E., Sastry S.K., (1996). Growth kinetics of Lactobacillus acidophilus under ohmic heating. *Journal of Biotechnology and Bioengineering,* 5, 49(3), 334-340.

Chuntranuluck S., Wells C.M., Cleland A.C., (1998a). Prediction of chilling times of foods in situations where evaporative cooling is significant: Method development. *Journal of Food Engineering*, 37, 111–125.

CODEX, (1997). Hazard Analysis and Critical Control Point (HACCP) System and Guidelines for Its Application Annex to CAC/RCP 1-1969, Rev. 3.

Chapman S., (2003). New machines use tumbling process to decontaminate food. Food Chem. News, 10:20.

Chen H.Q., Marks B.P., Murphy R.Y., (1999). Modelling coupled heat and mass transfer for convection cooking of chicken patties. *Journal of Food Engineering*, 42, 139–146.

Cho H.Y., Yousef A.E., Sastry S.K., (1996). Growth kinetics of Lactobacillus acidophilus under ohmic heating. *Journal of Biotechnology and Bioengineering,* 5, 49(3), 334-340.

Claeys W.L., Van Loey A.M., Hendrickx, M.E., (2002). Intrinsic time temperature integrators for heat treatment of milk. *Trends Food Science Tech*nology, 13, 293-311.

Coulter S., Pham Q.T., McNeil I., McPhail, N.G., (1995). Geometry, cooling rates and weight losses during pig chilling. *International Journal of Refrigeration,* 18, 456–464.

Datta A.K., Teixeira A.A., (1988). Numerically predicted transient temperature and velocity profiles during natural convection heating of canned liquid foods. *Journal of Food Science,* 53 (1), 191-195.

Davey L.M., Pham Q.T., (1997). Predicting the dynamic product heat load and weight loss during beef chilling using a multi-region finite difference approach. *International Journal of Refrigeration*, 20, 470–482.

De Cordt S., Hendrickx M., Maesmans G., Tobback P., (1992). Immobilised -amylase from *Bacillus licheniformis*: a potential enzymic time-temperature integrator for thermal processing. *International Journal of Food Science and Technology*, 27, 661-673.

De Elvira C., Sanz, P.D., Carrasco, J.A., (1996). Characterising the detachment of thermal and geometric centres in a parallelepipedic frozen food subjected to a fluctuation in storage temperature. *Journal of Food Engineering*, 29, 257–268.

Dostie M., Seguin J.N., Maure D, Tonthat Q.A., Chatingy R., (1989). Preliminary measurements on the drying of thick porous materials by combinations of intermittent infrared and continuous convection heating. New York, Hemisphere Press.

Dewanto V., Wu X., Kafui K. Adom, Liu R. H., (2002). Thermal Processing Enhances the Nutritional Value of Tomatoes by Increasing Total Antioxidant Activity. *Journal of Agriculture and Food Chemi*stry, 50, 3010−3014

Dunn J., (2015). Pulsed Light and Pulsed Electric Field for Foods and Eggs, Oxford Journals. *Science & Mathematics Poultry Science*, 75(9), 1133-1136.

Eliot-Godereaux S., Goullieux A., Queneudec T'kint M., (2003). Elaboration and kinetic modelling of the formation of a biochemical marker to quantify HTST processing. *Food Research International*, 36, 131-139.

Erdogdu F., Balaban M. O., Chau, K. V., (1998a). Modelling of heat conduction in elliptical cross section: I. Development and testing of the model. *Journal of Food Engineering,* 38, 223–239.

Estiaghi M.N., Knorr D., (1999). Method for treating sugar beet. International Patent Nr WO 99/6434.

Evans J., Russell S., James S., (1996). Chilling of recipe dish meals to meet cook-chill guidelines. *International Journal of Refrigeration*, 19, 79–86.

Evans R., Warboys M., (1997). Coupled heat and moisture during microwave vacuum drying. *Journal of Microwave Power and Electromagnetic Energy*, 32, 34–44.

FAO., (1984a). Food aid in figures. FAO, Rome, p.118.

Farkas J., Andrassy E ., Meszaros L., Reichart O., (1996). Effect of radiation damage on the apparent lag phase of *Listeria monocytogenes*. 16th *International Symposium of the ICFMH*, p. 158.

Farkas B.E., Singh R.P., Rumsey T.R., (1996b). Modelling heat and mass transfer in immersion frying. II, model solution and verification. *Journal of Food Engineering*, 29, 227–248.

Farkas J., (1998). Irradiation as a method for decontaminating food. *International Journal of Food Microbiology*, 44, 189–204.

Farkas J., (1999). Radiation processing: an efficient means to enhance the bacteriological safety of foods. *New Food*, 2, 31-33.

Fasina O.O. Fleming H.P., (2001). Heat transfer characteristics of cucumbers during blanching. *Journal of Food Engine*ering, 47, 203–210.

Food and Drug Administration (F.D.A), (1997). Irradiation in the production, processing and treatment in vacuum packaged ground pork. Fed. 59, 1164–1166, Registry 62, 64102–64121.

Fellows P.J., (2000). Food Processing Technology: Principles and Practice, second ed., CRC Press, New York.

Fenton G.A., Kennedy M.J., (1998). Rapid dry weight determination of kiwifruit pomace and apple pomace using an infrared drying technique. *New Zealand Journal of Crop and Horticulture Science,* 26, 35–38.

Flambert E., Deltour J., (1972). Localization of the critical area in thermally-processed conduction heated canned food. *Lebensm-Wiss U. Technology,* 5(1), 7.

Floros J.D., Ozdemir M., Nelson P.E., (1998). Trends in aseptic packaging and bulk storage. *Food Cosmetics and Drug Packaging,* 21, 236–239.

Floros J.D., (1993). Aseptic packaging technology: Principles of aseptic processing and packaging (2nd ed.). Washington, DC: Food Processors Institute, p 115–48.

Floros J., (2008). Food science: feeding the world. *Food Technol*, 62(5), 11.

Formanek Z., Kerry J.P., Galven K., Buckey D.J., Farkas J., (1996). Effect of dietary vitamin E supplementation and post slaughter addition of rosemary extract on oxidative stability of irradiated minced beef. 42nd ICOMST, Lillehammer, Norway, p. 90–91.

Foster A.M., Barrett R., James S.J., Swain M.J., (2002). Measurement and prediction of air movement through doorways in refrigerated rooms. *International Journal of Refrigeration*, 25, 1102–1109.

Fryer P.J., (1995). Electrical resistance heating of foods: New Methods of Food Preservation. Blackie Academic & Professional, London.

Fryer P.J., (1997). Thermal treatment of foods. In P.J. Fryer, D.L. Pyle, and C.D. Rielly (Eds.). *Chemical engineering for the food industry*, 331-382. London, Blackie A & P.

Fryer, P. J., Robbins P.T., (2005). Heat transfer in food processing: ensuring product quality and safety. *Applied Thermal Engineering,* 25(16), 2499–2510.

Fryer P.J., Simmons M.J.H., Mehauden K., Bakalis S., (2008). Validation of thermal processing using time temperature indicators as process probes. *Journal of Food Engineering,* 9 (1), 33-42.

Fujikawa H., Itoh T., (1998). Thermal inactivation analysis of mesophiles using the Arrhenius and z-value models. *Journal of Food Protection*, 7, 785-923, 910-912(3).

Gagnon M., Abdellaoui S., Lacroix M., Jobin M., Boubekri C., (1995). Effect of gamma irradiation combined with hot water treatment on the physico-chemical, nutritional and

organoleptic qualities of clementines., *International Journal of Food Science and Technology*, 15, 217-235.

García M.J., Acinas S.G., Antón A.I., Rodríguez V.F., (1999). Use of the 16S–23S ribosomal genes spacer region in studies of prokaryotic diversity. *Journal of Microbiological Methods,* 36, 55–64.

Ghani A.G.A., Farid, M.M., Chen, X.D., Richards P., (1999). Numerical simulation of natural convection heating of canned food by computational fluiddynamics. *Journal of Food Engineering,* 41, 55–64.

Ghazala S., Ramaswamy H.S., Smith J.P., Simpson M.V., (1995). Thermal process simulation of sous-vide processing of fish and meat foods. *Food Research International*, 28, 117–122.

Gaze J.E., Brown K.L., (1998). The heat resistance of spores of Clostridium botulinum 213B over the temperature range 120 8C to 140 8C. *International Journal of Food Science and Technology,* 23, 373 – 378.

Giovannoni S.J., Britschgi T.B., Moyer C.L., Field K.G., (1990). Genetic diversity in Saragasso Sea Bacterioplankton. *Nature,* 345, 60-62.

Gould G.W., (1989). Heat Induced Injury and Inactivation in Mechanisms of Action of Food Preservation Procedures: Safe at the plate. *Nutrition Today,* 12(6), 6–9, 28–31.

Gracias K.S., McKillip J.L., (2004). A review of conventional detection and enumeration methods for pathogenic bacteria in food. *Canadian Journal of Microbiology*, 50(11), 883-890.

Guiavarc̈h Y., (2003). Development and use of enzymic time-temperature integrators for the assessment of thermal processes in terms of food safety. PhD Thesis No.570, Katholike Universiteit Leuven, Belgium.

Guiavarc'h Y., Van Loey A., Zuber F., Hendrickx M., (2004a). Development characterization and use of a high-performance enzymatic time-temperature integrator for the control of sterilization process' impacts. *Biotechnology and Bioengineering*, 88, 15-25.

Gupta M.J., Irudayaraj J.M., Debroy C., Schmilovitch Z., Mizrach A., (2005). Differentiation of food pathogens using FTIR and artificial neural networks. *Trans. ASAE.*, 48, 1889-1892.

Hagen W, Drawert F., (1986). Determination of water content by infrared. *Monatsschrift Brauwissenschaft,* 40(6), 240–246.

Hall M.J., Ratledge C., (1977). *Applied and Environmental Microbiology*, 34, 230.

Hammer K.A., Carson C.F., Riley T.V., (1999). *Journal of Applied Microbiology*, 86, 985–990.

Han J.H., Floros J.D., (2007). Active packaging: a non-thermal process: Advances in thermal and non-thermal food preservation. Ames: Blackwell Publishing, p 167–83.

Head I.M., Saunders J.R., Pickup R.W., (1998). Microbial evolution, diversity, and ecology: a decade of ribosomal analysis of uncultivated microorganisms. *Microbiology and Ecology*, 35, 1 – 21.

Heldman D.R., Hartel R.W., (1997). *Principles of food processing.* New York: Chapman & Hall, p.288.

Hendrickx M., Maesmans G., De Cordt S., Noronha J., Tobback P., (1993). The evaluation of the integrated time-temperature effect in thermal processing of foods. *Critical Reviews in Food Science and Nutrition.*

Hendrickx M., Maesmans G., De Cordt S., Noronha J., Van Loey A., Tobback P., (1995). Evaluation of the integrated time-temperature effect in thermal processing of foods. *Critical Reviews in Food Science & Nutrition,* 35 (3), 231-262.

Heppell N.J., (1985). Measurement of the liquid-solid heat transfer coefficient during continuous sterilisation of liquids containing particles. Symposium, Aseptic Processing and Packaging of Foods, Tylosand, Sweden, p.108.

Herson A.C., Hulland, E.D., (1964). *Canned Foods, an Introduction to their Microbiology* (Baumgartner), 5th ed. Chem. Pub. Co. Inc., New York.

Herson A.C., Hulland E. D., (1980). Canned Foods. *Thermal Processing and Microbiology.*

Holdsworth S.D., (1985). Optimisation of thermal processing review, *Journal of Food Engineering,* 4, 89-116.

Holdsworth S.D., (1992). Aseptic processing and packaging of food products. *Elsevier Science Publishers* Ltd.

Holdsworth S.D., (1997). *Thermal processing of packaged foods.* Blackie Academic & Professional, London.

Hsu Y.C., Sair A.I., Booren A.M., Smith, D.M., (2000). Triose phosphate isomerise as an endogenous time temperature integrator to verify adequacy of roast beef processing, *Journal of Food Science,* 65(2), 236-240.

Icier F., Ilicali C., (2005a). The effects of concentration on electrical conductivity of orange juice concentrates during ohmic heating. *European Food Research and Technology, 220,* 406–414.10.

International Commission on Microbiological Specification for Foods (ICMSF), (1996). Microorganisms in foods: Characteristics of microbial pathogens. 5, p. 513.

IFT Food Technology, (2007). 61, 40–44

International Life Sciences Institute, (ILSI), (2004b). Nutritional and safety assessments of foods and feeds nutritionally improved through biotechnology: an executive summary. *Journal of Food Science,* 69:CRH62–8.

James M. Jay, (1995). Food Preservation with Chemicals Modern Food Microbiology. *Food Science Texts Series*, p. 273-303.

Jia C.C., Sun D.W., Cao C.W., (2000a). Mathematical simulation of temperature and moisture fields within a grain kernel during drying. *Drying Technology*, 18, 1305–1325.

Jia C.C., Sun D.W., Cao C.W., (2001). Computer simulation of temperature changes in a wheat storage bin. *Journal of Stored Products Research*, 37, 165–177.

Jorge C. Oliveira, Hendrickx M.E., (1996). Process Optimisation and Minimal Processing of Foods. COPERNICUS PROGRAMME Concerted action, CIPA-CT94-0195.

Johnston M. D., Lawson S., Otter, J. A., (2005). Evaluation of hydrogen peroxide vapour as a method for the decontamination of surfaces contaminated with *Clostridium botulinum* spores. *Journal of Microbiological Methods*, 60 (3), 403-411.

Johnson A.D., Barka A., Mertz J.E., (1982). Nucleotide sequence analysis of the recombination joints in 16 naturally-arising deletion mutants of SV40. *Virology,* 464–469.

Jonsson U., Snygg B.G., Harnulv, B.G., Zacrisson T., (1977). Testing two models for the temperature dependence of the heat inactivation rate of *Bacillus stearothermophilus* spores. *Journal of Food Scien*ce, 42, 1251-1252.

Jung A., Fryer, P.J., (1999). Optimising the quality of safe food: computational modelling of a continuous sterilisation process. *Chemical Engineering Science*, 54, 717–730.

Kader A.A., (2005). Increasing food availability by reducing postharvest losses of fresh produce. 5th International Postharvest Symposium Acta Hortic., 682, ISHS 2005.

Kim T., Silva J., Chen T., (2002). Effects of UV irradiation on selected pathogens in peptone water and on stainless steel and chicken meat. *Journal of Food Protecti*on, 65 (7): 1142-1145.

King C.J., (1968). Rates of sorption and desorption in porous, dried foodstuffs. *Food Technology,* 22, 165–171, 509.

Kiranoudis C., Markatos N., (2000). Pareto design of conveyor-belt dryers. *Journal of Food Engineering,* 46, 145–155.

Knap R.P., Durance T.D., (1998). Thermal processing of suspended food particles in cans with end-over-end agitation. *Food Research International*, 31(9), 635-643.

Kumar A. Bhattacharya, M. Blaylock J., (1990). Numerical simulation of natural convection heating of canned thick viscous food products. *Journal of Food Science,* 55, 1403–1411, 1420.

Kumar A., Bhattacharya M., (1991a). Numerical analysis of aseptic processing of a non-Newtonian liquid food in a tubular heat exchanger. *Chemical Engineering Comm*unity, 103, 27–51.

Lacroix M., Ouattara B., (2000). Combined industrial processes with irradiation to assure inequity and preservation of food products: a review. *Food Research International,* 33(9), 719–724.

Larousse J., Brown B.E., (1997). *Food Canning Technology*, 235-264, 297-332, 383-424, 489-530, New York: Wiley-VCH

Lee S., (2004). Microbial Safety of Pickled Fruits and Vegetables and Hurdle Technology. *Internet Journal of Food Safety*, 4, 21–32.

Leistner L., (1995). Principles and applications of hurdle technology: New Methods of Food Preservation. Springer, 1-21.

Leizerson S., Shimoni E., (2005). Effect of ultrahigh-temperature continuous ohmic heating treatment on fresh orange juice. *Journal of Agricultural and Food Chemistry, 53*, 3519–3524.

Lewis M.J., Heppell, N.J., (2002). Continuous Thermal Processing of Foods: Pasteurization and UHT Sterilization. *Journal of the Science of Food and Agriculture*, 82(4).

Lian G., Harris C.S., Evans R., Warboys M., (1997). Coupled heat and moisture transfer during microwave vacuum drying. *Journal of Microwave Power and Electromagnetic Energy,* 32, 34–44.

Liao H.J, Rao M.A., Datta A.K., (2000). Role of thermo-rheological behaviour in simulation of continuous sterilization of starch dispersion. *Trans. IChemE.*, 78, C, 48–56.

Lioliou E.E., Pantazaki A.A., Kyriakidis D.A., (2004). *Thermus thermophilus* genome analysis: benefits and implications. *Microbial Cell Factories*, 3:5.

Lin Y.E., Anantheswaran R.C., Puri V.M., (1995). Finite element analysis of microwave heating of solid foods. *Journal of Food Engineering*, 25, 85–112.

Ludwig W., Schleifer K.H., (1994). Bacterial phylogeny based on 16S and 23S rRNA sequence analysis. *FEMS Microbiological Rev*. 15, 155 – 173.

Lund D.B., (1975). Heat processing: Physical Principles of Food Preservation. Marcel Dekker, New York.

Mathioulakis E., Karathanos V.T., Belessiotis V.G., (1998). Simulation of air movement in a dryer by computational fluid dynamics: application for the drying of fruits. *Journal of Food Engineering*, 36, 183–200.

McKenna A.B., Tucker G.S., (1991). Computer modelling for the control of particle sterilization under dynamic flow conditions. *Food Control,* 2, 224-233.

Madigan M.T., Martino J.M., (2006). Brock Biology of Microorganisms (11th ed.). Pearson, p. 136.

Maesmans G., Hendrickx M., De Cordt S., Van Loey A., Noronha J., Tobback P. (1994). Evaluation of process value distribution with time temperature integrators. *Food Research International*, 27, 413-423.

Maggi P., Carbonara S., Fico C., Santantonio T., Romanelli C., Sforza E., Pastore G., (1997). Epidemiological, clinical and therapeutic evaluation of the Italian cholera epidemic in Europe. *Journal of Epidemiology*, 13, 95–97.

Marquenie D., (2003). Combinations of pulsed white light and UV-C or mild heat treatment to inactivate conidia of Botrytis cinerea and Monilia fructigena. *International Journal of Food Microbiology*, 85 (1-2), 185-196.

Marquis R. E., Baldec, J., (2007). Sporicidal interactions of ultraviolet irradiation and hydrogen peroxide related to aseptic technology. *Chemical Engineering and Processing*, 46 (6), 547-553.

Mattsson B., Sonesson U., (2003). Environmentally-friendly food processing. United Kingdom: Woodhead Publishing Limited, p. 337.

Miller J.J., (1989). Sporulation in *Saccharomyces cerevisiae.* Academic Press, New York, 3, p. 489-541.

McGee Harold, (2004). Wood Smoke and Charred Wood. On Food and Cooking .Scribner, p. 448–450.

Meade S.J., Reid E.A., Gerrard J.A., (2005). The impact of processing on the nutritional quality of food proteins. *Journal AOAC Int*ernational, 88, 904–922.

Mehauden K., Cox P.W., Bakalis S., Simmons M.J.H., Tucker G.S., Fryer P.J., (2007). A novel method to evaluate the applicability of time-temperature integrators to different temperature profiles. *Innovative Food Science & Emerging Technologies,* 8, 507-514.

Mirade P.S., Daudin J.D., (2000). Numerical study of the airflow patterns in a sausage dryer. *Drying Technology*, 18, 81–97.

Mongpreneet S., Abe T., Tsurusaki T., (2002). Accelerated drying of welsh onion by far infrared radiation under vacuum conditions. *Journal of Food Engineering,* 55, 147–156.

Monroe J.J., Loessner M.J., Allen G.D., (2005). Modern Food Microbiology, *Springer.*

Montville T.J., Matthews K.R., (2005). Food microbiology an introduction. American Society for Microbiology Press, p. 30.

Mossoba M.M., Al-Khaldi S.F., Kirkwood J., Fry F.S., Sedman J., Ismail A.A, (2005). Printing microarrays of bacteria for identification by infrared micro spectroscopy. Vibrational Spectroscopy, 38, 229-235.

Mudgett R.E., (1986). Electrical properties of foods: Engineering properties of foods. p. 329–390. New York, NY: Marcel Dekker, Inc.

Muyzer G., (1999). DGGE/TGGE a method for identifying genes from natural ecosystems. *Current Opinions in Microbiology.* 2, 317 – 322.

NACMCF, (2010). Reports and Recommendations Study of Microbiological Criteria as Indicators of Process Control or Insanitary Conditions.

Nanjundaswamy A.M., Saroja S., Ranganna S., (1973). Determination of thermal process for canned mango products. *Indian Food Packer* 27(6), 5.

Nath N., Ranganna S., (1983b). Determination of a thermal process schedule for guava Psidium guajava Linn. *Food Technol*ogy, 18, 301-316.

NAS, (1973). Toxicants occurring naturally in foods. Committee on Food Protection. Washington, DC: National Academy of Sciences, p. 624.

Navari P., Andrieu J., Gevaudan A., (1992). Studies on infrared and convective drying of no hygroscopic solids. *Drying 92, Amsterdam: Elsevier Science.* p. 685–94.

Nelson P.E. (1993). Principles of Aseptic Processing and Packaging (3rd ed.). p. 101-133.

Newsome R., Fisher W., (2007). Feeding the World Today and Tomorrow: The Importance of Food Science and Technology. An IFT Scientific Review by John D. Floros.

Nicolai B.M., De Baerdemaeker J., (1999). A variance propagation algorithm for the computation of heat conduction under stochastic conditions. *International Journal of Heat and Mass Transfer,* 42, 1513–1520.

Nicolai B.M., Scheerlinck N., Verboven P., De Baerdemaeker J., (2000). Stochastic perturbation analysis of thermal food processes with random field parameters. *Transactions of the ASAE,* 43, 131–138.

Nowak D., Levicki P.P., (2004). Infrared drying of apple slices. *Innovative Food Science Emerging Technologies,* 5, 353–360.

Ocio M.J., Salvador Fernandez P, Rodrigo M., Periago P., Martinez A., (1997). A time temperature integrator for particulated foods: thermal process evaluation. *Food Research and Technology*, 205(4), 325-328.

Ohlsson, (1980a). Optimal sterilisation temperatures for flat containers, *Journal of Food Science*, 45, 848-853.

Olmos A., Trelea I.C., Courtois F., Bonazzi C., Trystram G., (2002). Dynamic optimal control of batch rice drying process. *Drying Technology,* 20(7), 1319–1345.

Ozdemir M., Floros J.D., (2004). Active food packaging technologies. *CRC Critical Review in Food Science and Nutrition,* 44(3),185–193.

Özisik M.N., (1993). Heat Conduction (2nd edn.). Wiley, New York.

Paine F.A., (1991). The packaging user's handbook. New York: AVI, Van Nostrand Reinhold, p.158.

Pan Z., Singh R.P., Rumsey T. R., (2000). Predictive modelling of contact-heating process for cooking a hamburger patty. *Journal of Food Engineering,* 46, 9-19.

Patterson & Kilpatrick, (1998). The combined effect of high hydrostatic pressure and mild heat on inactivation of pathogens in milk and poultry. *Journal of Food Protection*, 61, 432–436.

Perrota N., Trelea I.C., Baudrita C., Trystram G., Bourginec P., (2011). Modelling and analysis of complex food systems: State of the art and new trends. *Trends in Food Science & Technology,* 22, 304-314.

Pflug I. J., (1987). Calculating Ft-values for heat preservation of shelf-stable, low-acid canned foods using the straight-line semi logarithmic model. *Journal of Food Pro*teins, 50 (7), 608–615.

Pflug G.Ch., (1996). Optimization of Stochastic Models: The Interface between simulation and optimization. Kluwer.

Powitz R.W., (2007). Water Activity: a New Food Safety Tool. Food Safety magazine.

Puri V.M., Anantheswaran R.C., (1993). The finite-element method in food processing: a review. *Journal of Food Engineering*, 19, 247–274.

Quass, D. W. (1997). Pulsed electric field processing in the food industry: A status report on pulsed electric field. Palo Alto, CA. Electric Power Research Institute, CR- 109742. p.23- 35.

Radomyski T., Murano E.A., Olson, D.G., Murano, P.S., (1994). Elimination of pathogens of significance in food by low-dose irradiation: A review. *Journal of Food Proteins,,* 57, 73-86.

Rahman M.S., (2009). Fat oxidation in freeze dried grouper during storage at different temperatures and moisture content. *Food Chemistry*, p.1257–1264.

Ramaiah Muthyala, (1997). Chemistry and Applications of Leuco DyesTopics in Applied Chemistry, Springer.

Ramaswamy H.S., Tung M.A., (1984). A Review on predicting freezing times of foods. *Journal of Food Process Engineering,* 7(3):169–203.

Rao S.S., (1989). The finite element method in engineering (2nd edition). New York, USA: Pergamon Press.

Ramaswamy R., Balasubramaniam V.M., Sastry S.K., (2005). Ohmic heating of foods: fact sheet for food processors. Extension Fact Sheet, The Ohio State University.

Raso J., Barbosa-Cánovas G.V., (2003). Nonthermal preservation of foods using combined processing techniques. *Critical Review of Food Science and Nutrition.,* 43(3), 265-285.

Resurreccion A.V.A., Galvez, F.C.F., Fletcher S.M., Misra S.K., Thayer D.W., Boyd, G., (1995). Consumer attitudes toward irradiated food: results of a new study. *Journal of Food Protection*, 58, 193–196.

Reute H., (1988). Aseptic Packaging of Food (Technomic, Lancaster, P.A.)

Reyes de Corcuera J.I., Cavalieri R.P., Powers J.R., Tang J., Kang D.H., (2005). Enzyme-electropolymer-based amperometric biosensors: an innovative platform for time-temperature integrators. *Journal of Agricultural and Food Chemistry*, 53, 8866-8873.

Rickman J.C., Bruhn C.M., Barrett D.M., (2007). Nutritional comparison of fresh, frozen, and canned fruits and vegetables II. Journal of the Science of Food and Agriculture, 87(7), 1185–1196.

Ruan R., Ye X., Chen P., (2004). Improving the thermal processing of foods: Developments in ohmic heating. Woodhead Publishing Ltd, Cambridge UK.

Rutherford G. C., Reidmiller J. S., Marquis R. E., (2000). Method to sanitize bacterial spores to subsequent killing by dry heat or ultraviolet irradiation. *Journal of Microbiological Methods*, 42 (3), 281-290.

Rickman J.C., Bruhn C.M., Barrett D.M., (2007b). Review: nutritional comparison of fresh, frozen, and canned fruits and vegetables II. Vitamin A and carotenoids, vitamin E, minerals and fiber. *Journal of Science in Food Agriculture.*, 87, 1185–1196.

Robertson G.L., (1993). Food packaging: principles and practice. New York: Marcel Dekker, p.686.

Rodrigo F., Martinez A., (1998). Evaluation of a new time temperature integrator in pilot plant conditions. *Food Research and Technology*, 206(3), 184-188.

Sakai N., Hanzawa T., (1994). Applications and advances in far-infrared heating in Japan. *Trends in Food Science and Technology,* 5, 357–362.

Sandoval A.J., Barreiro J.A., Mendoza S., (1994). Prediction of hot-fill-air-cool sterilization processes for tomato paste in glass jars. *Journal of Food Engineering,* 23, 33–50.

Sastry S. K., Li Q., (1996). Modeling the ohmic heating of foods. *Food Technology*, 50(5), 246–248.

Sastry S.K., Salengke S., (1998). Ohmic heating of solid-liquid mixtures: a comparison of mathematical models under worst-case heating conditions. *Journal of Food Process Engineering,* 21, 441-458.

Sawai J., Nakai T., Hashimoto A., Shimizu M., (2004). A comparison of the hydrolysis of sweet potato starch with b-amylase and infrared radiation allows prediction of reducing sugar production. *International Journal of Food Science and Technology,* 39, 967–974.

Seeboth A., Lötzsch D., (2014). Thermochromic and Thermotropic *Materials*. Pan Stanford Publishing

Selman J.D., (1987). The blanching process: Developments in Food Processing. *Elsevier Applied Science*, London, 4, 205-249.

Sharma G.P., Verma R.C., Pathare P.B., (2005). Thin-layer infrared radiation drying of onion slices. *Journal of Food Engineering,* 67:361–6.

Shyam S.S., Datta A.K., Rahman M.S., (2006). Handbook of Food and Bioprocess Modelling Techniques (Food Science and Technology).

Silley P., Forsythe S., (1996). Impedance microbiology-a rapid change for microbiologists. *Journal of Applied Bacteriology*, 80, 233-243.

Silva C., Hendrickx M., Oliveira F., Toback, P., (1992b). Optimal sterilisation temperatures for conduction heating foods considering finite surface heat transfer coefficients. *Journal of Food Science,* 57(3), 743-748.

Silva C.L.M., Oliveira F.A.R., Hendrickx M., (1993). Modelling optimum processing conditions for the sterilization of prepackaged foods. *Food Control,* 4, 67–78.

Silva C., Oliveira F., Hendrickx M., (1994a). Optimum sterilisation: A comparative study between average and surface quality. *Journal of Food Process Engineering*, 17, 155-176.

Silva C.K., Korczak, (1994). *Critical* evaluation of restrictions used to optimise sterilisation processing conditions. 4th Bath Food process Engineering Conference.

Silva F.V.M, Silva C.L.M., (1997). Quality Optimization of Hot Filled Pasteurized Fruit Purees: Container Characteristics and Filling Temperatures. *Journal of Food Engineering,* 32(4), 351-364.

Simpson R., Almonacid S., Solari P., (2000). Bigelow's general method revised. IFT Annual Meeting and Food Expo.

Singh R.P., Cadwallader K. R., (2004). Ways of measuring shelf-life and spoilage. Woodhead Publishing, Cambridge, p. 165-183.

Sivertsvik M., Jeksrud W., Wagane Aa., Rosnes J.T., (2004a). Solubility and absorbtion rate of carbon dioxide into non-respiring foods. *Journal of Food Engineering*, 61, 449-458.

Stoforos N.G., Taoukis P.S., (1998). Theoretical procedure for using multiple response time-temperature integrators for the design and evaluation of thermal processes. *Food Control,* 9(5), 279-287(9).

Straatsma J., Houwelingen G. V., Steenbergen A. E. & De Jong P., (1999). Spray drying of food products: simulation model. *Journal of Food Engineering,* 42, 67–72.

Stumbo C.R., (1965). Thermobacteriology in food processing. Academic Press, 111 Fifth Avenue, New York.

Sun D.W., (2002). CFD Applications in the Agri-Food Industry. *Computers and Electronics in Agriculture,* 34(1–3), 1–236.

Suppakul P., Miltz J., Sonneveld K., Biger S.W., (2003). Active packaging technologies with an emphasis on antimicrobial packaging and its applications. *Journal of Food Science,* 68(2), 408–420.

Swartlinga P., Lindgrena B., (1968). The sterilizing effect against *Bacillus subtilis* spores of hydrogen peroxide at different temperatures and concentrations, *Journal of Dairy Research,* 35(3), 423-428.

Taoukis P.S., Labuza T.P., (1989a). Applicability of Time Temperature Indicators as shelf life monitors of food products. *Journal of Food Science*, 54, 783–788.

Taoukis P.S., Labuza T.P., (1989b). Reliability of Time Temperature Indicators as food quality monitors under non isothermal conditions. *Journal of Food Science,* 54, 789–792.

Taoukis P.S., Koutsoumanis K., Nychas G.J.E., (1999). Use of time-temperature integrators and predictive modelling for shelf life control of chilled fish under dynamic storage conditions. *Int. Journal of Food Microbiology*, 53, 21-31.

Tewkesbury H., Stapley A.G.F., Fryer P.J., (2000). Modelling temperature distributions in cooling chocolate moulds. *Chemical Engineering Science*, 55, 3123–3132.

Texeira A.A., Dixon J.R., Zahradnik J.W., Zinsmeister G.E., (1969). Computer simulation of variable retort control and container geometry as a possible means of improving thiamine retention in thermally processed foods. *Journal of Food Science,* 40, 465-659.

Thijssen H.A.C., (1979). Optimization of process conditions during drying with regard to quality factors. *Lebensm-Wiss u-Technol.,* 12, 308–317.

Thorvaldsson K., Janestad H., (1999). A model for simultaneous heat, water and vapour diffusion. *Journal of Food Engineering*, 40, 167–172.

Thompson S.E., Foster N.S., Johnson T.J., Valentine N.B., Amonette J.E., (2003). Identification of bacterial spores using statistical analysis of Fourier transform infrared photoacoustic spectroscopy data. *Applied Spectroscopy*, 57, 893-899.

Toledo R.T., (1986). Post processing changes in aseptically packed beverages. *Journal of Agriculture and Food Chemistry*, 34(3), 405–408.

Togrul H., (2005). Simple modelling of infrared drying of fresh apple slices. *Journal of Food Engineering,* 71, 311–323.

Tucker G.S., Clark. P., (1990). Modelling the cooling phase of heat sterilization processes, using heat transfer coefficients. *International Journal of Food Science and Technology,* 25, 668–681.

Tucker G.S., Noronha J.F., Heydon C.J., (1996). Experimental validation of mathematical procedures for the valuation of thermal processes and process deviations during the sterilization of canned foods. *Transactions of the Institution of Chemical Engineers, Food & Bioproducts Processing,* 74, Part C, 140-148.

Tucker G.S., (2000). Estimation of pasteurisation values using an enzymic time-temperature integrator. *Food Australia,* 52 (4), 131-136.

Tucker G.S., Wolf D., (2003). Time-temperature integrators for food process analysis, modelling and control. R&D Report No.177, Campden & Chorleywood Food Research Association.

Tucker G., Cronje M., Lloyd E., (2005). Evaluation of a time-temperature integrator for mild pasteurisation processes. R&D Report No.215, Campden & Chorleywood Food Research Association.

Tucker G.S., (2004). Using the process to add value to heat-treated products. *Journal of Food Science,* 69 (3), 102-104.

Tucker G.S., Brown H.M., Fryer P.J., Cox P.W., Poole F.L., Lee H.S., Adams M.W.W., (2007). A sterilisation time-temperature integrator based on amylase from the hyperthermophilic organism *pyrococcus furiosus. Innovative Food Science and Emerging Technologies,* 8, 63-72.

Tuorila H., Cardello A.V., (2002). Consumer responses to an off flavour in juice in the presence of specific health claims. *Food Quality Pref* .,13, 561–569.

Vadivambal R., Jayas D.S., (2011). Applications of Thermal Imaging in Agriculture and Food Industry: A Review. *Food and Bioprocess Technology*, 4(2), 186-199.

Van Buggenhout S., Messagie I., Van Loey A., Hendrickx M., (2005). Influence of low-temperature blanching combined with high-pressure shift freezing on the texture of frozen carrots. *Journal of Food Science,* 70 (4), S304-S308.

Vaidya S., Orta-Ramirez A., Smith D.M., Ofoli R.Y., (2003). Effect of heat on phycoerythrin fluorescence: influence of thermal exposure on the fluorescence emission of R-phycoerythrin. *Biotechnology and Bioengineering,* 83, 465-473.

Van Der Sluis S. M., Rouwen W., (1994). TNO develops a model for refrigeration technology calculations. Voedingsmiddelen technologie, 26, 63–64.

Van Loey A.M., Hendrickx M. E., De Cordt S., Haentjens T.H., Tobback P. P., (1996). Quantitative evaluation of thermal processes using time-temperature integrators. *Trends in Food Science & Technology,* 7, 16-26.

Van Loey A.M., Haentjens T.H., Hendrickx M. E., Tobback, P. P., (1997b). The development of an enzymic time temperature integrator to assess the thermal efficacy of sterilization of low-acid canned foods. *Food Biotechnology*, 11 (2), 147-168.

Varma M.N., Kannan A., (2006). CFD studies on natural convective heating of canned food in conical and cylindrical containers. *Journal of Food Engineering,* 77, 1024–1036.

Verboven P., Scheerlinck N., De Baerdemaeker J., Nicolai B.M., (2000a). Computational fluid dynamics modelling and validation of the isothermal airflow in a forced convection oven. *Journal of Food Engineering*, 43, 41–53.

Verboven, P., Scheerlinck, N., De Baerdemaeker, J., Nicolai, B.M., (2001). Sensitivity of the food center temperature with respect to the air velocity and the turbulence kinetic energy. *Journal of Food Engineering*, 48, 53–60.

Venugopal V., Doke S.N., Thomas P., (1999). Radiation processing to improve the quality of fishery products. *Critical Reviews in Food Science and Nutrition*, 39, 391-440.

Vikram V.B., Ramesh M.N., Prapulla S.G., (2005). Thermal degradation kinetics of nutrients in orange juice heated by electromagnetic and conventional methods. *Journal of Food Engineering,* 69, 31–40.

Viollaz P.E., Alzamora S.M., (2005). Encyclopedia of food engineering: Food dehydration. p. 461–77.

Von Loesecke, (1943). Drying and dehydration of foods. New York: Reinhold Pub Co Inc. p.302.

Vorobiev E., Jemai A.B., Bouzrara H., Lebovka N.I., Bazhal M.I., (2004). Pulsed electric field assisted extraction of juice from food plants. In: Novel Food Processing Technologies Marcel Dekker, NewYork, p. 105-130.

Wallner-Pendleton E. A., Sumner S.S., Froning G.W., Stetson L.E., (1994). The use of ultraviolet radiation to reduce Salmonella and psychrotrophic bacterial contamination on poultry carcasses. *Poultry Science,* 73:1327–1333.

Wang Z. H., Chen G. H., (1999). Heat and mass transfer during low intensity convection drying. *Chemical Engineering Science*, 54, 3899–3908.

Wang L. J., Sun, D.W., (2002a). Modelling three conventional cooling processes of cooked meat by finite element method. *International Journal of Refrigeration*, 25, 100–110.

Wang C.W., Cook K.A., Sastry A. M., (2003). Conduction in Multiphase Particulate/Fibrous Networks: Simulations and Experiments on Li-ion Anodes. *Journal of The Electrochemical Society*, 150(3), 385-397.

Wang L. J., Sun D. W., (2003). Numerical analysis of the three dimensional mass and heat transfer with inner moisture evaporation in porous cooked meat joints during vacuum cooling process. *Transactions of the ASAE*, 46, 107–115.

Ward D.M., Weller R., Bateson M.M., (1990). 16S rRNA sequences reveal numerous uncultured microorganisms in a natural community. *Nature* 345, 63 – 65.

Wawerla M, Stolle A, Schalch B, Eisgruber H., (1999). Impedance microbiology: applications in food hygiene. *Journal of Food Prot*eins, 62(12), 1488-96.

Weissmann C., Enari M., Klohn P.C., Rossi D., Flechsig E., (2002). Transmission of prion. *Journal of Infectious Diseases,* 186 (Suppl.2), 157-165.

Whitaker S., (1977). Simultaneous heat, mass and momentum transfer in porous media: a theory of drying. 13,198, New York: Academic Press.

World Health Organization (WHO), (1994). Safety and Nutritional Adequacy of Irradiated Food. meat and poultry. *Journal of Food Safety*, 15, 181–192.

Wong C.F., Parisi A.V., (1999).Assessment of ultraviolet radiation exposures in photobiological experiments. Internet Photochemistry and Photobiology Conference.

Yam K.L., Takhistov P.T., Miltz J., (2005). Intelligent packaging: concepts and applications. *Journal of Food Sci*ence, 70(1):R1–R10.

Yang W. H., Rao, M. A., (1998). Transient natural convection heat transfer to starch dispersion in a cylindrical container: numerical solution and experiment. *Journal of Food Engineering,* 36, 395– 415.

Zhao Y., Kolbe E., Craven C., (1998). Computer simulation on onboard chilling and freezing of albacore tuna. *Journal of Food Science*, 63, 751–755.

Zhou L., Puri V.M., Anantheswaran R.C., Yeh. G., (1995). Finite element modeling of heat and mass transfer in food materials during microwave heating: Model development and validation. *Journal of Food Engineering*, 25(4), 509–529.

Chapter 3 Pasteurisation of model food packages by the inversion method

Abstract

In most food industries, the surface decontamination of food packages is achieved by the application of thermal processing. This research is concerned with the investigation of surface pasteurisation treatments in food packages, primarily for hot-filled food products.

Hot-filling is a thermal treatment based on the assumption that the heat transferred from the pasteurised food is sufficient to decontaminate the package. That is true for the surfaces that come in contact with the product, but it is not the case for the headspace and the lid of the package. Thus, a post-pasteurisation step usually in the form of a shower of hot water or steam is used. Inverting the filled jars is another way to give heat treatment to the lid and headspace of the pack, a method extensively used in the food industry for filling into glass jars, pouches, cartons and plastic trays.

The current research aims at assessing the effectiveness of inverting the pack as a thermal treatment of the headspace and the lid for model food packaging in the form of glass jars.

The target process to be achieved was 5 min at 70°C, for chilled foods with a shelf life < 10 days, and the model fluids used to evaluate the inversion process were tomato soup, and starch solutions of 3, 4, and 5% (w/w). The fluids used, were chosen based on their different viscosity, since that would potentially affect the heat transfer mechanism occurring during the cooling phase of the hot-fill process; the three model starch solutions, were compared with a real food product, the cream of tomato soup, with a viscosity that lies in between.

Rheological experiments were conducted in order to determine the flow properties of the model fluids used and dimensionless numbers were calculated giving an indication of the heat transfer mechanisms occurring during the cooling phase of the heat treatment.

Based on current industrial practice, the jars were hot-filled at a temperature of $80^{o}C$, inverted for 30 sec, sealed and then cooled down to room temperature.

The inversion time-filling temperature combination appeared to be very effective to achieve the goals set, the inverted jars showed significantly higher process values for the headspace and the lid, achieving the target process; the filling temperature was the most significant parameter. Based on these results, more t-T combinations were suggested for process values ≥5 min. Grashof numbers suggest that in some cases natural convection would have an effect.

A mathematical model was developed, using the dimensionless numbers calculated for confirming the existence of natural convection.

3.1   Introduction

The increased demand for less processed food products that retain their quality and nutritional characteristics is tensioned against requirements for food safety, which has led to stricter safety and quality regulations (Boero, 2011; Wilke et al., 2013).

To guarantee the safety of their products, food manufacturers use different food preservation techniques. The most commonly process is thermal treatment, where high temperatures are applied to the food in order to minimise the quantity of microorganisms and spores present (Fryer, Pyle, & Rielly, 1997). Depending upon the requirements, thermal treatment can be used for pasteurisation or sterilisation, and these are the most commonly used methods to ensure surface decontamination of food packaging.

Pasteurisation can be delivered 'in-pack' or to products that are heat processed before being filled. When the food packages are hot-filled, the food itself is sufficiently pasteurised but the internal surfaces of the packaging are not. The hot-fill method is used extensively in the food industry for filling into glass jars, plastic pots and pouches, cartons and plastic trays.

In order to ensure safety of the packaging surfaces and prevent contamination and spoilage, some form of 'top-up' pasteurisation e.g. a raining water tunnel at high temperature (usually 95°C), is often applied (Campden & Chorleywood Food Research Association, 1998).

Quantifying the heat treatment given to food packages during hot-fill operations would potentially improve food quality, increase line efficiency, reduce waste, energy input and the environmental burdens of food manufacturing.

In this work, the heat treatment is quantified based on the target lethality approach (F_o), at the slowest heating point within the food, as described in Chapter 2, §2.3. According to the F_o theory, the effect of a varying temperature on the applied thermal process can be described by a term called lethality (L), which refers to the thermal destruction of microorganisms achieved between a temperature (T) at any given time during the process and a reference temperature (T_{ref}), expressed as follows:

$$L = 10^{\frac{T-T_{ref}}{z}}$$
(3.1)

Where: T_{ref} = reference temperature of 121.1^{o}C and z = 10°C, based on the destruction of *Clostridium botulinum* in low-acid foods.

The total time–temperature combination received by a food product in order to achieve the desired thermal destruction of microorganisms, in the case of commercial sterilisation, is referred to as process value or *F-value* (Ball, 1923). The process value (*F* for sterilisation and

P for pasteurisation) is used as a basis for comparing heat sterilisation treatments and it can be calculated in two ways. The first is based on measurements of the initial and final loads of the heat-labile substance ($N_{initial}$ and N_{final}, respectively) while the second is based on the complete knowledge of the time-temperature history, T(t). This is expressed in the following equation:

$$F \text{ or } P = D_T \cdot \log\left(\frac{N_o}{N_f}\right) = \int_0^t 10^{\frac{T - T_{ref}}{z}} \cdot dt \tag{3.2}$$

Where: T(t) is the product temperature at the coldest point (°C), T_{ref} is the reference temperature for the D_T value (°C), t is the process time (min) and z is the number of degrees Celsius needed to bring about a ten-fold change in decimal reduction time.

In the current work, the process values were calculated based on the knowledge of time-temperature history obtained by temperature sensors located at six different locations inside the package.

This chapter is divided into the following parts:

- Description of the equipment and methodology of the hot-fill experiments conducted;

- Rheological analysis: the four pre-gelatinised model foods used were subjected to a variety of rheological tests in order to be characterised;

- Development of a mathematical model in combination with dimensional analysis for generating buoyancy flow.

3.2   Materials and Methods

3.2.1   Equipment

The model food packages used for conducting the hot-fill treatments were cylindrical glass jars of 7.3 cm × 9.3 cm diameter and height, respectively, giving a working volume of 325 mL. Thermocouples were located at six different locations inside the inverted and non-inverted jar, at the bottom, the bottom corner, the middle, the wall, the headspace and the lid as shown in Figure 3.1. The time-temperature history of the thermocouples was recorded using a USB-TC-08 data logger (Pico Technology, Cambridgeshire, UK), with a temperature accuracy ±0.5 °C and a sampling rate of up to 10 Hz.
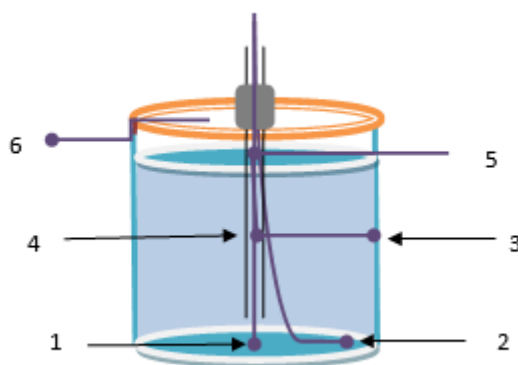
Figure 3.1: Location of thermocouples inside the glass jar at 1. Bottom, 2. Corner, 3. Middle, 4. Wall 5. Headspace, and 6. Lid

The time-temperature profiles obtained were then converted into process values based on Equation 3.2. The kinetic parameters (z-value) used to calculate the process values, were obtained from the calibration of bacterial α-amylases. A z-value of 10.8°C was used for achieving a target of 5 min at 70°C.

The fluids used in the hot-fill treatments were aqueous solutions of maize starch (Colflo 67, Ingredion, Manchester, UK) of 3, 4 and 5% (w/w), and cream of tomato soup (Heinz Foods, Wigan, UK), and their pasteurisation was conducted in a well-stirred water bath (Grant, UK). For convenience, the model fluids will be referred to as A, B, C and T for the 3, 4, 5% of starch solution, and tomato soup, respectively.

The samples were pre-gelatinised at the reference temperature of 80°C in the well-stirred for approximately 80 min (the time needed for the model foods to reach the reference temperature in the water bath) and were cooled down to ambient temperature. Samples of 2 mL of the pre-gelatinised fluids were then taken for rheological characterisation using a TA AR1000 cone and plate rheometer (TA Instruments, Newcastle, Delaware, USA) equipped with 0.06 m diameter 2° steel cone and plate geometry.

3.2.2   Inversion method

Duran® glass beakers of 1000 mL (Fisher Scientific UK Ltd) were filled with 700 mL of each of the model foods and were immersed in the water bath, until the required filling temperatures of 80°C was reached. A compact overhead stirrer (Fisher Scientific UK Ltd) was used to continuously stir the liquid foods while being heated, to ensure thermal uniformity. Once the desired fluid temperature was reached, two glass jars with their lids screwed in were fully immersed into the water bath for approximately 5s, at the same temperature as the fluid. Each of the two already heated glass jars was hot-filled with 290 mL of the model food and sealed; the headspace of the container was kept lower than 10%, volumetrically. After the two jars were sealed, one of them was inverted for 30 s, whilst the other was at the upright position. After the 30 s, the inverted jar was brought back to the upright position and was kept together with the non-inverted jar at ambient temperature for approximately 10 min, as illustrated in Figure 3.2. At the end of the process, the lids of both

glass jars were removed and the time-temperature profile recorded by the thermocouples is

stopped. The thermocouples were removed from the jars, cleaned properly and re-used for

the next set of experiments. The inversion process was repeated seven times for each fluid.

$$P = \int_0^t 10^{\frac{T_t - T_{ref}}{z}} . dt$$
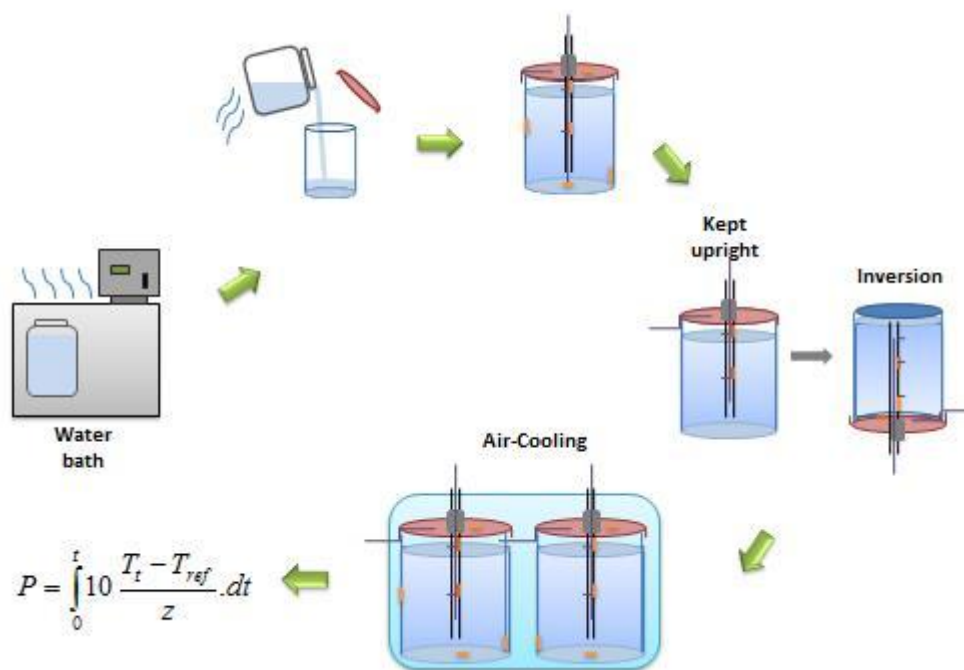
Figure 3.2: Hot-fill process with the method of inversion.

The time-temperature profiles and process values illustrated in Figures 3.18-3.20 and 3.21

respectively are a result of seven replicates. The standard deviation of all the replicates was

lower than 2, thus the average value of the data obtained was shown in the Figures.

3.2.3   *Rheology*

Rheology is important for determination of a product's stability and quality and for selecting

proper design and process equipment (Fischer and Windhab, 2011). The rheological

characteristics of food products can be determined by several methods, such as flow and oscillatory measurements, which are performed to determine the flow behaviour and to provide information about the viscoelastic properties of the materials tested, respectively.

The time-temperature profiles and process values illustrated in Figures 3.7-3.13 are a result of five replicates. The standard deviation of all the replicates was lower than 2, thus the average value of the data obtained was shown in the Figures.

3.2.3.1 Oscillatory measurements

Oscillation tests are used for determining the strength and stability of a material. They give a clear indication of the behaviour of the sample, whether viscous or elastically dominated, over a given frequency range. The nature of the tests is non-destructive, enabling measurements to be made without incurring structural damage to the sample. Thus, the dynamic rheological parameters are related to the sample's molecular structure. These tests also provide a very sensitive means of studying the molecular motions that give rise to the phenomenon like glass transition temperature (Winter H.H., 1997).

By subjecting a specimen to an oscillatory stress (σ) and determining the response, both the elastic and viscous characteristics can be obtained. In the case of the cone-plate geometry, the cone is forced into oscillatory shear with angular frequency ω and the sample is placed between the plate and the cone, as illustrated in Figure 3.3.
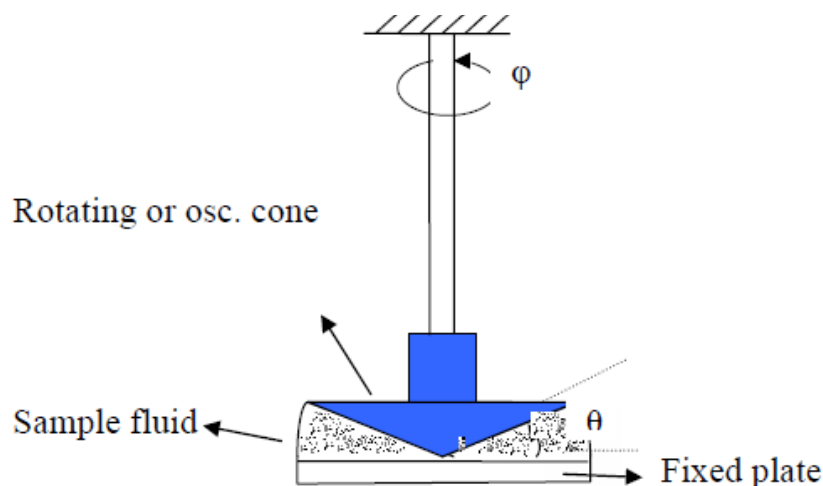
Figure 3.3: Configuration of the cone-plate rheometer.

Stress Sweep Test

Usually the rheological properties of a viscoelastic material are independent of stress up to a critical stress level. Beyond that level, the material's behaviour is non-linear and the storage modulus declines. So, measuring the stress amplitude dependence of the storage and loss moduli, (G', G'') is a good first step taken in characterising viscoelastic behaviour; a stress sweep will establish the extent of the material's linearity. The linear viscoelastic region can be determined easily in dynamic testing by changing the amplitude of the input stress function (Nielsen and Landel, 1994). When applicable, data from oscillatory tests can be utilized in time-temperature superposition technique to expand the frequency range which otherwise would be inaccessible experimentally (Bird et al., 1987). Knowledge of dynamic properties such as G' and G'' allows computation of all other linear viscoelastic properties as well as the material behaviour in other types of deformations such as tension.

The Linear Viscoelastic Region (LVR) was determined by performing an amplitude sweep over a stress at a constant frequency of 1 Hz and a temperature of 25°C. The test shows how the applied stress would affect the sample, in essence where does the structure begin to breakdown and how quickly does it breakdown. Information is provided about the rigidity

and strength of products, such as delicately-structured fruit juices and thickened drinks (Menard, 2008).

The behaviour of the fluids is expressed in terms of complex shear stress, and phase angle against the oscillation stress applied (Figures 3.9 and 3.10). The complex modulus results from the varying strain in the product and is the ratio of shear stress to shear strain (Figure 3.2), expressed as follows:

$$G* = \frac{\tau_{max} - \tau_{min}}{\gamma_{max} - \gamma_{min}} = G' + i \cdot G'' \tag{3.3}$$

Where: G', G'' and i are the dynamic storage modulus, the dynamic loss modulus and the complex number $\sqrt{-1}$ respectively. τ_{min} / τ_{max} (Pa) and γ_{min} / γ_{max} (s^{-1}) are the minimum and maximum shear stress and shear rate, respectively.
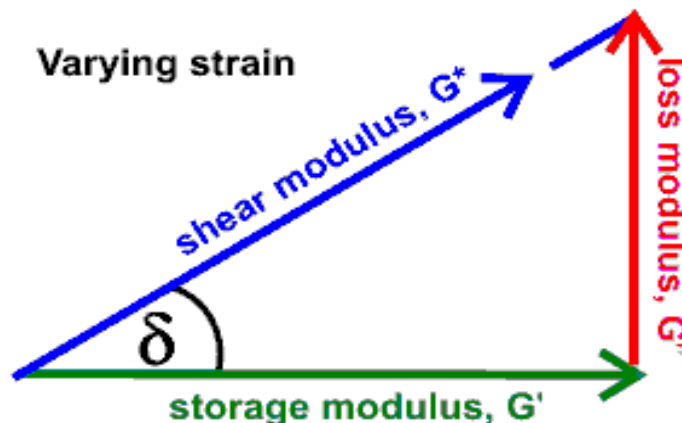
Figure 3.4: Complex shear modulus

$G*$ is the material's overall resistance to shear deformation, and it is a good indicator of the material's flexibility or stiffness.

δ is the phase difference between the stress and strain, and if close to zero degrees means that the material is highly elastic, whilst approaching the 90 degrees it is highly viscous and

demonstrates the greatest capability to dissipate energy. At 45 degrees, the material is perfectly viscoelastic.
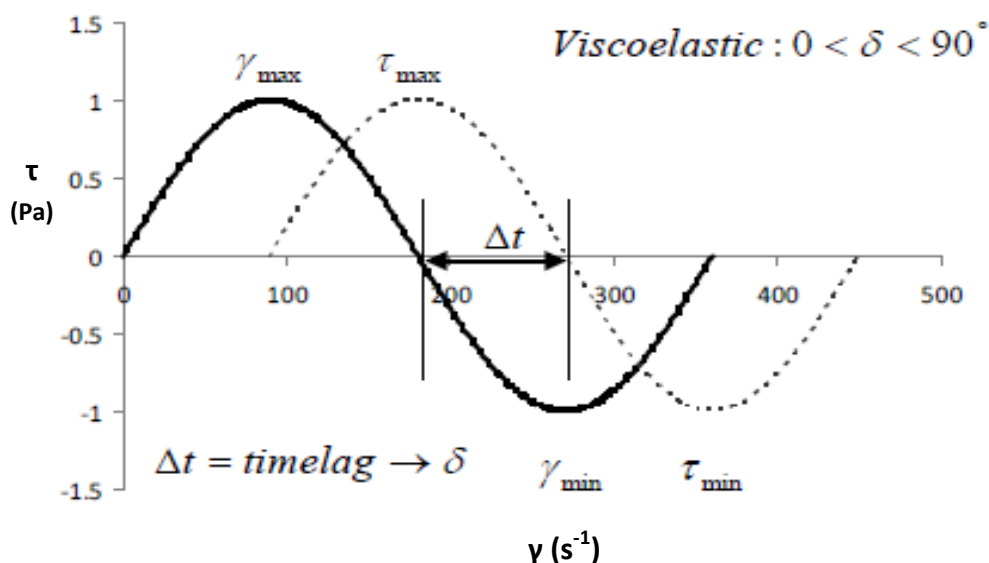
Figure 3.5: Viscoelasticity (Hesp, S. A. M.; Soleimani, 2009).

The LVR can be defined as the level where the complex modulus, drops to 90% of its original value (Dealy et al., 2006). The viscoelastic behaviour of the fluids is characterised by a critical oscillation value below which $G' > G''$, indicating highly structured solutions and above which G' progressively declines until G'' eventually exceeds it and the materials behave in a fluid-like manner.

The length of the LVR is a measure of stability; all further oscillation analysis was being performed within the LVR.

Frequency Sweep Test

After the fluid's linear viscoelastic region has been defines by the stress sweep test, its structure can be further characterised using a frequency sweep at a stress below the critical stress σ. This provides more information about how time affects the sample and the effect of colloidal forces and the interactions among particles. Materials usually become stronger (G'

increases) as the rate increases or the measurement time decreases. Cross over points for G'

and G'' are commonly used as an indication of the sample's relaxation time G'=G''.

The materials' response over a range of oscillation frequencies from 0.1-100 Hz, was

monitored at a constant temperature of 25oC and oscillation stress of 1 Pa, chosen from the

LVR region (determined from the stress sweep test). The frequency was plotted against the

complex modulus and phase angle δ, as shown in Figures 3.11 and 3.12, respectively.

Temperature Sweep Test

The temperature dependence of the steady and dynamic shear parameters was observed by

the conduction of a temperature sweep test. The samples were submitted to a shear rate of

$10s^{-1}$ and the stress was maintained at 1 Pa for a frequency of 1 Hz. (Figure 3.13).

3.2.3.2 Flow measurements

Steady State Flow Test

The final test to be performed was that of steady state flow, for estimating the apparent

viscosities of the different solutions. The fixtures used were 50 mm diameter, 0.0399 rad

cone and plate, with the cone truncated at 0.048 mm from its vertex; the tests were run by

taking ten points per decade. Measurements at each shear rate were made in both the

clockwise and counter clockwise directions, with the shear applied for 20 s and then

measurements of the torque and normal force averaged over the next 30 s. Before loading

each sample, the cone and plate fixtures were installed and set to a nominal gap of 1 mm; the

gap was then zeroed using the Autozero capability of the AR1000 rheometer. The

temperature control chamber was then opened, and the upper fixture was raised

approximately 60 mm. A sample was then transferred to the lower plate fixture using a 3 mL syringe. The upper cone fixture was lowered to a position of 0.040 mm and then the cone was repositioned to the specified gap of 0.048 mm; this procedure was used in an effort to compensate for the expansion of the sample and the fixtures when changing from room temperature to the test temperature of 25 °C. The total time for a single test was approximately 70 min, including the 10 min delay to ensure thermal steady state before measurements were begun.

Approximately 2 mL of each sample was placed on the plate and a pre-shear phase was used in order to ensure reproducible results; by pre-shearing the normal forced induced when the geometry is closing reduces and the results become more reproducible. The samples are fully hydrated and the previous history is destroyed enabling the measurement of the viscosity at a defined point. Heymann et al., (2002), found that differences between storage (G´) and loss moduli (G´´) were distinct when samples were pre-sheared; both moduli appeared to show higher values after oscillatory pre-shear. For gel-like fluids, pre-shear is applied in order to restore potential microstructural disruption in the tested fluid (Srinivasa et al., 1995). The authors showed that G´ increases with increasing the pre-shear strain.

During the conditioning step, the samples were set at equilibration for 2 min and were pre-sheared for 1 min at a shear stress of 100 s^{-1}. After the completion of the conditioning step, the pre-gelatinised samples were subjected to a constant temperature of 25°C and a frequency of 1 Hz, for a shear rate range of 0.01-1000 s^{-1}.

The data were best fitted by the Carreau rheological model (Figure 3.6), which describes a wide range of fluids; it is mostly used to fit viscosity data for middle to high range of shear rates. The model pieces together functions for Newtonian and shear-thinning ($\eta<1$) non-Newtonian laws and it is expressed as follows:

$$\frac{\eta - \eta_\infty}{\eta_o - \eta_\infty} = \left[1 + (c \cdot \dot{\gamma})^2\right]^{\frac{d-1}{2}} \tag{3.4}$$

Where c and d are the consistency and rate index constants, respectively and η_o and η_∞ are the viscosities at shear rate $\dot{\gamma} = 0$ and $\dot{\gamma} = \infty$ respectively.
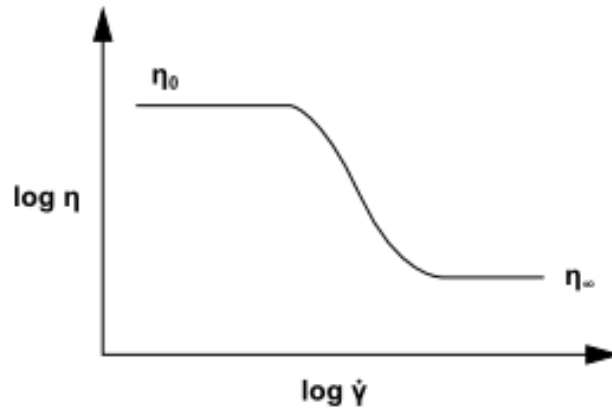
Figure 3.6: Variation of viscosity with shear rate, according to Carreau model.

The figure shows how viscosity is limited by η_o and η_∞ at low and high shear rates, respectively.

The viscosities were estimated based on equation 3.4 for a shear rate of $10\mathrm{s}^{-1}$ which belongs to the shear rate range used for food products (10^0-10^2) (Somwangthanaroj, 2010).

The specific heat (C_p) and thermal conductivity (k) of the starch solutions were estimated based on equations 3.5 and 3.6 respectively, as a function of their moisture content (Peleg, Normand, and Corradini, 2012).

$$C_p = 4.19 \cdot M/100 + 0.84 \cdot (100 - M)/100 \ (\mathrm{kJ \ kg^{-1} \ K^{-1}}) \tag{3.5}$$

$$k = 0.55 \cdot M/100 + 0.26 \cdot (100 - M)/100 \quad (\mathrm{W \ m^{-1} \ K^{-1}}) \tag{3.6}$$

Where: M is the percentage moisture content on a wet basis

The specific heat of the cream of tomato soup was estimated based on equation 3.7 (Choi and Okos, 1983), taking into account the composition of the solid components contained in the soup.

$$C_p = 4.180 \cdot X_w + 1.711 \cdot X_p + 1.928 \cdot X_f + 1.547 \cdot Xc + 0.908 \cdot X_a \ (\text{kJ kg}^{-1} \text{K}^{-1}) \qquad (3.7)$$

Where: X is the mass fraction of each component and w, p, f, c and a, correspond respectively to water, protein, fat, carbohydrates, and ash.

When data are not available, the thermal conductivity of biological materials such as the cream of tomato soup can be estimated based on the water content. According to Anderson (1950), the thermal conductivity can be estimates as follows;

$$k = k_w \cdot X_w + k_s \cdot (1 - X_w) = 0.056 + 0.57 \, X_w \qquad (3.8)$$

Where: k_w is the thermal conductivity of water and k_s is that of the solid portion.

Finally, the densities of all fluids were measured/weighed on an Analytical Balance (Sartorius ENTRIS224-1S, Massachusetts). The viscosities and thermal properties of the fluids tested are presented in Table 3.2.

During the experiments, a solvent trap was used to minimise solvent loss.

All oscillatory and flow tests were repeated at least five times and the average was taken for analysis.

3.2.4   Mathematical modelling

The steady state of free convection in a rectangular cavity filled with the model fluids used in the experiments was studied by developing a mathematical model. COMSOL Multiphysics 4.3b (COMSOL Ltd, Cambridge, UK) was used to set up a convection model; the model calculates the steady state velocity and temperature field with a predefined non-isothermal flow interface which couples the heat transfer and fluid dynamics, provided in the Heat Transfer Module.

The geometry and boundary conditions are shown in Figure 3.7. The cavity is consisted of impermeable walls, i.e. with a zero flow boundary condition. To generate the buoyancy flow, the left and right edges of the cavity were set at 20 and 30°C, respectively; the temperature difference produces the density variation that drives the buoyant flow. The choice of the two temperatures was random, since the parameter of interest was the temperature difference, rather than the temperatures themselves. The goal of the developed model was to indicate whether there is natural convection occurring in fluids of a specific viscosity or not. The specific model was not aiming at mimicking the experimental conditions. Based on the results obtained from the simulations, a new model was developed including the module of natural convection, when the actual experiment was predicted.

The upper and lower boundaries are insulated i.e. zero heat flux boundary condition.

No-slip fluid boundary conditions were applied resulting in zero velocity at the wall, with pressure remaining unidentified; the model contains information only about the pressure gradient and it estimates the pressure field up to a constant (Incropera, 2006). Thus, in order to define that constant and achieve convergence, the initial pressure field is set to be consistent with the volume force. The initial pressure field must be also consistent with the

pressure constraint, which is arbitrary fixed at a point setting of $p = 0$, at the left, top surface; that is necessary for defining a well-posed model.

The volume force and initial pressure, which accounts for the hydrostatic pressure in the fluid column, are expressed as follows:

$$F = -\rho_o \cdot g \cdot \beta \cdot (T - T_o) \tag{3.9}$$

$$p_o = -\rho_o \cdot g \cdot (H - y) \tag{3.10}$$

Where: T, T_o, g, ρ_o, and β represent the temperature, reference temperature, gravity acceleration, reference density, and the volumetric thermal expansion coefficient, respectively. p_o, H and y are the reference pressure, the geometrical height, and the horizontal reference location, respectively.
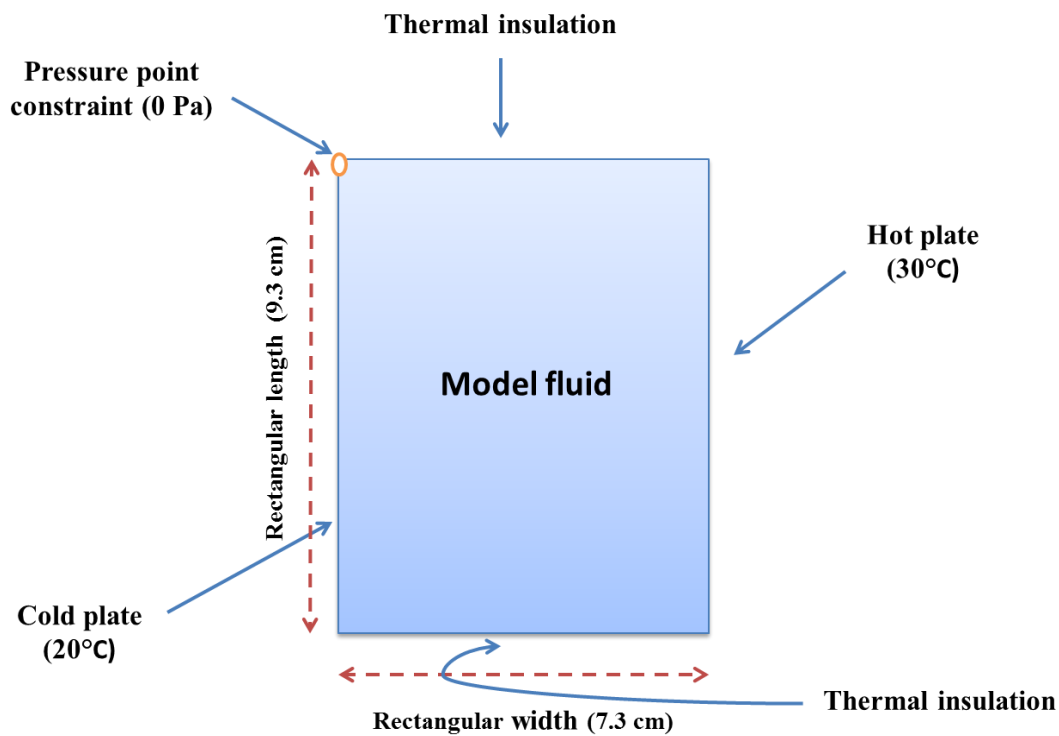
Figure 3.7: Domain geometry and boundary conditions of the rectangular cavity.

The Boussinesq buoyancy term that appears on the right-hand side of the Navier-Stokes equations accounts for the lifting force due to thermal expansion:

$$\rho(u \cdot \nabla)u = -\nabla p + \nabla \cdot \mu \cdot \left(\nabla u + (\nabla u)^T\right) + \rho_o \cdot g \cdot \beta \cdot (T - T_o) \tag{3.11}$$

$$\nabla \cdot u = 0 \tag{3.12}$$

Where: u and p is the vector of fluid velocity and pressure (dependent variables for the flow), respectively, and μ represents the dynamic viscosity.

The heat balance is expressed through the steady state conduction-convection equation:

$$\rho_o \cdot C_p \cdot u \cdot \nabla T - \nabla \cdot (k \cdot \nabla T) = 0 \tag{3.13}$$

Where: k is the thermal conductivity and C_p is the specific heat capacity of the fluid.

It is important to choose how fine the mesh needs be in order to resolve the velocity and temperature gradients and ensure the results are mesh independent. An extra fine grid was used for the domain whilst extra elements were added at the boundaries due to greater velocity and temperature variations adjacent to the walls. The complete mesh consists of 4474 domain and 188 boundary elements, and the convergence criterion used was 10^{-8}.

3.2.4.1 Model analysis

Before any simulations are started the flow regime needs to be estimated; that is achieved by using non-dimensional parameters such as the Prandtl, Grashof and Rayleigh numbers. They are calculated using the thermo-physical properties of the model solutions listed in Table 3.2.

The thermo-physical properties are given at 25$^{\text{o}}$C which is in the range of the temperatures used in the model.

In fluid mechanics working with non-dimensional numbers is a common and convenient way to reduce the number of dependent and independent parameters. The non-dimensional numbers used in the current work are the following:

The **Prandtl number**, **Pr**, is defined as the ratio of fluid viscosity to thermal diffusivity and it is expressed by:

$$\Pr = \frac{\nu}{\alpha} = \frac{c_p \cdot \mu}{k} \tag{3.14}$$

Where:
$$\alpha = \frac{k}{\rho \cdot C_p} \tag{3.15}$$

α = thermal diffusivity (m^2 s^{-1}), C$_p$ = specific heat (J kg^{-1} K^{-1}), ν = kinematic viscosity (m^2 s^{-1})=μ/ρ (dynamic viscosity/density).μ= dynamic viscosity (Pa s), and k = thermal conductivity of the fluid (W m^{-1} K^{-1}).

The **Reynolds number**, **Re**, is defined as the ratio of inertial forces to viscous forces and it is used to predict the flow regime of the fluids; it is expressed by the following expression:

$$\Re = \frac{\rho \cdot U \cdot L}{\mu} \tag{3.16}$$

Where: U is the typical velocity (m s$^-$1) and L the typical length (m)

When a viscous fluid flows along a fixed impermeable wall, the velocity at any point on the wall will be zero due to the no-slip condition. The extent to which the boundary layer at the wall develops along the length of the wall depends upon the value Re, and hence on the viscosity.
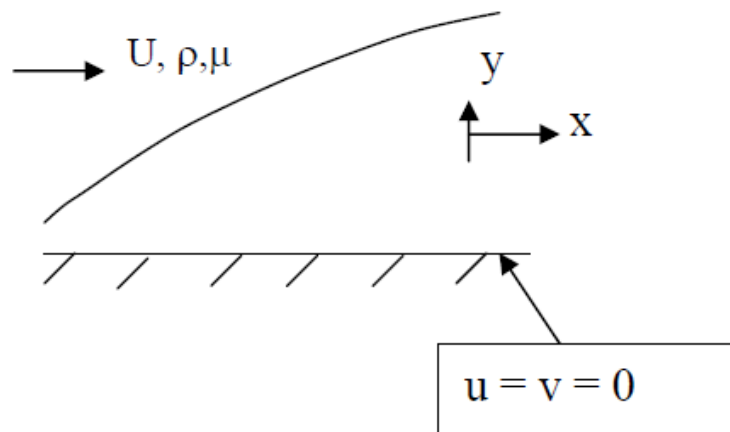
Figure 3.8: No-slip condition and boundary layer development.

Where: u and v are the velocities (m s^{-1}) at the wall along x and y, respectively.

The viscosity of the model fluids used in the current work is high and the flow is in the laminar/transitional regimes. Hence the boundary layers are important; the fluid velocity within the boundary layers changes rapidly from zero to its main-stream value possibly implying a steep gradient of shear stress (Burr, 2010). The majority of the resistance to heat transfer takes place within the boundary layer, whilst the pressure distribution throughout it remains constant.

The velocity boundary layer thickness can be defined as the distance from the wall at which the viscous flow velocity is 99% of the free stream velocity and can be obtained in terms of the Reynolds number, using the following equation:

$$\delta_M \approx \frac{L}{\sqrt{Re}} \tag{3.17}$$

The thermal boundary layer, δ_T, which similarly to the velocity boundary layer is the distance from the wall, at which the temperature is 99% of the temperature found at the region where the fluid stabilises, can be defined by the Prandtl number.

For Pr>>1, the ratio of the two thicknesses is governed by the following equation:

$$\frac{\delta}{\delta_T} = \sqrt{\text{Pr}} \qquad (3.18)$$

The **Grashof number**, **Gr**, is defined as the ratio of buoyancy to viscous forces and it is described as follows:

$$Gr = \frac{\rho^2 g\beta(T_s - T_\infty)L^3}{\mu^2} \qquad (3.19)$$

Where: g = acceleration due to Earth's gravity (m s^{-2}), β = volumetric thermal expansion coefficient (K^{-1}), T_s = surface temperature (K), T_∞ = bulk temperature (K), L = the distance between the highest (bulk) and lowest temperature (headspace) along the cylinder (m).

The volumetric thermal expansion coefficient was estimated based on the Boussinesq approximation, as expressed by Adrian, (1993):

$$\beta = -\frac{1}{\rho}\frac{\Delta\rho}{\Delta T} \qquad (3.20)$$

Where: $\Delta\rho = \rho_\infty - \rho$ (kg m^{-3}) and $\Delta T = T_\infty - T$ (^{o}C) between the bulk of the fluid and the headspace.

The Grashof number can also be expressed as the velocity ratio:

$$Gr = \frac{U_0{}^2}{\left(\mu/(\rho \cdot L)\right)^2} \qquad (3.21)$$

Where U_o = typical velocity due to buoyancy forces, defined by:

$$U_0 = \sqrt{g \cdot \beta \cdot \Delta T \cdot L} \qquad (3.22)$$

The critical Grashof number value that indicates the transition between laminar (larger buoyancy forces) and turbulent (larger viscous forces) flow is 10^9.

The **Rayleigh number**, **Ra**, is another indicator of free convection, and is defined as:

$$Ra_L = \frac{\rho^2 \cdot g \cdot \beta \cdot \Delta T \cdot L^3}{\mu \cdot \alpha} = Gr_L \cdot Pr_L \qquad (3.23)$$

Like the Grashof number, a critical Rayleigh value indicates the transition between laminar and turbulent flow, which is about 10^9.

The viscous forces limit the buoyancy effects and may result in an overestimated typical velocity, obtained by U_o. Thus, another approach, where the thermal diffusivity and viscosity of the fluids are included should be more accurate in estimating the typical velocity. U_1 is used instead and is defined as follows:

$$U_1 = \frac{\alpha}{L} \cdot \sqrt{Ra} \qquad \text{or} \qquad U_1 = \frac{U_o}{\sqrt{Pr}} \qquad (3.24)$$

The Grashof and Rayleigh numbers need first to be calculated in order to characterise the flow regime. If they are significantly below the critical order of 10^9, the regime is laminar and in that case Equation 3.21 or Equation 3.24 provide estimates of the typical velocity U that can be used to validate the model after performing the simulation.

3.3   Results and Discussion

3.3.1   Rheology

The model fluids' (A, B, C, and T) response to increasing stress was monitored by the stress sweep test, see Figure 3.9; the samples were subjected to small amplitude oscillatory shear. Initially the applied stress is low and the material structure is preserved, but as the test progresses, the increased stresses cause disruption, which is demonstrated by a decrease in elasticity, with a phase angle (δ) rise (Figure 3.10), and a decrease in rigidity, which is expressed by the complex modulus (G*).

The LVR of the solutions was defined for a constant frequency of 1 Hz and a temperature of 25°C, and it lies in the range of 0.01-1 Pa, 0.01-1.5 Pa, 0.01-2 Pa, and 0.01-6 Pa for solutions A, B, C and T, respectively. The longer the LVR, the more stable the system is, expecting the solution of 5% starch (C) to show higher resistance in amplitudes of stress, strain, frequency or temperature when those are applied.

The value of oscillation stress chosen for subsequent testing was 1 Pa, which is below the critical oscillation stress for all fluids (1, 1.5, 2 and 6 Pa for A, B, T and C, respectively) and consequently lies within their LVR region.
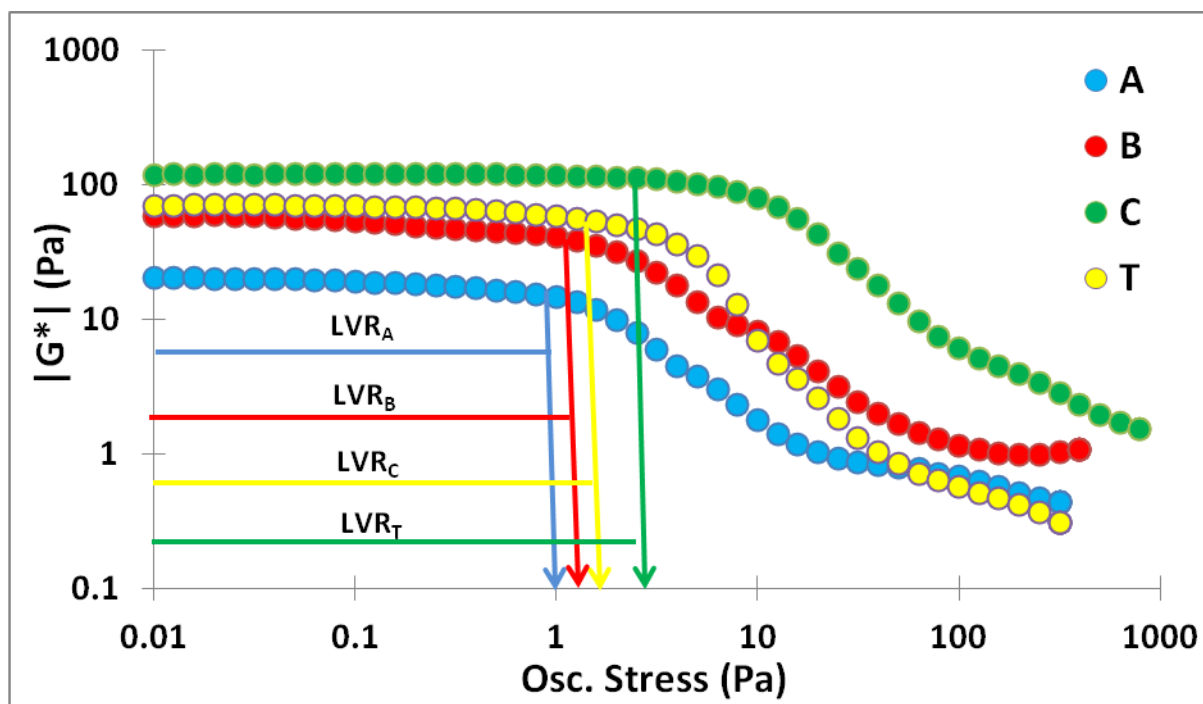
Figure 3.9: Oscillation stress sweep test.

The phase angle was also plotted against the oscillation stress, shown in Figure 3.10, in order to confirm that the drop in complex modulus was due to a decrease in elasticity. The samples exhibit constant phase angle until the critical stress value, and afterwards they increase towards being progressively more viscous. The phase angle starts increasing for each solution at 1, 1.5, 2 and 6 Pa, the critical values that G* (elasticity) starts decreasing and the material exits the LVR. The gel point, which is indicated by a phase angle of 45°, of A, B and T, and C, is observed at 2, 5 and 11 Pa, respectively, where the values of elastic (G´) and viscous (G´´) modulus cross (i.e. G´= G´´).
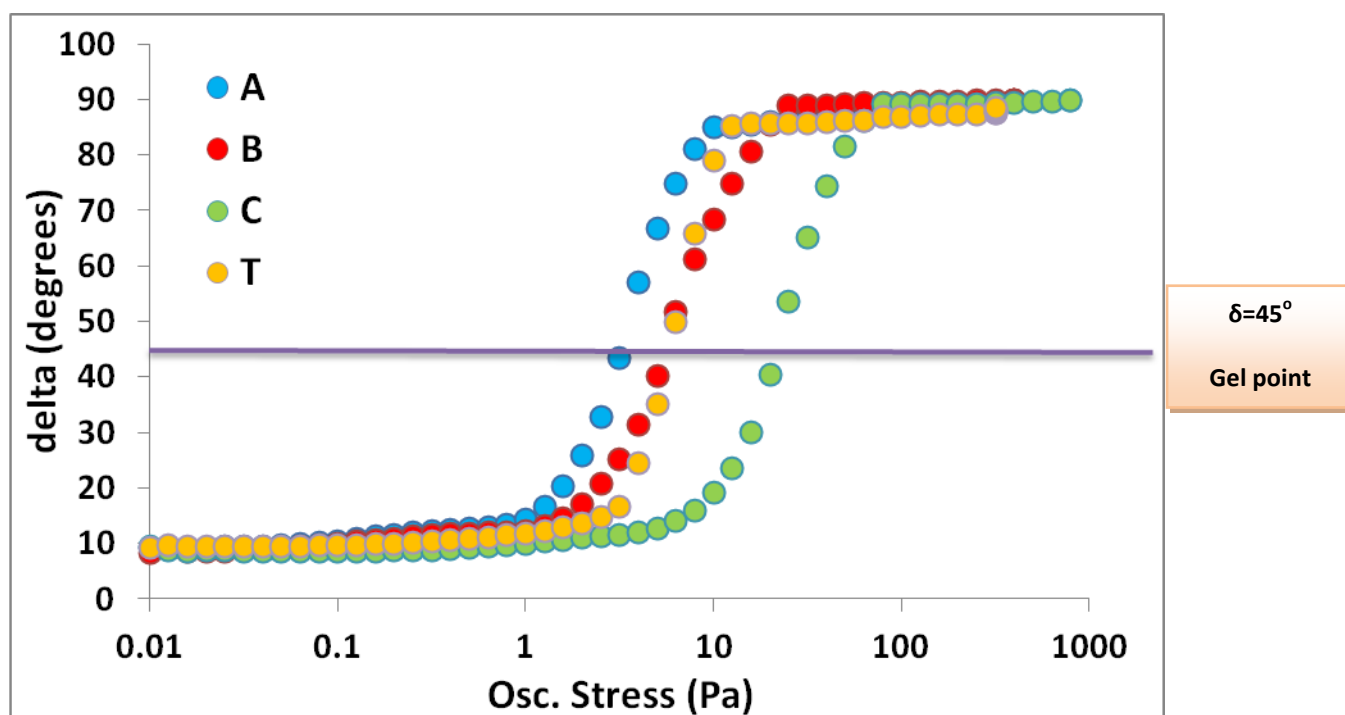
Figure 3.10: Oscillation stress sweep test with phase angle.

After the LVR region was defined, the fluids were further characterised by a frequency sweep test at an applied stress of 1 Pa, chosen from the stress sweep test, at a constant temperature of 25°C and a frequency range of 0.01 to 100 Hz.

Figure 3.9 suggests that the complex modulus of solution A is highly dependent on the frequency, especially after 4 Hz. That leads to the conclusion that the fluid becomes more elastic, as the frequency applied increases. Between 1 and 4 Hz, solution A behaves like a gel, as $1 > \tan \delta > 0.5$, as illustrated in Figure 3.10. The fact that $\tan \delta < 1$, means that there is no crossover point of G' and G'' over this frequency range. The structure of fluid A becomes weaker with increasing frequency, and sedimentation is more likely to occur.

The point where $G' = G''$ or $\tan \delta = 1$, the viscoelastic behaviour changes from a dominant elastic solid-like ($G' > G''$) to viscous liquid-like ($G'' > G'$), is called the gel point. Fluids B and T remain independent of frequency up to 10 Hz, they increase slightly from 10 to 40 Hz and then they show a peak at 100 Hz. They start behaving gel-like after 11 and 12 Hz,

respectively (1 > tan δ > 0.5), and there is no cross point of the elastic and viscous modulus at any point throughout the test (tan δ < 1).

When 1 > tan δ > 0.5, the material tested behaves gel like (Augusto, 2012).

Solution C is the most stable, as expected from the stress sweep test (the longest LVR). G* is independent of frequency throughout the test, and tan δ range is the lowest of all fluids (tan δ < 0.5); it is the most elastic fluid. Fluids B, T, and C have strongly associated particles, and sedimentation is unlikely to occur. The storage modulus (G´) is higher than the loss modulus (G″), for all fluids, along the whole frequency range studied, which indicates that the fluids have dominant elastic properties rather than the viscous ones. Thus, the product can be classified as weak gels (Rao, 2005). This kind of behaviour is mostly observed in suspensions with network-like structure, such as fruit products, tomato products and fruit purees (Massa et al., 2010). The frequency chosen to be used for subsequent tests was 1 Hz, a value at which all the fluids are frequency independent and more stable.
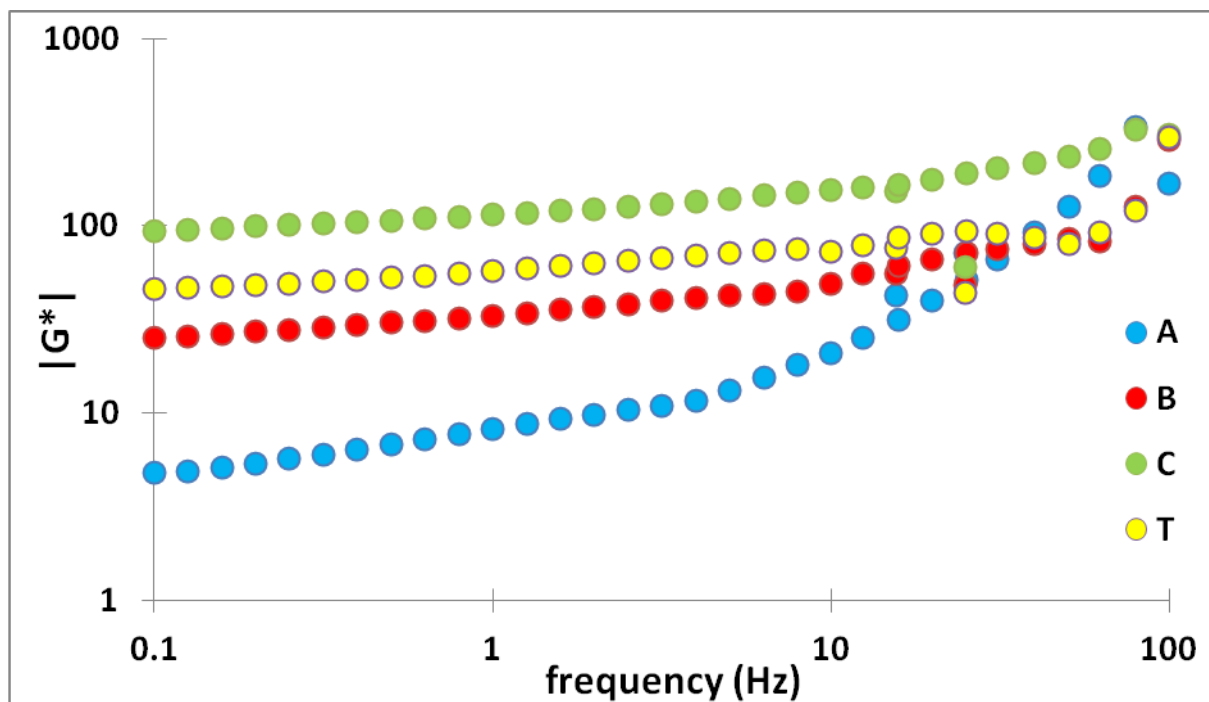
Figure 3.11: Frequency sweep test at 25°C and oscillation stress 1 Pa.
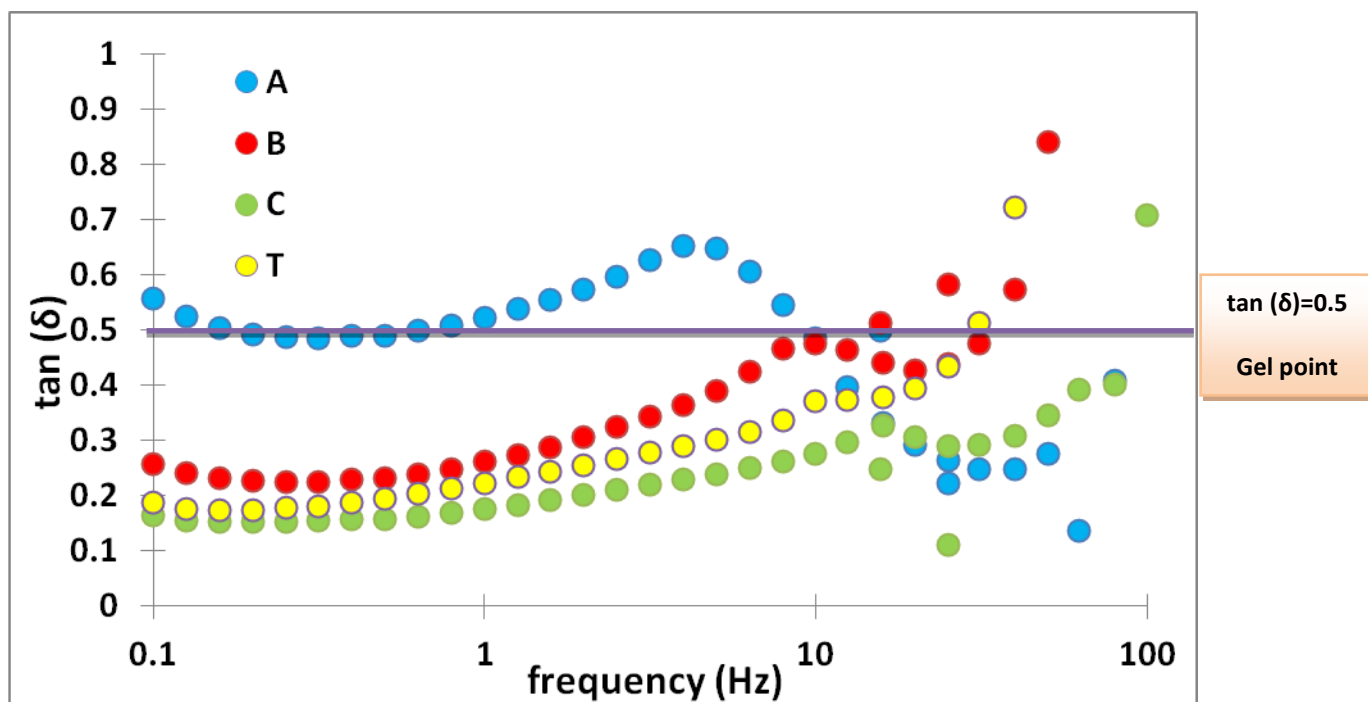
Figure 3.12: Frequency sweep test at 25^oC and oscillation stress 1 Pa with phase angle.

For the temperature sweep test, the model foods were prepared at room temperature and were heated up on the Peltier plate of the rheometer for 40 min at a temperature range between 25 and 85^oC, at a rate of 5^oC min^{-1}. The stress and frequency were maintained at 1 Pa and 1 Hz, respectively. The temperature was plotted against the complex modulus, Figure 3.13, and the tangent phase angle, Figure 3.14. As the temperature increases, the complex modulus (G*) remains constant until the fluids start gelatinising and reach the maximum viscosity and volume at approximately 85^oC.

Starch granules, when heated in excess water (i.e., water-starch ratios > 1.5:1) lose their molecular order in an irreversible way (gelatinisation), resulting in an increased granule hydration, swelling and possibly the leaching of soluble components, such as amylose. The hydrated molecules progressively vibrate, inducing hydrogen bonds disruption, which eventually leads to the plasticisation of the starch molecules within granules. If the starch concentration present is sufficiently high (typically 2–7%), the granules swell and start to

press against one another, until they occupy nearly the entire volume of the aqueous phase, leading to significantly increased viscosity (BeMiller, 2009).

In the current work, waxy maize starches are used, which are primarily consisted of amylopectin. This means that they gelatinise more easily and yield solutions that cannot form firm gels, as they have relatively short branch chains; amylopectin molecules retrograde very slowly (Shim, 2001). For the performance of the test, the shear rate was kept constant at $10s^{-1}$ and a frequency of 1 Hz. No crossover point was observed for G′ and G″, with G′ > G″ throughout the temperature range. This means that the fluids' behaviour is predominantly elastic and they are in between the elastic and perfectly viscoelastic state (tan δ < 0.5) for most of the process.

Solutions A and C start gelatinising at $72^{o}C$ and after $75^{o}C$, with tan δ > 0.5, they behave more gel-like. Solutions B and T gelatinise around $65^{o}C$ and are affected less by temperature increase.
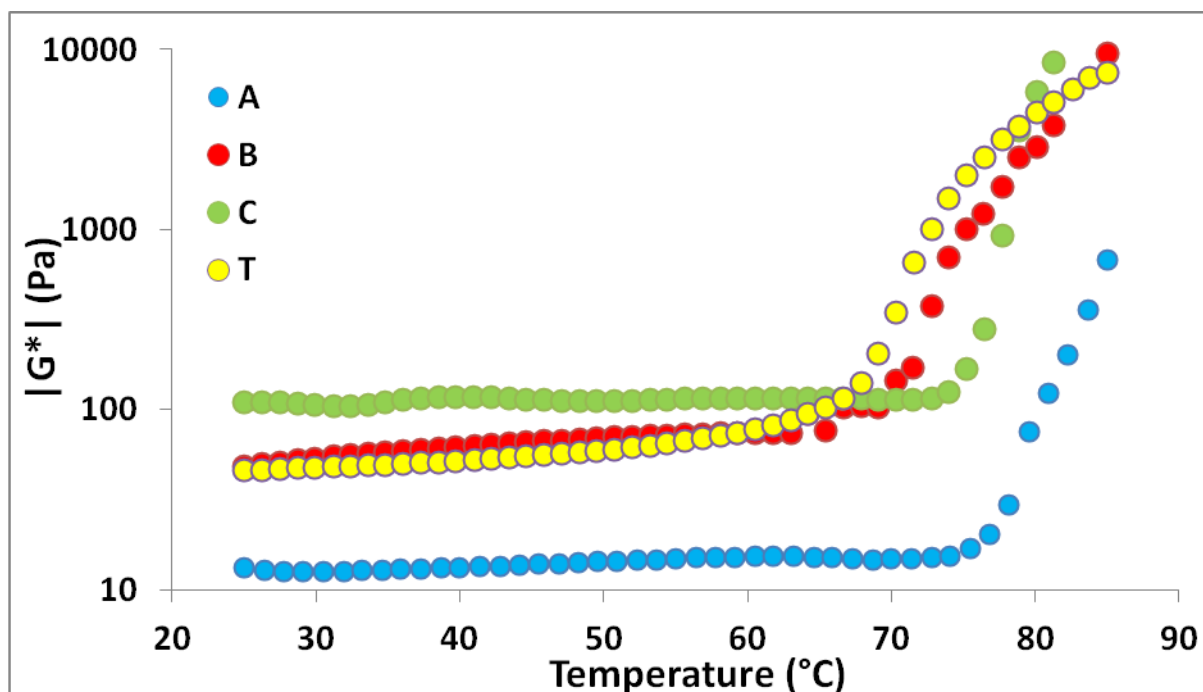
Figure 3.13: Temperature sweep step at 1 Pa stress and f=1 Hz.
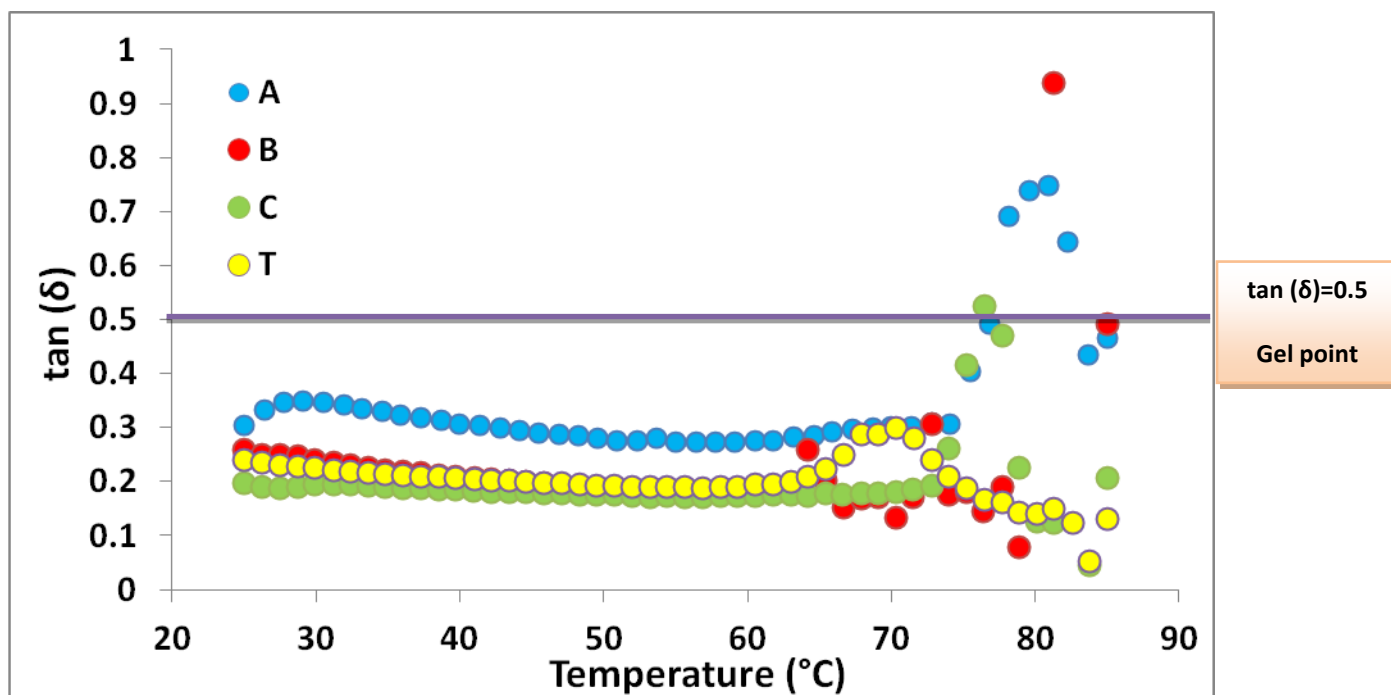
Figure 3.14: Temperature sweep step at 1 Pa stress and f=1 Hz with phase angle.

Fluid A seemed to consistently escape the rheometer plate by the end of the experiments, making it behave in a different way than the rest of the fluids. The oscillation stress used for all fluids and experiments was 1 Pa, which is very close to the critical stress of fluid A; that can possibly explain the fluctuating behaviour of the fluid (the shortest LVR).

The fact that the fluid is the least elastic one, can also mean that the centrifugal forces are created which throw the volume elements outwards.

A smaller amount of sample (< 2 mL) would probably be a way of solving the problem (less sample to escape).

The steady state flow test used for estimating the apparent viscosities of the different solutions was conducted at a constant temperature of $25^{o}C$ and a frequency of 1 Hz a shear rates range between 0.01 and 1000 s^{-1}, as shown in Figure 3.13. All fluids show a shear-thinning behaviour (n < 1) and the model parameters for each fluid are shown in Table 3.1;

Once the model fluids were rheologically characterised, their thermal properties were then estimated. Based on equations 3.4 to 3.8, the dynamic viscosity at $\gamma = 10 \text{ s}^{-1}$ and the thermal properties of the fluids used are described in Table 3.2.

Table 3.1: Model parameters of the fluids used.

Fluid	η_∞ (Pa. s)	η_0 (Pa. s)	c (s)	d	At $\gamma=10\text{s}^{-1}$
A	0.064	598.6	2172	0.749	0.3 Pa s
B	0.224	1420	2589	0.734	1.0 Pa s
C	0.360	7212	2600	0.760	3.3 Pa s
T	0.076	4533	2651	0.818	1.3 Pa s

Table 3.2: Thermal properties of fluids used.

Model fluid	k (W m^{-1} K^{-1})	C_p (kJ kg^{-1} K^{-1})	ρ (kg m^{-3})	η (Pa. s) at $\gamma=10$ (s^{-1})
A	0.26	4.008	1010	0.30
B	0.26	4.005	1043	1.00
T	0.28	3.670	1034	1.30
C	0.26	4.001	1065	3.30
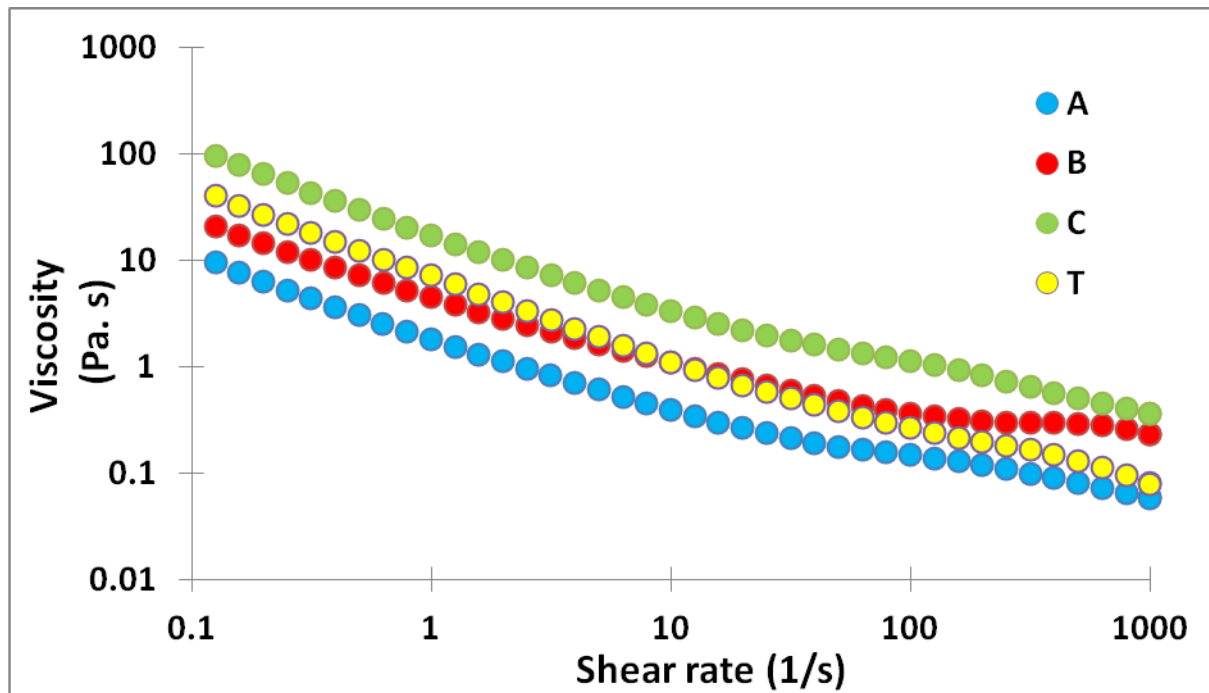
Figure 3.15: Steady state flow at $\gamma = 10$ s^{-1} and T = 25°C

3.3.2   Numerical simulations

As indicated in §3.2, the flow regime of the fluids in a rectangular cavity consisted of a cold and hot wall and insulated bottom and top surface, was examined by calculating the dimensionless Grashof, Rayleigh, Prandtl and Reynolds numbers. From the results obtained the Ra number for all four model fluids belongs to the range $10^4 < \text{Ra}_L < 10^9$ and thus laminar regime is expected; according to LeFevre, (1956), the above range indicates the occurrence of laminar natural convection. Heat transfer is conduction dominated until a critical Ra number is reached; according to Heslot et al. (1987) and Henkes (1990), that critical Ra number equals to 1708. By increasing the temperature difference, the Ra number is increased and the flow pattern changes.

Experiments conducted from the above authors in cylindrical geometries and square cavities heated from the vertical walls and insulated from the horizontal ones, support that for $6 \times 10^3 <$

Ra $<1.5\times10^5$ laminar convection occurs, whilst from 1.5×10^5 to $2.5\times10^{5,}$ the flow becomes chaotic; turbulence appears at a Ra $\geq 10^6$.

According to the values estimated in the current work and based on the above findings, steady laminar convection is expected by fluids T and C, the most viscous ones, whilst a more chaotic behaviour is expected by fluid B and especially by fluid A. The typical velocity (U_1) was estimated to be in the range of 0.3 to 1 mm s^{-1}, with the lowest and highest value corresponding to fluids C and A, respectively; the least viscous solution, fluid A, appears to reach a velocity up to three times higher than the rest of the fluids, making the occurrence of convection more possible and/or evident as compared to the rest of the fluids.

The dimensionless parameters and typical velocities for each model fluid are presented in Table 3.3.

Table 3.3: Dimensionless numbers and velocity used in heat treatment.

Fluid	Gr	Pr	Ra	Re	U_1 (mm s^{-1})
A	200	3.7×10^3	7.0×10^5	0.2	1
B	20	1.3×10^4	2.0×10^5	0.04	0.5
T	10	1.6×10^4	1.5×10^5	0.03	0.4
C	2	4.0×10^4	7.0×10^4	0.01	0.3

The simulated data were presented in terms of velocity magnitude and temperature isotherms for a temperature difference of 10°C between the cold and hot vertical wall, for all the model fluids as illustrated in Figures 3.16 and 3.17, respectively.

The highest velocity values for all fluids appear to be located at the lateral boundaries where the highest variations of temperature occur, indicating that the natural convection occurs from the boundaries. The maximum velocity values for fluid A, B, T and C is 1.3, 0.4, 0.4 and 0.1

mm s^{-1}, respectively; the velocities are of similar order of magnitude to the estimated typical

velocities U_1 of the order 1, 0.5, 0.4 and 0.3 mm s^{-1} shown in Table 3.3.

A)   B)

T)   C)
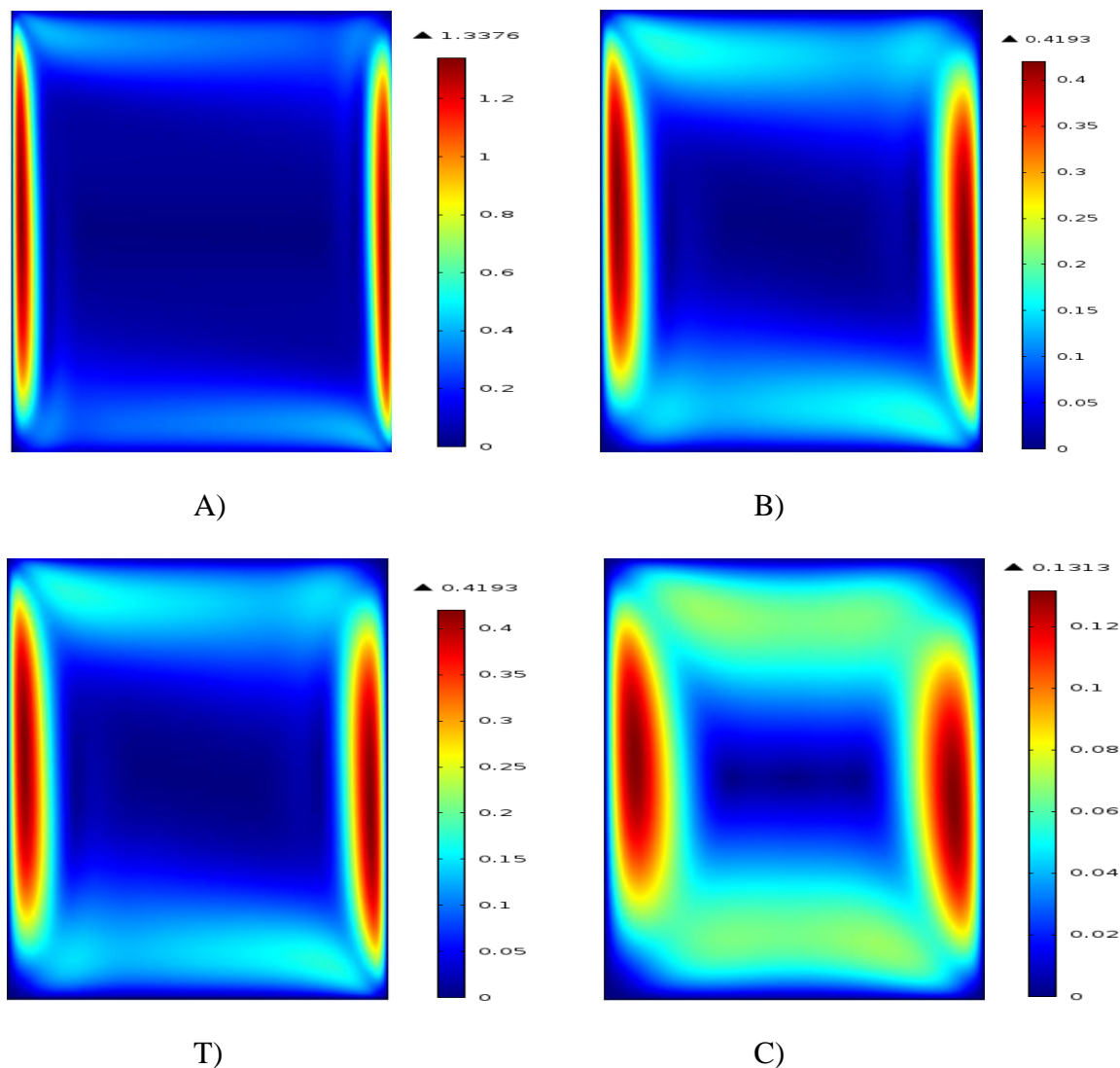
Figure 3.16: Velocity magnitude (mm/s) of A, B, T and C fluids at $\Delta T = 10^{o}C$.

Figure 3.17 shows the temperature field (surface) and velocity field (arrows) of the 2D

model. The fluid flow seems to follow the boundaries, with the highest variations observed at

the boundaries, especially at lateral walls, which are responsible for the free convection; the

temperature and velocity variations are smoother at the core of the fluid, with the most

viscous one (fluid C) showing a more distinct separation of the cold and hot zone; that is due

to the fact that fluid C cools down the slowest, since it records the lowest velocity at the boundaries.

A)

B)

T)

C)
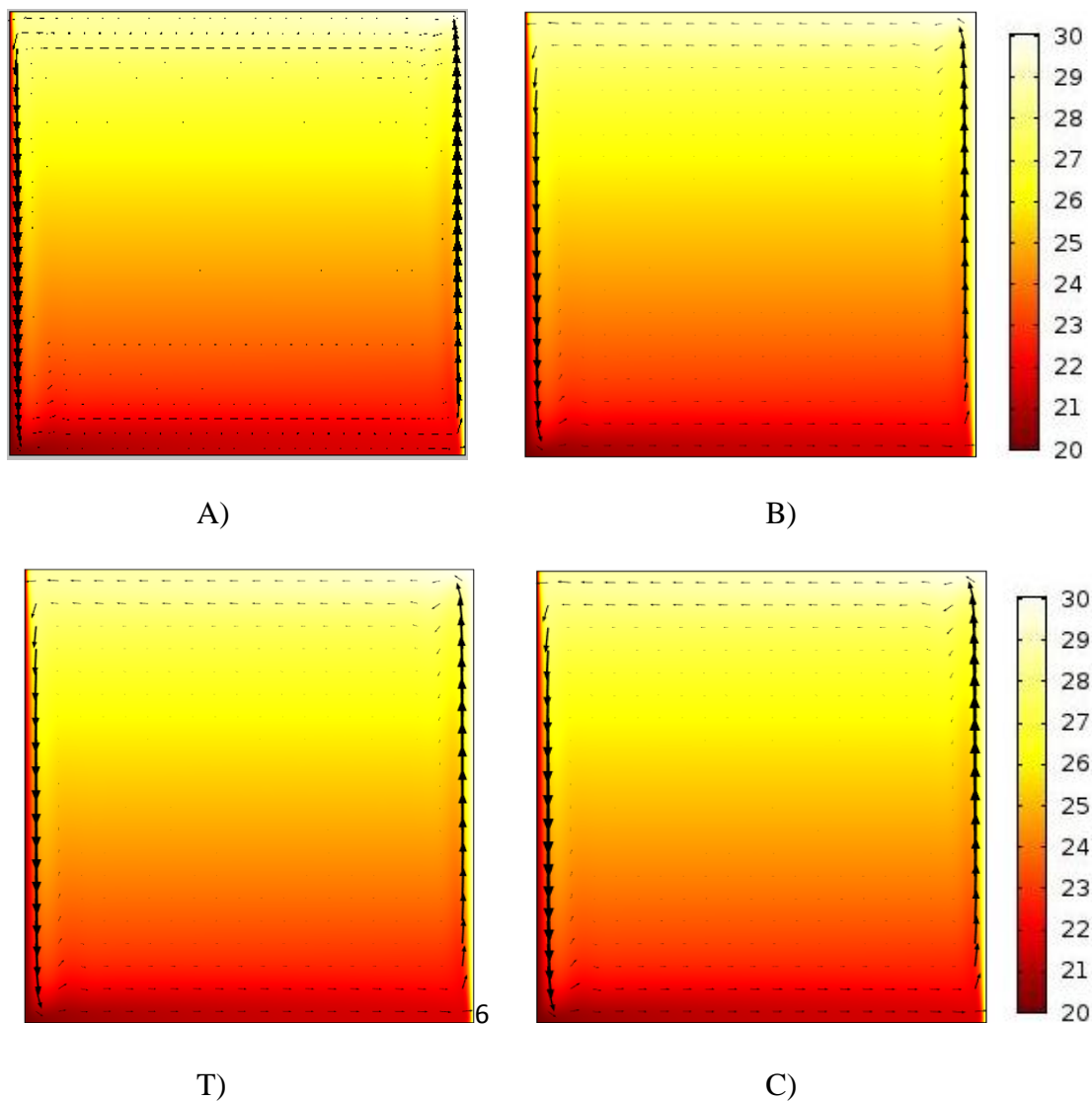
Figure 3.17: Temperature field (surface plot) and velocity (arrows) of A, B, T and C fluids at ΔT = 10°C.

The momentum layer thickness at the left boundary was plotted against velocity, as illustrated in Figure 3.18. The thickness of fluid A was estimated to be of order 4 mm, whilst for fluids B, C and T it was approximately 9 mm. The results are expected, as the velocity of fluid A is significantly higher than the rest of the fluids, leading to a higher Re number and consequently to a lower boundary layer thickness, according to Equation 3.14.
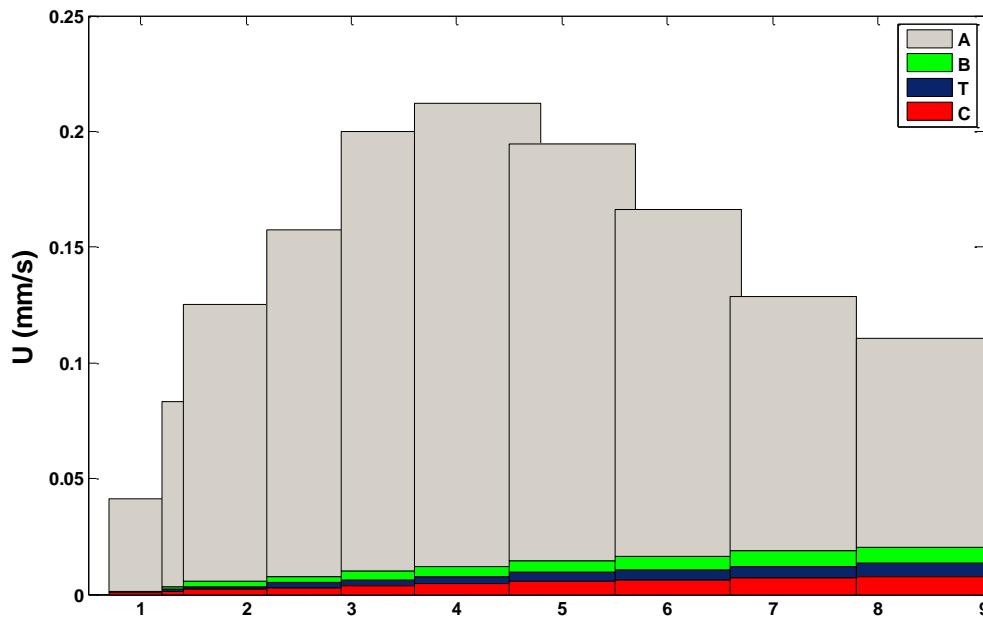
Figure 3.18: Velocity profile of the model fluids at the left boundary, at $\Delta T = 10^{o}C$.

Kumar and Bhattacharya (1991) reported that the thickness of ascending viscous liquids near the wall was greater than that for Newtonian fluids such as water, attributed to the large viscosity difference between the fluids.

In the current work, the temperature profile of the fluids was plotted against the thickness at the left boundary, Figure 3.19, resulting in values from 2.5 to 4.5 mm for the least viscous (fluid A) and most viscous fluid (fluid C), respectively. The results confirm the findings of Kumar and Bhattacharya, although the viscosity difference of the fluids is not that significant as in the case between Newtonian and non-Newtonian fluids.
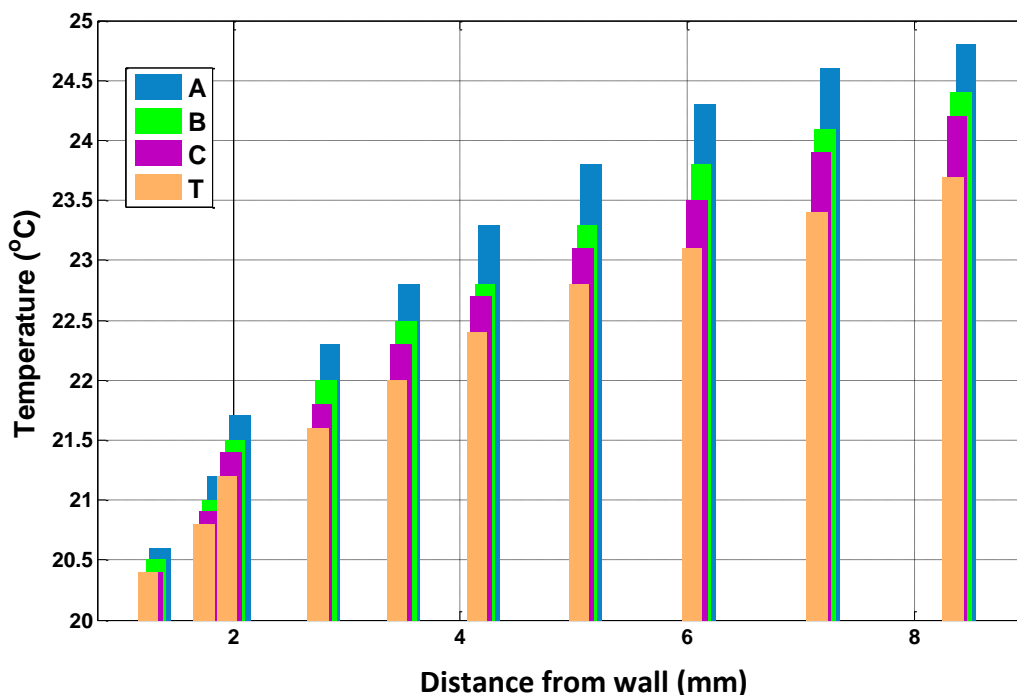
Figure 3.19: Temperature profile of the model fluids at the left boundary, at $\Delta T = 10^{o}C$.

According to the results and observations obtained from the numerical simulations, laminar convection is expected to occur in all fluids through the vertical walls and be more profound in fluid A during the hot-fill treatment; the heating/cooling temperatures and consequently the process values calculated for the headspace and the lid of the package should be higher in fluid A.

If the convection is turned off, the temperature and velocity distribution is significantly different, as illustrated in Figure 3.20. Without the temperature difference, no buoyancy occurs and the fluid is static; the velocity magnitude is almost zero. Conduction is the dominating mechanism occurring and consequently the fluid is treated as a solid.

The same conclusions are drawn for the rest of the fluids.
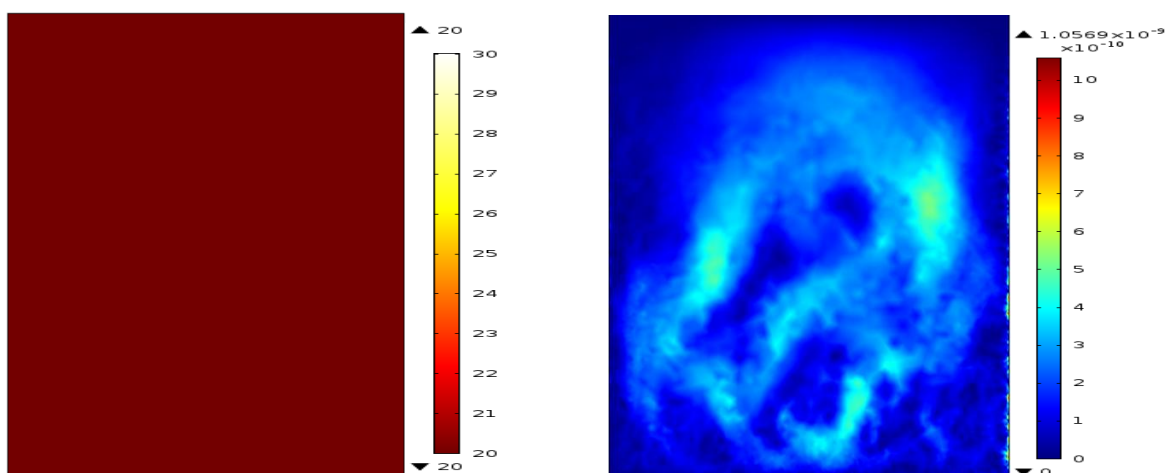
Figure 3.20: Temperature field and velocity magnitude (mm/s) of fluid A, with $\Delta T = 0^{o}C$, between the two walls (Figure 3.5).

3.3.3   *Effectiveness of the inversion method*

The recorded time-temperature history of the model fluids at the six different locations inside the inverted and non-inverted jars, are illustrated in Figures 3.21-3.23.

The temperature at the bottom and corner of the non-inverted jars is recorded to be the lowest for fluid A and the highest for fluid C, which is expected since the least viscous fluid cools down faster. That is confirmed by the estimated higher velocity and consequently higher heat transfer within fluid A, shown in Table 3.3. As far as the inverted jars are concerned, an average temperature drop of 1, 2, 2 and $3^{o}C$ is recorded for fluids A, B, T and C, respectively since the two locations are exposed to air for 30 seconds; the highest drop, $3^{o}C$ is observed for fluid C which exhibits the lowest heating rate.
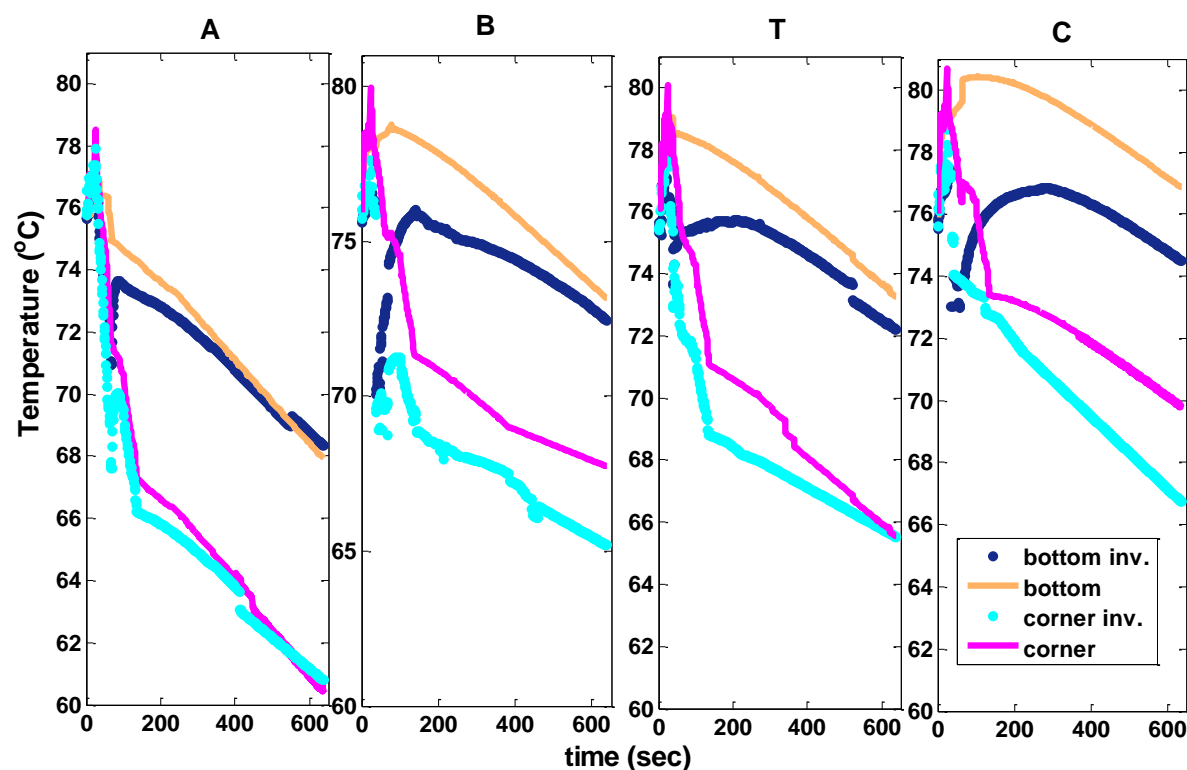
Figure 3.21: t-T profiles of fluids A, B, T and C at the bottom and bottom-corner of the inverted and non-inverted jars.

At the core of the fluids and the wall of the package there is a small temperature drop of 0.3-1°C for fluids A and B, whilst there is almost no difference observed in the more viscous fluids T and C. The temperature drop is expected since the flow is moving due to inversion and some energy is exchanged between the cold and hot regions. The temperature at the bulk remains almost constant throughout the process, as it is the furthest location from the wall and it cools down the slowest. Almost two hours were required for the core of the fluid to reach the cooling medium temperature of 20°C.
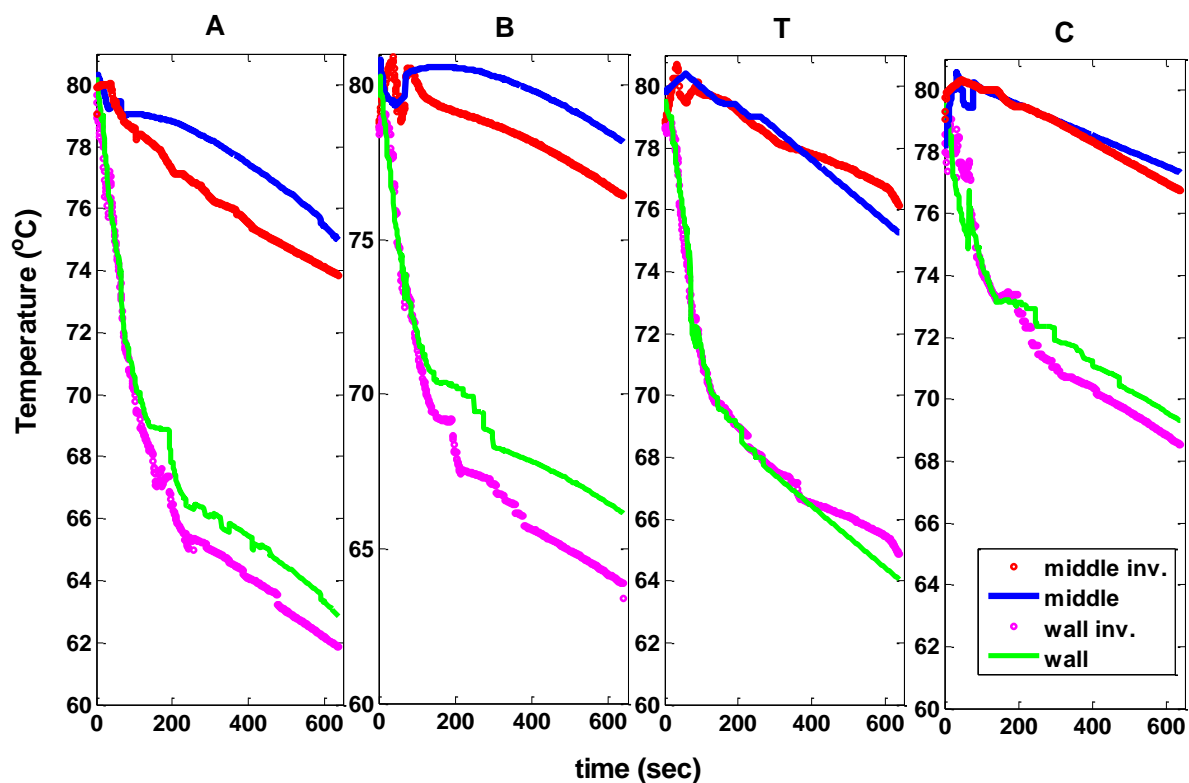
Figure 3.22: t-T profiles of fluids A, B, T and C at the middle and wall of the inverted and non-inverted jars.

The average temperature of the headspace and the lid, which are the locations of interest, appear to increase significantly with inversion; an increase of 3 and 6°C for fluids A and B, and T and C, respectively for both locations. The highest increase in temperature during inversion was recorded for fluid A, confirming the simulation results. The higher velocity and heat rate at the least viscous fluid leads to a more profound effect of buoyancy currents in the fluid, and consequently to increased temperatures for both the inverted and non-inverted containers.

By inverting the jars, some forced convection occurs due to mixing; the Re number was calculated in order to satisfy that assumption, based on Equation 3.16. Finally, the ratio $Gr_L / \mathrm{Re}_L{}^2$ was calculated, resulting in a value of approximately 1 for all fluids, indicating that both free and forced convection is evident during the thermal process (Churchill, 2002), confirming the simulation results.
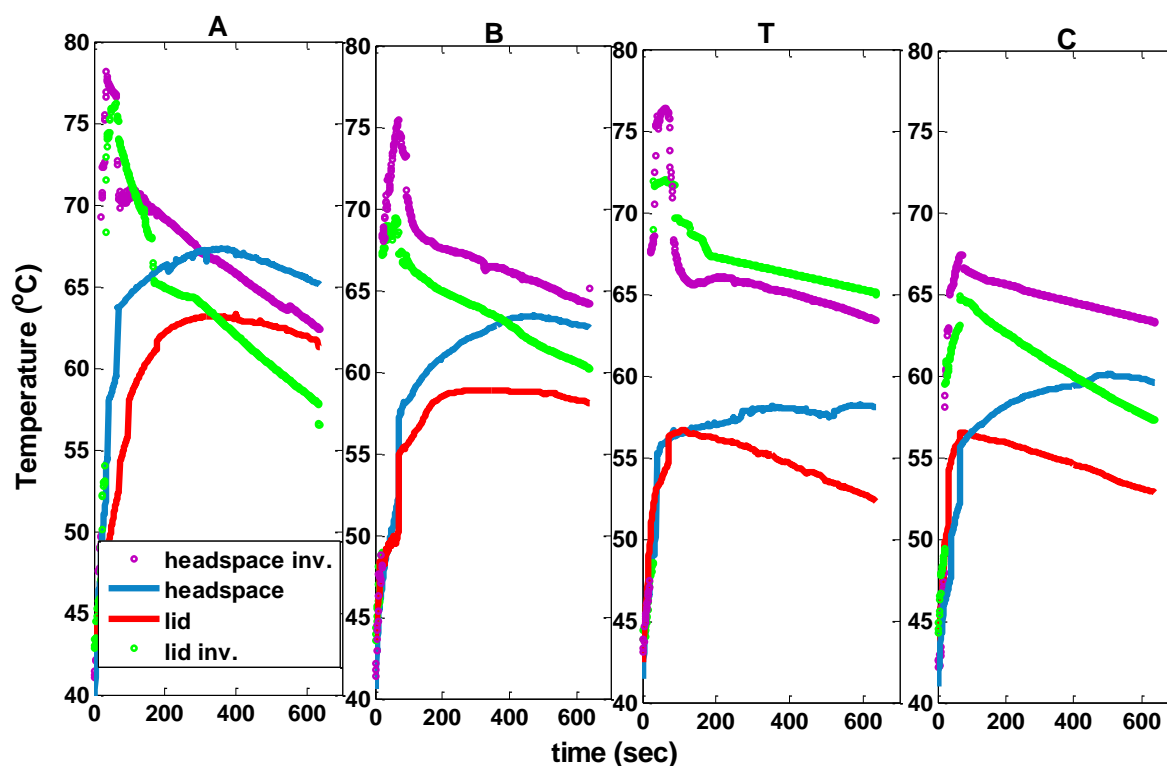
Figure 3.23: t-T profiles of fluids A, B, T and C at the headspace and lid of the inverted and non-inverted jars.

Although the free convection appears to be evident for all fluids, the small to moderate Gr numbers of 4%, 5% starch solution and tomato soup (2-20), indicate that the buoyancy currents are weak and the heat transfer occurs predominately by conduction; the flow properties are relatively unimportant in that case (Mahmud and Das, 2002).

This would lead to the expectation of lower process values for the headspace and the lid for the above mentioned fluids, as compared to the 3% of starch solution that shows a Gr number up to 100 times higher.

The time-temperature history recorded at the different fluids and locations is converted into process values, according to Equation 3.2 and illustrated in Figure 3.24, where the above observations   are

refle
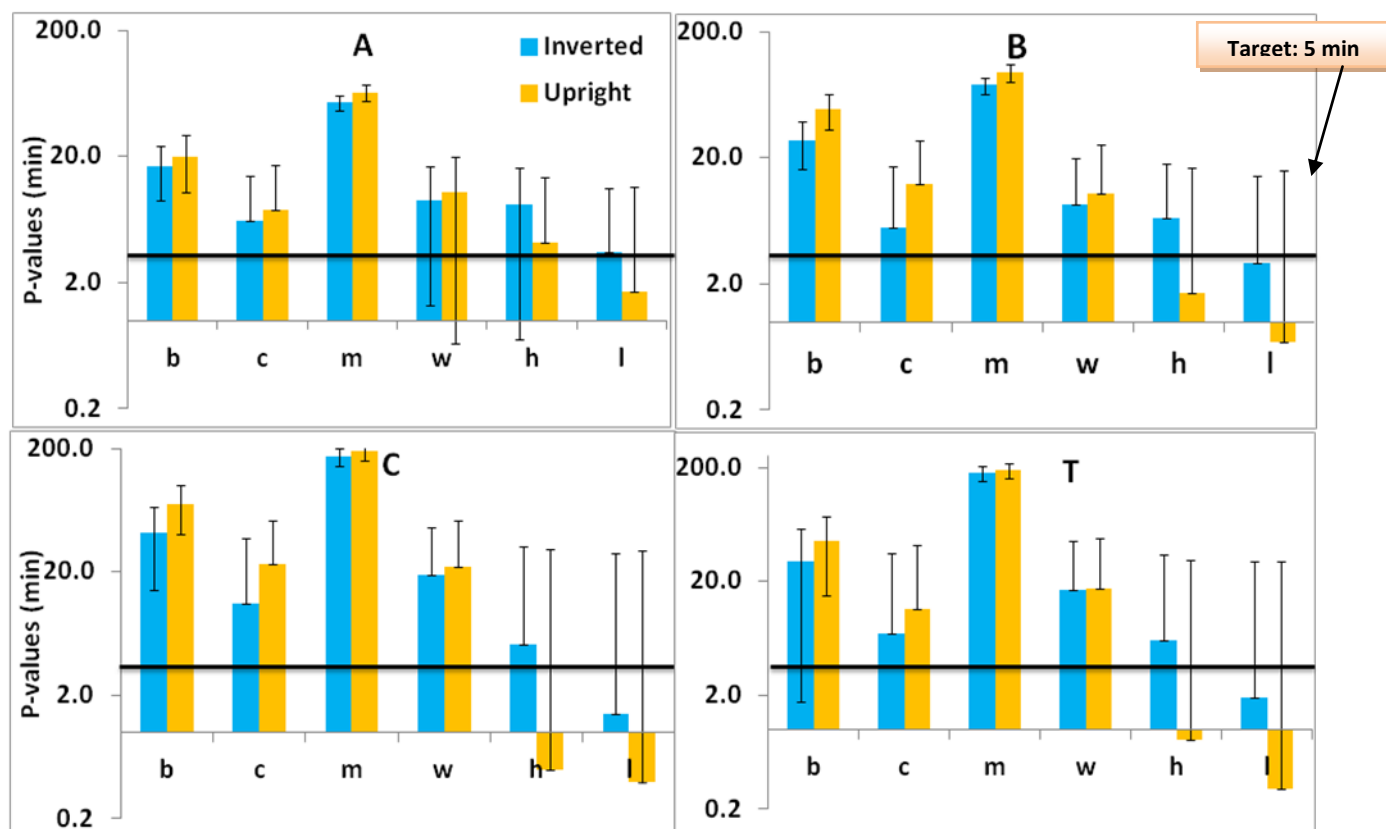
Figure 3.24: Calculated process values for fluids A, B, T and C at a T_{ref} of 70°C and a z-value of 10.8^{o}C.

According to Figure 3.24, the target process is achieved by all locations for fluids A and T, but not achieved for fluid B at the lid and fluid C at neither the headspace nor the lid.

The model fluids follow the same trend with the time-temperature profiles, with the process values increasing with viscosity at the bottom, corner, middle and wall, but decreasing at the headspace and the lid. An important point to be made from the above Figure is that the bottom and corner of the jars do not get significantly colder with inversion; it appears that the length of inversion time is sufficient to heat up the headspace and the lid but not long enough to significantly cool down the bottom and the corner.

The target process line drawn shows by how much the chosen inversion time and filling temperature combination, exceeds or misses the target set. Based on the above figure,

equivalent inversion time- filling temperature combinations were suggested for achieving a

process 5 min for the headspace and the lid illustrated in Figures 3.25 and 3.26, respectively.
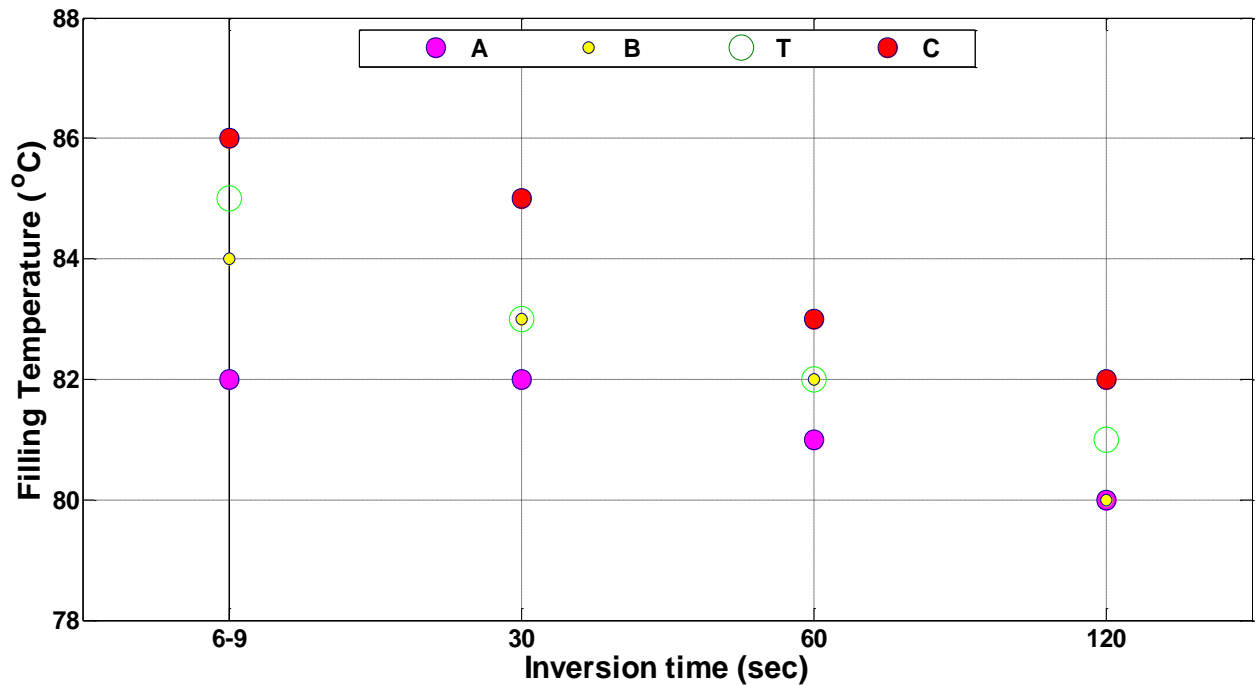
Figure 3.25: t-T combinations for achieving the target process at the headspace
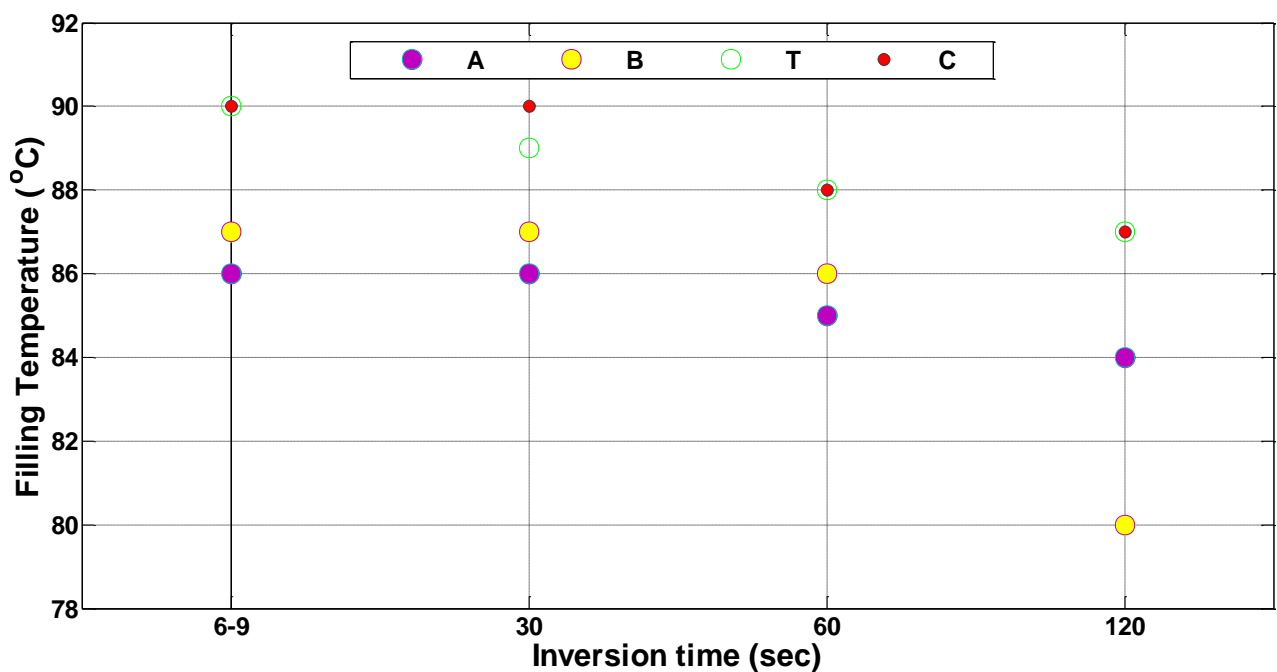
Figure 3.26: t-T combinations for achieving the target process at the lid**.**

Provided that the accumulative lethality calculated for the 10 min of the thermal treatment given to the coldest point of the product is equivalent to that obtained by holding at the reference temperature of 70°C for 5 min, then any temperature between 60 and 80°C can be used for heating. Based on that, it is possible to calculate the process time required at a variety of temperatures for achieving an equivalent process for other pasteurisation temperatures. A range of time lengths required for achieving an equivalent process of 5 min at 70°C, at temperatures between 60 and 80°C was calculated and presented in Table 3.4.

Table 3.4: Equivalent processes of 5 min at 70°C at a calculated z-value of 10.8°C.

Temperature ($^{\circ}$C)	Time required (min) to achieve an equivalent process
60	47.80
62	30.43
64	19.37
66	12.33
68	7.85
70	5.00
72	3.18
74	2.03
76	1.29
78	0.82
80	0.52

3.4   Conclusions

The effectiveness of the inversion method as a treatment for the headspace and the lid, for hot-filled model foods, tomato soup, and starch solutions of 3, 4, and 5% (w/w), was investigated targeting a process of 5 min at 70°C.

The jars were hot-filled at a temperature of 80°C, sealed, inverted for 30 sec, brought back to the upright position and cooled at room temperature for approximately 10 min. The inversion time and filing temperature combination chosen appeared to be sufficient for achieving the goal set, for fluids A and B at all locations, whilst it was not sufficient for the headspace and the headspace and nor the lid of fluids T and C, respectively. The inverted jars showed significantly higher process values for the headspace and the lid with the filling temperature being the most important parameter. Based on the time temperature profiles used during the thermal treatment, more inversion time and filling temperature combinations were suggested for achieving process values ≥5 min for all fluids, at all locations.

The rheological study conducted, revealed that the most stable model fluid, in terms of stress, strain, frequency and temperature resistance was fluid C (most viscous), whilst the most dependent one was fluid A (least viscous). Fluid A is highly dependent on a frequency ≥ 4 Hz, after which it becomes more elastic; at the frequency range between 1 and 4 Hz, it behaves like a gel, with $1 > \tan \delta > 0.5$. Fluids B and T and C are independent of frequency, with the latter being the most elastic one ($\tan \delta < 0.5$). The storage modulus (G´) is greater than the loss modulus (G″) for all fluids, along the whole frequency and temperature range studied, indicating that the fluids have dominant elastic properties rather than viscous ones. All fluids show a shear-thinning behaviour ($n < 1$) and are best described by the Carreau model.

A mathematical model based on finite element method was developed using dimensionless numbers, for generating natural convection. A rectangular cavity filled with the model fluids, consisted of a cold and hot vertical wall with the bottom and top surface being insulated, was examined. From the Ra numbers obtained, the model fluids appear to belong to the range $10^4 <$ Ra $< 10^9$, indicating the occurrence of laminar flow. That was confirmed by the high velocity values that appeared to be located at the lateral boundaries, where the highest variations of temperature occur; the natural convection occurs from the boundaries. The maximum velocity of fluids A, B, T and C was calculated to be 0.4, 0.2, 0.1 and 0.06 mm s^{-1}, respectively. The values are in good agreement with the values estimated from the dimensionless numbers, validating the model developed. The mathematical model confirms the observations made from the inversion method analysis; the higher velocity calculated for fluid A explains its faster cooling rate and consequently higher temperatures and process values at the headspace and the lid during the hot-fill treatment, as compared to the rest of the fluids.

References

Adams J.B., (1996). Determination of D80 for α-amylase inactivation. Internal Project Report, Ref: 12598/, Campden & Chorleywood Food Research Association.

Anderson S.A., (1950). Automatic Refrigeretion. MacLaren &Son Ltd., Norberg, Denmark.

Ball C.O., Olsen, F.C.W., (1957). *Sterilization in Food Technology*.

Bee G.R., Park D.K., (1978). *Heat* penetration measurement for thermal process design. McGraw-Hill Book Co., New York.

BeMiller J., (2009). Pasting, paste, and gel properties of starch–hydrocolloid combinations. *Carbohydrate Polymers,* 86(2):386–423.

Bird R.B., Armstrong R.C., Hassager O., and Curtiss C.E. (1987). Dynamics of Polymeric Liquids (2nd ed.). Wiley, New York vol. 1

Boero R. (2011). Food quality as a public good: cooperation dynamics and economic development in a rural community. *Mind & Society, 10*, 203–215.

Burr K.P., Nemoto R.H., (2010). Modelling and simulation of severe slugging in air water pipeline–riser systems. *International journal of multiphase flow*.

Choi I., Okos M.R., (1983). The thermal properties of liquid foods. Paper No 83-6516, *Winter Meeting,* Chicago, AL.

Churchill S.W., (2002). Heat Exchanger Design Handbook: Combined Free and Forced Convection Around Immersed Bodies. Section 2.5.9, Begell House, New York.

Dealy J.M., Larson R.G., (2006). Structure and rheology of molten polymers. Hanser Publishers, Munich.

Ferry J.D., (1980). *Viscoelastic Properties of Polymers*, 3rd ed., Wiley, New York.

Fischer P., Windhab, E. J. (2011). Rheology of food materials.*Current Opinion in Colloid & Interface Science*, 16, 36-40.

Fryer P.J., Pyle D.L., Rielly C.D., (1997). Chemical Engineering for the Food Industry Handbook. Section 9.1.

Henkes, (1990). Natural convection boundary layers. Ph.D thesis, Delft University of Technology, Delft, Netherlands.

Heslot F., Castaing B., Libchaber A., (1987). Transition to turbulence in helium gas. *Phys. Rev.A,* 36, 5870–5873.

Hesp, S.A.M., Soleimani, A., (2009). Asphalt Pavement Cracking: Analysis of Extraordinary Life Cycle Variability in Eastern and North eastern Ontario, *International Journal of Pavement Engineering*, 10(3), 209-227.

Heymann L., Sigrid P., Aksel N., (2002). On the solid-liquid transition of concentrated suspensions in transient shears flow. *Rheologica Acta*, 41(4), 307-315.

Incropera F.P., DeWitt D.P., Bergman T.L, Lavine A.S., (2006). Fundamentals of Heat and Mass Transfer, John Wiley & Sons, Sixth edition.

Kumar A., Bhattacharya M., (1991). Transient temperature and velocity profiles in a canned non-Newtonian liquid food during sterilization in a still-cook retort. *International Journal of Heat and Mass Transfer,* 34, 1083–1096.

LeFevre E. J. (1956). Laminar Free Convection from a Vertical Plane Surface. *Proc. Ninth Int. Congr. Appl. Mech.*, Brussels, 4, 168.

Menard K.P., (2008). Dynamic Mechanical Analysis: A Practical Introduction (2nd ed.).

Mahmud S., Das P.K, Hyder N., (2002). Laminar natural convection around an isothermal square cylinder at different orientations., *International communications in heat and mass transfer,* 29 (7), 993-1003.

Peleg M., Normand M.D., Corradini M.G., (2012). The Arrhenius Equation Revisited.*Critical Reviews in Foods Science and Nutrition*, 52(9), 830–851.

Shim J., Mulvaney S.J., (2001). Effect of heating temperature, pH, concentration and starch/whey protein ratio on the viscoelastic properties of corn starch/whey protein mixed gels. *Journal of the Science of Food and Agriculture*, 81(8):706–717.

Somwangthanaroj A., (2010). Rheology and polymer characterisation. http://pioneer.netserv.chula.ac.th/~sanongn1/course.html

Srinivasa R.R., Saad A.K., (1995). Shear-induced microstructural changes in flocculated suspensions of fumed silica. *Journal of Rheol*ogy, 39, 1311.

Wilke T., Raab V., Breuer O., Hamer M., Peterson B., (2013). Lebensmittelsicherheit und die Entwicklung von Public-Private-Partnership-Strukturen. *Die Zeitschrift für Außen- und Sicherheitspolitik*, 6, 23– 33.

Chapter 4 - Modelling of temperature distributions in hot-filled food packages

Abstract

The pasteurisation of food packages by the method of hot filling is a well-established and widely used thermal processing technique in food industry, commonly combined with a post pasteurisation step in order to ensure safety. That step can either be the application of raining shower or steam, before the containers reach the cooling section or by inverting the jars; in the current work inversion was used as a step for headspace and lid pasteurisation. The filling temperature and inversion time used in the current work for achieving a target process of 5 min at 70°C were 80°C and 30s, respectively.

Transient flow patterns and temperature profiles within a model liquid food, 3% starch solution (w/w) and a real food product, cream of tomato soup the liquids, for both the inverted and non-inverted package, during the cooling phase of the heat treatment were predicted and modelled by a finite element method. The fluids were assumed to reach the filling temperature of 80°C instantaneously and after being filled into the glass jars, cooling takes place by conduction. The model assumes a finite cylindrical geometry and constant properties (thermal conductivity k, specific heat C_{p}, thermal expansion coefficient b, and density); the Boussinesq approximation was applied and viscosity was used as a function of temperature. The temperature isotherms and velocity field plots indicated the occurrence of a

weak laminar, natural convection for both model fluids, with higher velocities observed when the jars were inverted. The mathematical model developed was validated by the experimental data and the calculation of the Root Mean Sum Error (RMSE).

4.1   Introduction

The objective of thermal processing is to ensure the safety of the final food products whilst maintaining their quality (Teixeira, 1992). The simultaneous achievement of product sterility and minimum quality losses has been a challenge for the food industry (Abdul Ghani et al., 2002). The temperature profiles recorded during the process and within the food are of great importance for accomplishing the above objective. The development of mathematical models has been proved to be useful in determining the temperature distribution within the food product as well as calculating the inactivation kinetics of microbial and quality factors (Avila and Silva, 1999).

The transient temperature and velocity profiles in natural convection-heated liquid foods were first predicted numerically by Datta and Teixeira (1988). Later, simulations were used by Kumar and Bhattacharya (1991) to predict the temperature distribution within viscous liquid foods in a vertical can, and Abdul Ghani et al. (1999) used computational fluid dynamics to describe natural convection-heated canned foods. The computational time was significantly reduced by the use of axi-symmetric approach along the vertical direction (*y*-axis), which was adopted by all the above authors (Erdogdu et al.*,* 2010, Erdogdu and Tutar 2011, Kiziltas et al.*,* 2010; and Moraga et al.*,* (2011)). Sandoval, Barreiro & Mendoza (1994) developed a model for describing the pasteurisation by hot-filling of a tomato paste that was air-cooled and predicted the heat transfer mechanisms and lethalities occurring during the cooling phase. Joseph et al.,(1996) also described the hot-fill treatment in fruit purees, using

both air and water as cooling media and carried out a number of simulations in order to investigate the effect of filling temperature, type of cooling medium and pasteurisation value on the quality of the product. The complex behaviour of the fluids in such thermal processes makes the prediction of temperature profiles and heat transfer a rather challenging task.

Another challenge during thermal processing of liquid foods is the presence of headspace, which is required for the vacuum forming during processing (Cox and Fryer, 2002); air may not be eliminated during sealing (Ramaswamy et al.,1996) and the headspace might act as an insulator, retarding the heat transfer mechanisms (Ghani et al., 1999; Mohamed, 2007). Controversial findings related to the effect of headspace on the heat transfer rates have been reported in literature. Weintraub et al., (1989); Ramaswamy et al., (1996), reached the conclusion that the heating rates are decreased in the presence of headspace, whilst Kumar et al., (1990); Joseph et al., (1996) and Erdogdu and Tutar (2011) pointed out that the rate is enhanced in canned liquid foods due to the effect of condensing steam. On the other hand, Erdogdu et al., (2010), stated that the headspace effect ($< 5\%$ in volume) was not significant on the simulation results and was neglected. In a coupled liquid–gas system the velocity fields between air and fluid, in the case of canning are influenced and the heat transfer rate is consequently altered due to the effect of natural convection occurring during thermal processing (Bukhari et al., 2007). Not much attention has been given in literature to numerically solve such systems, and simulations are carried out taking into account only the liquid phase (Ghani et al., 2006; Kannan et al., 2008; Erdogdu et al., 2010).

The objectives of the current work were:

- To develop a mathematical model that mimics the behaviour of the 3% starch solution and tomato soup during the cooling phase of a hot-fill treatment, by predicting the transient temperature, velocity and flow patterns.

- To validate the model developed, by comparing the predicted data with experimental results.

4.2   Materials and methods

For achieving the given objectives, the current study consists of experimental and computational elements. As described in Chapter 3 § 3.2.1, glass jars of a total 325 mL working volume, including a 10% headspace (in volume) were hot-filled with 3% (w/w) of starch solution, and cream of tomato soup; the jars were then air-cooled for approximately 10 min. The cooling phase of the hot-filled model fluids was numerically studied and analysed using a Heat Transfer Module, coupled by the non-isothermal incompressible fluid flow physics interface, available in the COMSOL Multiphysics 4.3b (COMSOL Ltd, Cambridge, UK) software package.

The thermo-physical properties of the model fluids, thermal conductivity k, thermal expansion coefficient β and specific heat C_p were assumed to be constant during the simulations. The density was assumed to be constant in the governing equations except in the buoyancy term, where the Boussinesq approximation is used, as expressed in Eq. 3.11, Chapter 3 § 3.2.4 for describing its variation with temperature. The viscosity was modelled as a as temperature dependant variable; the Carreau viscosity model was used in the non-isothermal flow model, using the properties of Table 3.1 and described by Equation 3.3, Chapter 3 § 3.2.3.1.

4.2.1   Model equations and computational procedure

The model considers free convection in a glass jar of hot fluid at room temperature. The non-isothermal laminar flow interface, coupled with the Heat Transfer interface, was used for computing the temperature distribution and the flow pattern. Based on the non-dimensional analysis conducted and analysed in Chapter 3 § 3.2.4.1 the flow regime of the model fluids was determined to be laminar and the heat transfer mechanism dominating was conduction. The computations were performed for a glass jar of 0.073 m diameter (R), 0.095 m height (H), 0.003 (x_wall), and 0.0015 (x_bot) m thickness for the glass wall and bottom, respectively. The lid dimensions were also incorporated in the simulations, of the same radius, 0.003 m height, and 0.001 m thickness; ≈5% of the total volume was assumed to be occupied by the headspace. The package was assumed to be homogeneously cooled, allowing consideration of a 2D-axi symmetric geometry (Figure 4.1).
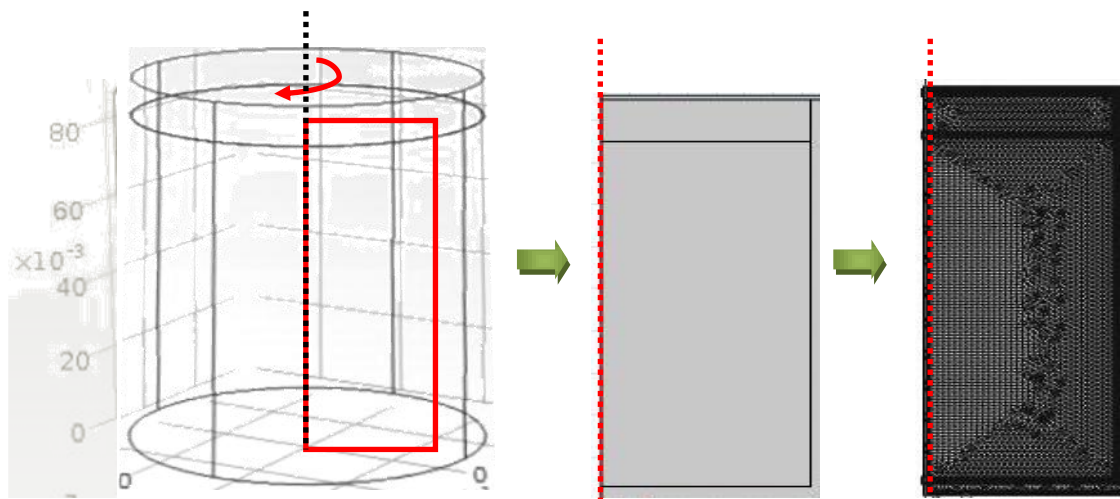
Figure 4.1: Geometry definition for model simulation.

Initially, the glass jar and the fluid are both set at 80°C, and the surrounding air and lid at 20°C, the room temperature. In the case of the inverted glass jars a parametric sweep step function available in COMSOL Multiphysics, was added into the model in order to simulate

the temperature distribution at inclination angles from 0 to π rad for the first inversion, which lasted approximately 1s. The jar remained at the inverted position (π rad) for 30 s and then a second parametric sweep step was used to describe the fluid behaviour from π to 2 π rad. After the jar being brought back to the upright position (2 π rad), the simulation continues for 600 s at that angle. The "if condition" was used for approximating the inversion step with the parametric sweep step; at zero time, the geometry was kept at zero rad, at time between 1 and 30 seconds, the geometry was simulated at π rad, and finally at time between 31 and 600 seconds it was simulated at 2π rad. By incorporating the time sweet test and the if condition, the inversion step can be accurately approximated, by allowing the headspace to appear to the top of the jar, every time the geometry is inclined.

The inclination angle is exactly the same as the angle of the gravity vector from its initial vertical position and the fluid movement is driven by the fact that the gravitational vector direction is varying periodically. The global mass and momentum balances for non-isothermal flow are coupled to an energy balance, where heat transport occurs through convection and conduction.

The fluid and headspace air were simulated as a single phase fluid including flow and heat continuation at the interface of the two different materials, instead of two-phase. That is because the materials have significantly different densities, making the convergence almost impossible.

The temperature at the outer surfaces (glass bottom and side, and lid) was simulated as a function of temperature, due to cooling taking place. During the cooling phase, the difference between the surface temperature of the glass jar, lid and the surrounding medium, T_s- T_∞, is reduced, because T_s is reduced. Thus, the surface temperature is a time varying parameter and interpolation is used, in order to accurately represent the actual experimental conditions. The external natural convection heat transfer coefficient (h_c), which is proportionally dependent

on the temperature difference $T_s - T_\infty$ will also be reduced during the cooling phase; it was determined based on the empirical equations predicted by Holman (1990), for a laminar flow with air as the cooling medium in vertical cylindrical walls and expressed as follows:

$$h_c = 1.42 \cdot \left(\frac{T_s - T_\infty}{y} \right)^{\frac{1}{4}} \qquad (4.1)$$

No holding time was considered in the simulations and the pasteurisation values obtained were based on a filling temperature-inversion time combination.

The effect of the headspace ($< 10\%$) on the heat transfer rates was not taken into consideration; Erdogdu et al. (2010) and Kiziltas et al. (2010) reported that a headspace volume of approximately 5%, had no significant effect on the simulations. Thus, the fluid-air interface analysis was not included in the model but flow and heat continuity boundary was used instead and the fluids were treated as a single phase problem. No mass transfer was taken into account during computation. The atmospheric pressure and the surface tension at the intersection of the air/fluid were set to zero and 0.072 N m^{-1}, respectively. The gravitational effects (9.81 m s^{-2}) were also expressed as body forces.

The governing differential equations for solving a single-phase, time dependent non-isothermal flow model were solved by coupling the Fluid Dynamics module, for the momentum and continuity equations, and the Heat Transfer module, for the energy balance equations. For the energy balance in the glass wall and the lid only the conduction is considered. The thermal properties for the glass wall and lid are assumed to be of silica glass and steel, respectively. The results were presented in terms of temperature isothermals and flow patterns and the predicted data were validated by the experimental ones.

The Root Mean Square Error (RMSE) statistical values were calculated for confirming the time-temperature profile correlations between the experimental and predicted data, based on the equation given by Atkinson, (1993):

$$RMSE = \sqrt{\frac{1}{n} \cdot \sum_{i=1}^{n} \left(T_{experimental} - T_{simulations}\right)^2} \qquad (4.2)$$

Where: n is the number of experimental data and T refers to the temperature values obtained from the experimental and simulated data at each of the six points inside the inverted and non-inverted jars, for all fluids. The lower the calculated RMSE value the better the correlation between the experimental and predicted data.

4.2.2   Meshing

The boundary layers occurring at the walls being cooled and at the interface between the fluid and the air are of great importance to the numerical convergence of the solution, keeping the discretization error small. In order to adequately represent the boundary layer flow and make the model more realistic, the mesh elements should be carefully chosen; a larger concentration of grid points is needed near the boundaries, when compared with the rest of the domain, where the temperature and velocity variations are smaller due to the fact that the liquid adjacent to the walls is more temperature dependant via the effect of heat transfer, leading to buoyancy forces due to the density differences. Thus, a non-uniform grid system needs to be was used throughout the geometric entity (Boz, Erdogdu, Tutar, 2014).

Erdogdu et al., (2010) demonstrated that inflation at the boundaries, which resulted in very fine grid structure, resolved the velocity and temperature components accurately, whilst Tu et al., (2008) reported that maximum flexibility in matching mesh cells with boundary surfaces

was achieved by the combination of different elements, such as triangular and quadrilateral (hybrid grids); the quadrilateral or hexahedral elements were used to enhance the grid quality at the boundary layers near the solid walls, while triangular or tetrahedral elements were used for the rest of the flow domain for accurate solutions and faster convergence. Mesh independency cannot always be achieved though, due to the restrictions in computational power and time. For ensuring accuracy of the simulated results and mesh independency, 3 different mesh sizes, fine, finer and extra fine, were investigated and validated by the experimental data at the wall, headspace and middle of the glass jar. The choice of the points was made due to the difference in their mesh resolution; higher grid points are applied at the boundaries, as compared to the less dense grid at the domain (Figure 4.2). The RMSE values were calculated for demonstrating the differences between the mesh cases and the experimental data. The value of the time step size used was 1 s.

4.2.3   Assumptions made for simplification

The following assumptions need to be made for defining the numerical problem and simplifying it:

1. An axi-symmetric vertical geometry was selected in order to reduce the problem from three-dimensional to two-dimensional; the computational time needed was significantly reduced.

2. The thermal properties of the model fluids (specific heat (C_p), thermal conductivity (k), and thermal expansion coefficient (β) are kept constant; temperature dependence of density (ρ) is only used in the Boussinesq term.

3. The no-slip condition was applied at the inside walls of the jar, between the glass, lid and the fluid.

4. The pressure within the fluid domain is unknown, making it difficult to achieve convergence. Thus, the pressure was arbitrarily fixed at a point.

5. Heat generation due to viscous dissipation was considered to be negligible, due to the low velocities of the highly viscous fluids used (Mills, 1995).

6. Boussinesq approximation is valid; the density difference has a linear relationship with temperature.

7. The thermal boundary conditions are applied to the outer boundaries of the package, as the thermal resistance of the glass and lid wall are taken into account.

8. The convective boundary condition, driven by the temperature difference between the glass, lid and the surrounding atmosphere was applied in the simulations, at the top, bottom, and side surfaces; no other thermal boundary condition was required for describing the flow.

9. Laminar flow mode was assumed to hold through the whole cooling process.

4.2.4   *Governing Equations*

The study models the fluid motion with the incompressible Navier-Stokes equations since the mass density remains more or less constant during motion and so the state equation can be written as follows:

$$\rho = \rho(t,x) = \rho_o \tag{4.3}$$

For $\rho_o > 0$ the mass conservation equation is expressed as:

$$\nabla \cdot v = 0 \tag{4.4}$$

The required governing equations of continuity, momentum and energy, in cylindrical coordinates (Bird, Stewart & Lightfoot, 1960) are described as follows:

Continuity equation

$$\frac{1}{r} \cdot \frac{\partial}{\partial r}\left(r \cdot \rho_f \cdot v_r\right) + \frac{\partial}{\partial z}\left(\rho_f \cdot v_z\right) = 0 \qquad (4.5)$$

Energy equation

$$\frac{\partial T}{\partial t} + v_r \cdot \frac{\partial T}{\partial r} + \frac{v_\theta}{r} \cdot \frac{\partial T}{\partial \theta} + v_z \cdot \frac{\partial T}{\partial z} = \frac{k_f}{\rho_f \cdot c_{p_f}}\left[\frac{1}{r} \cdot \frac{\partial}{\partial r}\left(r \cdot \frac{\partial T}{\partial r}\right) + \frac{1}{r^2} \cdot \frac{\partial^2 T}{\partial \theta^2} + \frac{\partial^2 T}{\partial z^2}\right] \qquad (4.6)$$

Momentum equation in vertical direction

$$\rho_f \cdot \left(\frac{\partial v_z}{\partial t} + v_r \cdot \frac{\partial v_z}{\partial r} + v_z \cdot \frac{\partial v_z}{\partial z}\right) = -\frac{\partial P}{\partial z} + \mu \cdot \left[\frac{1}{r} \cdot \frac{\partial}{\partial r}\left(r \cdot \frac{\partial v_z}{\partial r}\right) + \frac{\partial^2 v_z}{\partial z^2}\right] + \rho_f \cdot g \qquad (4.7)$$

Momentum equation in radial direction

$$\rho_f \cdot \left(\frac{\partial v_r}{\partial t} + v_r \cdot \frac{\partial v_r}{\partial r} + v_z \cdot \frac{\partial v_r}{\partial z}\right) = -\frac{\partial P}{\partial r} + \mu \cdot \left[\frac{\partial}{\partial r}\left(\frac{1}{r} \cdot \frac{\partial}{\partial r}\left(r \cdot v_r\right)\right) + \frac{\partial^2 v_r}{\partial z^2}\right] \qquad (4.8)$$

Where: T is temperature (^{o}C), t is the cooling time (s), P is the pressure (Pa), g is the gravitational acceleration (m s^{-2}), μ is the dynamic viscosity (Pa s), v is the velocity component (m $^-$s^1) and k_f, c_{pf}, and ρ_f are the thermal conductivity (Wm^{-1} K^{-1}), the specific heat (J kg^{-1} K^{-1}) and the density (kg m^{-3}) of the fluid, respectively. r, and z refer to the radial and vertical axial direction, respectively.

The angular direction was not included in the momentum equation, since axi-symmetry was assumed, reducing the computational time significantly. The ρ_f g term is assumed to be the external force driving the natural convection process. The model treated the density as a constant value in all solved equations except for the buoyancy term in the momentum

equation. Thus, the variation in density was neglected everywhere except in the buoyancy term. The momentum equations were linearised and solved for a pressure set to zero. Energy and flow equations were coupled to determine the heat transfer between water–air fluid side and wall surface. The 1st-order numerical discretization scheme for the convection terms of each governing equation and a 1st-order accurate implicit time integration scheme for time discretization were used.

4.2.1.1 Boundary and Initial conditions

The initial and boundary conditions were obtained from the experimental results.

Initially, the fluid is at rest (u=0) and shows a uniform initial temperature:

$T(r, z, t) = T_o = 80^oC$ (filling temperature);

u=0, v=0 at $0 \leq r \leq R$, $0 \leq z \leq H + x\_lid$

The boundary conditions used, were the following:

- At the glass boundary, r=R:

  $T = T_{gw}$, u=0, v=0, for $0 \leq z \leq H$

- At the glass bottom, z = 0:

  $T = T_{gw}$, u=0, v=0, for $0 \leq r \leq R$

- At the top of the jar, where the boundary condition is applied at the lid, z = H + x_lid:

  $\dfrac{\partial T}{\partial z} = 0$, for $0 \leq r \leq R$

- At the symmetry:

  $\dfrac{\partial T}{\partial r} = 0$, for $0 \leq z \leq H + x\_lid$

At the top and outer surfaces, the convective heat flux boundary condition was used, driven by the temperature difference between the glass/lid and the surrounding atmosphere:

$$q = -h\,(T - T_{ext}) \tag{4.9}$$

Where: q is the inward heat flux and h is the heat transfer coefficient of the surrounding air.

4.3   Results and Discussion

4.3.1 Meshing

According to Figures 4.2 and 4.3 for fluid A and T, respectively, a noticeable difference between the three mesh resolutions and the experimental data was observed. It appears that when finer and extra fine resolution was applied to the domain, the fluid structures near the boundaries (walls and interface) increased the discretization of the flow equations and apparently led to cumulative computational errors. The fine mesh size appeared to be the most compatible with the experimental results. Another reason for the difference in mesh resolutions could be the choice of the time step (1s) for the given convergence criterion (Cornelissen et al., 2007). A more refined mesh should result in more accurate results, due to the minimised discretization errors as compared to coarse or normal mesh resolutions. Druzeta et al., (2009), reported that excessive mesh refinement could lead to deterioration of the results because of faster accumulation of computational errors on higher mesh resolutions caused by the Courant–Friedrichs–Lewy (CFL) condition. Breuer et al., (2000) explained this contradiction using a filtering approach, which requires additional resources for time-dependent laminar flows that bring resource limitations into the solution. If no filtering is applied, as in the case of the current work, it is possible that modelling and discretization errors will cancel each other leading to differences between mesh resolutions.
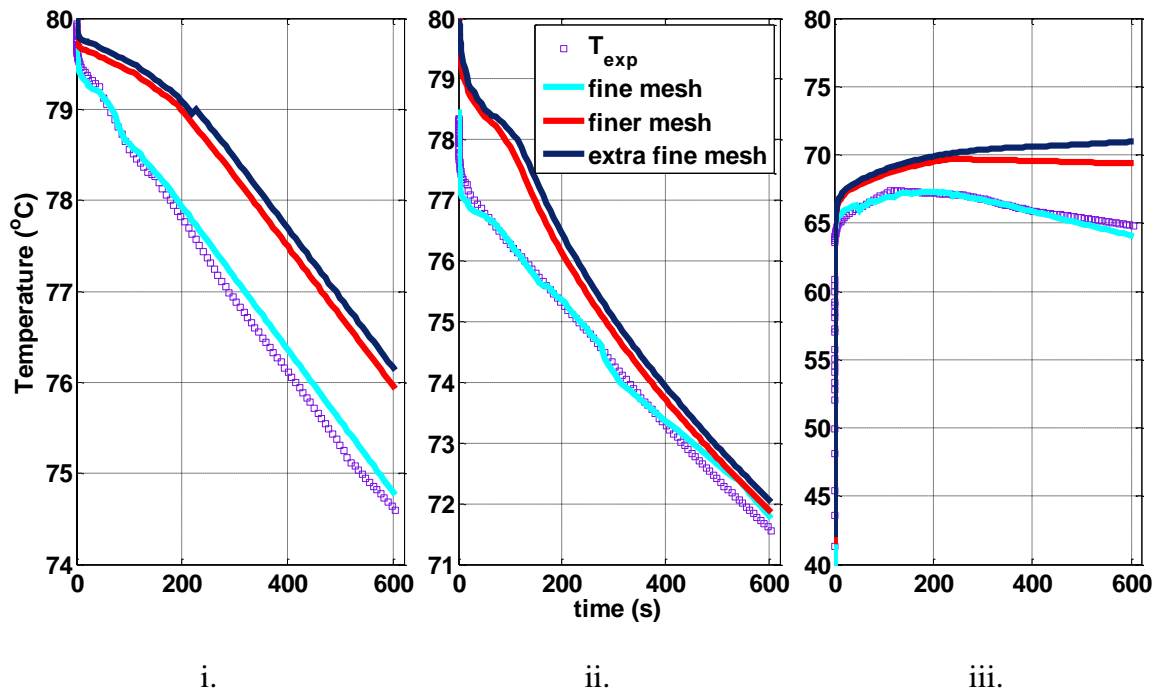
Figure 4.2: Comparison of predicted and experimental data obtained with fine, finer, extra fine mesh resolution for fluid A at the: i. middle, ii. wall and iii. headspace.
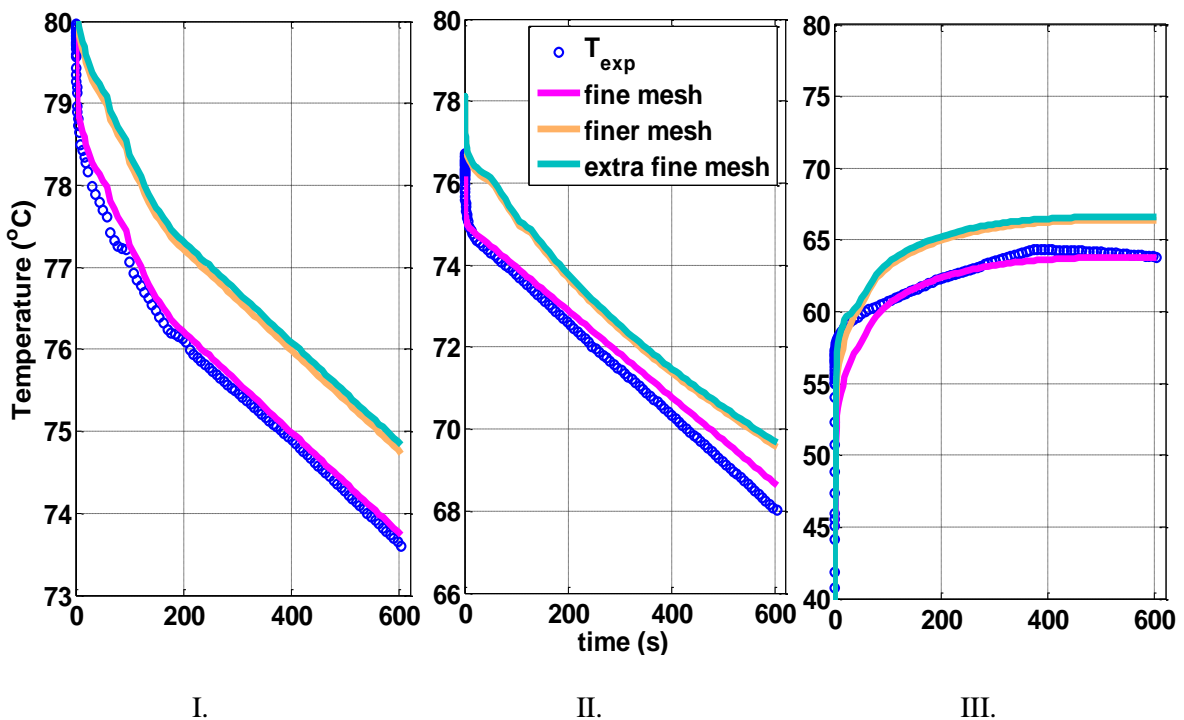
Figure 4.3: Comparison of predicted data obtained with fine, finer, extra fine mesh resolution and experimental data for fluid T at the: I. middle, II. wall and III. headspace.

The differences observed between the mesh sizes applied, were confirmed by the calculation of the RMSE values (Table 4.1). The more profound differences were shown to be between the fine and extra fine resolution for the wall (up to 9 times higher) and the headspace (up to 15 times higher) of fluid A and T, respectively. That seems to confirm the above argument, that the fluid structures near the boundaries lead to increased discretization and computational errors. The difference at the middle is also noticeable for both fluids when the mesh is further refined.

Table 4.1: RMSE values (^{o}C) obtained from the three cases of mesh resolution.

Fluids	Location within the jar	Fine	Finer	Extra fine
3% starch	middle	0.17	1.03	1.17
	wall headspace	0.16	1.28	1.41
		1.24	3.42	4.26
Tomato soup	middle	0.17	1.04	1.12
	wall headspace	0.43	1.25	1.41
		0.51	6.03	7.80

Based on the above, fine grid was used for the domains of the fluid and air, with corner refinement and triangular elements, whilst a layered quadrilateral mesh with finer grid was used for the non-slip boundaries at the wall and bottom, which are subjected to sudden changes over time, and at the interface of the coupled liquid-air system.

7031 nodal points were used with a finer grid in the domains and a finer grid near the wall and the interface of fluid-air. The convergence criterion and the time step used was 10^{-8} and 1 second, respectively.

4.3.2   Heat treatment

Temperature isotherms and velocity fields were plotted to describe the temperature distribution and the flow behaviour of 3% starch (A) and tomato soup (T) during the cooling phase of the hot-fill treatment. The model fluids were examined for the two cases of non-inverted (Case I) and inverted glass jars (Case II).

Case I: Fluid A

Figure 4.4 illustrates the temperature evolution of fluid (A), Case I at different cooling periods of 1, 100 and 600 s; these times were arbitrarily chosen from the experimental results. Initially, the fluid and the glass jar are at the same temperature, since the jars were preheated before being hot-filled, and the headspace and the lid were set at an initial temperature of $20^{o}C$; the initial and boundary conditions were again chosen based on the experimental results. During the hot-filling, the fluid starts cooling through the walls and moves downwards, as the density near the walls increases. The core of the fluid, which is the slowest cooling point in the jar (the furthest from the walls) remains at high temperature and moves upwards heating up the headspace and the lid (Figure 4.4 a). The process time (10 min) is not sufficient to enable the hot regions of the fluid to cool down significantly; approximately 1.5 hours of processing time was needed for the bulk of the fluids to reach the medium (air) temperature ($20^{o}C$). The hot fluid moving upwards is deflected by the lid and starts moving in radial direction, downwards as it gets heavier. The headspace is heated instantaneously (in the first 5 seconds, Figure 4.4 a) whilst the lid starts being heated at approximately 100 seconds (Figure 4.4 b). At the end of the process the dominating effect of conduction is clearly demonstrated (Figure 4.4 c), with convection occurring only through the latter boundaries. That is due to the relatively high viscosity of the fluid and the short process time,

which was chosen to be the same as the time used in the experimental work, for the predicted results to be comparable with the experimental ones.
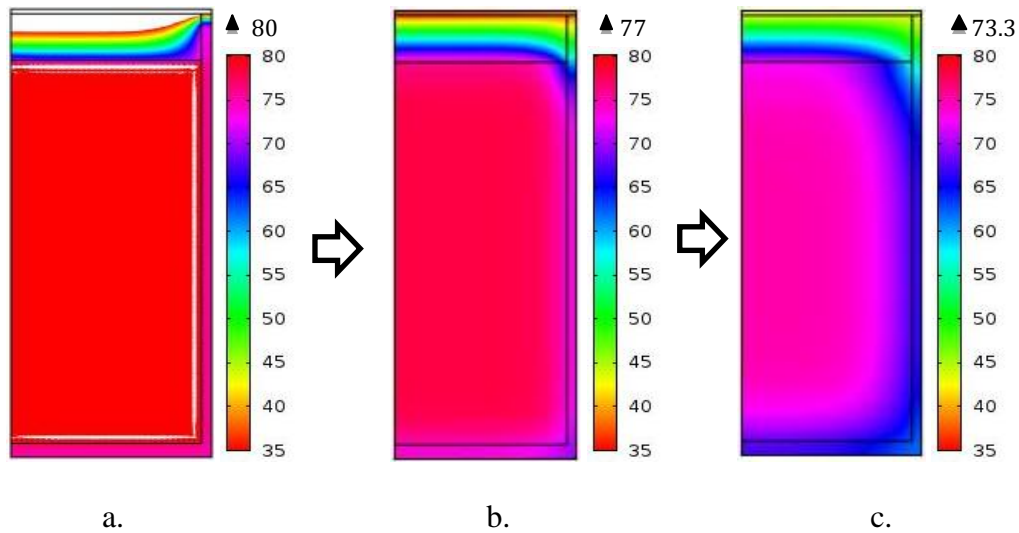
Figure 4.4: Temperature isotherms of fluid A at a. 1s, b. 100s, c. 600s. The key shows the temperature in ^{o}C.

The changes due to temperature differences between the cold surfaces (walls, lid of the jar) and the hotter liquid create a recirculating flow, indicating the existence of convection currents during the process. The flow behaviour of fluid A is expressed in terms of velocity vectors for 1, 10, 100, 200, 400 and 600 s during the cooling phase of the heat treatment, as illustrated in Figure 4.5.

At first the fluid is at rest, so no indication of flow is observed (Figure 4.5i); the heat exchange between the headspace air and the fluid at the early stages, heats the cold zone (headspace) increasing the velocity and creating a secondary flow near the wall. As the process progresses and after approximately 2 min, the simulated results show that the flow is recirculating within the jar, with the fluid rising near the wall and moving downwards near the axis (Figure 4.5iii). After the first 2 min and until the end of the process, more eddies are formed (secondary and tertiary flows), which become smaller in size and more distinct in

terms of location, with time; there is weak recirculation at the interface and near the wall and bottom, which are the cold spots within the jar (Figure 4.5 iv-vi). The secondary flow at the bottom is pushed towards the wall.

Figure 4.5: Velocity field of fluid A at: i. 1s, ii. 10s, iii. 100s, iv. 200s, v. 400s, and vi. 600s. The key shows the velocity in m s^{-1}.

Case I: Fluid T

The observations made from the temperature isotherms of fluid T (Figure 4.6) were similar to the ones from fluid A; the headspace is being heated instantaneously (Figure 4.6a) whilst it takes approximately 180 s for the lid to be heated. The highest temperatures reached at the bulk of the fluid, are higher than those observed for fluid A, which is expected, since the tomato soup cools down slower.


A.   B.   C.
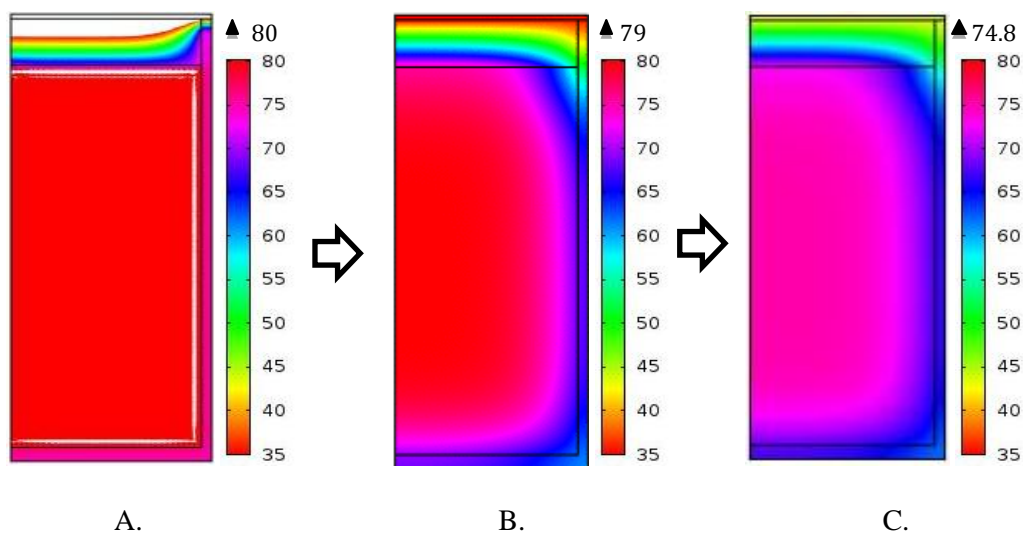
Figure 4.6: Temperature isotherms of fluid T at a. 1s, b. 100s, c. 600s. The key shows the temperature in ºC.

The velocity field plotted for describing the flow of tomato soup (Figure 4.7) indicates that the fluid seems to be at rest for the first 70-80 seconds with the temperature being uniform at this stage and then gradually, as the cooling progresses convection currents become evident at the boundaries. That is illustrated by the movement of the cold zone close to the interface, towards the bottom of the container. The cold spot continues to move until it eventually remains at a region that is about 20% from the bottom of the jar.

Studies carried out by Datta and Texeira, (1987) on the sterilisation of cans consisting of a viscous fluid such as CMC (carboxy-methyl cellulose), showed that a secondary flow is

formed at the bottom of the can, near the centre line, whilst later on, Kumar and Bhattachary, (1991) simulated the same fluid but no secondary zones were indicated. From the simulation obtained in the current work, the formation of eddies was evident in both fluids, with tomato soup having similar viscosity with CMC ($\approx$1 Pa s at a reference temperature of 80°C, based on Equation 3.3, Chapter 3 § 3.2.) and the starch solution with a value of ≈ 0.3Pa s, confirming the findings of the Datta and Texeira. However, the results in this work refer to the cooling effect on the fluid behaviour instead of heating. Thus, more research needs to be conducted for testing the similarities of the heating and cooling effect on the formation of secondary zones. Kumar and Bhattacharya (1991) reported that the thickness of ascending viscous liquids (CMC) near the wall (the distance between the location of the stagnant region and the wall) in the case of cans' sterilisation was greater (12 mm) than that for water (6 mm), attributed to the large viscosity difference between the two fluids.

According to calculations made upon actual container dimensions, the thickness of the starch solutions and the tomato soup was 3 and 4 mm, respectively. The difference in thickness is not significant, since the viscosity difference is not sufficiently large and it can explain the small differences observed in flow behaviour between the two fluids.
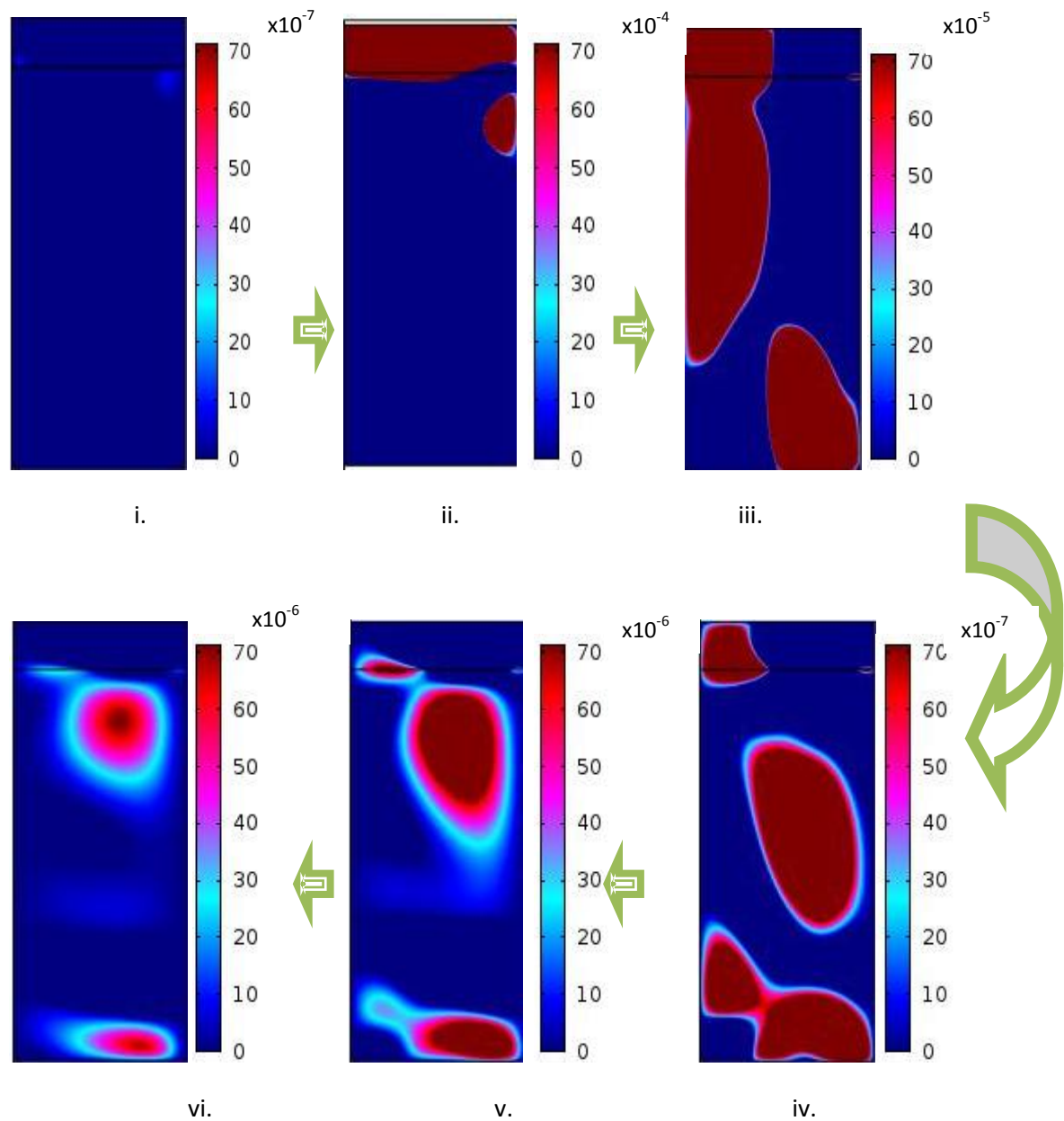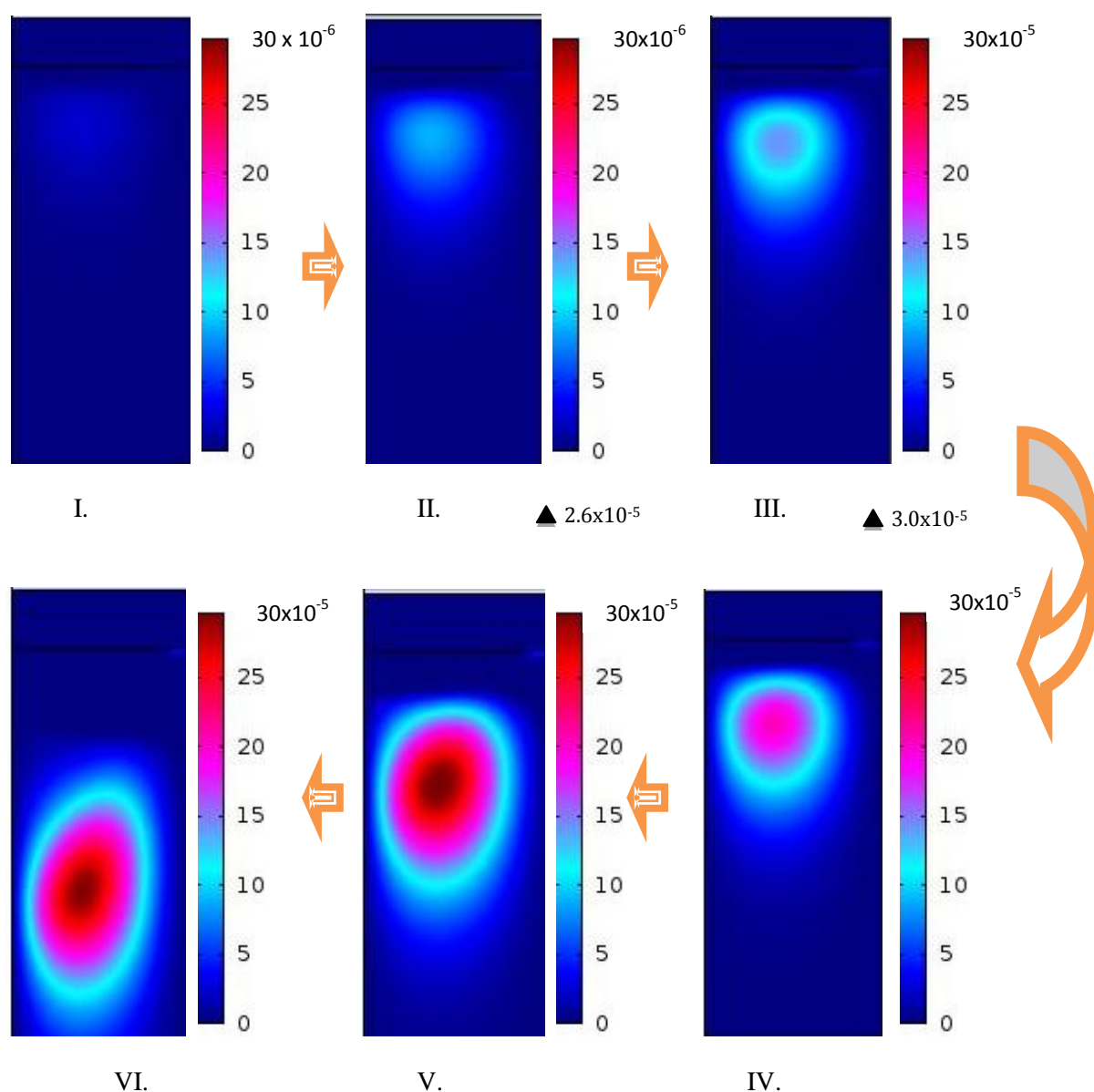
Figure 4.7: Velocity field of fluid T at: I. 100s, II. 200s, III. 300s, IV. 400s, V. 500s, and VI. 600s. The key shows the velocity in m s^{-1}.

In order to examine the reason for the velocity of the circulating fluid to decrease with time, the temperature difference between the bulk of the fluid and the wall was plotted against time for both model fluids (Figure 4.8). It appears that for fluid A, the temperature difference increases with time for about five minutes and then it is stable, whilst fluid T shows a higher temperature difference which is stable almost throughout the process. That indicates that fluid A cools faster (higher heat transfer) than fluid T, although the temperature difference for the latter is higher. After a certain amount of time, the temperature difference is not sufficiently

large and the viscosity doesn't allow the fluid to move anymore. Thus, the buoyancy force is reduced and conduction dominates, which is indicated by the very low velocity values for both fluids. The fact that the temperature difference stabilises slower for fluid A, explains the higher predicted velocities, which was expected due to the lower viscosity.
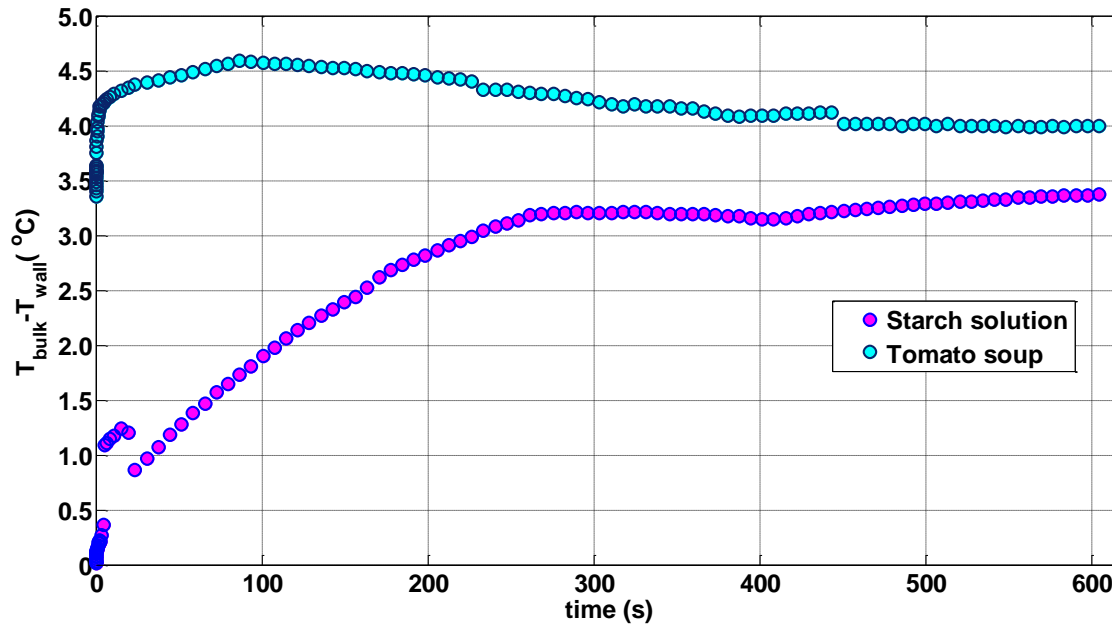
Figure 4.8: Temperature difference between the surface and the bulk of the fluid with time.

Temperature isotherms and velocity field of fluids A and T were also plotted for Case II. The fluids and the glass jar were set at an initial temperature of $80^{\circ}C$, whilst the headspace and lid were set at $20^{\circ}C$. The jars were inverted for 30 s and then inverted back to the upright position until the end of the process.

Figures 4.9 and 4.10 illustrate the temperature evolution of fluids A and T at the following cooling times (chosen arbitrarily from the experimental results):

i.   t=1s, at inclination angle phi=0 rad (upright)

ii. t=2s, at inclination angle phi=π rad (the jar is inverted)

iii.   t=32s, at inclination angle phi=π rad (at the end of inversion)

iv.   t=33s, at inclination angle phi=2π rad (after the 2nd inversion), and

v.   t=600s, at inclination angle phi=2π rad, at the end of the process

Case II: Fluid A

Initially, the jar is cooling down from the walls creating a flow downwards, while the bulk of the fluid flows upwards heating up the headspace. Once the jar is inverted, the headspace and the lid show a temperature increase of approximately 20°C, whilst close to the interface of fluid-air and at the centreline (Figure 4.9b) the fluid flow is disrupted and a decrease in temperature is observed. The forced convection caused by inverting the jars, created recirculating zones within the fluid and especialy near the boundaries. The disruption observed at the interface and near the wall could in reality be because of an existing bubble or the coldzone movement from the headspace towards the bottom of the jar.

At the end of the first inversion, after 30 s at an inclination angle of π rad (Figure 4.9c), the headspace and lid become hotter, whilst the temperature of the bottom starts decreasing. When the jar is inverted again at the upright position, it seems that the cold zone moved from the headspace, towards the bottom and then appears close to the interface and right wall. That could theoretically support the existence of bubbles during the process, but cannot be described numerically with the single-phase flow module used in the current work; air and fluid would have to be treated as a two phase-model system. By the end of the process, the flow reaches stability and whist the bulk of the fluid is conduction-dominated, the interface and walls are convection dominated.
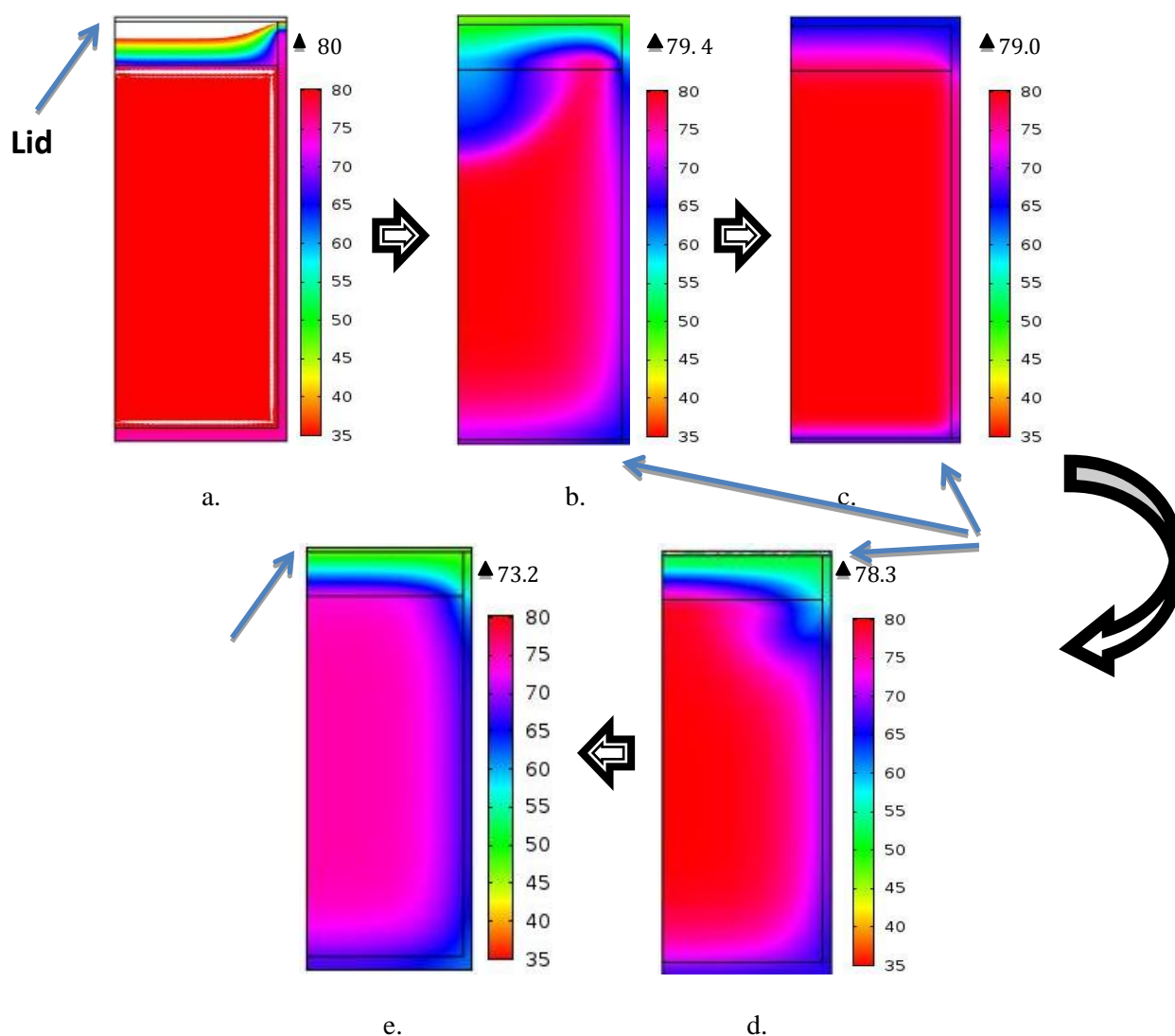
Figure 4.9: Temperature isotherms of fluid A at a. 1s, b. 2s, c. 32s, d. 33s and e. 600s.

The observations made from the temperature isotherms are reflected in the velocity field plots. Initially, the headspace air mixes with the fluid and moves towards the bottom of the container, creating at the end of the first inversion secondary and tertiary flows near the axis and at the bottom wall of the jar. By inverting the jar upright, the fluid flows over the whole surface of the jar relatively fast, and then once it mixes with the headspace air again, it is separated into two main flows, covering the colder zones of the headspace and the bottom wall and a third one close to the interface and right side wall (Figure 4.10 C-D). After approximately two minutes, there are two distinct flows; the cold zones of both the headspace

and the bottom are pushed towards the wall, with their size being decreased (velocity significantly reduced).
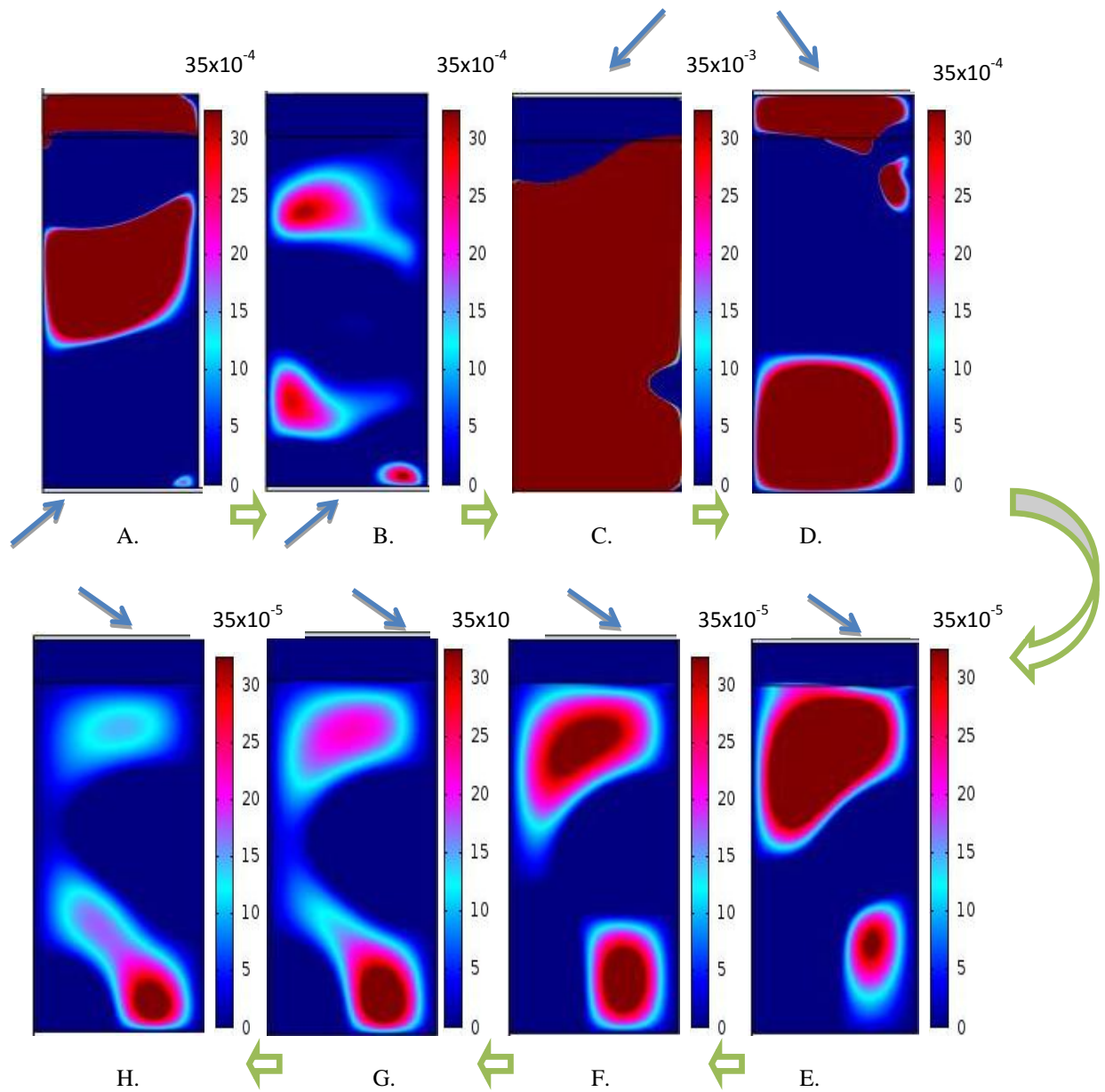
Figure 4.10: Velocity field of fluid A at: A. 1s, B. 30s, C. 31s, D. 100s, E. 300s, F. 400s, G. 500s, H. 600s.

Case II: Fluid T

In the isotherms concerning the tomato soup, the observations are similar to the ones concerning the starch solution, except from the slightly higher temperatures recorded due to the slower cooling of the fluid. Convection occurs through the walls and the interface, whilst the bulk of the fluid is mostly conduction dominated. By inverting the jars, the temperature of the headspace and the lid is increased, whilst it is decreased at the bottom and the interface, since the fluid is mixed with the headspace air (Figure 4.11ii). The interface is also disrupted in the case of fluid T, indicating the heat exchange between hot and cold zones, but it is less profound than in fluid A which would be expected from the lower viscosity and consequently the lower velocities occuring. At the end of the first inversion (Figure 4.11iii), the headspace and lid reach their highest temperature, whilst the bottom reaches its lowest. The flow becomes more stable after approximately six minutes, no more disruptions at the interface and the walls, with the bulk of the fluid being dominated by conduction and the latter boundaries being responsible for the laminar convection.
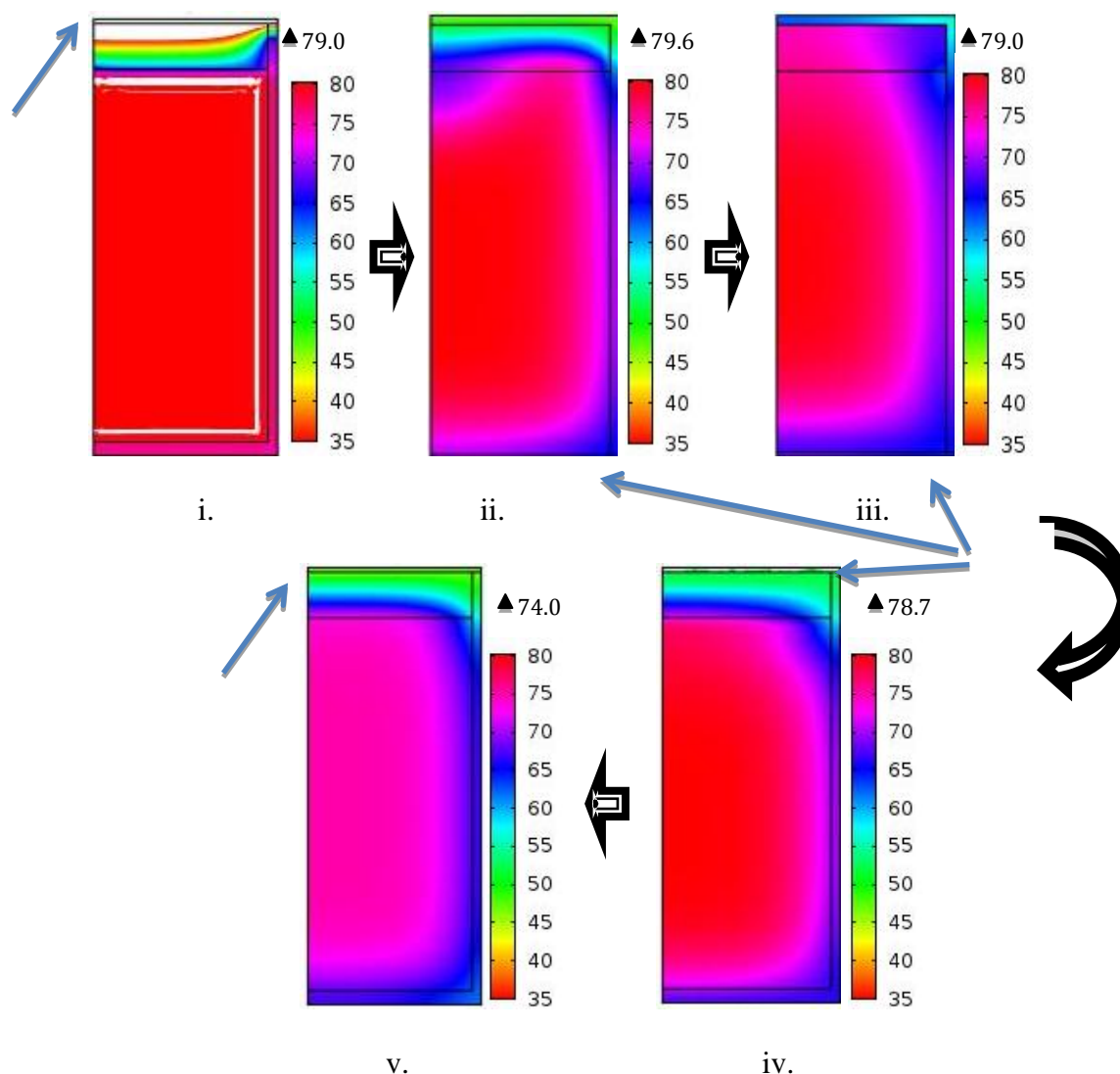
Figure 4.11: Temperature isotherms of fluid T at: i. 1s, ii. 2s, iii. 32s, iv. 33s, v. 600s.

The heat exchange occurring during the cooling phase for fluid T is illustrated by the velocity vectors at the defined cooling times. At the first second of inversion the cold zone of the headspace is moving towards the bulk and the bottom of the jar, creating a secondary cold zone near the centreline and a tertiary one at the bottom, near the right wall (Figure 4.12I). At the end of the first inversion, at 30 s, the reduced size of the cold zones near the interface and the bulk of the fluid, indicate the significantly reduced velocity at the specific locations, as compared to the increased size of the cold zone at the bottom, near the right wall (Figure 4.12II); that means the temperature difference at the bottom wall is higher than the rest of the

fluid at the specific time. When the container is inverted again to the upright position, there is an increased velocity throughout the fluid, shown by the bulk movement over most of the jar surface (Figure 4.12III). At approximately the first three minutes after the jar is inverted upright, a low velocity secondary flow is formed at the headspace, near the lid, whilst big part of the rest of the flow is moving downwards, until it reaches the bottom wall. The rest of the time until the end of the process, the velocity of the cold zone at the bottom wall is gradually reduced, until the fluid finally stops circulating at that point whilst at the meantime, a secondary flow is formed again at the headspace, increasing with time. The results reflect the observation from the temperature isotherms, since the velocity plots show that the cold spots are located near the interface and the walls.
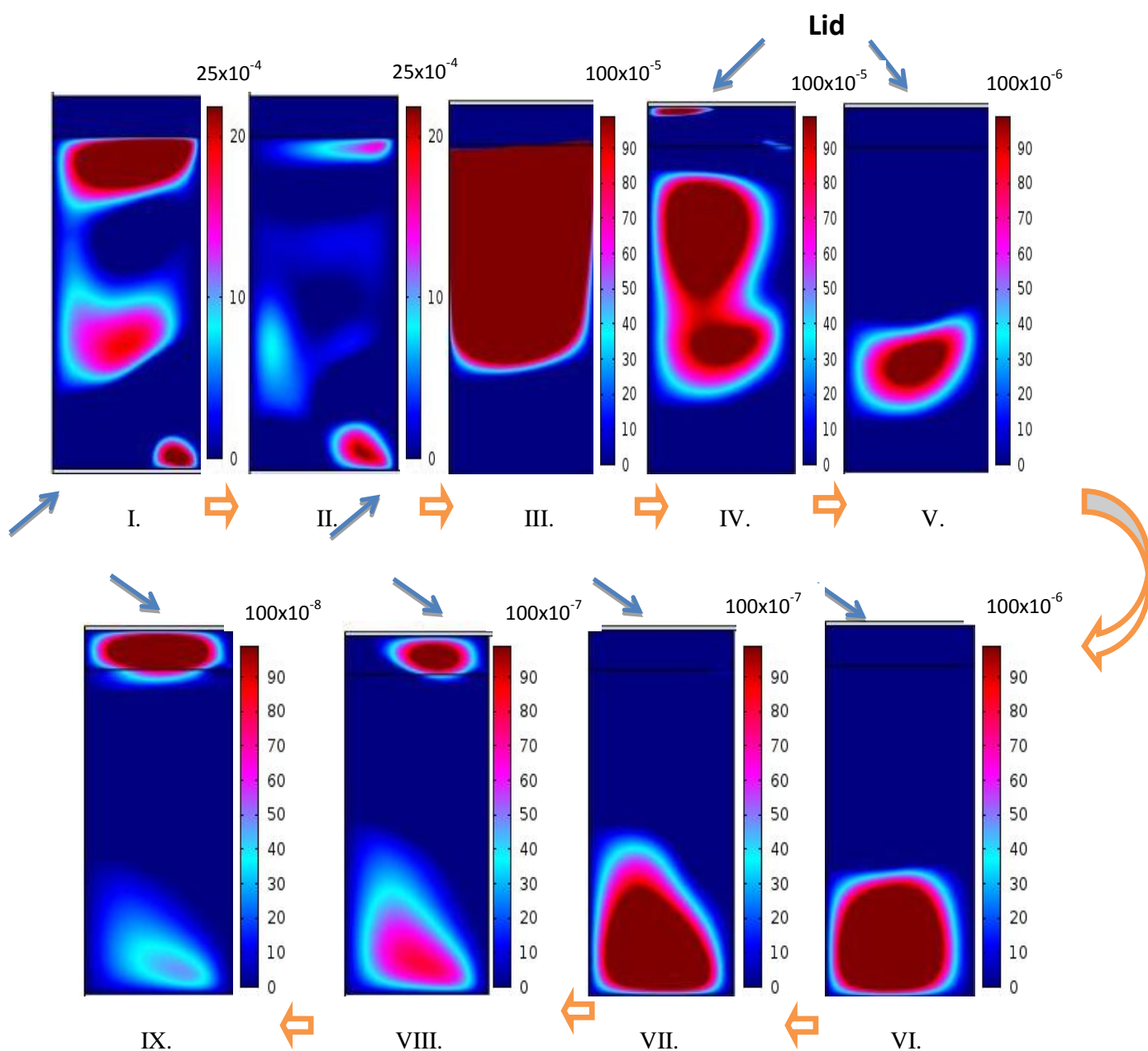
Figure 4.12: Velocity field of fluid T at I.1s, II. 30s, III. 31s, IV. 50s, V. 100s, VI. 200s, VII. 400s, VIII. 600s.

4.3.3   Model validation

The predicted time-temperature data were validated by being compared with the experimental data for both cases and fluids. The RMSE values were calculated for confirming the time-temperature profile correlations between the experimental and predicted data, presented in Table 4.2, based on equation 4.2.

Fluid A

According to Figures 4.13 and 4.14, the simulated data appear to be in a very good agreement with the experimental ones for both the inverted and non-inverted case. The difference of $\leq$ 0.5^oC for the bottom, corner and the bulk, and $\leq 2^oC$ for the headspace, lid and the wall, obtained from the RMSE calculations, confirm the good correlation between the two sets of data; the higher difference at the lateral boundaries is expected due to the increased temperature fluctuation at the specific locations.
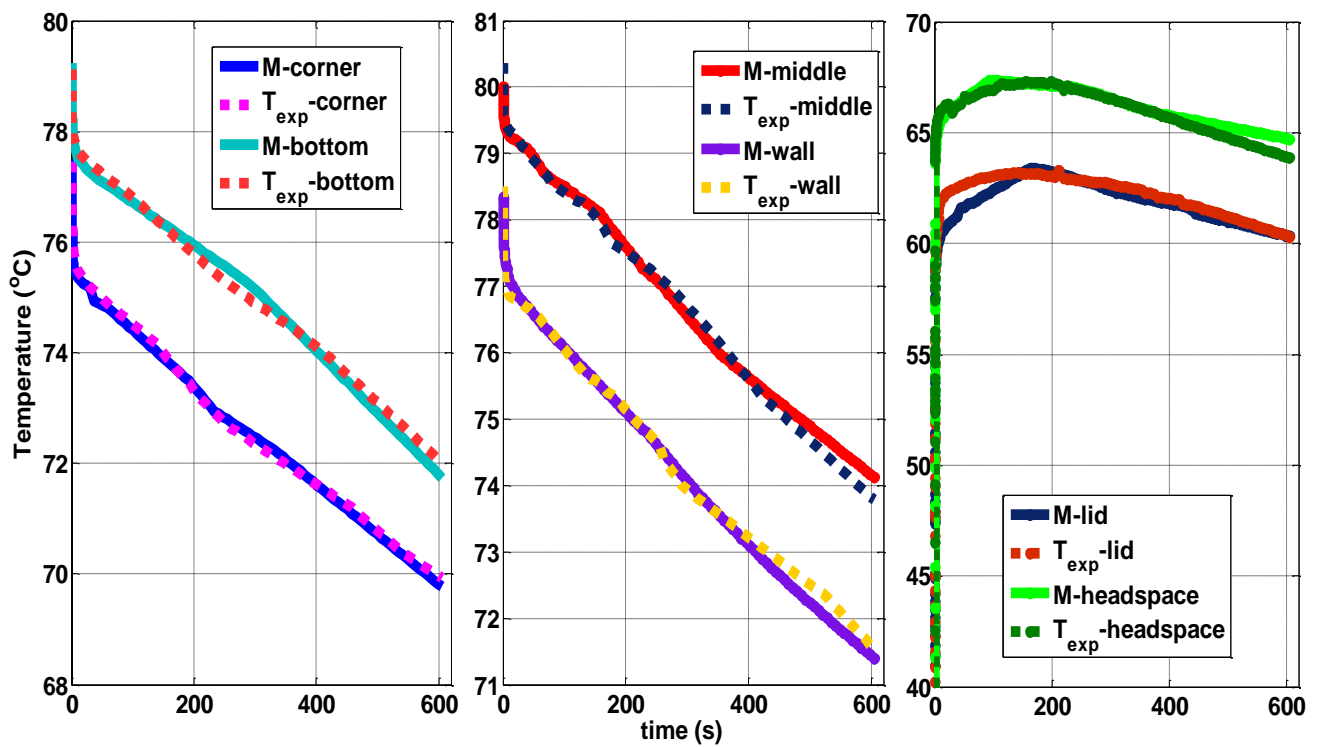
Figure 4.13: Time-temperature profiles of predicted versus experimental data for fluid A-Case I.
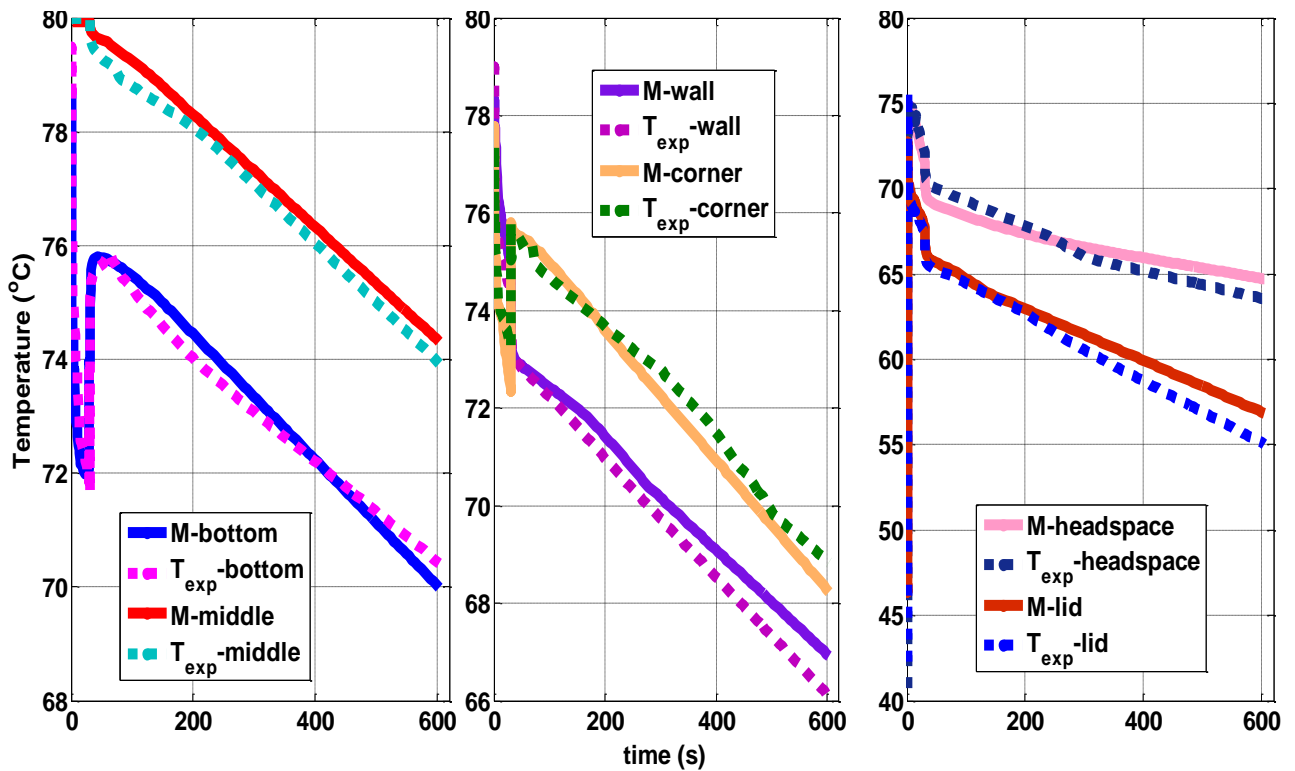
Figure 4.14: Time-temperature profiles of predicted versus experimental data for fluid A-Case II.

Fluid T

The same results are obtained for fluid T; the predicted and experimental data correlate very well, with RMSE values of $\leq 0.5\,^{\circ}$C for the bottom, corner and the bulk, and $\leq 1\,^{\circ}$C for the headspace, lid and the wall (Figure 4.15 and 4.16). The fact that the agreement is slightly better as compared to fluid A is possibly because the temperature fluctuations in fluid T are less profound at the boundaries (lower velocities).

For both fluids and cases the RMSE values show the accuracy and the reliability of the developed mathematical model (Table 4.2).
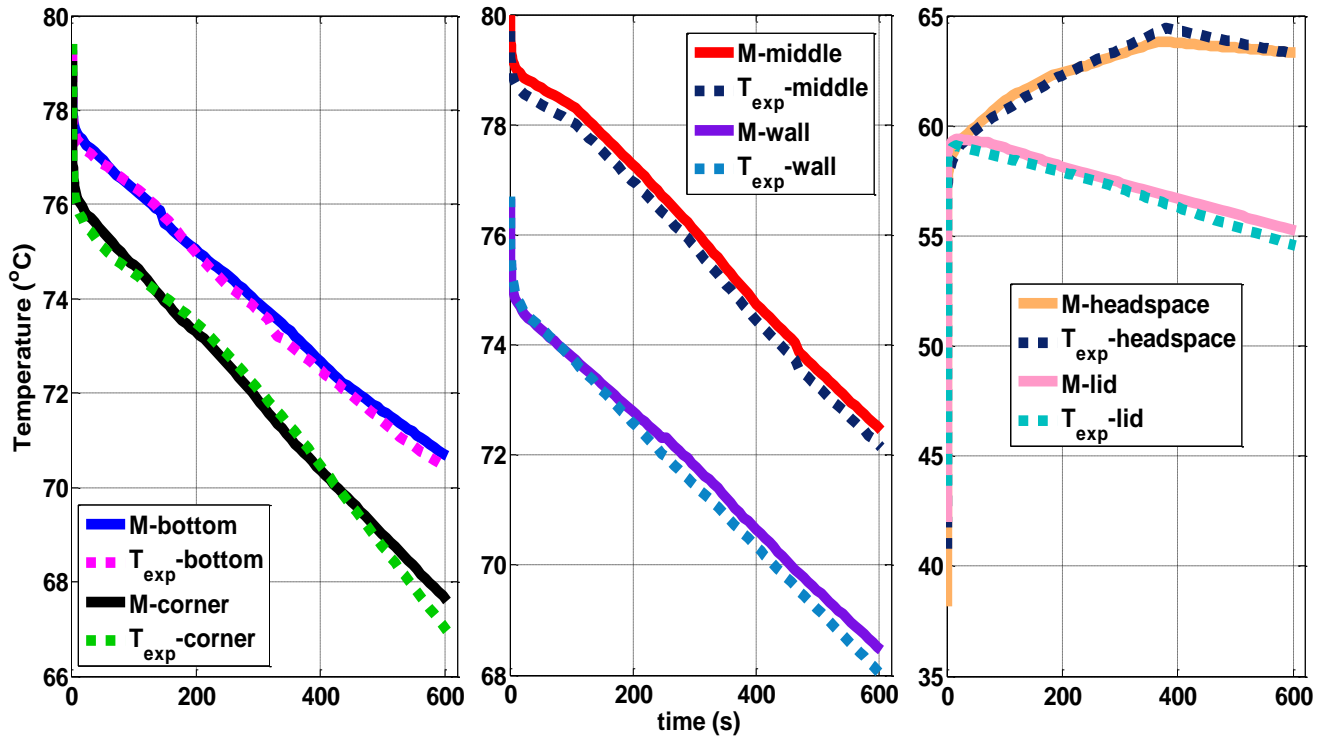
Figure 4.15: Time-temperature profiles of predicted versus experimental data for fluid T-Case I.
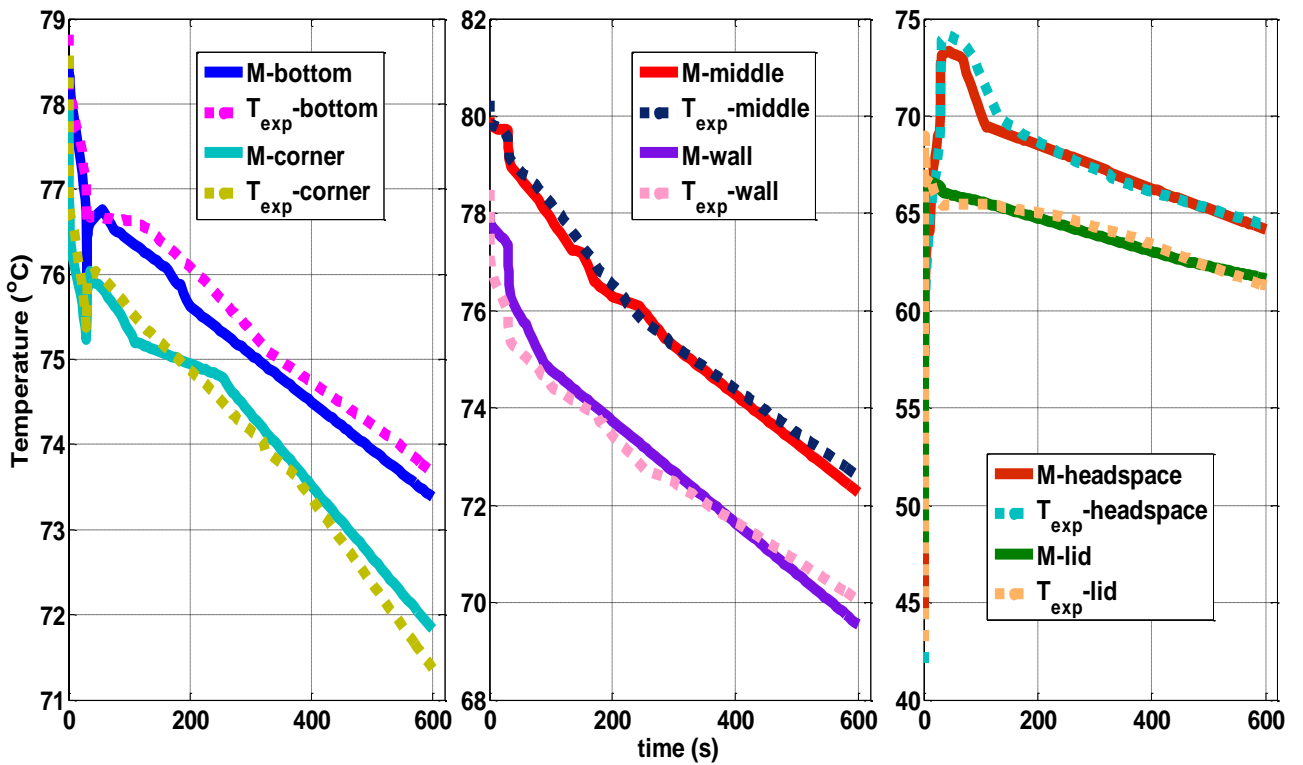
Figure 4.16: Time-temperature profiles of predicted versus experimental data for fluid T-Case II.

Table 4.2: RMSE values (^{o}C) for fluids A and T and Cases I and II.

	Fluid A		Fluid T	
	Inverted	**Upright**	**Inverted**	**Upright**
Bottom	0.5	0.3	0.3	0.3
Corner	0.5	0.5	0.3	0.3
Middle	0.3	0.4	0.2	0.3
Wall	0.6	1.1	0.6	0.3
Headspace	1.6	1.8	1.0	0.5
lid	1.4	2.1	0.8	0.3

4.4   Conclusions

A model and real liquid food of 3 % starch solution (w/w) (Fluid A) and cream of tomato soup (Fluid T), respectively, were hot-filled at a temperature of 80°C into glass jars and were air-cooled for 10 min; the two fluids were chosen due to their viscosity difference. The method of inversion was used as a post-pasteurisation step for sufficiently heating up the headspace and lid of the package; the jars were inverted for 30 s.

The temperature distribution and flow behaviour of the two fluids for both the inverted (Case I) and non-inverted package (Case II), during the cooling phase of the hot-filling were predicted by the dynamic finite element mathematical method. 7031 nodal points were used with a fine grid at the domain and finer grid near the walls and the interface of air-fluid; a time step of 1s and a convergence criterion of 10^{-8} were used. The fluids were assumed to have a finite axi-symmetric cylindrical geometry and constant thermo-physical properties

(thermal conductivity k, specific heat Cp, thermal expansion coefficient b, and density); the density was assumed to be constant in the governing equations except in the buoyancy term, where the Boussinesq approximation is used, for describing its variation with temperature. The viscosity was modelled as a as temperature dependant variable.

The inversion step was numerically solved by the use of a parametric sweep step which simulated the temperature distribution at inclination angles (angle of the gravity vector from its initial vertical position) from 0 to π rad for the first inversion (upright to inverted position), and from π to 2π rad (inverted to upright position again) for the second inversion. The temperature isotherms plotted for illustrating the temperature evolution during the cooling phase of the treatment show that the fluid is rapidly cooled down near the walls creating a downward flow, whilst the core remains at high temperatures and moves upwards, heating up the headspace and the lid; that created recirculation zones which were reflected in the velocity plots. In both fluids and cases, the cold zones are located near the walls and the interface between the fluid and air. The convection currents push the cold zones of the fluid to move from the headspace towards the bottom of the jar and near the wall, creating secondary and tertiary flows. The forced convection caused by the inversion of the package, created higher recirculation within the fluid; the disrupted interface of the fluids indicated the existence of either a bubble, created during inversion or the movement of cold spots within the fluid. The velocity plots showed faster heat transfer in fluid A, with the velocities being up to ten times higher than those in fluid T. The comparison of the predicted temperature profiles with the experimental ones showed good agreement for both cases and fluids. The correlation of the two data sets was confirmed by the low RMSE values obtained.

The validation of the mathematical model developed, makes the future design, control and optimisation of thermal processes promising.

References

Atkinson K., (1993). Elementary Numerical Analysis (2nd ed.). John Wiley & Sons, Inc., New York, NY, USA (Chapter 8).

Avila I.M.L.B., Silva, C.L.M. (1999). Modelling kinetics of thermal degradation of colour of peach puree. *Journal of Food Engineering*, 39, 161–166.

Boz Z., Erdogdu F., Tutar M., (2014). Effects of mesh refinement, time step size and numerical scheme on the computational modeling of temperature evolution during natural-convection heating. *Journal of Food Engineering,* 123, 8–16.

Breuer M., (2000). A challenging test case for the large eddy simulation: high Reynolds number circular cylinder flow. *International Journal of Heat and Fluid Flow,* 21, 648‑654.

Bukhari S.J.K., Siddiqui M.H.K., (2007). Characteristics of air and water velocity fields during natural convection. *Heat Mass Transfer*, 43, 5, 415-425.

Cornelissen J.T., Taghipour F., Escudie R., Ellisa N., Grace J.R., (2007). CFD modelling of a liquid‑solid fluidized bed. *Chemical Engineering Science*, 62, 6334‑6348.

Cox P.W. and Fryer P.J., (2002). Modelling thermal processes: heating. *Food process modelling*, 340–364.

Datta A.K., Teixeira A.A., (1987). Numerical modelling of natural convection heating in canned liquid foods. Transactions of American Society of Agricultural Engineers, St. Joseph, MI: American Society of Agricultural Engineers.

Datta A.K., Teixeira, A.A., (1988). Numerically predicted transient temperature and velocity profiles during natural convection heating of canned liquid foods. *Journal of Food Science*, 53 (1), 191-195.

Druzeta S., Sopta L., Macesic S., Crnjaric-Zic N., (2009). Investigation of the importance of spatial resolution for two-dimensional shallow-water model accuracy. *Journal of Hydraulic Engineering* 11, 917‑925.

Erdogdu F., Uyar R., Palazoglu T.K., (2010). Experimental comparison of natural convection and conduction heat transfer. *Journal of Food Process Engineering,* 33, 85–100.

Erdogdu F., Tutar M., (2011). Velocity and temperature field characteristics of water and air during natural convection heating in cans. *Journal of Food Science,* 76, 119–129.

Ghani A.A.G., Farid M.M., Chen X.D., Richards P., (1999). Numerical simulation of natural convection heating of canned food by computational fluid dynamics. *Journal of Food Engineering,* 41, 55–64.

Ghani A.A.G., Farid M.M., Chen X.D., Richards P., (1999). An investigation of deactivation of bacteria in a canned liquid food during sterilization using computational fluid dynamics (CFD). *Journal of Food Engineering,* 42, 207-214.

Ghani A.A.G., Farid M.M., Chen X.D., (2002). Numerical simulation of transient temperature and velocity profiles in a horizontal can during sterilization using computational fluid dynamics. *Journal of Food Engineering,* 51, 77–83.

Ghani A.G., Farid M.M., (2006). Using the computational fluid dynamics to analyse the thermal sterilization of solid–liquid food mixture in cans. *Innovative Food Science Emerging Technologies,* 7, 55–61.

Holman J. P., (1992). Heat transfer, UK: McGraw-Hill.

Joseph S.J., Speers R.A., Pillay V., (1996). Effect of head space variation and heat treatment on the thermal and rheological properties of non-agitated, conduction-heated materials. *Lebensm Wiss u. Technologie*, 29, 556–560.

Kannan A., Sandaka P.Ch.G., (2008). Heat transfer analysis of canned food in a still retort. *Journal of Food Engineering,* 88, 213–228.

Kiziltas S., Erdogdu F., Palazoglu T.K., (2010). Simulation of heat transfer for solid–liquid food mixtures in cans 3 and model validation under pasteurization conditions. *Journal of Food Engineering,* 97, 449–456.

Kumar A., Bhattacharya M., Blaylock J., (1990). Numerical simulation of natural convection heating of canned thick viscous liquid food products. *Journal of Food Science,* 55, 1403–1411, 1420.

Kumar A., Bhattacharya M., (1991). Transient temperature and velocity profiles in a canned non-Newtonian liquid food during sterilization in a still-cook retort. *International Journal of Heat and Mass Transfer,* 34, 1083–1096.

Mills A.F., (1995). Basic heat and mass transfer, USA: Irwin.

Moraga N., Torres A., Guarda A., Galotto M.J., (2011). Non-Newtonian canned liquid food, unsteady fluid mechanics and heat transfer prediction for pasteurization and sterilization. *Journal of Food Process Eng*ineering, 34, 2000–2025.

Mohamed I.O., (2007). Determination of an effective heat transfer coefficients for can headspace during thermal sterilization process. *Journal of Food Engineering,* 79, 1166–1171.

Ramaswamy S., Grabowski S., (1996). Influence of entrapped air on the heating behaviour of a model food packaged in semi-rigid plastic containers during thermal processing. *Food Science Technology,* 29, 82–93.

Sandoval, Barreiro, Mendoza, (1994). Prediction of hot-fill-air-cool sterilization processes for tomato paste in glass jars. *Journal of Food Engineering* 23, 33–50.

Teixeira A.A., (1992). *Food Engineering Handbook*: Thermal process calculations. Marcel Dekker, Inc, New York, NY, 563-619.

Tu J., Yeoh G.H., Liu C., (2008). Computational Fluid Dynamics: A Practical Approach. *Elsevier Applied Science Publishers*, New York, NY, USA, p. 36.

Tutar M., Erdogdu F., (2012). Numerical simulation for heat transfer and velocity field characteristics of two-phase flow systems in axially rotating horizontal cans. *Journal of Food Engineering,* 111, 366–385.

Weintraub S.E., Ramaswamy H.S., Tung M.A., (1989). Heating rates in flexible packages containing entrapped air during overpressure processing. *Journal of Food Science,* 54, 1417–1421.

Chapter 5 - TTI validation for hot-fill processes

Abstract

Traditionally, thermal processes are quantified by using temperature sensors (thermocouples). However, in processes where complexities such as particulate foods or continuously cooked products are introduced, the application of thermocouples is not convenient and the process validation can be challenging.

The use of time temperature integrators (TTIs) as an alternative means to process evaluation of either temperature or microbial systems has recently received considerable attention (Van Loey, & Hendrickx, 2002). In the current chapter, TTIs were tested for their reliability and accuracy under isothermal and non-isothermal conditions, and were then used for the validation of the hot-fill process, for a target process of 2 min at 70°C (Target I) and 5 min at 85°C (Target II). The TTI systems used in the following experiments are based on α-amylase from *Bacillus amyloliquefaciens (BAA)* prepared as two different solutions for evaluating the two target processes at the reference temperatures of 70 and 85°C, referred to as BAA70 and BAA85, respectively. When tested under isothermal conditions, the TTIs resulted in a D_{70}-value of 4.1 min and a z-value of 10.8^{o}C for BAA70 and a D_{85}-value of 8.7 and a z-value of 10.3^{o}C for BAA85; the heat duration was calculated to be 7 and 16 min for BAA70 and BAA85, respectively.

A Peltier stage was used for investigating the response of the two TTI systems under non-isothermal conditions. The TTIs appeared to be reliable in picking up small temperature

differences, but they cannot reach the temperature that the Peltier stage is set to deliver. Finally, their response was investigated under hot-fill treatments and was compared to that of the thermocouples, subjected to the same thermal treatments. The heating mediums used for the thermal process were water, 3% starch solution and tomato soup; the process values were obtained at five locations inside the glass jar, the bottom, corner, wall, headspace and the lid. The target process was achieved by the bottom, bottom-corner and wall for BAA70 TTI and all three fluids, but he filling temperature was not sufficient to pasteurise the headspace and the lid. Both TTI systems record lower temperatures than thermocouples under any of the conditions they were submitted in the current work.

A statistical analysis was performed for illustrating how significantly different the two monitoring techniques are; results obtained from ANOVA showed that the two methods are not significantly different at a 5% confidence level and that given the potential for discrepancy, the TTI systems could be safely used for evaluating pasteurisation processes.

5.1   Introduction

Food thermal processing is still one of the most widely used food preservation methods aiming to deliver safe food to the consumer, by inactivating the pathogenic micro-organisms within it, and to extend the foods' shelf life (Bellara et al., 1999).

As the variety of food products, processes and container types is increasing, food manufacturers are faced with the challenge of proving that their products are microbially safe. Consumers' awareness of healthy food and the tighter regulations in terms of additives maximise the challenge of food producers, since the product delivered to the consumer needs to be safe and of high quality at the same time; this is an optimisation problem. Thus, the validation of thermal processes has become of ever-increasing importance. The use of

conventional temperature probes is the most common method of validating thermal processes, since they are accurate over a defined temperature range and are sensitive to temperature change. However, they are not always convenient to be used due to complexities introduced by products cooked in continuous ovens, such as poultry joints, burgers and bread, and products with discrete pieces cooked in agitated vessels or heat exchangers such as ready meals, soups, cook-in-sauces, and dressings (Tucker, 2003). Because of the above mentioned complexities, other monitoring techniques need to be adopted for evaluating the impact of a heat treatment on safety and quality of a food product.

Alternative options available are the following:

o   *Microbiological methods:* they are divided into the count reduction method, which refers to the inoculation of the entire food with organisms of known heat resistance, and the method of spores encapsulated in an alginate bead. The bead mimics the food pieces in their thermal and physical behaviour so that its heating rate is similar to the food (Brown et al., 1984). The method relies on the measurement of the log reductions obtained by enumerating the surviving organisms or spores, which are converted into process values.

o   *The in situ method*: the approach relies on the direct evaluation of a quality attribute such as colour and vitamin content, before and after the thermal treatment. Detection limits, sample size requirements, in the case of inactivation of microorganisms and their spores, and recontamination are examples of the method having a restricted application (Mulley et al., 1975).

o   *The physical-mathematical approach*: it is frequently used as an alternative to the *in situ* method. The technique is based on the combination of *a priori* determined kinetic parameters for thermal inactivation of a safety or quality factor, with the time-temperature

history obtained from a developed mathematical model. The temperature profile can be obtained either from direct physical measurement (Bigelow et al., 1920) or analytical heat transfer models (e.g. Teixeira et al., 1969).

The process design, evaluation and optimisation of the approach have been abundantly demonstrated. However, the limited information on convective heat transfer coefficients, the lack of accurate thermo-physical data, and the complexities caused during physical experimental work in processes such as in-pack thermal treatment of solid/liquid mixtures in rotary retorts or aseptic processing installations, have led to restricted use of the approach.

o   *Time Temperature Integrators (TTIs):* small measuring devices that are time-temperature dependent. They can be enzyme based, usually amylase or peroxidase when it comes to pasteurisation treatments and goes through an irreversible change when heated that mimics the change of a target attribute when exposed to the same conditions. If the reaction kinetics of the temperature-induced denaturation matches those of the microbial kinetics, the enzyme can be used as a biochemical marker of a process.

Microbial destruction typically follows first order kinetics. The microbial counting data obtained can then be used to determine the D- and z-value key kinetic parameters that will further characterise microbial lethality. The D-value is the required heating time to reduce microbial population by 90% and the z-value is the temperature change required to result in a 10-fold change in D-value. In a similar way, the D- and z-value concept can be used to characterise loss of nutrients. Differences between the D- and z-values of microorganisms and quality attributes can be exploited to optimise thermal processes by using model based approaches (Banga et al.,(1991); Moles et al., (2003).

A lot of different types of enzymatic TTIs have been developed recently, including α-amylase, *Burkholderia cepacia* lipase, polyphenol oxidase, and glucoamylase based TTIs

(Guiavarc'h, 2003; Jin, Jin, Guanglin, & Qin, 2012; Kim, Park, & Hong, 2012; Moritz, Balasa, Jaeger, Meneses, & Knorr, 2012; Tucker et al., 2007; Van Loey, Guiavarc'h, Claeys, & Hendrickx, 2004; Yan et al., 2008).

Time–temperature integrators used in commercial pasteurisation processes have been developed successfully from a few minutes at 70 °C up to many minutes at 95 °C (Tucker, Lambourne, Adams & Lach, 2002, Fryer et al., 2011). Most of the TTIs used in pasteurisation treatments are amylase based, extracted from bacterial sources such as *Bacillus subtilis*, *amyloliquefaciens* or *licheniformis* (Tucker et al., 2007). One such system that has suitable kinetics for estimating pasteurisation values, is the amylase extracted from *Bacillus amyloquefaciens* (BAA), which is the amylase used in the current work. The denaturation of the amylase is minimal at ambient temperature so it can be easily transported. The key attributes of a BAA system are presented in Table 5.1 and some examples of product types and processes where the TTIs have been used are shown in Table 5.2.

Enzymic TTIs have also been used as quality indicators of horticultural products (Bobelyn et al., 2006) and for predicting losses of food quality ascribed to enzymatic changes, hydrolysis, and lipid oxidation (Kim et al., 2012).

Table 5.1: *Bacillus amyloquefaciens* α-amylase (BAA) characteristics (Tucker, 1999).

Operating principle	Amylase activity reduction
Measurement method	Amylase assay
Temperature range (^{o}C)	60-100
z-value (^{o}C)	9.7 ± 0.3
D-value at 80.7^{o}C (min)	$D_{80.7} = 18.7$
Sample size (L)	0.02

Table 5.2: Application of BAA and BLA (*Bacillus licheniformis*) in food processing (CCFRA, Pasteurization heat treatments, 1992).

Product type	Process type	Amylase type
Hot-fill sauces	Pasteurisation topped up with sprayed water/steam	BAA and BLA
Fruit products in liqueurs	In-container pasteurisation	BAA
Ready meals	Sous-vide	BLA
Fruit products with particulates	Ohmic heating	BAA

In order to extend the range of temperatures that the TTIs can be used, upwards into sterilisation temperatures, amylases were dried to precise moisture levels (De Cordt et al.*,* 1994; Van Loey et al.*,* 1997 Guiavarc'h, 2003). Lab-scale experimental results showed that a range of heat stabilities were obtained for different levels of moisture content. The method relied on enthalpy change measurements for a dried amylase in a stainless steel pan, using a differential scanning calorimeter. However, issues concerning the sealing and high density of the pan were reported when used in industrial canning plants (Tucker & Wolf, 2003). Thus, a different method needs to be developed for a sterilisation TTI.

Some potential limitations of the TTIs include:

- TTIs are typically located in the surface of the product; that will lead to significant differences between the product and surface temperature, since the thermo-physical properties will change from product to product, for different process and type of package.

- Different microorganisms and quality attributes require different TTIs.

- Extensive experimentation is required for every time the product or the package is altered.

In the current chapter TTIs are tested under the following conditions:

- Isothermal: water bath experiments

    − Calculation of D- and z- value kinetic parameters;

    − Calculation of process values;

    − Estimation of TTIs' heat duration.

- Non-isothermal: Peltier Stage experiments

    − Reliability of TTIs under a variety of time-temperature profiles;

- Hot-fill treatment: validation of thermal treatment by comparing TTIs with thermocouples, submitted under the same conditions.

5.2   Materials and Methods

5.2.1   Preparation of TTIs

TTI solutions are based on commercial α-amylases (powder A6380 Type II A, and liquid A7595, supplied by Sigma, UK) isolated from *Bacillus amyloliquefaciens* (BAA). The amylases denature when heated in buffer solutions and the residual activity, measured using the Randox colorimetric technique, provides a measure of the thermal process applied to the food. TTI solutions were formulated by dissolving powder amylase for BAA70, and liquid amylase for BAA85, in the appropriate buffer systems. Amylase activity was then measured by using an amylase assay reagent (Randox).

Preparation of Tris Buffer for BAA85 (0.05 Tris Buffer, pH 8.6 at 25°C)

3.0285 g of Trizma base (Sigma T-6066) (tris hydroxymethyl aminomethane) were weighed in a 50 mL beaker and dissolved in 500 mL distilled water. The temperature was adjusted to 25°C, using a water bath and the pH was adjusted to 8.5-8.6 using 1 M HCl (Sigma H-7020), added with a Pasteur pipette (Adams, 1996; Van Loey et al., 1997a). The buffer solution was kept in the fridge for maximum of one month from its preparation.

Preparation of 10mM acetate buffer for BAA70 (pH 5.0 containing 1mM calcium chloride (CaCl$_2$.2H$_2$O))

1.36 g of sodium acetate trihydrate were weighed in a 50mL beaker and 40mL of distilled water were added (100 mM solution). Then 0.036 g of calcium chloride (CaCl$_2$.2H$_2$O) was weighed into a 50 mL beaker and 25 mL of 100 mM sodium acetate solution were added. The pH was adjusted to 5.0 using glacial acetic acid.

Bacillus amyloliquefaciens α-amylase at 85°C (BAA85) solution

BAA85 TTI was used for high acid food products in a pH range of 3.7 to 4.2, targeting a process of 5 minutes at 85°C (CCFRA, 1992a). The solution was prepared by dissolving 50 mg of α-amylase powder from *Bacillus amyloliquefaciens* (BAA) in 5 mL of 0.05 M Tris Buffer, giving a final enzyme concentration of 10 mg/mL.

Bacillus amyloliquefaciens α-amylase at 70°C (BAA70) solution

BAA70 was used for the measurement of mild pasteurisation treatments, targeting a process of the order of a few minutes at 70°C at the core of the food. The food products that receive these mild treatments are intended for distribution under refrigerated conditions for up to ten days storage time, or are naturally high in acid, and are stored under ambient conditions for many

months. The solution was prepared by dissolving 25 mg of liquid α-amylase in 50 mL of 10 mM Sodium Acetate Buffer at 25°C, giving a final enzyme concentration of 0.5 mg/mL.

Both BAA85 and BAA70 solutions were encapsulated into Altesil (Altec, Cornwall, UK) high strength silicone tubing with a 2 mm internal bore and 0.5 mm wall thickness cut into lengths of 15 mm. The two ends of the tube were dipped into silicone elastomer (Sylgard 170, Dow Corning, USA), heated in a conventional oven at 70°C for the silicone to dry, and then they were immersed in the buffer solution and stored in the freezer at -18°C.

5.2.1.1 Randox Amylase Calorimetric Method

The Randox amylase test method (Randox Laboratories Ltd) was used to measure the enzyme activity of both the BAA70 and BAA85 solutions. The method uses ethylideneblocked p-nitrophenyl-maltoheptaoside as substrate (Substrate 2 from the kit), which is cleaved by BAA70 and BAA85 into fragments that are further hydrolysed by the indicator enzyme α-glucosidase, releasing p-nitrophenol and glucose. p-nitrophenol creates a yellow coloured solution, which can be detected using a spectrophotometer and the rate of which can be expressed as an activity. The terminal glucose of the substrate is chemically blocked preventing cleavage by the indicator enzymes (Monza, 2009).

Enzyme Assay procedure

Randox provide a kit containing an amylase substrate and a buffer solution. These kits are supplied in quantities for 5 assays or 20 assays. Preparation was carried out according to the manufacturer's instructions, as follows:

The kit reagents were allowed to equilibrate at room temperature before opening. 20 mL of Buffer 1 (calcium chloride and sodium chloride) were added to Substrate 2, from the kit. The amylase solutions of BAA85 and BAA70 were extracted from the TTI silicone tubes using a

syringe. 10 μL of BAA85 solution were diluted with 290 μL of 50 mM Tris Buffer (30-fold dilution), while 15 μL of BAA70 were diluted with 15 μL of 10 mM Acetate Buffer (2-fold dilution). 20 μL of each diluted solution was added to a cuvette containing 1 mL of the enzyme essay reagent from Randox (Crumlin, UK). The cuvette was then immediately placed into the chamber of the spectrophotometer (CECIL, Cambridge, UK) and the absorbance, at a wavelength of 405 nm and 30°C, was measured. The readings from the spectrophotometer were taken over a 5 minute period.

5.2.1.2 Determination of BAA70 and BAA85 activity

According to the above, the reaction rate of both solutions can be determined by plotting the absorbance readings of BAA70 and BAA85 against time.

Highly active solutions, such as the control samples, reached a constant gradient soon after starting the assay, whereas samples with low enzyme activity required more time. The amylase activities were calculated based on the gradient with the fastest reaction rate of absorbance with time. Figure 5.1 illustrates the reaction rate curve for a control (unheated) amylase, sample of BAA70, prepared according to § 5.2.1, in which the initial rate r_A is $0.014s^{-1}$, based on equation 5.1:

$$r_A = k_f \cdot C_{BAA} \qquad\qquad (5.1)$$

Where: r_A is the reaction rate, k_f is the first order rate constant and C_{BAA} is the active BAA concentration.
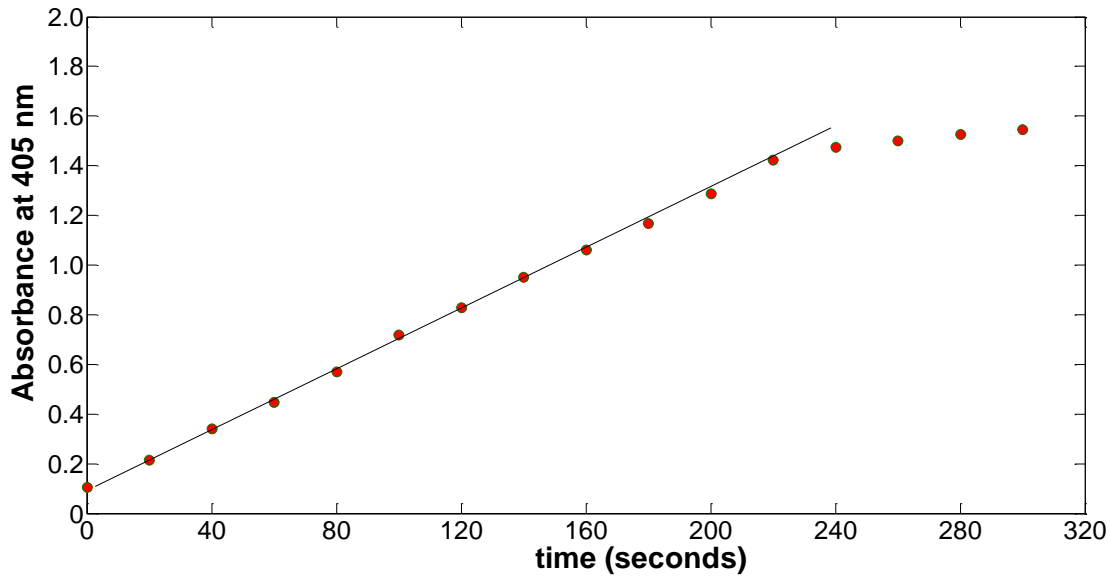
Figure 5.1: Reaction rate curve from BAA70 amylase assay.

The ratio of initial and final activity of the enzyme solutions can then be calculated based on equation 5.2 (Cornish and Wharton, 1988):

$$\frac{A_{initial}}{A_{final}} = \frac{C_{BAA_0}}{C_{BAA}} = \frac{r_{A_o}}{r_A} \qquad (5.2)$$

Where: r_{Ao} is the initial reaction rate and C_{BAAo} is the initial, untreated BAA concentration.

5.2.2   *Isothermal conditions*

5.2.2.1 Calculation of D- and z-values

Before any validation tests were carried out, the TTIs were calibrated so that the enzyme kinetics, D_T- and z-value to be determined. The process lethality was then estimated. According to Tucker et al. (2002) the maximum immersion time should be within a period of approximately one and two log reductions of the initial activity value in order to maximize the accuracy of the measurements.

Thus, after a series of heating trials, the combination of temperatures and immersion times for both TTI systems was chosen based on the achievement of a one to two log reduction of the initial enzyme activity. The time-temperature combinations used for calibrating BAA70 and BAA85 TTIs are presented in Tables 5.3 and 5.4, respectively.

A typical calibration consists of three control TTIs, as a measure of the initial activity, and three TTIs processed at different lengths of time at a defined reference temperature. The TTIs were removed at regular intervals depending upon the maximum length of time they can be still active at the specific temperature. Once the enzyme activities were calculated, based on equation 5.2, the gradient of log A_f/A_0 can be plotted against time. The D_T-values for the above temperatures were then determined, using the following equation:

$$\log\left(\frac{A_{final}}{A_{initial}}\right) = -\frac{t}{D_T} \qquad (5.3)$$

Table 5.3: Experimental immersion times and temperatures for BAA70 TTI.

Temperature (^{o}C)	Water bath immersion times (min)
60	1,2,3,4,6,8,10,12,14,16,18,20,22,24,26,28,30
63	1,2,3,4,6,8,10,12,14,16,18,20,22,24
65	1,2,3,4,6,8,10,12,14
70	1,2,3,4,6
75	1,2,3

Table 5.4: Experimental immersion times and temperatures for BAA85 TTI.

Temperature (^{o}C)	Water bath immersion times (min)
80	1,2,3,4,6,8,10,12,14,16,18,20,22,24,26
83	1,2,3,4,6,8,10,12,14,16,18,20,22
85	1,2,3,4,6,8,10,12,14
87	1,2,3,4,6,8,10
90	1,2,3

After the D_T-values were estimated for the above time-temperature combinations, the second key parameter, z-value was calculated. The gradient of log D_T-values is plotted against the defined temperatures and the z-value is determined based on Equation 5.4:

$$z = -\frac{T_1 - T_2}{\log\left(D_{T_2} / D_{T_1}\right)} \tag{5.4}$$

5.2.2.2 Determination of P-values

Assuming that first order kinetics are employed for the enzymes' inactivation, the same as for the destruction of micro-organisms, the process values were obtained based on the initial and final enzyme activities measured at the beginning and at the end of the thermal process, using the following equation:

$$P = D_{T.} \log\left(\frac{A_{initial}}{A_{final}}\right) \tag{5.5}$$

The calculation of the process values can also be obtained by integrating the time-temperature history experienced by the product. The P-values obtained, should be equal to

the ones calculated from the TTIs, provided that the assumption of first order kinetics holds for the enzymes over the whole temperature range they have experienced. The combination of the two monitoring techniques used to validate the thermal process is expressed as follows:

$$P = \int_{0}^{t} 10^{\frac{T(t)-Tref}{z}} .dt = D_{T.} \log\left(\frac{A_{initial}}{A_{final}}\right) \tag{5.6}$$

T_{ref} equals the value of 85°C and 70°C, for BAA70 and BAA85, respectively, with the appropriate, estimated z-values.

5.2.3   *Non-isothermal conditions: Peltier stage*

The TTIs were tested under non-isothermal conditions for their sensitivity to be evaluated at various time-temperature profiles. A Peltier stage (Linkam, Tadworth, UK), was used to provide the time temperature profiles by control of the applied voltage to its thermoelectric module – the Peltier and its operational principle are illustrated in Figure 5.2.

The thermoelectric module was connected to a water circulating pump (ECP 220-240V/50 Hz, Linkam, Tadworth, UK) that keeps the device from overheating and being damaged, and a computer, where the time-temperature profiles were set and controlled. The software used was Linksys 32 (Linkam, Tadworth, UK).
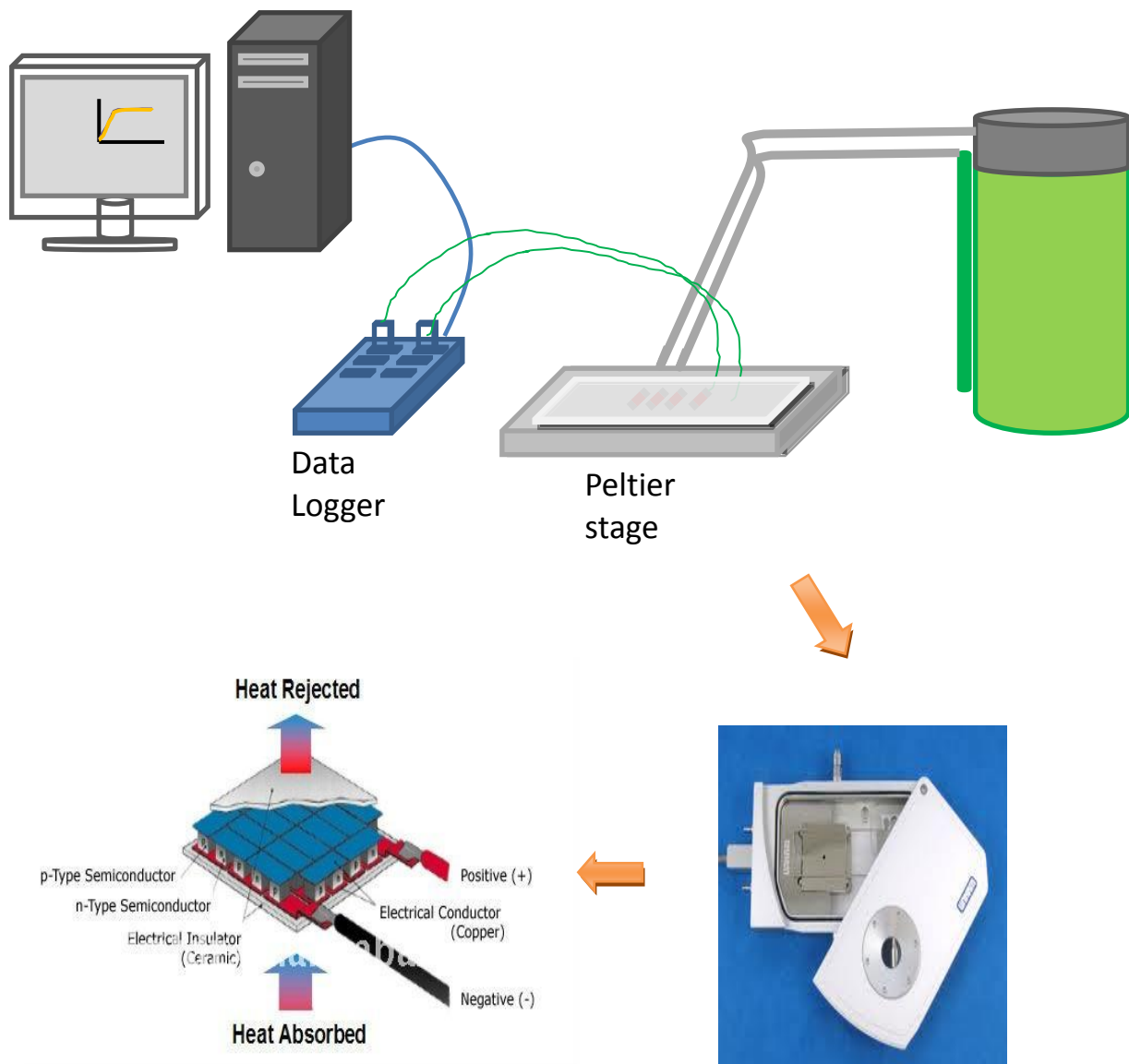
Figure 5.2: Experimental configuration of Peltier stage (top), Linkam Peltier module used and its principle of operation (bottom) (http://www.huimao.com/).

The reliability of the Peltier system was checked by attaching a thermocouple on the thermoelectric module using adhesive tape. The time-temperature history recorded from the thermocouple data logger was compared to that obtained from the internal temperature measurement from the Peltier stage.

In order to test the sensitivity of the TTIs on temperature changes, three TTIs and one more with a calibrated thermocouple (type K) inside, were attached to the thermoelectric module,

using a heat sink compound (RS, Corby, UK, thermal conductivity = 0.9 (W m^{-1} K^{-1}) that ensured good thermal contact between them and the Peltier plate. The enzyme activities obtained from the TTIs were compared to the time-temperature history recorded from the thermocouple inside the fourth TTI, in terms of process values, using equation 5.6. The above non-isothermal conditions were repeated five times.

The experiments conducted on the Peltier stage, were separated into two different sets:

5.2.3.1 Simple cycles

The heating and cooling rate of the process is kept constant, and the holding time is of great importance, as it is the factor that affects the lethality of the process the most. Such a process is usually batch, where a retort is used for the heating, holding and cooling phases of the treatment. The calculation of lethality in these types of processes is easier as compared to variable time-temperature conditions. The evaluation of thermal processes at a constant lethal temperature is relatively easy; but the temperature throughout a process is rarely constant.

The TTIs were heated up at two different reference temperatures, 70 and 85°C, at a constant heating/cooling rate of 30°C min^{-1}. The holding time at which the TTIs and the thermocouples were kept, for the above two T_{ref}, varied from 2 to 10 min. The TTIs were then cooled down to 20°C, at the same rate of 30°C min^{-1}. The holding time, the number of repetitions for each T_{ref} and the number of TTIs and thermocouples used on the plate are shown in Table 5.5.

Table 5.5: Experiments conducted on Peltier stage at constant heating/cooling rate.

Holding time (min) at T_{ref}=70°C (BAA70)	Holding time (min) at T_{ref}=85°C (BAA85)	Repetitions	Number of TTIs	Number of thermocouples
1	2	5	15	10
2	4	5	15	10
3	6	5	15	10
4	8	7	21	14
6	10	7	21	14
8	12	7	21	14

5.2.3.2 Complex cycles

The second set of experiments refers to complex time-temperature profiles which are more relevant to industrial continuous processes, such as hot-fill treatments; the product is continuously processed usually into tunnels with the sections of heating, holding, and cooling. The TTIs were heated up at two different rates, 15 and 30°C min^{-1}, until the reference temperature of 70 or 85°C was reached, with no holding time, and were immediately cooled down to 20°C, at the same rates. The repetitions and number of TTIs and thermocouples used are summarised in Table 5.6.

Table 5.6: Complex cycles produced on Peltier stage for a heating/cooling rate of 15 and 30°C min^{-1}.

Holding time (min)	T_{ref} (°C)	Repetition of t-T profiles	Repetitions	Number of TTIs	Number of thermocouples
0	70/85	x1	5	15	10
0	70/85	x2	5	15	10
0	70/85	x3	5	15	10
0	70/85	x4	5	15	10

For both simple and complex cycle, the standard deviation between the repetitions resulted in a value lower than 3. Thus, the average values were taken as representative for illustrating the data obtained in Figures 5.6-5.9.

5.3   Results and Discussion

5.3.1   Isothermal conditions: kinetic parameters and heat treatment duration

The log of initial (A_o) /final (A) amylase activity was plotted against a defined heating time for both BAA70 and BAA85 as illustrated in Figure 5.3. The values of $D_{70°C}$ and $D_{85°C}$ were then calculated based on equation 5.3 and are presented in Table 5.7.
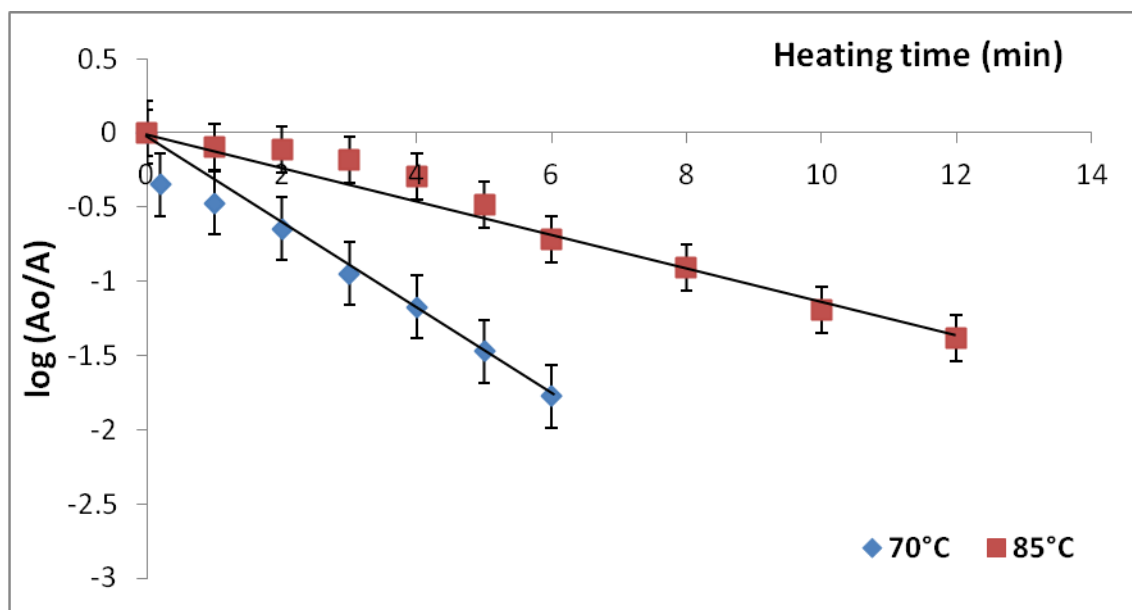
Figure 5.3: The BAA70 and BAA85 D_T-value calculation curves.

Table 5.7: Calculated D_T-values for BAA70 and BAA85 solutions.

Test temperature (°C)	D_T-value (min)	Test temperature (°C)	D_T-value (min)
BAA70		**BAA85**	
60	40.8	80	25.0
63	18.3	83	16.6
65	7.3	**85**	**8.7**
70	**4.1**	87	6.6
75	1.6	90	2.7

The log of the above determined D_T-values was then plotted against temperature, Figure 5.4, for both solutions and the z-values were calculated based on equation 5.5.
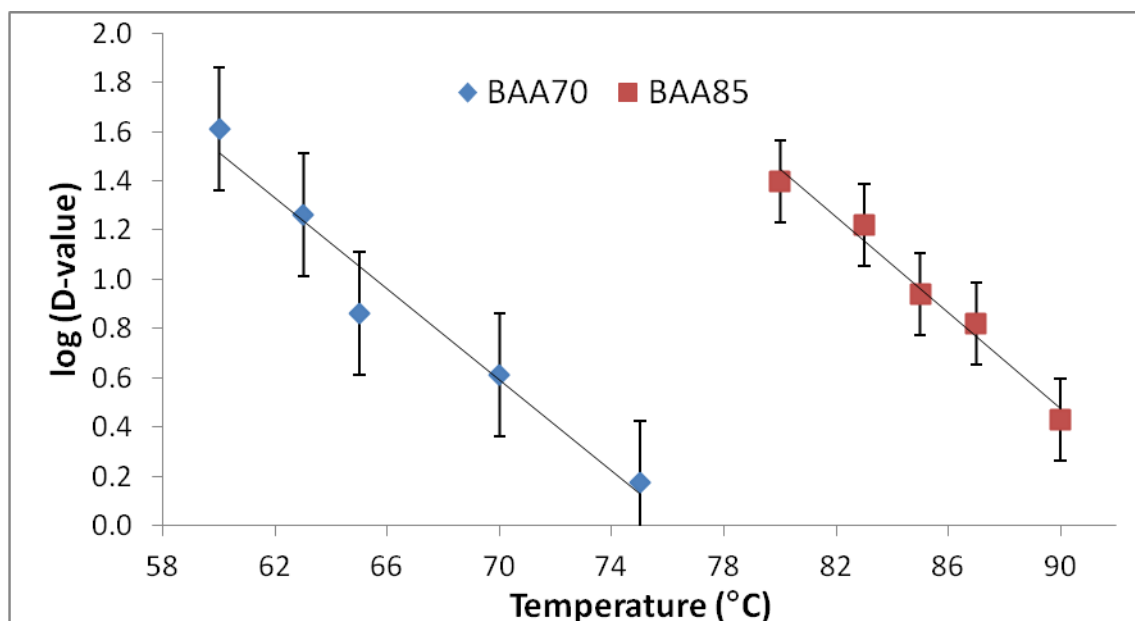
Figure 5.4: The BAA70 and BAA85 z-value curve.

A $D_{70°C}$-value of 4.1 ± 0.4 min was obtained for BAA70 at $T_{ref}=70°C$, which is significantly low in comparison to the value of 8.4 min reported in literature (Lambourne and Tucker, 2001). That is probably due to the different amylase batches being used and/or the storage conditions of the TTIs. The z-value of BAA70 was calculated to be $10.8\pm0.5°C$, which is within the range of the values used for the evaluation of safety of the pasteurisation processes for several microorganisms with z-values from 5 to $12°C$ (Van Loey et al., 1997).

The $D_{85°C}$-value for BAA85 was calculated to be 8.7 ± 0.3 min, higher than the value of 6.8 min found by Lambourne and Tucker, (2001). That is possibly owing to the different α-amylase used in the current project. The liquid form of amylase used, shows optimal activity at the range between $70°C$ and $90°C$, in comparison to the powder amylase used in experimental work reported from literature (Hendrickx et al., 1992), where the amylase shows an optimum at $65°C$. The higher D_T-value obtained from the liquid amylase, indicates that the specific amylase is more heat resistant than the powder one, and would possibly be more accurate in monitoring higher temperatures in pasteurisation treatments. The z-value of

BAA85 was 10.3±0.3°C, consistent with the values used for monitoring pasteurization processes. The kinetic parameters obtained from the experimental work are shown as compared to the values reported in literature, in Table 5.8.

In order for the TTIs to accurately represent the effect of a thermal treatment on microorganisms of interest, it is important that their kinetics resemble that of the target organism, which would result in similar lethality. Thus, TTIs could accurately mimic the destruction rate of microorganisms and be used safely in validating thermal processes.

Table 5.8: α-amylase TTIs used in pasteurisation treatments of foods
(CCFRA guidelines, 2006b).

Product pH	Target microorganisms	Target process	D_T-value (min)	z-value (°C)	D_T-value (min)	z-value (°C)
			Literature		Experimental	
Cook-chill <3.5	Acid-philic yeasts and moulds, and lactobacilli	2 min at 70°C BAA70	8-10	8-9	4.1±0.4	10.8±0.5
High acid 3.5-4.0	Acid tolerant yeasts and moulds, spore-forming bacteria	5 min at 85°C BAA85	8-10	9-9.5	8.7±0.3	10.3±0.3
Sous-vide 4.0-4.2	spore-forming bacteria	10 min at 90°C BLA90	15-25	9-9.5	-	
Acid 4.2-4.5	spore-forming bacteria	5 or 10 min at 93.3°C BLA93	8-12	9-9.5	-	

In the current work, the denaturation of *Bacillus amyloliquefaciens* α-amylase was used as the TTI system that can be used in pasteurisation treatments (60–105°C). The kinetics obtained under non-isothermal conditions was proved to be reliable for its use in measuring integrated process values (Van Loey and Arthawan, 1997a).

The z-values of both BAA70 and BAA85 enzymes appear to be higher than those of the targeted processes, which is in agreement with what is found in literature about enzymes

implicated in mild thermal processes concerning acid and high-acid food products (Hendrickx et al., 1996). Hence, if the process values of the enzymes are used to predict the actual values of the thermal treatment, the filling temperature needs to be larger than the reference temperature, so that the target process value to be achieved. As far as the heat duration of the TTIs is concerned, the chosen immersion times resulted in one to two log reductions of activity for both enzymatic solutions, maximizing the accuracy of the measurements (Tucker et al., 2002). Consequently, TTIs should be able to endure heat treatments for maximum $2D_T$-values. According to the kinetics obtained, the BAA70 and BAA85 solutions should be accurately used for heat duration of maximum 8.2 min and 17.4 min, respectively.

The calculation of the process values was based on equation 5.3. The obtained values were plotted against the defined immersion times, in order to estimate the heat duration of the two TTI systems. Figure 5.5 illustrates the correlation of the TTIs with the processing time using the ideal Y=X curve; R^2 was calculated to be 0.993 and 0.995 for BAA70 and BAA85 respectively. According to Figure 5.5, the maximum heat duration of BAA70 is 7 min, and that of BAA85 is 16 min, which are slightly lower than the ones expected to be achieved, according to the $2D_T$-value theory. The fact that the BAA70 has a shorter shelf life than BAA85 is possibly owing to the significant difference in their D_T-values, D_{70}-value is half of D_{85}, indicating that BAA70 is less temperature resistant than BAA85.
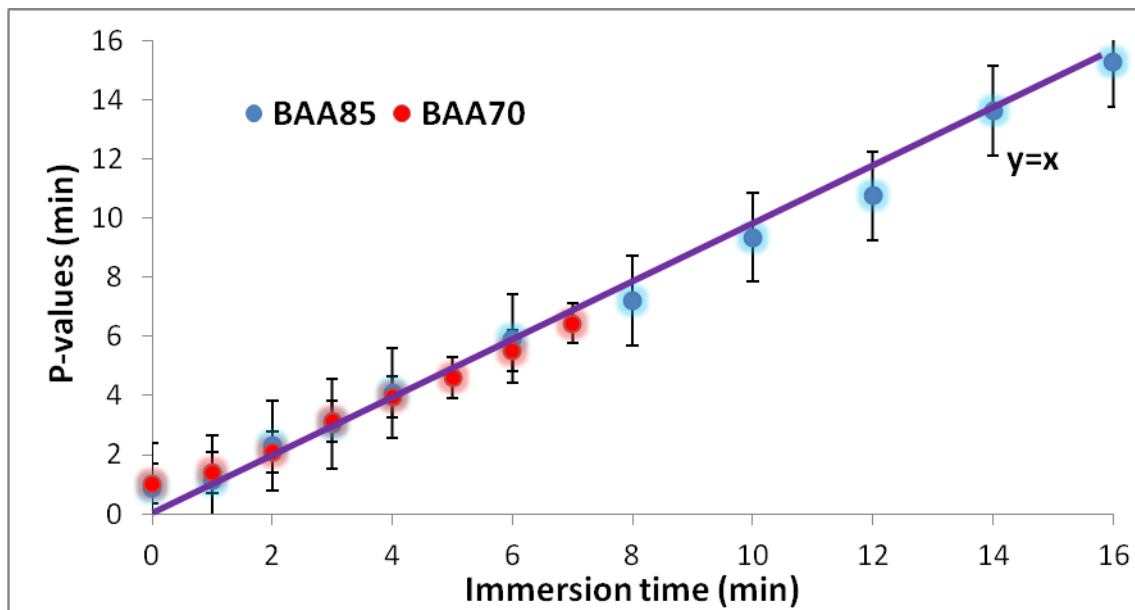
Figure 5.5: Heat duration curve of BAA70 and BAA85.

5.3.2   Non-isothermal conditions: Peltier Stage

5.3.2.1 Reliability of the stage

The Peltier Stage was tested for its reliability, before being applied as a heat treatment to the TTIs. The reliability of the system was checked by comparing the time-temperature history within the Peltier stage with that obtained from the attached thermocouple on the thermoelectric module, as recorded from the data logger.

The stage and the plate time-temperature profiles were compared at the two different conditions that the TTIs will later on be submitted to. The stage was set to heat up at the reference temperature of $70^{o}C$, for a holding time of 10 min, at a constant heating/cooling rate of $30^{o}C$ min^{-1}, Figure 5.6 (a), and at the reference temperature of $85^{o}C$, with no holding time, twice at the same rate, Figure 5.6 (b).

a. b.
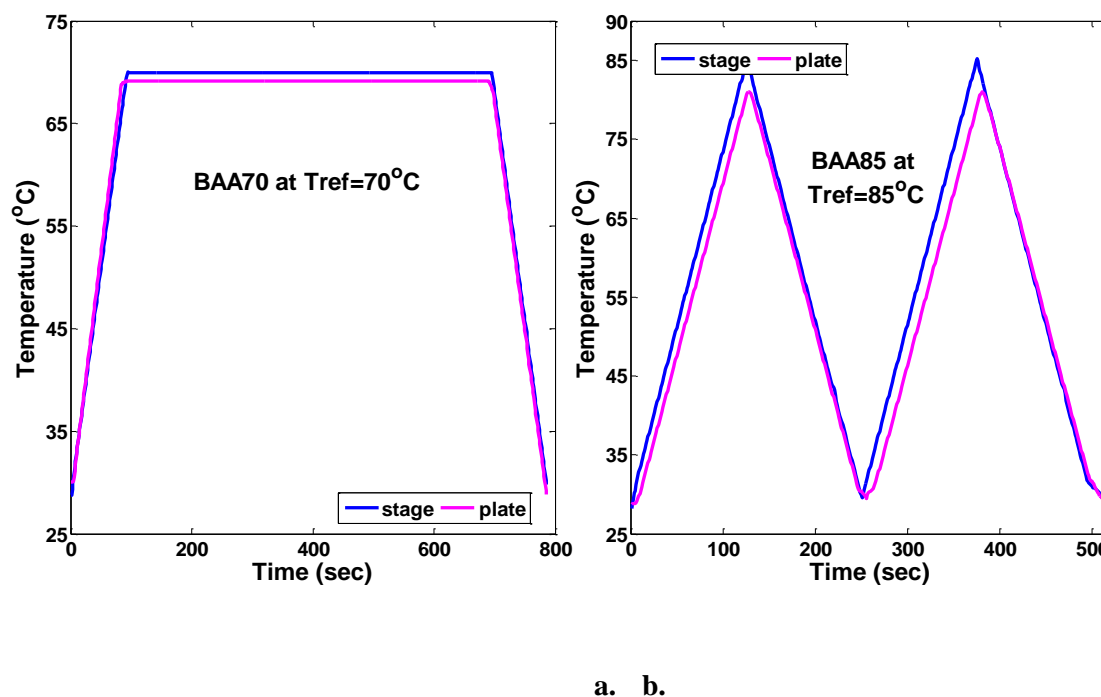
Figure 5.6: Time-temperature profiles of the Peltier stage and the thermoelectric module for a. BAA70 and b. BAA85.

It appears that the temperatures recorded on the plate, are very consistent with the ones obtained from the stage, in both conditions, making the method reliable for testing the TTIs' sensitivity under tightly controlled time-temperature conditions. The slight difference of 0.5-1°C is possibly due to measurement sampling rate; the stage temperature is recorded every 0.30 seconds, whilst the one of the thermocouple is recorded every second. Another reason can be the thermocouples moving during the treatment.

After the accuracy of the Peltier stage was confirmed, three TTIs plus one with a thermocouple inside were attached to the thermoelectric module. The thermocouple was inserted in the TTI in order to test whether the process values obtained from the amylase reduction are consistent with the values obtained from the time-temperature profile that the thermocouple records inside the TTI. That way, the TTIs can be comparable with the time temperature recorded on the thermoelectric module, since the TTIs cannot record the changes in a continuous process; they would have to be removed and measured in every step of the

heat treatment applied. The Peltier stage was set to heat up at the reference temperatures of $70^{\circ}C$ for a range of holding times from 2 to 10 min for BAA70, and at a reference temperature of $85^{\circ}C$, with no holding time, repeated twice in a consequent cycle. The time-temperature profiles were recorded until both TTI systems reached the temperature of $70^{\circ}C$, at a rate of $30^{\circ}C$ min^{-1}; the experiments were repeated 5 times for both TTI solutions. The time-temperature profile obtained from the thermocouples and the enzyme activities measured at the beginning and the end of the process were compared in terms of process values, based on Equation 5.6; the process values shown in Figure 5.7 are the average values obtained from the 5 replications, for all the time-temperature histories applied on the module. The linear fit curve indicated a very good agreement between the two process-value sets; the observation was confirmed by the calculated standard deviation values of 0.024 and 0.014 min for BAA70 and BAA85, respectively.

The results indicate that recording the time-temperature profile of the amylase by the inserted thermocouple, instead of measuring its activity, is reliable. Thus, the heating/cooling profiles applied by the stage, will make the comparison of TTIs and thermocouples placed on the module more convenient.
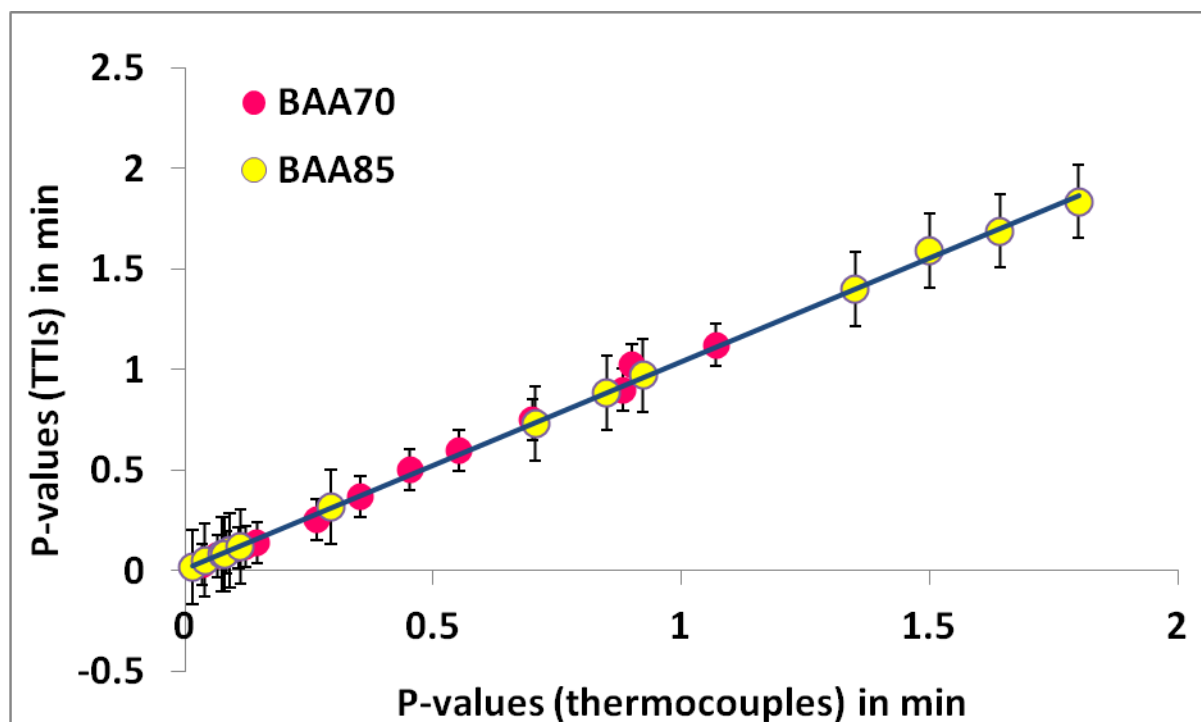
Figure 5.7: Correlation between the temperatures recorded from the thermocouple inside the TTIs, and the enzyme activity of the TTIs.

5.3.2.2 Simple cycles

The Peltier stage was set to heat up the module until the reference temperatures of 70, 85 and 90°C were reached. The holding time was set from 2 to 12 min, for all three reference temperatures and the cooling cycle was set to reach 20°C; the heating/cooling rate was kept constant at 30°C min⁻¹. The different reference temperatures and holding times were chosen in order to test the sensitivity of the TTIs under a variety of conditions.

Three BAA70 and BAA85 TTIs were attached to the thermoelectric module, with inserted thermocouples; an extra thermocouple also used, which was in direct contact with the module; the time-temperature profiles of the two monitoring techniques were recorded by the Peltier stage and were compared.

BAA70 was used for the reference temperature of 70°C, whilst BAA85 was used for the reference temperatures of 85, and 90°C. Figure 5.8 illustrates the two TTI systems for 10, 8 and 4 min of holding time, as the best obtained results from the range of 2 to 12 min, for each reference temperature.

The profiles shown are obtained from the average values of 7 replicate experiments.
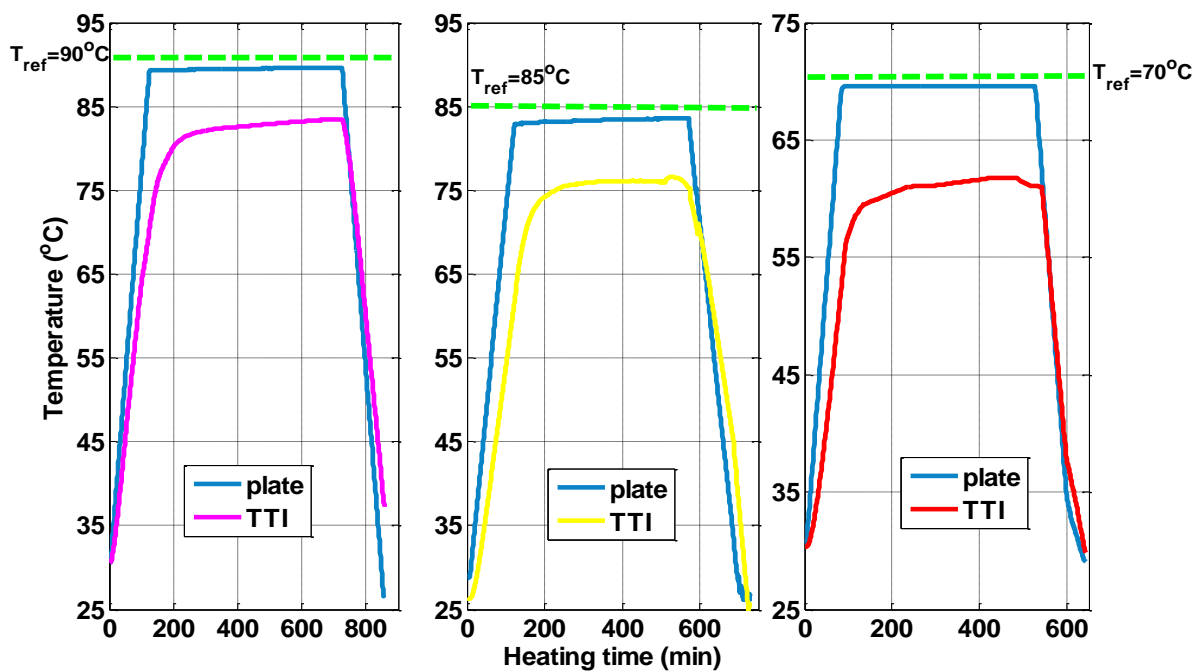
Figure 5.8: Time-temperature profiles of the thermocouples (plate) and BAA85/BAA70 TTIs at 90, 85 and 70°C, respectively, for 10, 8 and 4 min holding time.

From the time-temperature profiles illustrated in Figure 5.8, it can be observed that the temperature recorded inside both TTI systems doesn't reach the temperature that the Peltier stage is set to deliver. The thermocouple on the module records temperatures of 5, 7 and 8°C higher than the TTIs, for the reference temperatures of 90, 85 and 70°C, respectively.

Reasons for that can be:

- The thickness of the silicone tube used, which can give rise to larger heating lags;

- The faster heat received by the thermocouples (prone to conduction), due to their higher thermal conductivity and small size;

- Experimental error: non-proper application of the heat sink compound on the TTIs, the thermocouples moving during the process.

5.3.2.3 Complex cycles

The second set of experiments refers to complex time-temperature profiles that are more relevant to industrial, continuous thermal processes. The TTIs were heated up at a rate of 30°C min^{-1}, until the reference temperature of 70, 85 and 90°C was reached. No holding time was set and the solutions were immediately cooled down to 30°C, at the same rate. The cycle was repeated for 1 to 4 times for both enzymes. The repetitions and number of TTIs and thermocouples used are summarised in Table 5.5. The cycles chosen to be illustrated as the best obtained result for BAA70 TTI, at a reference temperature of 70°C, were four consequent heating/cooling cycles, three for 85°C and 2 for 90°C, referring to BAA85 TTI. Similarly to the simple cycles, three BAA70 and BAA85 TTIs were attached to the thermoelectric module, with inserted thermocouples and an extra thermocouple in direct contact with the module. The time-temperature profiles of the two monitoring techniques were recorded by the Peltier stage and were compared under a variety of complex conditions for testing the sensitivity of the TTIs.
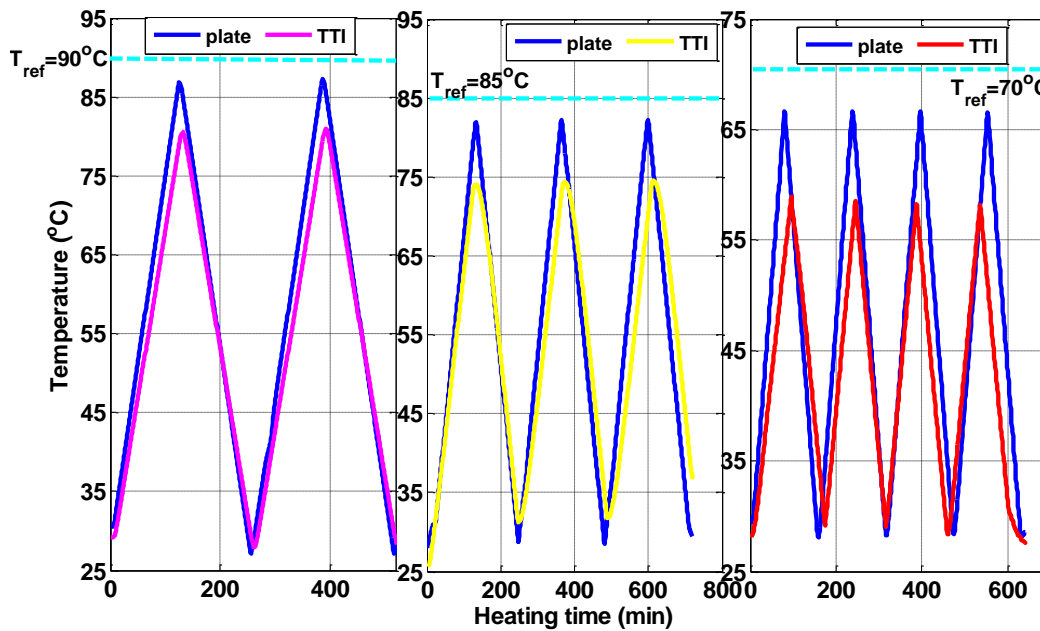
Figure 5.9: Complex time-temperature profiles of the thermocouples (plate), BAA85 and BAA70 TTIs at 90 °C (2 heating/cooling cycles), 85 °C (3 heating/cooling cycles), and 70°C, (4 heating/cooling cycles), respectively.

The temperature recorded at the core of the TTIs indicates that the enzymic solutions are able to pick up small temperature changes throughout the process, but are not sensitive enough to reach the temperature that the thermocouples record on the module. Similarly as with the simple cycles, the higher the reference temperature, the lower the temperature difference between the TTI systems and the thermocouples is; a difference of 5, 7 and 8°C, is observed for the reference temperatures of 90, 85 and 70°C, respectively.

The above observations are reflected in Figure 5.9, where the process values of the thermocouples attached on the thermoelectric module are plotted against those obtained from the TTIs under both the simple and complex heating/cooling conditions defined earlier. The time-temperature history illustrated in Figures 5.8 and 5.9 is integrated and converted into process values based on the left part of Equation 5.6.
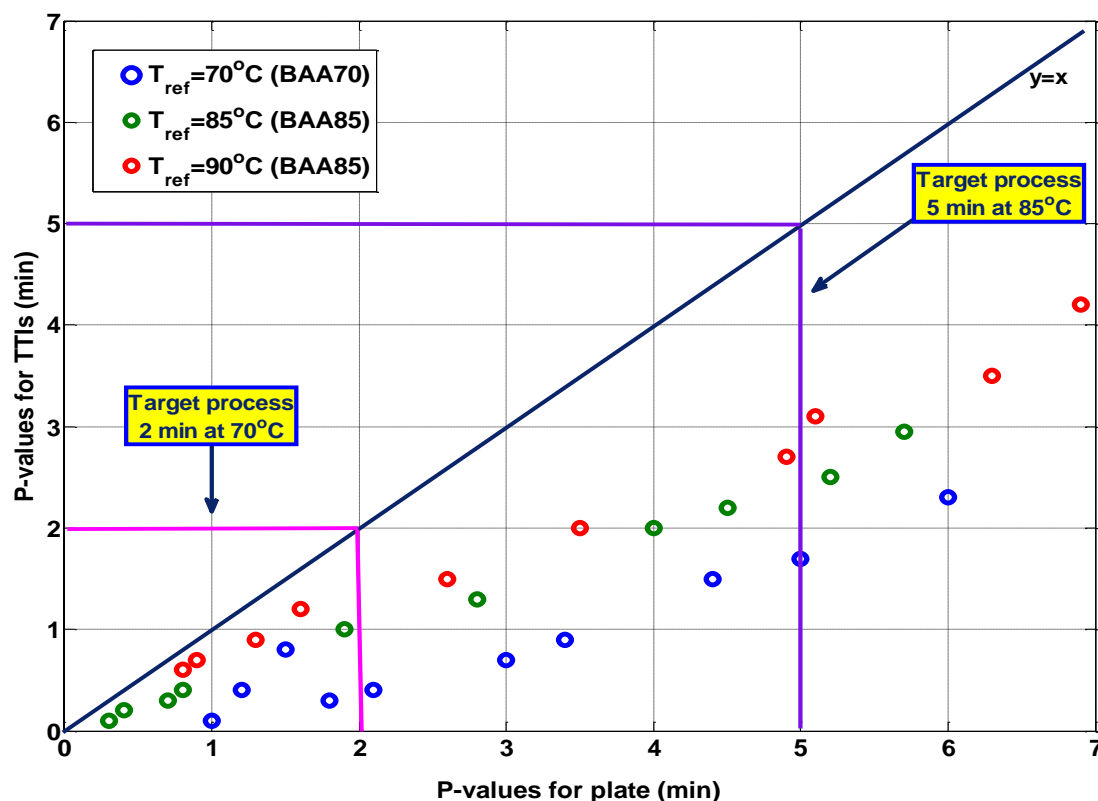
Figure 5.10: Correlation of TTIs and thermocouples under simple and complex non-isothermal conditions set by the Peltier stage.

From Figure 5.10 it is indicated that the TTIs are underestimating the process for both enzyme solutions, under all different conditions (simple and complex). That was expected, since the TTIs record temperatures from 5 to 8^oC lower than the thermocouples attached to the thermoelectric module.

The temperatures used for the non-isothermal conditions were set to be equal to the reference temperatures, which inevitably lead to low process values; the highest average process value obtained for BAA70 was 2.3 min and for BAA85 was 3 and 4.1 min for the reference temperature of 85 and 90^oC, respectively. The highest value calculated for the thermocouples on the module, were 6.0, 5.8 and 6.9 min for the reference temperatures of 70, 85 and 90^oC; the process value of BAA85 TTI was increased by 1 min, when the temperature used (90^oC) was higher than the reference one. That is probably due to the fact that BAA70 TTI has a slightly higher z-value (z=10.8±0.5^oC) as compared to the BAA85 TTI (z=10.3±0.3^oC)

leading to a higher process value and consequently smaller temperature difference with the thermocouples on the plate.

The BAA85 TTIs do not reach the target process for neither of the reference temperatures, whilst the BAA70 TTIs reached the target of 2 min under the simple cycle conditions applied for a holding time ≥4 min. Thus, the TTI systems are not appropriate for assessing hot-fill treatments, under the specific time-temperature conditions. In order to avoid the need for top-up pasteurisation they need to be tested under conditions where the temperatures used, will be higher than the reference ones. In the following section, the TTIs are submitted to conditions more industrially realistic.

5.3.3   Hot-filling by the method of inversion

In the third set of experiments conducted, the TTIs are being tested under the non-isothermal conditions of the hot-fill treatment, described in Chapter 2.

Based on the above derived conclusions, from the sensitivity tests conducted, it appeared that the TTI systems cannot reach the temperature applied to them by the thermoelectric module and they record lower temperatures than the thermocouples attached on the same plate, when the temperatures applied are equal or close to the reference temperatures. Thus, in order to overcome that problem, in the hot-fill treatments in which the TTI solutions were subjected, the filling temperatures were higher than the reference ones, for the TTIs to be possibly more comparable with the thermocouples, subjected under the same conditions.

The TTIs and the thermocouples were positioned in places of interest, where the cold spots are likely to be, on the inside of a glass jar, as illustrated in Figure 5.11. Positions 1, 2, 3, 4 and 5 refer to the bottom, bottom-corner, wall, headspace and the lid, respectively.
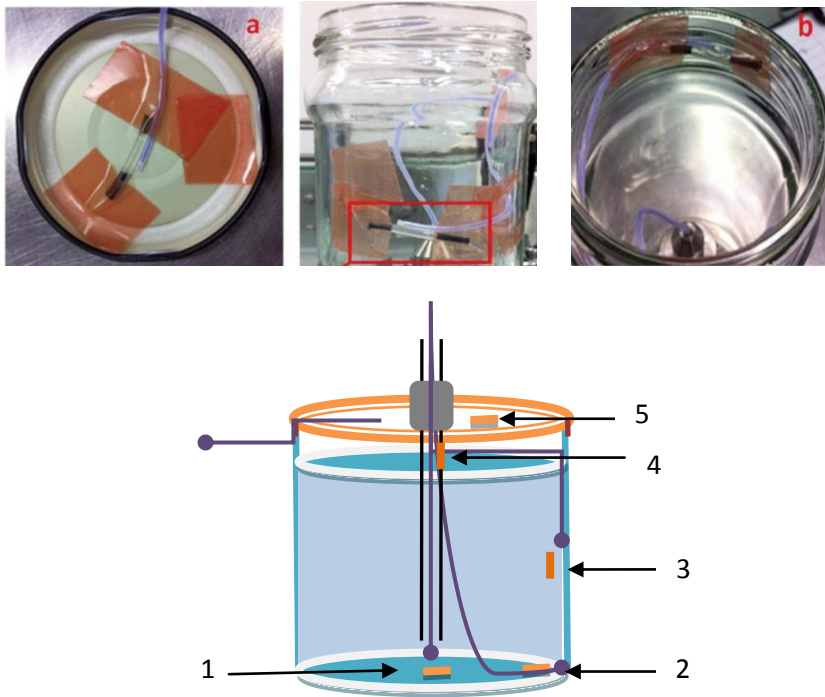
Figure 5.11: Location of TTIs and thermocouples in a glass jar.

The hot-fill treatment experiments were conducted for three different fluids: water, 3% of starch solution (w/w) and cream of tomato soup. The choice was made based on the different thermal properties of the fluids in order to test the response of the TTIs under a variety of fluid conditions. The thermal properties of the fluids were calculated based on Equations 3.4-3.8, Chapter 3, §3.2.3.1, and are presented in Table 5.9.

Table 5.9: Properties of the fluids used at 70°C.

	k (W m^{-1} K^{-1})	C$_p$ (kJ kg^{-1} K^{-1})	ρ (kg m^{-3})	η (Pa s) at γ=10 s^{-1}
water	0.590	4.181	998.2	0.001
3% starch	0.313	4.011	1026	0.30
Tomato soup	0.315	3.673	1050	1.30

The fluids were chosen to be pasteurised at 75 and 90°C for BAA70 and BAA85, respectively. The reasons for the specific filling temperatures were:

- The need for higher temperatures than the reference ones, for minimising the tendency of the TTIs to underestimate the process, as explained above, and

- The heat duration of the TTI systems (BAA70 at 70°C = 7 min and BAA85 at 85°C = 16 min); the enzyme activity recorded within 5°C, for both enzymes didn't affect significantly the process values obtained. For a process time of 10 min, at the above chosen temperatures, the TTIs could endure the heat treatment and be more comparable to the thermocouples.

After being pasteurised, the fluids were filled into a glass jar, which was sealed and air-cooled for approximately 10 min.

The jars were preheated before being hot-filled, at the same temperature the fluids were pasteurised, in order to minimise any heat losses that can occur between the times the fluid is hot-filled and the jar is sealed, and to avoid a possible thermal shock of the package.

The obtained enzyme activity of the TTIs and the time-temperature history of the thermocouples were converted into process values, based on Equation 5.6, and were then compared for both target processes of 2 min at 70°C and 5 min at 85°C.

Figures 5.12 and 5.13 compare the process values of the thermocouples and TTIs at a filling temperature of 75°C and 90°C for BAA70 and BAA85, respectively at all the locations of interest.

Figure 5.12: P-values of BAA70 TTIs and thermocouples for: i. water, ii. 3% starch solution and iii. tomato soup at $T_{fil}=75^{\circ}C$, for all locations.

Where: b, c, w, h and l refer to the bottom, bottom-corner, wall, headspace and lid, respectively.

The coldest points are as expected, at the headspace and the lid of the package, since they are the only locations during the heat treatment that do not come to contact with the pasteurised product. According to common industrial practice, the lid is separately pasteurised from the product, usually by the application of steam. The target process was achieved for the bottom, bottom-corner and wall for all three fluids, but not for the headspace and the lid, under the specific conditions. The TTIs show lower values than the thermocouples for all fluids, with the water showing the smallest difference. That can be can be explained by the poorer heat transfer in the more viscous fluids, since their layer boundary thickness is greater, as compared to water.

The underestimation of the process by the TTIs has possibly to do with the high z-values ($Z_{BAA70} = 10.8^0C > Z_T = 7.5^0C$, and $Z_{BAA85} = 10.3^0C > Z_T = 8.3^0C$) of both enzymes and the fact that the filling temperatures are higher than the reference temperatures, which are responsible for most of the accumulated lethality recorded by the thermocouples, leading to higher process values.

The process values of the TTI and thermocouples were also calculated for the target process of 5 min at 85°C at a filling temperature of 90°C. The values recorded by both monitoring techniques were low, with those of the thermocouples being slightly higher; the target process is not achieved by the BAA85 TTIs, under the specific conditions. It would appear that the filling temperature of 90°C is not sufficiently high for achieving the required target for high acid foods. Thus, the TTIs used under the specific conditions cannot be appropriately used for pasteurisation treatments.
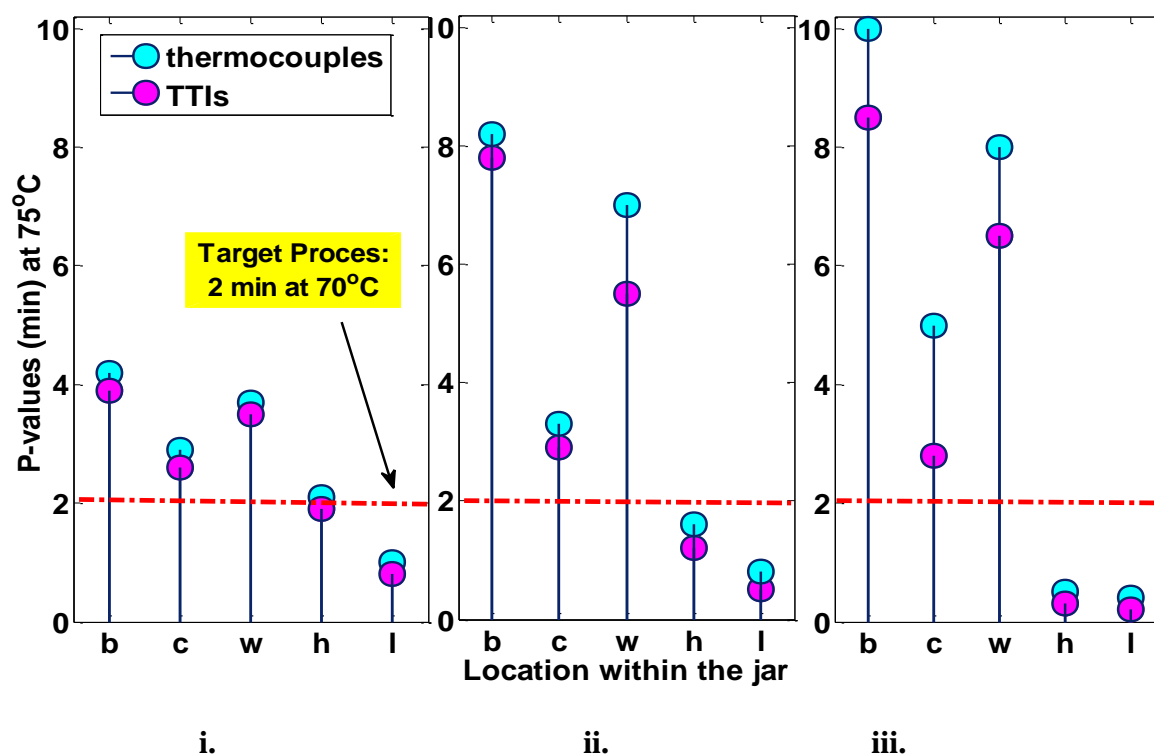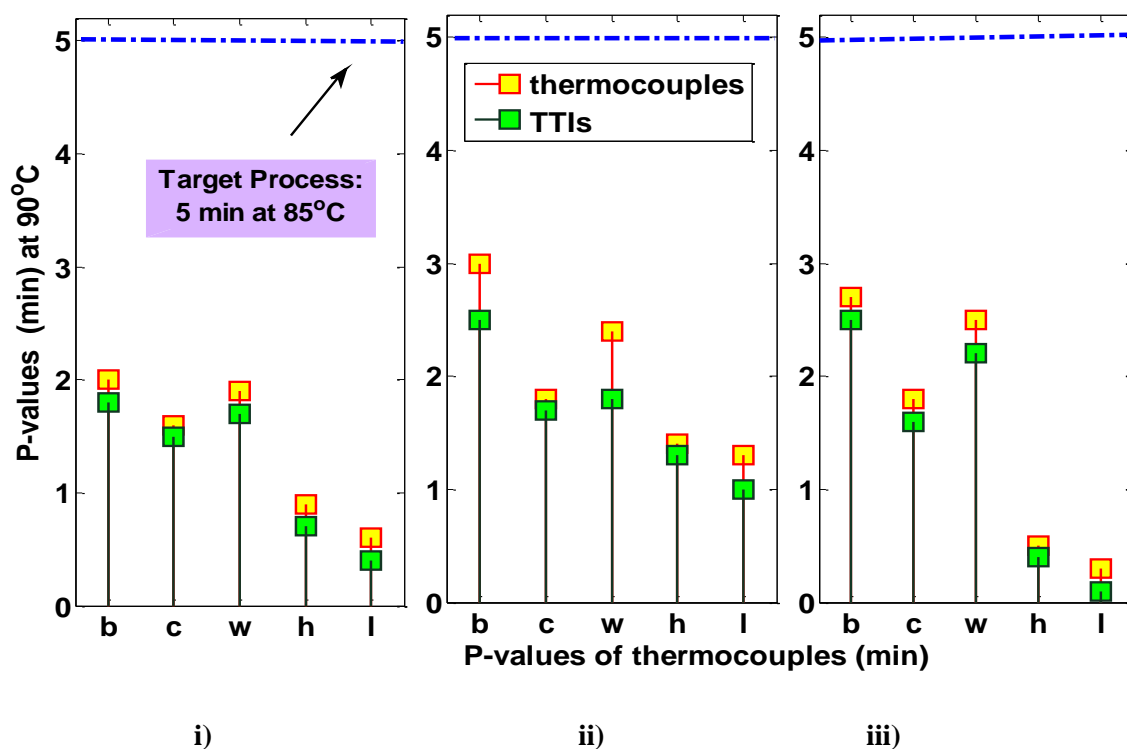

Figure 5.13: P-values of BAA85 TTIs and thermocouples for i) water, ii) 3% starch solution and iii) tomato soup at T_{fil}=90°C for all locations.

In both target processes the filling temperature is higher than the reference temperature and the z-values are higher than the ones of the target processes leading to underestimation of the process, which confirms the results reported in literature (Van Loey et al., 1996), as presented in Table 5.10.

Table 5.10: Possible scenarios for hot-fill processes.

	$T_{fil} > T_{ref}$	$T_{fil} < T_{ref}$
$Z_{TTI} > Z_T$	**Underestimation**	**Overestimation**
$Z_{TTI} < Z_T$	Overestimation	Underestimation

Where: T_{fil} = filling temperature, T_{ref} = reference temperature, Z_{TTI} = z-value of the enzyme, Z_T = z-value of the target process.

According to Table 5.10, The TTIs would overestimate the process at temperatures lower than the reference temperatures, as the lethality at temperatures lower than 60 and 75^0C, for BAA70 and BAA85, respectively, is negligible. Thus, the thermocouples would record much lower temperatures than the TTIs, which would overestimate that way the process, for the given z-values. This scenario would be the worse in terms of safety.

The measurement limit of the spectrophotometer was three log reductions in amylase activity with a reading to 3 decimal points. An average initial amylase activity for the BAA85 TTI and BAA70 was 1.000 and 0.9 units/minute, which for 3 log reductions would result in 0.001 units/minute activity for both TTI solutions. The highest process-values calculated from the amylase activities were ≤ 0.002 min^{-1}, which was the limit of the measuring accuracy of the spectrophotometer; thus, it was not possible to measure an amylase activity in excess of two log reductions with the present amylase assay method. That is another reason why the thermocouples will always be measuring higher process values than the thermocouples, for the current available equipment and assay.

5.3.4 Statistical analysis

In order to determine whether the two validation techniques are significantly different, an analysis of variance (ANOVA) test was performed for both process targets (2 min at 70°C and 5 min at 85°C). ANOVA is a procedure that compares two or more groups and is consisted of one independent variable, in the case of one-way ANOVA, with two or more conditions. In our case, the independent factor is the location of the thermocouples and TTIs within each fluid, and the two conditions compared are the process values of each monitoring technique at the defined locations; one-way ANOVA was chosen for analysing the difference between the two data sets. The test is based on the assumption that all sample populations are normally distributed and all group means are equal versus the alternative hypothesis that at least one group is different from the others; thus, the normality assumption was firstly checked.

The process values obtained from the thermocouples and the two TTI systems of BAA70 and BAA85 (Tables 5.11 and 5.12), were used as the data sets for the ANOVA analysis.

The statistical analysis was performed using the MatLab & Simulink software (Math Works, UK).

Table 5.11: Process values of thermocouples and BAA70 TTIs.

Locations	Process values (min)					
	Water		3% starch solution		Tomato soup	
	Thermocouples	TTIs	Thermocouples	TTIs	Thermocouples	TTIs
Bottom	4.2	3.9	8.2	7.8	10	8.5
Corner	2.9	2.6	3.3	2.9	5.0	2.8
Wall	3.7	3.5	7.0	5.5	8.0	6.5
Headspace	2.1	1.9	1.6	1.2	0.5	0.3
Lid	1.0	0.8	0.8	0.5	0.4	0.2
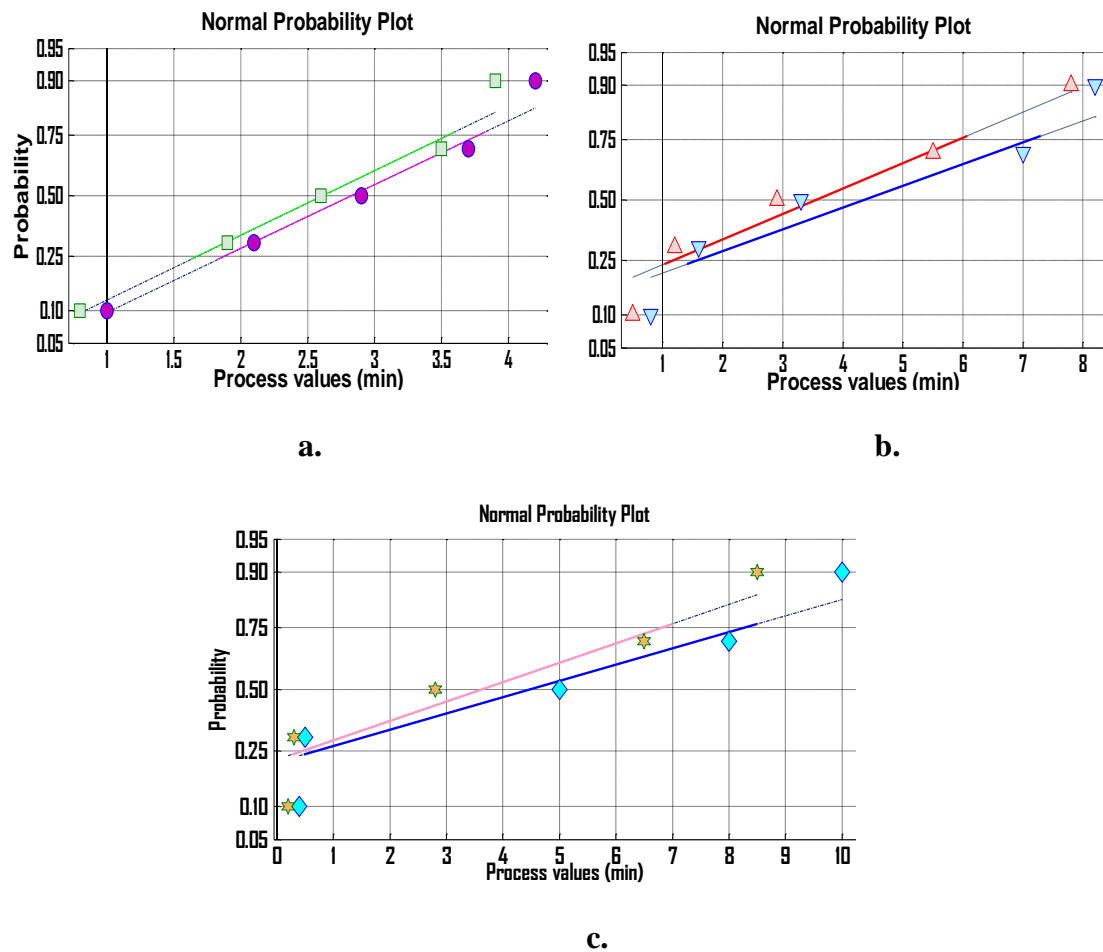
Figure 5.14: Normal probability plots for a. Water, b. 3% starch solution and c. tomato soup. The left and right hand lines refer to the BAA70 TTIs and thermocouples, respectively.

The scatter graphs give approximately straight lines through the first and third quartiles of the data, indicating approximate normal distributions. In the case of 3% starch and tomato soup, a slight departure from normality is observed in the lower tail. The shift in the mean from thermocouples to TTIs is not strongly evident; Wilcoxon rank sum hypothesis test was used to quantify that shift of distributions. The null hypothesis assumes that the two independent samples come from continuous distributions with equal medians, whilst the alternative would mean that they are not. If the null hypothesis is satisfied, the test will confirm that the shift between the two samples is not significant.

For all three fluids the logical output of h = 0, and the quite high p-values of approximately 0.6, indicate a failure to reject the null hypothesis at the default significance level of 1%. Thus, the normality assumption was satisfied and the ANOVA test was next performed.

Table 5.12: ANOVA test for the correlation of BAA70 TTIs and thermocouples.

Source	SS	df	MS	F	Prob>F
Water					
Columns	0.144	1	0.144	0.09	0.7711
Error	12.72	8	1.59		
Total	12.864	9			
3% starch					
Columns	0.9	1	0.9	0.09	0.7719
Error	80.076	8	10.0095		
Total	80.976	9			
Tomato soup					
Columns	3.136	1	3.136	0.19	0.6728
Error	130.66	8	16.3325		
Total	130.796	9			

The ANOVA table shows the between-groups variation (Columns) and within-groups variation (Error). ss is the sum of squares, and df is the degrees of freedom. MS is the mean squared error, which is SS/df for each source of variation. The F-statistic is the ratio of the mean squared errors, and the p-value is the probability that the test statistic can take a value greater than or equal to the value of the test statistic.

The high *p*-values of 0.77 and 0.67 ($p > 0.05$) indicate that the differences between column means are not statistically significant; the null hypothesis that the two groups' means are close to equal is satisfied.

The fact that there are no significant differences between the groups in a population level means that any differences observed, should be due to error.
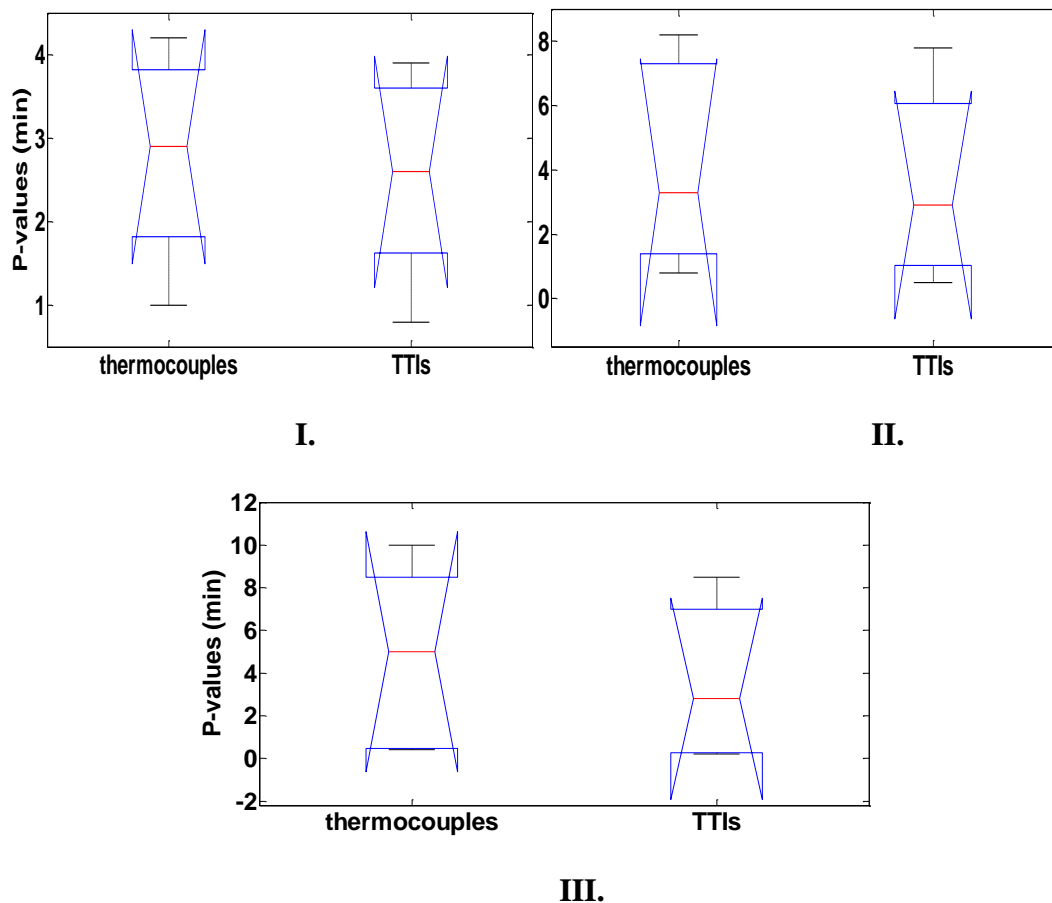
Figure 5.15: Notched box-plots of the two groups tested for I. Water, II. 3% starch, III. Tomato soup.

One-way ANOVA returns notched box plots of the observations in y, by group. Notched box plots apply a "notch" or narrowing of the box around the median and display the variability of the median between samples. Notches are useful in offering a rough guide to significance of difference of medians; if the notches of two boxes do not overlap, this offers evidence of a statistically significant difference between the medians at the 5% significance level, which is

based on a normal distribution assumption. The width of the notches is proportional to the interquartile range of the sample and inversely proportional to the square root of the size of the sample. The "flipped" appearance in the notched box plots means that the 1st quartile has a lower value than the confidence of the mean and vice versa for the 3rd quartile.

Figure 5.15 shows that the notches overlap, for all three fluids, indicating that there is no significant statistical difference between the two mediums of each fluid at the 5% significance level. This is confirmed by the low F-values and the high p-values, shown in the ANOVA table. Thermocouples exhibit more heterogeneous values than TTIs, since the boxes and the whiskers of thermocouples cover a larger range of the y-axis and its notches are larger, which represents a larger dispersion of the data values for thermocouples (Gries 2009a: 204f).

The same procedure was followed for the second target, were thermocouples and BAA85 TTIs are the groups analysed. The normality of the data sets was firstly checked and was followed by the Wilcoxon rank sum hypothesis test.

Table 5.13: Process values of thermocouples and BAA85 TTIs.

Locations	Process values (min)					
	Water		3% starch solution		Tomato soup	
	Thermocouples	TTIs	Thermocouples	TTIs	Thermocouples	TTIs
Bottom	2.0	1.8	3.0	2.5	2.7	2.5
Corner	1.6	1.5	1.8	1.7	1.8	1.6
Wall	1.9	1.7	2.4	1.8	2.5	2.2
Headspace	0.9	0.7	1.4	1.3	0.5	0.
Lid	0.6	0.4	1.3	1.0	0.3	0.1

i)

ii)

iii)
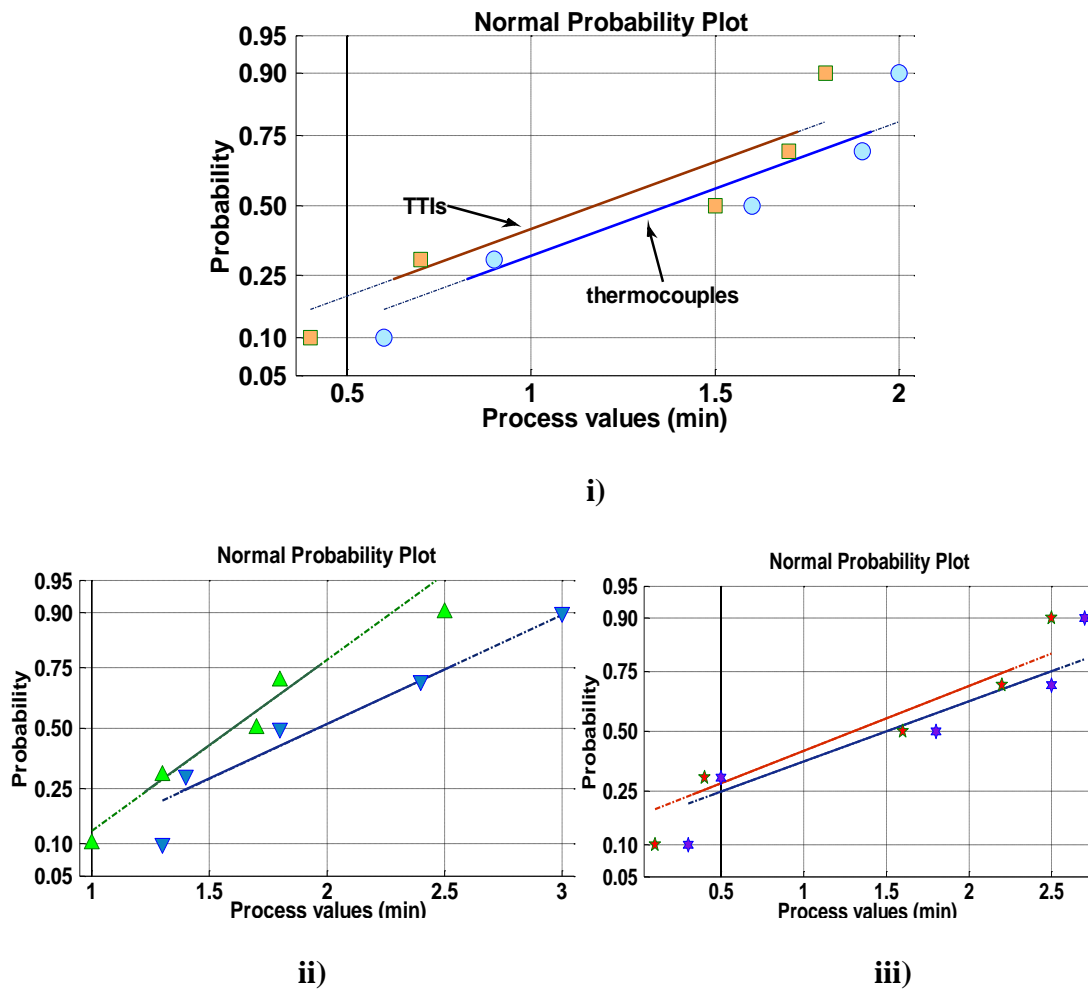
Figure 5.16: Normal probability plots for **i)** Water, **ii)** 3% starch solution and **iii)** Tomato soup. The left and right hand lines refer to the BAA85 TTIs and thermocouples, respectively.

In Figure 5.16, the scatter graphs follow straight lines through the first and third quartiles of the data, indicating normal distributions, in the case of water. As far as the 3% starch solution is concerned, some departure from normality is observed in the lower tail and shift in the mean from TTIs to thermocouples is evident.

For all three fluids the logical output of h = 0, and the high p-values of 0.5, 0.4 and 0.6 for water, starch solution and tomato soup, indicate a failure to reject the null hypothesis at the

default significance level of 1%. Thus, the normality assumption was satisfied and the ANOVA test was next performed (Table 5.14).

Table 5.14: ANOVA test for the correlation of BAA85 TTIs and thermocouples.

Source	SS	df	MS	F	Prob>F
Water					
Columns	0.144	1	0.144	0.09	0.7711
Error	12.72	8	1.59		
Total	12.864	9			
3% starch					
Columns	0.9	1	0.9	0.09	0.7719
Error	80.076	8	10.0095		
Total	80.976	9			
Tomato soup					
Columns	3.136	1	3.136	0.19	0.6728
Error	130.66	8	16.3325		
Total	130.796	9			

I)

II)

III)

Figure 5.17: Notched box-plots of the two groups tested for I) Water, II) 3% starch, III) Tomato soup.

The high *p*-values of 0.66, 0.46 and 0.78 ($p > 0.05$) indicate that the differences between column means are not statistically significant; the null hypothesis that the two groups' means are close to equal is satisfied. The results obtained from the ANOVA analysis are confirmed by Figure 5.17, which shows that the notches overlap, for all three fluids, indicating that there is no significant statistical difference between the two mediums of each fluid at the 5% significance level.

Similar to the results from the 1st process target, the boxes and the whiskers of thermocouples cover a larger range of the y-axis, with larger notches, indicating a larger dispersion of the data, as compared to BAA85 TTIs.

Based on the process values obtained during the hot-fill treatment, for both target processes, a variety of filling temperatures at the locations of interest within the glass jar was calculated for achieving the equivalent processes of 2 min at 70°C and 5 min at 85°C, for BAA70 and BAA85, respectively. The suggested combination of the filling temperatures and the TTI locations in the container is illustrated in Figure 5.18.
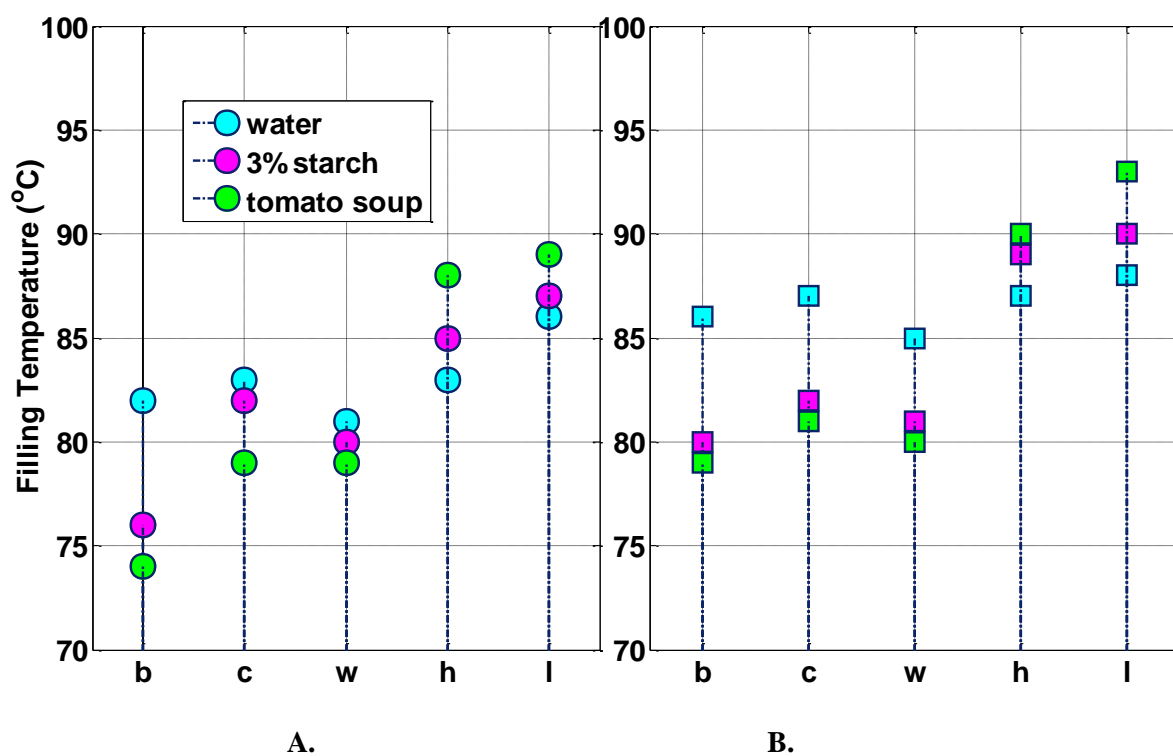

Figure 5.18: Filling temperatures required for A. BAA70 to achieve a target process of 2 min at 70°C and B. BAA85 for a target process of 5 min at 85°C.

5.4   Conclusions

Time Temperature Integrators (TTIs) were tested as an alternative validation method to temperature sensors, for measuring pasteurisation treatments. The method uses an encapsulated *Bacillus amyloliquefaciens* α-amylase (BAA) TTI, and it was applied to assess hot-fill treatments targeting the two processes of 2 min at $70^{o}C$ and 5 min at $85^{o}C$ for cook-chilled and high acid food products, respectively. The TTIs were tested under isothermal and tightly controlled non-isothermal conditions for the kinetic parameters to be obtained and for testing their sensitivity to a variety of temperature profiles, respectively.

In the first set of experiments, the calibration of the two TTI systems resulted in a D_{70}-value of 4.1 min and a z-value of $10.8^{o}C$ for BAA70 and a D_{85}-value of 8.7 and a z-value of $10.3^{o}C$ for BAA85. The z-values of both enzymes are consistent with the values required for pasteurization processes, but higher than the values of the target processes, ($7.5^{o}C$, and $8.3^{o}C$, respectively), which lead to underestimation of the thermal process. For overcoming this problem, the TTIs were submitted to temperatures higher than the reference ones, at 75 and $90^{o}C$, for predicting real process time and for being consistent with the heat duration time estimated from the isothermal experiments; the maximum heat duration was calculated to be 7 and 16 min for BAA70 and BAA85, respectively.

In the second set of experiments, TTIs were tested under non-isothermal conditions using the Peltier stage, which generated various time-temperature profiles under constant heating/cooling rate for a variety of holding times (simple cycles) and subsequent heating/cooling with no holding time (complex cycles). The TTIs appeared to pick up small temperature differences, but they do not reach the temperature that the Peltier stage is set to deliver; both BAA70 and BAA85 TTIs recorded temperatures 5 to $8^{o}C$ lower than the thermocouples. That is possibly due to the silicone tube thickness, which acts like a barrier in transferring the applied heat, the higher conduction received by the thermocouples and the

limitations coming from the assay method and the spectrophotometer. Another possible problem with the design of the specific TTIs is that the majority of their volume is positioned above the surface of the package, which means that only a small area of the TTIs will be in contact with the surface. Thus, in the case that there is a large temperature difference between the surface of the package and the bulk of the fluid, the TTIs would be exposed to a temperature slightly higher than that of the package, resulting to higher process values.

After the sensitivity tests were performed, the response of the TTIs was investigated under the hot-fill treatment conditions, and was compared to that of the temperature sensors under the same conditions and locations. The two monitoring techniques were compared for a filling temperature of 75 and 90°C, for BAA70 and BAA85, respectively, with water, 3% of starch solution and tomato soup being the heating mediums. The process values were calculated at five different positions inside the glass jar, as shown in Figure 2.11, with the headspace and the lid being the coldest points. The target process was achieved by the bottom, bottom-corner and wall for BAA70 TTI and all three fluids. The filling temperature was not sufficient to pasteurise the headspace and the lid. The time-temperature combination of 10 min at 90°C, did not achieve the target process of 5 min at 85°C, with the TTIs showing lower process values than the thermocouples. Both TTI systems record lower temperatures than thermocouples under any of the conditions they were submitted in the current work. In order to investigate whether the two validation methods are significantly different, a statistical analysis of variance was performed. Results from the ANOVA tables and the box-plots, showed that the two methods are statistically not significantly different at a 5% confidence level. That means that the agreement between the two methods can be considered to be good, given the potential for discrepancy; the TTI systems could be safely used for evaluating pasteurisation processes.

References

Banga J.R., Perez-Martín R.I., Gallardo J.M., Casares J.J., (1991). Optimisation of thermal processing of conduction-heated canned foods: study of several objective functions. *Journal of Food Engineering, 14, 25.*

Bellara S.R., Fryer P.J., McFarlane C.M., Thomas C.R., Hocking P.M., Mackey B.M., (1999). Vizualization and modelling of the thermal inactivation of bacteria in a model food. *Applied Environmental Microbiology*, 65, 3095-3099.

Brown K.L., Ayres C. A., Gaze J. E., and Newman, (1984). Thermal destruction of bacterial spores immobilised in food/alginate particles. *Food Microbiology*, 1:187-198.

Bobelyn Els, Hertog Maarten, Nicolaï Bart M., (2006). Applicability of an enzymatic time temperature integrator as a quality indicator for mushrooms in the distribution chain. *Postharvest Biology and Technology,* 42(1):104–114.

Campden & Chorleywood Food Research Association (CCFRA), (1992a). Food Pasteurisation Treatments. Technical Manual No.27.

Campden & Chorleywood Food Research Association (CCFRA), (2006b). Pasteurisation: A food industry practical guide (second edition). Guideline No.51.

De Cordt S., Hendrickx M., Maesmans G., and Tobback P. (1992). Immobilised -amylase from *Bacillus licheniformis*: a potential enzymic time-temperature integrator for thermal processing. *International Journal of Food Science and Technology*, 27, 661-673.

De Cordt S., Avila I., Hendrickx M. & Tobback P., (1994). DSC and protein-based time temperature integrators: Case study of -amylase stabilised by polyols and/or sugar. *Biotechnology & Bioengineering*, 44, 859-865.

Fryer P. J., Simmons M.J.H., Cox P.W., Mehauden K., Hansriwijit Suwijak, Challou Flora, Bakalis Serafim, (2011). Temperature Integrators as tools to validate thermal processes in food manufacturing. *Procedia Food Science,* 1:1272–1277, 11th International Congress on Engineering and Food (ICEF11).

Gries S. T., (2009a). Quantitative corpus linguistics with R. A practical introduction. London: Routledge.

Guiavarc"h Y., (2003). Development and use of enzymic time-temperature integrators for the assessment of thermal processes in terms of food safety. PhD Thesis No.570, Katholike Universiteit Leuven, Belgium.

Hendrickx M., Saraiva J., Lyssens J., Oliveira J. & Tobback P., (1992). The influence of water activity on thermal stability of horseradish peroxidase. *International Journal of Food Science & Technology*, 27, 33-40.

Hendrickx M., De Cordt S., Van Loey., (1995). Evaluation of the integrated time-temperature effect in thermal processing of foods. *Critical Reviews in Food Science and Nutrition,* 35(3).

Jin Q., Jin W., Guanglin Z., Qin F., (2012). A time–temperature indicator based on glucoamylase. China Patent 201110394281.X.

Kim W., Park E., Hong K., (2012). Development of a time–temperature integrator system using *Burkholderia cepacia* lipase. *Food Science and Biotechnology*, 21:497–502.

Maesmans G., Hendrickx M., De Cordt S., Van Loey A., Noronha J., Tobback P., (1994). Evaluation of process value distribution with time temperature integrators. *Food Research International*, 27, 413-423.

Moles C.G., Alonso A. A., (2003). Improving food processing using modern optimization methods. *Trends in Food Science & Technology 14 (4), 131-144.*

Moritz M., Balasa A., Jaeger H., Meneses N., Knorr D., (2012). Investigating the potential of polyphenol oxidase as a temperature–time-indicator for pulsed electric field treatment. *Food Control,* 26:1–5.

Mulley E.A., Stumbo C.R. and Hunting W.M., (1975). Thiamine: A chemical index of the sterilization efficacy of thermal processing. *Journal of Food Science*, 40: 993.

Tucker G.A., and Holdsworth S.D., (1996). Optimization of Quality factors for Foods Thermally Processed in Rectangular Containers. Technical Memorandum 627, CCFRA, Chipping Campden, UK.

Tucker G.S., (1999). A novel validation method: Application of time-temperature integrators to food pasteurization treatments. *Transactions of the IChemE, Food and Bioproducts Processing*, 77, Part C, 223-231. Campden and Chorleywood Food Research Association, Chipping Campden, UK.

Tucker G.S., Lambourne T., Adams J.B., and Lach A., (2002). Application of biochemical time-temperature integrators to estimate pasteurisation values in continuous food processes. *Innovative Food Science & Emerging Technologies*, 8 (1), 63-72.

Tucker G.S. and Wolf D., (2003). Time-temperature integrators for food process analysis, modelling and control. R&D Report No.177. Campden & Chorleywood Food Research Association.

Tucker S., Brown H.M., Fryer P.J., Cox P.W, Poole F.L., Lee H.S., (2007). Sterilisation time–temperature integrator based on amylase from the hyperthermophilic organism *Pyrococcus furiosus*. *Innovative Food Science & Emerging Technologies,* 8:63–72.

Van Loey A., Hendrickx M., De Cordt M.E., Haentjens T.H and Tobback P.P., (1996). Quantitative evaluation of thermal processes using time-temperature integrators. *Trends in Food Science and Technology*, 7, 16-26.

Van Loey A., Arthawan A., Hendrickx M., Haentjens T.H. and Tobback P.P., (1997a). The development and use of an a-amylase based time-temperature integrator to evaluate in-pack pasteurization processes, *Lebensmittel-Wissenschaft und-Technologie*, 30: 94 –100.

Van Loey A., Guiavarc'h Y., Claeys W., Hendrickx M., (2004). Improving the thermal processing of foods: The use of time–temperature integrators (TTIs) to validate thermal processes. P. Richardson (Ed.), Woodhead Publishing Ltd., Cambridge, UK p. 365–379.

Yan S., Huawei C., Limin Z., Fazheng R., Luda Z., Hengtao Z., (2008). Development and characterization of a new amylase type time–temperature indicator. *Food Control*, 19:315–319.

Chapter 6 - Conclusions and Future Work

6.1   Conclusions

In this thesis, the inversion method was investigated for its effectiveness as a thermal treatment of the headspace and the lid, for hot-filled model foods. Starch solutions and cream of tomato soup were used for evaluating a heat treatment targeting a process of 5 min at 70°C. The model fluids were hot-filled in pre-heated glass jars at a temperature of 80°C, were inverted for 30 s, brought back to the upright position and cooled at room temperature for 10 min. The chosen set of inversion time and filing temperature appeared to be sufficient for achieving the goal set, for the least viscous fluids, 3% and 4% starch solution, whilst it was not for the tomato soup and the 5% starch solution (the most viscous fluid). The inverted jars showed significantly higher process values for the headspace and the lid with the filling temperature being the most important parameter.

The behaviour of the model fluids was investigated by carrying out a series of rheological experiments and developing a dynamic mathematical model. Results showed a shear-thinning behaviour for all model fluids, with dominating elastic properties, and the finite element method used, based on dimensionless numbers and the viscosities calculated from the steady state rheological test, indicated that the fluids could generate natural convection from the lateral boundaries. The temperature distribution and flow behaviour of tomato soup and 3% starch solution for the inverted and non-inverted packages, was further analysed and predicted mathematically using the finite element method; the predicted data were compared with the experimental ones, for validating the model. A two-dimensional, axi-symmetrical

geometry was used for computational simplification and fluids were assumed to have constant thermo-physical properties, but temperature dependant viscosity. 7031 nodal points were used with a finer grid near the walls and the interface of air-fluid with a convergence criterion set to 10^{-8}. For both fluids and cases investigated, the temperature isotherms and velocity vectors plotted, showed that cold zones are located near the walls and the interface between the fluid and air. The convection currents push the cold zones of the fluid to move from the headspace towards the bottom of the jar and near the wall, creating secondary and tertiary flows. The forced convection caused by the inversion of the package, created higher recirculation within the fluid; the disrupted interface of the fluids indicated the existence of either a bubble created during inversion or the movement of cold spots within the fluid. The velocity values of fluid A (7.8×10^{-3}) were up to ten times higher than those in fluid T(6.3×10^{-4}), explaining the faster heating of the headspace and the lid and the lower temperatures observed. The comparison of the predicted temperature profiles with the experimental ones showed good agreement for both cases and fluids. The correlation of the two data sets was confirmed by the low RMSE values obtained, validating the model developed.

The heat treatment of hot-filling was also evaluated by *Bacillus amyloliquefaciens* α-amylase (BAA) based Time Temperature Integrators (TTIs), which are used as an alternative validation method to temperature sensors. The method was applied to target the two processes of 2 min at 70^{0}C and 5 min at 85^{0}C for cook-chilled and high acid food products, respectively. The TTIs were tested under isothermal conditions, resulting in a D_{70}-value of 4.1 min and a z-value of 10.8^{0}C for BAA70 and a D_{85}-value of 8.7 and a z-value of 10.3^{0}C for BAA85; the heat duration of BAA70 and BAA85 was 7 and 16 min, respectively. The TTIs appeared to pick up small temperature differences, when tested under tightly controlled, non-isothermal conditions but, they consistently record temperatures lower than the thermocouples. The ANOVA statistical analysis conducted showed that the two monitoring

techniques are statistically not significantly different at a 5% confidence level, indicating that the correlation between the thermocouples and the TTIs can be considered to be good, given the potential for discrepancy. Thus, the TTI systems could be safely used for evaluating pasteurisation processes.

6.2   Future work

The inversion of glass packages as a thermal treatment of the headspace and the lid has been shown to be promising for targeting yeasts and moulds in acid foods. Further studies on a variety of inversion time and filling temperature combinations could help reduce the time of post-pasteurisation treatments used currently in the food industry. Different package materials and sizes could also be investigated in evaluating the effectiveness of the inversion step. Preliminary experiments on hot-fill treatments with Polyethylene terephthalate (PET) and carton packages showed a noticeable difference in the effectiveness of the method, expressed in terms of process values. That is due to the significantly different thermal properties of the package material making them worth investigating. The two materials and the different package sizes were not expanded in this work due to time limitation.

The use of temperature sensors for validating the degree of thermal process achieved will probably remain the most used method, since on-line process control is feasible, as compared to the TTIs. Both the temperature sensors and the TTIs lack predictive power for processing conditions different from the ones under which the experiments are run. Thus, advanced mathematical models have been developed in the last decades to overcome that problem and predict process times and temperatures based on empirical formulae or theoretical heat transfer models. Most of the food companies rely on the General method for setting up time-temperature plans, but the method does not allow process deviations to be assessed. By the

use of predictive modeling the batches of food products that undergo process deviation, would be able to be controlled and the process establishment would be more straightforward (Tucker et al., 2003). Based on experiments from current work, modelling the heat process would potentially show by how much the temperature difference between the two monitoring techniques can underestimate the process and what would the ideal filling temperature be for the best correlation.

TTIs would be very advantageous if combined with temperature sensors; being used in monitoring critical control points is fundamental. In traditional canning process, lethal rates are evaluated at time steps of one minute, due to current capabilities of data loggers, but with modern processes they can be estimated at time steps of one second. The application of TTIs to various thermal processes, such as pasteurisation and sterilisation is active, especially for food products that are heated and cooled in large vessels or heat exchangers where wire-based systems cannot be used.